Tesis doctoral

Methodology and analysis of gas embolism: experimental models and stranded cetaceans

(Metodología y análisis de la embolia gaseosa: modelos experimentales y cetáceos varados)

Yara Bernaldo de Quirós Miranda

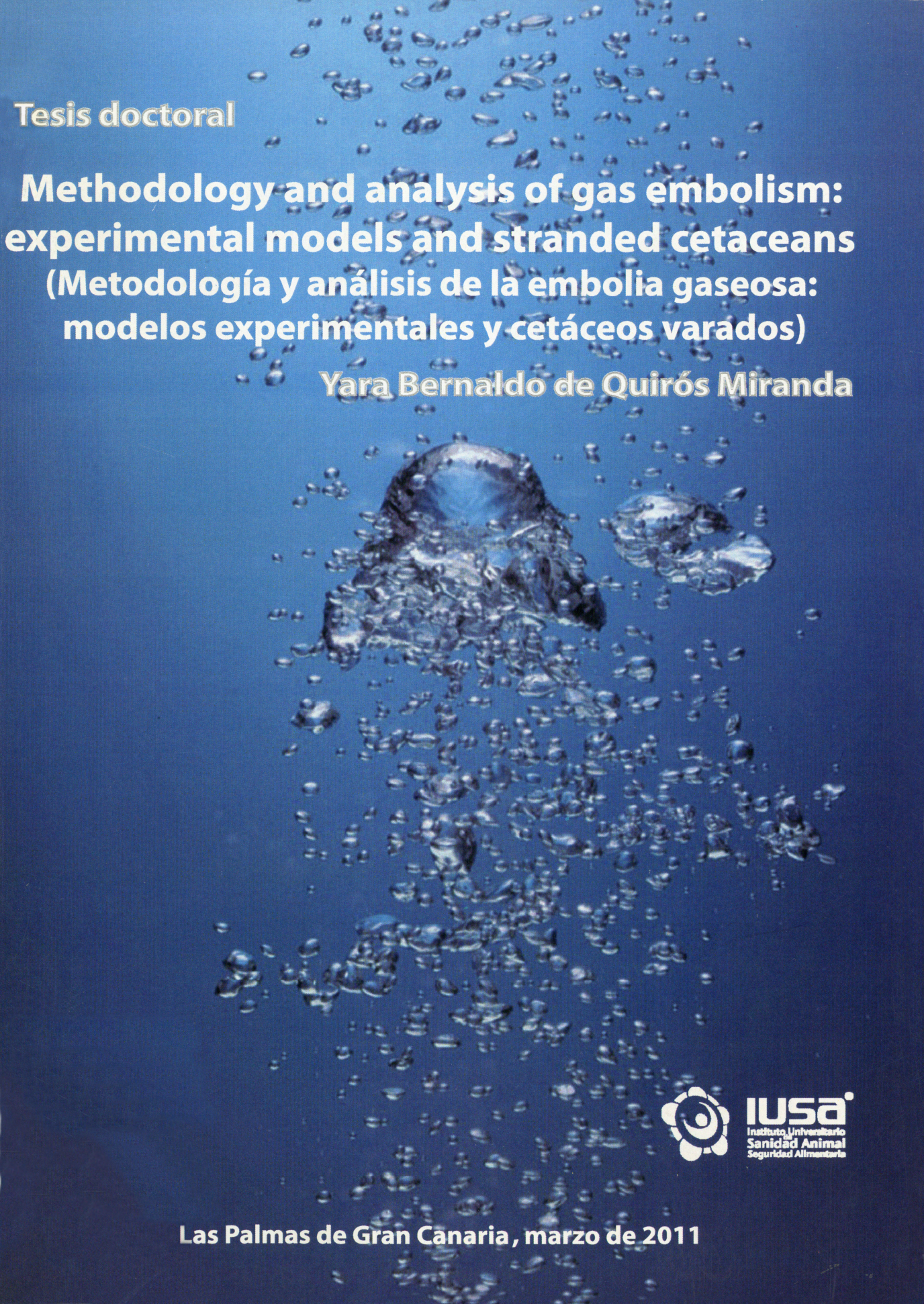

IUSA
Instituto Universitario de Sanidad Animal y Seguridad Alimentaria

Las Palmas de Gran Canaria, marzo de 2011

UNIVERSIDAD DE LAS PALMAS DE GRAN CANARIA

IUSA Instituto Universitario de Sanidad Animal Seguridad Alimentaria

Anexo I

Dª. BEGOÑA ACOSTA HERNÁNDEZ, SECRETARIA DEL INSTITUTO UNIVERSITARIO DE SANIDAD ANIMAL Y SEGURIDAD ALIMENTARIA (IUSA) DE LA UNIVERSIDAD DE LAS PALMAS DE GRAN CANARIA (ULPGC)

CERTIFICA:

Que el Consejo de Doctores del Instituto en su sesión de fecha 28 de febrero de 2011 tomó el acuerdo de dar el consentimiento para su tramitación, a la tesis doctoral europea titulada: **"METHODOLOGY AND ANALYSIS OF GAS EMBOLISM: EXPERIMENTAL MODELS AND STRANDED CETACEANS". ("METODOLOGÍA Y ANÁLISIS DE LA EMBOLIA GASEOSA: MODELOS EXPERIMENTALES Y CETÁCEOS VARADOS")**, presentada por la doctoranda Doña Yara Bernaldo de Quirós Miranda, dirigida por el Doctor D. Antonio J. Fernández Rodríguez y el Doctor D. Óscar González Díaz.

Y para así conste, y a efectos de los previsto en el Artº 73.2 del Reglamento de Estudios de Doctorado de esta Universidad, firmo le presente en Las Palmas de Gran Canaria, a veintiocho de febrero de dos mil once.

UNIVERSIDAD DE LAS PALMAS DE GRAN CANARIA Instituto Universitario de Sanidad Animal y Seguridad Alimentaria

UNIVERSIDAD DE LAS PALMAS DE GRAN CANARIA

IUSA Instituto Universitario de Sanidad Animal Seguridad Alimentaria

Anexo II

UNIVERSIDAD DE LAS PALMAS DE GRAN CANARIA

Departamento: Instituto Universitario de Sanidad Animal Y Seguridad Alimentaria.

Programa de Doctorado: Sanidad Animal.

Título de la Tesis

"METHODOLOGY AND ANALYSIS OF GAS EMBOLISM: EXPERIMENTAL MODELS AND STRANDED CETACEANS". ("METODOLOGÍA Y ANÁLISIS DE LA EMBOLIA GASEOSA: MODELOS EXPERIMENTALES Y CETÁCEOS VARADOS").

Tesis Doctoral Europea presentada por Doña Yara Bernaldo de Quirós Miranda.

Dirigida por el Doctor D. Antonio J. Fernández Rodríguez y el Doctor D. Óscar González Díaz.

El Director **El Codirector** **La Doctoranda**

Las Palmas de Gran Canaria, a 28 de febrero de 2011

“Ever since humankind has lived by and gone down to the sea, we have been awestruck by the creaturas that make it their home. First we feared them, later we ate them and now we try to emulate them”

Gerald Kooyman

"Every person has the right to inherit an uncontaminated planet on which all forms of life may flourish"

Jaques Yves Cousteau 1910-1967

“The impossible missions are the only ones which succeed”

“Les missions impossible sont les sueles qui réussissent”

Jaques Yves Cousteau 1910-1967

Tabla de contenido

1 INTRODUCTION

1.1 INTRODUCTION AND OBJECTIVES

The impact of anthropogenic sound on the marine environment and conservation of species has increased exponentially at national and international levels resulting in a high social and scientific concern in recent years (European-Parliament, 2004).

One of the best examples of this assertion lies in whales stranding and death related to noise emissions during naval maneuvers. The beaked whales (family *Ziphiidae*) are the most often whales involved in this kind of mass stranding temporally and geographically related to the use of antisubmarine active mid-frequency sonar .

Atypical mass stranding of beaked whales (BW) had not been referenced prior to 1963 (date from which, antisubmarine acoustic technology started to be used). Since then, mass strandings have been reported associated with military maneuvers in different world geographic locations as Bonnaire 1974, Canary Islands 1985, 1988, 1989 and 2002, Greece 1996, and in Bahamas in 2000 (Cox et al., 2006).

Except in the Bahamas, where a partial pathological study was done in three whales and authors concluded a diagnosis of "acoustic trauma", none systematic pathological analysis had been previously done in other similar cases. Until 2002, the “acoustic hypothesis” (Cox et al., 2006) was the only option that had received scientific attention, especially in the United States, although this has still not been scientifically proven.

An alternative, but not exclusive, "non-acoustic" hypothesis was published by Jepson et al. (2003) and Fernández et al. (2005), after the study of the lesions in dead BWs involved in a mass stranding coincidentally with naval exercises in the Canary Islands. Our group provided a possible explanation of the relationship between

anthropogenic, acoustic (sonar) activities and the stranding and death of those marine mammals.

Fourteen BWs stranded in the Canary Islands close to the site of an international naval exercise (Neo-Tapon 2002) held the 24th of September 2002. Strandings began about 4 hours after the onset of midfrequency sonar activity. Eight Cuvier's BW's *(Ziphius cavirostris)*, one Blainville's BW *(Mesoplodon densirostris)*, and one Gervais' BW *(Mesoplodon europaeus)* were examined postmortem and studied histopathologically. No inflammatory or neoplastic processes were noted, and no pathogens were identified.

Macroscopically, whales had severe, diffuse congestion and hemorrhage, especially around the acoustic jaw fat, ears, brain, and kidneys. Gas bubble-associated lesions and fat embolism were observed in the vessels and parenchyma of vital organs. In vivo bubble formation associated with sonar exposure that may have been exacerbated by modified diving behavior caused nitrogen supersaturation above a threshold value normally tolerated by the tissues (as occurs in decompression sickness).

Alternatively, the effect of the sonar on different tissues that have been supersaturated with nitrogen gas could be such that it lowers the threshold for the expansion of in vivo bubble precursors (gas nuclei). Exclusively or in combination, these mechanisms may enhance and maintain bubble growth or initiate embolism. Severely injured whales died or became stranded and died due to cardiovascular collapse during beaching.

That study demonstrated a new pathologic entity in cetaceans. The syndrome was apparently induced by exposure to mid-frequency sonar signals and particularly affects deep, long-duration, repetitive-diving species like BWs.

The new pathological entity named "Gas Bubble Disease" or " Decompression like Sickness" in cetaceans was deeply discussed in a specific Workshop Marine Mammal

Commission of the United States (2004) with the participation of international experts and one of its main conclusions was that:

"Induced Gas-bubble disease is a plausible pathologic mechanism for the morbidity and mortality seen in cetaceans associated with sonar and merits further investigations".

Simultaneously, this hypothesis raised an important public controversy and a scientific replay in *Nature 2004* (Piantadosi and Thalmann, 2004), which clearly disagreed with that interpretation, requiring investigations on analysis of the composition of the gas in the bubbles in order to approach a diagnosis of Decompression Sickness (DCS).

Attempts have been made to analyze the gas produced during decompression, using a wide variety of methods in humans and experimental animal pathology but not, so far, in cetaceans. However, appropriate and accurate measurement of respiratory gases while avoiding atmospheric air is difficult, and the peculiar circumstances of cetacean strandings and *in situ* necropsies make this goal even more difficult.

There are many issues in this complex problem which should be addressed scientifically in order to approach and scope responses, which may contribute to understanding “what”, "how", "why" of this new pathology described in cetaceans. In this direction, this project addresses generically “what” (gas analysis) and “how” (gas sampling and storing) addressing the following specific objectives:

1. To develop and standardize an accurate and handy feasible methodoly that enables gas analysis and sampling for field necropsy of stranded cetaceans.

2. To obtain experimentally in rabbits referenced guideline data (presence, amount and analysis) of intravascular gas bubbles generated both “in vivo”

(compression / decompression or iatrogenic venous gas embolism) and "*postmortem*" (putrefaction model).

3. To use gas analysis for diagnosis of gas embolic related pathologies in stranded cetaceans.

1.2 STATE OF THE ART

1.2.1 PHYSICAL CHEMISTRY OF RESPIRATORY GASES

Normal respiratory gases (nitrogen, oxygen and CO_2) are expected to be found in the blood and to interfere with bubble dynamics. For a better understanding of this dynamic equilibrium, we should first go through the physical and chemical properties affecting these gases inside the body. This review is based in the textbook of Medical Physiology of (Guyton, 1981).

1.2.1.1 Free diffusion

Gases are free molecules, with inner energy expressed usually as kinetic motion. Molecules move randomly, striking each other resulting on the dispersion of molecules. Therefore, if gas molecules are placed in a closed system, they will occupy the total volume. The impact of the random movements of the molecules against the walls of the system is the pressure. This means that gas pressure is concentration dependant. If this closed system has a concentration gradient, it will result on a net movement of molecules from the concentrated area (high pressure area, P_A) to the most diluted one (low pressure area, P_B). This net movement of molecules is the **net diffusion,** and its rate (D) will be directly proportional to gradient pressure and inversely proportional to the distance (d) between the two areas.

$$D = \frac{(P_A - P_B)}{d} = \frac{\Delta P}{d} \tag{1.1}$$

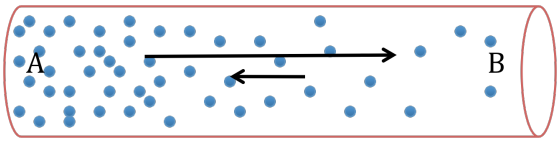

Fig. 1.1: Net diffusion of free gas molecules.

In biological systems, we will find most of the times, a mixture of gases. The total pressure (P_t) is now the sum of different molecules hitting the surface and therefore the pressure of each gas (named partial pressure) is directly proportional to its molar fraction (fraction of these molecules hitting on the surface, y), being the total pressure the sum of the different partial pressures composing the system. This is known as the **Dalton law**:

$$P_A = y_A \cdot P_t \tag{1.2}$$

$$P_t = \sum_{i=A}^{N} P_i = P_A + P_B + P_C + \cdots \tag{1.3}$$

As a consequence the rate of diffusion of each gas is also directly proportional to its partial pressure.

1.2.1.2 Diffusion of gases through fluids

If we now introduce a fluid on this closed system, we will have two different phases in contact with each other and once more with a pressure gradient. Thus, molecules will move from the high-pressure area towards the low one until equilibrium is reached. At the equilibrium state the pressure of the dissolved gas is exactly equal to the pressure of the gas in the gas state. But this time there will be other factors affecting the net diffusion. Depending on the polarity of the molecule and polarity of the fluid, they will have different solubility coefficient (S). This is, polar molecules will be attracted by polar fluids, and therefore will be more soluble than non-polar molecules on this fluids. Each compound has its own solubility for each fluid. Now the concentration of the dissolved gas depends on its partial pressure and on the solution temperature. This is expressed thorough the **Henry's law**:

$$P_i = K^i_{H,c} \cdot C_i^{aq} \tag{1.4}$$

Where P_i is a partial pressure of gas i (atm), C_i^{aq}, is the concentration of dissolved gas (mol·L^{-1}) and $K^i_{H,c}$ is the Henry constant (atm·L·mol^{-1}) which depends on the

solute, the solvent and the temperature (Wikipedia, 2011). Henry's equation can be expressed in terms of solubility of gas dissolved and the pressure gradient by:

$$C_i^{aq} = S_i \cdot \Delta P \tag{1.5}$$

Where *ΔP* is a pressure gradient, S_i is the solubility coefficient of gas *I* and C_i^{aq} is the concentration of *i* in aqueous solution (Wikipedia, 2011).

There is another way of expressing Henry's law in terms of gas concentration ratio between the two phases (Wikipedia, 2011):

$$C_i^{aq} = K_{H,cc}^{i} \cdot C_i^{g} \tag{1.6}$$

Where $K_{H,cc}^{i}$ represents the Henry constant that it is expressed in terms of the ratio of concentrations of gas *i* between both phases. The remaining terms of equation (1.6) has the usual meaning.

Besides the concentration gradient or pressure, other additional factors affecting diffusion of gas through fluids are cross-sectional area of the fluid (*A*), molecular weight (*MW*) and the temperature of the fluid. In the body, the temperature remains very constant; therefore temperature is usually not considered. Net rate diffusion in fluids remains as follows:

$$v_D = \frac{A \cdot S_i \cdot \Delta P}{d \cdot \sqrt{MW}} \tag{1.7}$$

Where v_D is the diffusion rate, *ΔP* is the pressure difference, *A* is the cross-sectional area of the fluid, S_i is the solubility coefficient of the gas, *d* is the distance of diffusion, and MW_i is the molecular weight of the gas.

Physicochemical properties of a given gas that affect the diffusion rate are its solubility coefficient and its molecular weight. We can define the diffusion coefficient taking into account these two characteristics only:

$$D_i = \frac{S_i}{\sqrt{MW_i}} \tag{1.8}$$

As a result, under the same pressure level, different gases will diffuse faster or lower depending on its diffusion coefficient. Considering the diffusion coefficient for oxygen to be 1 for the body fluids, the relative diffusion coefficient for other respiratory gases is:

Table 1.1: Relative diffusion Coefficient for different gases of respiratory importance.

Gases	Relative Diffusion Coefficient.
O_2	1
CO_2	20.3
N_2	0.53

Roughly, CO_2 diffusion coefficient is 20 times higher than oxygen and 60 times higher than nitrogen.

1.2.1.3 Diffusion of gases through tissues

Respiratory gases are more soluble in lipids that in water. Therefore diffusion of gases through tissues is limited by diffusion rates in fluids, thus diffusion through cell membranes is the same as for fluids.

1.2.1.4 Diffusion of gases through the respiratory membrane

Respiratory or pulmonary membrane is the overall membrane surfaces where gaseous exchange takes place. The ultrastructural components of the respiratory membrane are:

1) A layer of fluid in the alveolus

2) The alveolar epithelium

3) The basement membrane of the alveolar epithelium

4) Interstitial space (very thin)

5) The basement membrane of the endothelium (in many places is fused with the endothelium)

6) Endothelial membrane.

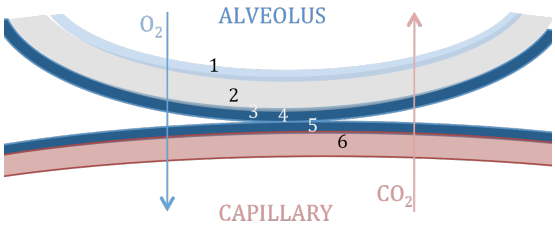

Fig. 1.2: Ultrastructural components of the respiratory membrane and net diffusion of oxygen and CO_2. Illustration adapted from Guyton (1981).

According to equation 1.5, factors that determine how fast a gas diffuses through the respiratory membrane are: the thickness of the membrane, surface, diffusion coefficient of the gas and pressure difference for that gas.

1.2.2 HUMAN RESPIRATORY PHYSIOLOGY

This review is based in the textbook of Medical Physiology of (Guyton, 1981).

1.2.2.1 Gaseous exchange in the alveolus

Alveolar gas composition is different from atmospheric air because only 1/7 of total volume is replaced with new atmospheric air, oxygen is constantly diffusing from the alveolus and CO_2 is constantly diffusing into the alveolus, and air is humidified as soon as gets in contact with body fluids. Thus, perfusion and ventilation determine the alveolar gas composition.

During normal pulmonary blood flow the blood becomes almost saturated with O_2 when it has passed only through one-third of the pulmonary capillary. If because of metabolic reasons, more oxygen is demanded, there are several ways to increase body uptake and all of them are intrinsically correlated:

Increase cardiac output. Increases total volume of blood passing through the pulmonary capillaries at the same time. Exposure time can be decreased 2/3rds and still blood will be oxygenated.

Increase the surface of the respiratory membrane; by opening of previous dormant pulmonary capillaries, dilatation of pulmonary capillaries previously opened.

Increase of ventilation rate. Several breaths are needed to replace most of the alveolar air by new atmospheric air.

1.2.2.2 Transport of respiratory gases

Oxygen is transported mainly (97%) in combination with hemoglobin, and only 3% in dilution. Oxygen binds loosely and in a molecular way (and therefore easily reversible) with one of the iron of the hemoglobin. It does not become ionic oxygen. Thus, it is released into the tissue fluids in the form of dissolved molecular oxygen.

Diluted CO_2 represents as well a small proportion (2.7%); the rest reacts with the water molecules and is transported as carbonic acid. About 70% of the carbonic acid is transported in the red blood cells (RBC) because they have an enzyme (carbonic anhidrase) that catalyzes and speeds the reaction with the water inside the cells. 30% of CO_2 is transported in combination either with hemoglobin (to form carbaminohemoglobin) or with plasma proteins.

Nitrogen is an inert gas (meaning that it does not react chemically with other materials), thus it will always be transported in dilution.

1.2.2.3 Gaseous exchange in tissues

Respiratory gases are more soluble in lipids that in water. Diffusion of gases through tissues is limited by diffusion rates in fluids, thus diffusion through cell membranes is the same as for fluids (Guyton, 1981). But because of the same reason, fatty tissues may act as a sink for these gases, especially for nitrogen that is about 6 times as soluble in fat as in blood (Vernon, 1907).

Pressure differences are very important attending to Equation 5. In tissues there is a large pressure difference (55mmHg) for oxygen to diffuse from capillaries to interstitial tissues and since the cells are always using oxygen, intracellular PO_2 will be always lower than interstitial fluid PO_2. The normal intracellular PO_2 ranges from as low as 5mmHg to 60 mmHg.

CO_2 acts just in the opposite way. Large quantities of CO_2 are formed in the cells that diffuse into the interstitial fluid and into the capillary veins. Pressure differences are very small in this case, but since CO_2 solubility coefficient (S_{CO2}) is 20 times higher than oxygen, it does not need such a great pressure difference in order to diffuse.

1.2.2.4 Gaseous exchange in humans

In the figure bellow the normal PO_2 and PCO_2 values in a human body is described in mmHg. Because of the high solubility of nitrogen, PN_2 in tissues is expected to be in equilibrium with PN_2 in the alveolus.

All tissues have water, and water has the propensity to evaporate into the gas phase. The water vapor pressure at normal body temperature (37˚C) is of 47mmHg. As atmospheric air enters in contact with the respiratory passages is humidified.

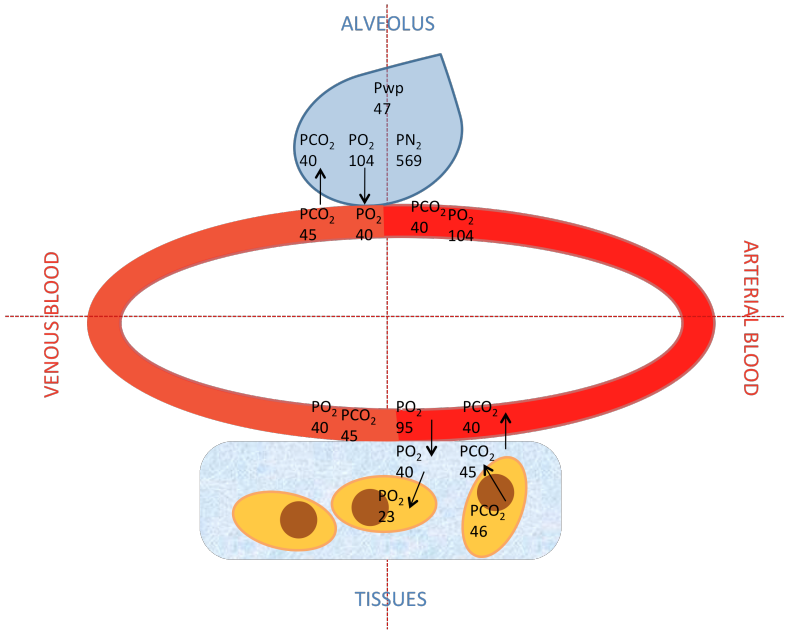

Fig 1.3: Schematic figure showing partial pressure and net diffusion of oxygen and CO_2 in the alveolus and tissues. Illustration adapted from Guyton (1981).

1.2.2.5 Physiology of Scuba diving

A scuba diver normally breathes high-pressure air. The blood becomes saturated with nitrogen to the same pressure as that within the alveolar air. Because nitrogen is an inert gas and because is about 6 times as soluble in fat as in water, it is accumulated in the tissues. Tissues can become saturated if remained at depth for several hours. When a diver comes back to the surface, alveolar PN_2 decreases and the reverse respiratory process removes the nitrogen. If pressure drops suddenly because of ascent, gases can escape from the dissolved state and form bubbles.

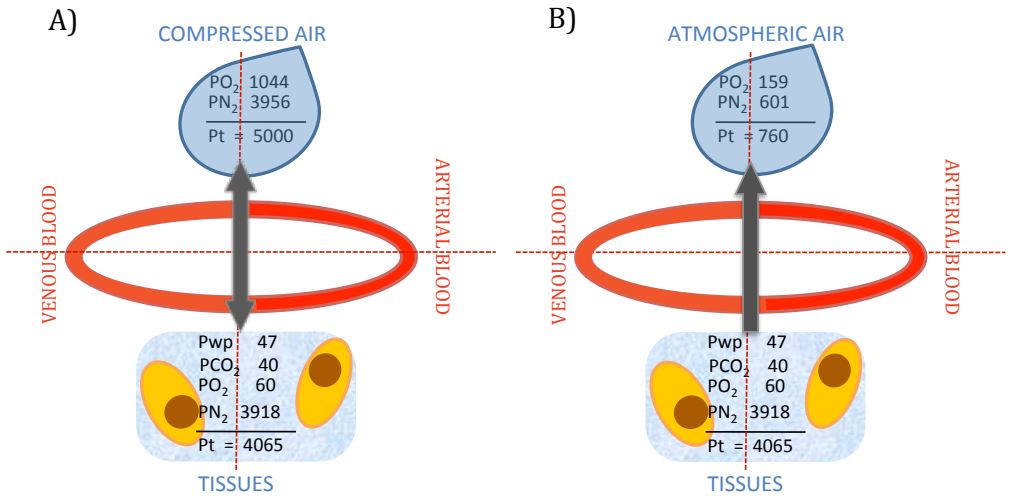

Fig 1.3: Schematic figure showing partial pressure of respiratory gases in breathing gases and tissues in two different conditions; at depth (A) and back to the surface after a long dive (B). Illustration adapted from Guyton (1981).

1.2.2.6 Physiology of breath-hold diving

Breath-hold divers do not breathe high-pressure air but PN_2 in the alveolus is increased because of depth and is taken up by the blood and tissues. During ascent, N_2 diffusion from tissues to blood and alveolus is more slowly, thus N_2 can build up in tissues (Ferrigno and Lundgren, 2003).

1.2.3 DECOMPRESSION SICKNESS

1.2.3.1 Definition

Decompression illness is a term used to describe diseases caused by intravascular or extravascular bubbles that are formed as a result of reduction in environmental pressure (decompression). The term covers both arterial gas embolism and decompression sickness (DCS) (Vann et al., 2011).

In diving, arterial gas embolism usually occurs during the ascent when expanding gas stretches and ruptures alveolar capillaries (pulmonary barotraumas) allowing alveolar gas to enter the arterial circulation (Vann et al., 2011).

We will refer to air embolism (AE) to the one caused by direct entrance in the vascular system of either alveolar gas (such as in pulmonary barotrauma) or atmospheric air as a consequence of an iatrogenic problem.

DCS alone is the disease caused by bubble formation due to gas phase separation in the body. Gas phase may arise from supersaturated gas tissues after decompression this is when the sum of the dissolved gas tensions (oxygen, carbon dioxide, nitrogen, helium) and water vapour exceeds the local absolute pressure (Hamilton and Thalmann, 2003; Vann et al., 2011).

Still, the pathophysiological mechanism of DCS is not fully understood but there are evidences that some manifestations of DCS are caused by autochtonous bubbles while others are by intravascular bubbles (Francis and Simon, 2003). Additionally, statistical relationship between the amount of vascular of gas bubbles and DCS has been reported (Sawatzky, 1991).

1.2.3.2 History

Robert Boyle was the first in describing gas bubbles formed by decompression in 1656 (Boyle, 1670), while Paul Bert did the first systematic study of gas bubbles in blood and tissues after decompression (Bert, 1878).

Bert described bubble formation and DCS three centuries later, explaining that bubble formation is due to supersaturation and that the only gas "which would threaten life on being liberated would be exclusively the one the proportion of which was considerably increased in the blood", this was nitrogen (Bert, 1878).

Following his theory, J.S. Haldane developed a physiological model of nitrogen kinetics resulting on decompression tables for avoiding DCS by controlling the depth, the duration of the dive, and the decompression time (Boycott et al., 1908). The model divided the body into 5 different compartments with different saturation rates. Each compartment represented the overall tissues with similar saturation rates in the body. The saturation rates were established by blood perfusion and nitrogen solubility, based on the results from Vernon who determined that nitrogen is approximately six times more soluble in fat than in blood (Vernon, 1907). The model is based on the tolerance to a certain degree of a superstaturation without development of bubbles. This critical value is given by the difference between nitrogen tension in tissue and the absolute pressure (Boycott et al., 1908).

Later, in 1938, Harvey suggested that gas nuclei could be present in biological systems (Harvey, 1938), and Evans and Walder showed the existence of these gas nuclei in living organisms (Evans and Walder, 1969).

In the 1950's, the ultrasound Doppler was developed for inspection of cardiac functions (Satomura, 1957). This technology was later improved and used as a non-invasive system for detection of intravascular bubbles. Thanks to this new tool, bubbles could be observed on diving schedules following Haldane's theory (Hills, 1977). This observation suggested that Haldane assumption of a degree of supersaturation without

bubble formation might not be correct. Nowadays, vascular gas bubbles are known to occur in most decompressions (Eckenhoff et al., 1990).

Later studies have shown that this assumption is not correct and that considerable bubble formation is associated with these diving profiles (Hills, 1977).

1.2.3.3 Origin and formation of bubbles

Mechanisms of bubble formation and growth are not completely understood. Bubbles are thought to grow from preexisting gas nuclei formed through heterogeneous nucleus rather than de novo formation by supersaturation since bubbles have been observed at lower saturation grade needed for this phenomenon to occur(Harvey, 1938; Tikuisis and Gerth, 2003).

Supersaturation can be defined as the excess of partial pressure compared to barometric pressure on a given fluid. If the partial pressure of a gas held in solution exceeds the barometric pressure, the gas will tend to effervesce and to form bubbles (Shaw et al., 1935). The formation of spontaneous gas bubbles from supersaturated liquid phases is called homogenous nucleation. It arises from the liquid phase without the prior presence of additional phases. It is based on the statistical fluctuations on the thermal energy of the molecules causing the failure of cohesive forces of the liquid and resulting on the formation of vaporous nuclei by cavitation (Blatteau et al., 2006). Hence, the main mechanism triggering bubble formation is the molecular interactions (Tikuisis and Gerth, 2003).

On the other hand, heterogeneous nucleation comprises different processes where solid-liquid or liquid-liquid interfaces are involved, and which require much lower saturations (Tikuisis and Gerth, 2003). Processes proposed for heterogeneous nucleation can be broadly divided in two categories:

A. Cavitation produced by thermal changes or either hydrodynamic or mechanic effects, which in turn will decrease hydrostatic pressure while

increasing supersaturation at specific locations. Thus, musculoskeletal activity has long been suggested as facilitating DCS (Whitaker et al., 1945). Some of the cavitation processes include:

a. Reynolds cavitation: when a fluid is circulating through a tube with a constriction, fluid velocity is increased at this point thus reducing hydrostatic pressure, and under certain circumstances, a cavity will be formed (Blatteau et al., 2006; Dean, 1944; Harvey, 1951)
b. Viscous adhesion or tribonucleation. If two surfaces in intimate contact but separated by a viscous liquid film are suddenly separated in an abrupt way, the viscosity will avoid sudden filling and cavities can occur (Banks and Mill, 1953; Blatteau et al., 2006; Campbell, 1968; Hayward, 1967; Ikels, 1970). This phenomenon has been proposed to happen with movements, exercise (McDonough and Hemmingsen, 1985a; McDonough and Hemmingsen, 1984a; McDonough and Hemmingsen, 1984b; McDonough and Hemmingsen, 1985b), within the joints (Fick, 1911) or in the heart valves (Hennessy, 1989).

B. Hydrophobic nuclei, which will be filled by gas according to Dalton's law (Equations 1.2 and 1.3), produced by hydrophobic crevices or by surface-active coatings such as micelles. (These processes have been also purposed for bubble stabilization).
   a. Hydrophobic crevices might be cracks on a solid surface or an acute angled cavity, like that of an inverted cone that would be wetted or not depending on the angle. Whether a certain liquid can wet a given surface depends on its cohesive and adhesive forces. Cohesive force is the attraction between molecules of the same nature, while adhesive forces is the attraction between molecules of different nature and it differs for different pair of substances. An example of this is the different attraction of water and mercury to glass. Water is more attracted to glass than mercury is, thus although the strong cohesive

force of water it forms a concave meniscus, while mercury forms a convex meniscus due to weak adhesive forces.

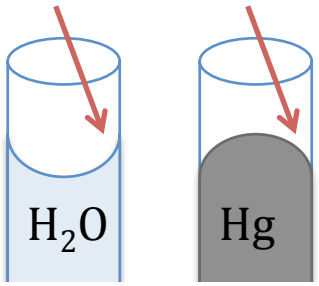

Fig 1.4: Schematic figure showing the meniscus formed by water and mercury in contact with the glass as a representation of different adhesive forces to glass.

Molecules in the bulk of a liquid are attracted to neighbors on all sides (cohesive forces). The molecules on the surface of the liquid are attracted to molecules below but not above. This results in a net force pulling the surface molecules inward. This force per unit length is called surface tension (N/m).

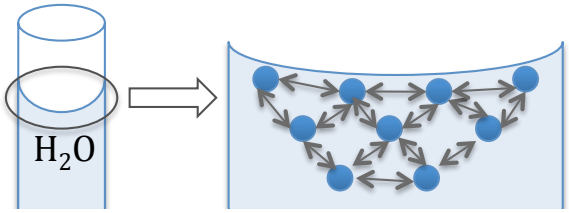

Fig 1.4: Schematic figure representing the cohesive forces.

The surface tension of a liquid increases with increasing intermolecular forces therefore is higher for polar liquids (Wallwork and Grant, 1977). Lower surface tension will wet smaller angles.

In the steady state, the **Laplace equation** describes the effect of surface tension on a bubble as:

$$P_i = P_{amb} + 2\sigma/R \qquad (1.9)$$

where P_i is the pressure in the bubble (Nm^{-2}), P_{amb} the ambient pressure (Nm^{-2}), σ the gas–liquid interface surface tension (Nm^{-1}) and R is the interface radius of curvature (m). For a bubble to be stable

under an applied pressure increase, the surface tension term needs to be negative, which can only occur if *R* is negative (Chappell and Payne, 2006). Hydrophobic crevices have negative radius of curvature (surface concave towards the liquid phase) so LaPlace surface tension acts against the liquid stabilizing the gas nuclei in undersaturated gas-liquid solutions (Tikuisis and Gerth, 2003).

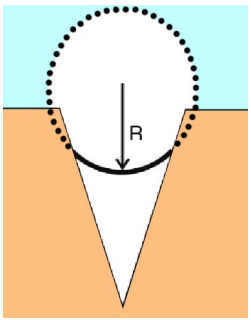

Fig 1.5: Schematic figure representing a crevice model with a negative radius curvature. Illustration adapted from Tikuisis and Gerth (2003).

b. The other way of preventing the bubble to reduce is the adsorption of surface-active materials to the gas-liquid interface, such as micelles. Micelles are aggregates of surfactants (amphilic molecules with a polar hydrophilic and a lipophilic group) with the hydrophilic "head" regions in contact with surrounding solvent, sequestering the hydrophobic single tail regions in the micelle centre. As the bubble shrinks, these molecules form a continuous surface that prevents the bubble shrinking further (Fox and Herzfeld, 1954; Vanliew and Burkard, 1995; VanLiew and Raychaudhuri, 1997; Yount, 1979).

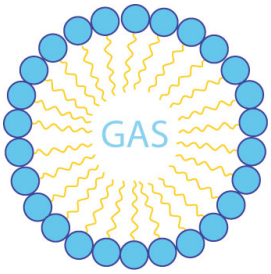

Fig 1.6: Schematic figure representing a micelle with a gas nucleus.

1.2.3.4 Bubble growth

Once the bubble has been formed it will grow or shrink according to LaPlace equation (1.9) thus, pressure difference may be regarded as the driving force for bubble growth (Blatteau et al., 2006). The pressure gradient is given by the difference between dissolved gas tension and the bubble gas pressure at the gas-liquid interface (Tikuisis and Gerth, 2003). Gas tension inside a bubble is inversely proportional to bubble size. Thus, the larger the bubble, the larger the gradient for bubble growth, and consequently the smaller the gradient for bubble decay (Mollerlokken et al., 2007). Therefore, the rate of growth of these bubbles will be influenced by their initial size.

The rate of bubble growth is largely determined by gas diffusion, which depends not only on pressure difference, but also on surface area, diffusion constants, and gas solubility (Blatteau et al., 2006). Water vapor is assumed to always be in equilibrium between bubble and tissue and metabolic gases (oxygen and CO_2) have being largely included in this equilibrium assumption (Tikuisis, 1986).

Models adopting this equilibrium assumption of metabolic gases result in single inert gas dynamics models, but multigas dynamics models have shown that although the metabolic gases may only represent a small amount of the gas in the bubble, their presence has a significant effect on the behavior of the bubble under decompression due to the high diffusivity of these gases (Chappell and Payne, 2006). For example, a highly soluble gas like CO_2, even at low tension, may play an important role in the early growth of a bubble by diffusion (Harris et al., 1945a; Harris et al., 1945b). A rapid passage of CO_2 out of bubbles as well as entrance into bubbles can be observed 38 times more rapidly than with nitrogen in the same conditions (Ishiyama, 1983).

1.2.3.5 Decompression summary

To summarize, bubble formation during decompression is not simply the consequence of inert gas supersaturation. A large body of evidence indicates that bubbles originate as persistent bodies of undissolved gas called pre-existing gas nuclei. Heterogeneous nucleation processes are involved first for generating these gas entities. Musculoskeletal activity could be the main promoter of gas nuclei from stress-assisted nucleation, such as Reynolds' cavitation and/or viscous adhesion (Blatteau et al., 2006) The formation and increase in size of extravascular and intravascular bubbles occurs when the sum of the dissolved gas tensions (oxygen, carbon dioxide, nitrogen, helium) and water vapor exceeds the local absolute pressure (Vann et al., 2011). Although nitrogen is expected to be the main responsible for bubble growth (Bert, 1878) the presence of metabolic gases might have a significant effect on the behavior of the bubble under decompression due to the high diffusivity of these gases (Chappell and Payne, 2006).

1.2.4 ADAPTATIONS OF MARINE MAMMALS TO DIVING

Marine mammals moved from land to water around 55 to 60 million years ago (Ponganis et al., 2003). Marked anatomical and physiological modifications were necessary to meet the physical demands of living in water instead of air (Williams and Worthy, 2002). These required variations include adaptations for breath-hold diving, temperature regulation in cold water, water and salt balance, underwater navigation, and high pressure at great depth (Elsner, 1999). We will review those adaptations more directly related to deep-diving capabilities.

Marine mammals are the champions at breath-holding in the mammalian world (Elsner, 1999). Some marine dolphins can dive to depths in the 300-500 meters of sea water (msw) while others such as and pilot whales (*Globicephala*) are capable of dives to 600 msw or more (Ponganis et al., 2003). Maximum depth and maximum duration for BWs and sperm whales (SWs) is of 1888 msw, 2035 msw and 85min, 73 min respectively. They are deep and long duration divers (Kooyman, 2009).

The study of these adaptations and capabilities started long time ago with the great physiologist Paul Bert (1870). He found out that when ducks were experimentally submerged they experience a dramatic slowing of the heart rate. He also suggested that the highest resistance to diving asphyxia in ducks compare to chickens was because of their larger blood volume and related oxygen storage.

An increased total body oxygen store is considered essential for the breath-hold capacity of diving mammals. The oxygen is stored in three compartments: the respiratory system, the blood, and the body musculature (Kooyman, 2009). When comparing blood and lung oxygen stores of the major groups of diving mammals, some interesting differences become evident (Fig. 3). The most prolonged diver, the Weddell seal, has the largest blood oxygen and the smallest lung oxygen storage capacity. Seals dive on only about 20-60% of total lung capacity. The sea otter, which is a short

duration diver, has potentially the largest oxygen store of all, and it is attributable to the lung volume (Kooyman, 1973).

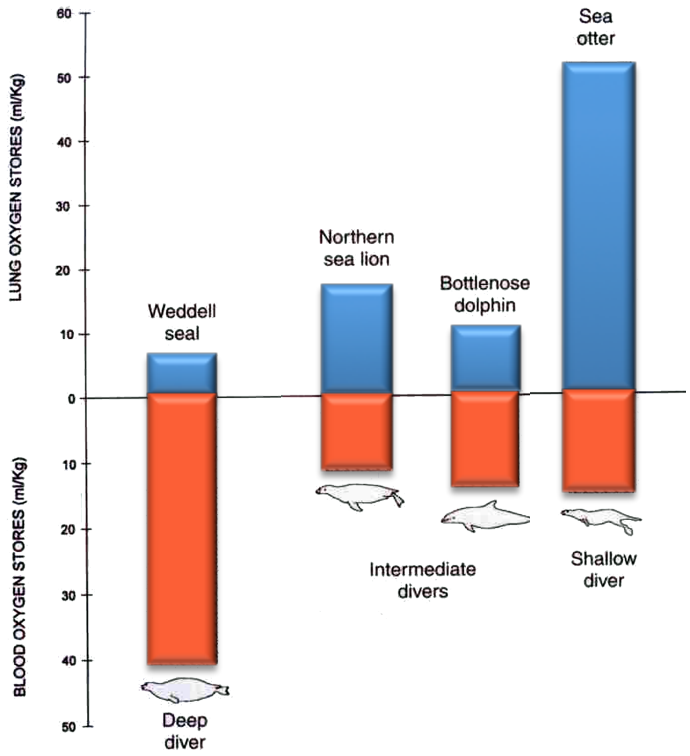

Fig 1.7: oxygen stores in lung versus blood in shallow and deep diving mammals. Illustration adapted from Pabst (1999).

Adaptations and degree of the development of these adaptations varies among species. We would go through general adaptations, which might be absent or present and more or less developed in some species than others.

1.2.4.1 Morphological adaptations

1.2.4.1.1 Respiratory system

The respiratory oxygen store is dependant on lung volume and the concentration of oxygen in the lung at the start of a breath hold (Kooyman, 2009). The only way the oxygen store of the lung can be increased is by increasing the lung volume during the dive (Kooyman, 1973). Lungs are a liability for deep divers in contrast to the muscle and blood, because they are a better nitrogen store than oxygen store (Kooyman and Ponganis, 1998). Perhaps this is why the lungs of marine mammals are the most structurally modified of any mammalian group (Belanger, 1940; Denison and Kooyman, 1973). The most notable examples are the reinforcement of peripheral airways, the loss of respiratory bronchioles, and the presence of a series of bronchial sphincters (Belanger, 1940; Kooyman et al., 1973).

The lung volume is smaller in the prolonged divers compare to short duration divers. Actually behavioral observations indicate that sea lions and porpoises (short duration divers) dive on inspiration in which case they may be taking full advantage of their lung store. But in general terms, lung oxygen stores represent a small proportion of the total body oxygen stores of long-term divers (Kooyman, 1973).

In addition to the reduction of lung volume, the terminal airways leading to the alveoli are reinforced with cartilage or thickened muscle (Belanger, 1940; Denison and Kooyman, 1973) to avoid this structures to collapse before the alveoli is emptied, trapping air in the alveolus where gas exchange would occur (Denison et al., 1971). Instead, the alveoli will collapse first under compression, forcing the air into the reinforced upper airways. There are radiographic evidences in Weddel seals that these adaptations allow graded lung collapse, forcing the air into the upper airways (Kooyman et al., 1970). A gradation in the architecture of small and large airways occurs in parallel with the degree of aquatic specialization in mammals (Williams and Worthy, 2002).

On the other hand the function of the circular muscular and elastic sphincters at the entrance of the alveoli, unique to cetaceans, is not well understood (Drabek and Kooyman, 1983; Kooyman, 1973; Scholander, 1940). It has been hypothesized that they trap air in the alveoli and they regulate air flow from the alveoli during the dive (Drabek and Kooyman, 1983).

Efficient gas exchange in these animals is achieved with large tidal volumes, which are (80-90%) of lung capacity. Since tidal volumes are so large, it is important to know if they dive on inspiration or expiration. There is still a debate, but most cetologists consider whales and dolphins to dive on inspiration (Ridgway, 1986)

In summary, lung oxygen stores represent a small proportion in long-term divers. Instead, major modifications have occurred in the blood-vascular system which has resulted in a considerable increase in oxygen storage capacity (Kooyman et al., 1973) (See figure 1.7).

1.2.4.1.2 Cardiovascular system

The main oxygen stores (80-90%) in deep divers are blood and muscle (Kooyman and Ponganis, 1998).

Oxygen storage capacity in the blood is enhanced by increase in blood volume, the number of RBCs and hemoglobin concentration (Williams and Worthy, 2002). Blood volumes can be three times human values and hemoglobin concentrations can reach twice human values (Ponganis et al., 2003). There is a positive relationship between blood volume and maximum dive duration in mammals (Ridgway and Johnston, 1966).

Some of the anatomic adaptations might include (depending the specie) large capacitance structures (spleens and venous sinuses), venous sphincters muscles, aortic windkessels, and vascular retia (Ponganis et al., 2003).

It has been suggested that the spleen could act as a reservoir of RBC in some species such as phocid seals. During the dive the spleen would contract and expel RBC into circulation elevating the hematocrit as high as 60% during the first 10 minutes of the dive. This is commonly known as splenic contractions (Williams and Worthy, 2002). However, our observational experience in cetaceans indicates that spleen volume is smaller in deep divers compare to shallow divers.

The inferior vena cava of most pinnipeds (and of some whales) had a striated muscle sphincter located cranial to the large hepatic sinus. Its contraction and relaxation is postulated to regulate venous return to the heart (Ponganis et al., 2003).

The aortic windkessels are dilations of the aorta (aortic bulb) and aortic arch that thanks to their elastic properties, have a gradual contraction that might help to maintain blood flow during diastole (Ponganis et al., 2003).

An other interesting morphological adaptation of the cardiovascular system is the *retia mirabilia* which is a plexus of anastomosing arteries and veins. Vessels from the aorta supply the thoracic rete that lies between ribs in the dorsal thoracic cavity. The vascular tissue form the thoracic rete extends around the vertebrae and enters into the neural canal where it forms the primary arterial supply to the brain (Pabst et al., 1999). These structures have been proposed to act as windkless just like the aortic bulb does. In this case they will assure the maintenance of blood flow supply to the brain. Other interesting hypothesis about their function include the prevention of the bends by entrapping bubbles acting like a filter, intrathoracic vascular engorgement to prevent lung squeeze, and modifications of blood composition (Ponganis et al., 2003).

1.2.4.1.3 Musculoskeletal system

The importance of myoglobin concentration for oxygen storage capacity was demonstrated first by Scholander et al. (1942) in seals. From the measurements of myoglobin concentration in the muscles of many species of divers it is clear that the most consistent compartment for oxygen storage in all birds and mammals that dive to depth is an elevated myoglobin concentration (Butler and Jones, 1997). This is more characteristic than any changes in respiratory or blood volume and hemoglobin concentration (Kooyman and Ponganis, 1998). Marine mammals present myoglobin contents approximately 10 to 15 times that in human muscle (Ponganis et al., 2003). Muscle myoglobin concentrations increase proportionately with diving capacities and are highest in penguins, pinnipeds, and cetaceans (Kooyman and Ponganis, 1998).

1.2.4.2 Physiological adaptations: the dive response

Reviewing adaptations to hypoxia is important to consider the role of body mass, relative metabolic rate, oxygen stores and the rate of depletion of those oxygen stores (Butler and Jones, 1997; Kooyman and Ponganis, 1998). Although the oxygen stores in the body is greater in diving than in non-diving species, it is insufficient to enable aerobic metabolism during a prolonged dive (Butler and Jones, 1997).

Table 1.2: Species, body mass, distribution and quantity of oxygen stores, maximum and routine dives depth and duration. Data obtained from (Kooyman, 2009)

Specie	Body mass (Kg)	Total store (mL/Kg)	Lung	Blood (%)	Muscle	Routine depth (m)	Maximum depth (m)	Routine duration (min)	Maximum duration (min)
Human	70	20	24	57	15	5	214	0.25	6
Weddell seal	400	87	5	66	29	200	741	15	93
Elephant seal	400	97	4	71	25	500	1653	25	120
California sea lion	100	40	21	45	34	40	275	2.5	10
Bottlenose dolphin	200	36	34	27	39		535		
Cuvier's BW	3000					1070	1888	58	85
Sperm whale	10000	77	10	58	34	500	2035	40	73

This is achieved by a suite of physiological changes known as the dive response. These response was first described in restrained animals forced to dive(Scholander, 1940). The dive response consists on an overall reduction in the level of anaerobic metabolism achieved by selective peripheral vasoconstriction except for those tissues more sensitive to hypoxia together with a decrease in heart rate (bradycardia) (Butler and Jones, 1997). Studies on freely birds and mammals, suggest that most, if not all, dives performed naturally are aerobic in nature and that peripheral vasoconstriction during diving should not take place in the locomotor muscles, which are working organs, but in the viscera alone (Butler and Jones, 1997). Still, a reduction in the level of metabolism of splanchnic organs will reduce significantly total metabolic rate since these organs account for nearly 50% of the total resting metabolism.

The level of response is variable and depends on such factors as the degree of aquatic specialization, species, dive duration, behavior and type of dive (Williams and Worthy, 2002).

1.2.5 EVIDENCES OF DECOMPRESSION IN MARINE MAMMALS

Marine mammals were not considered to suffer from decompression sickness since gas supersaturation was not expected to occur because the gas available for supersaturation is limited to that of the lungs, which are compressed during the dive forcing the residual air to the upper airways where non-gas exchange should take place. In addition, partial pressure of nitrogen in the blood would decrease as nitrogen is distributed among tissues (Piantadosi and Thalmann, 2004).

However there is an increasing body of evidences suggesting that this might not be completely right. Depth for alveolar collapse is not expected to be the same for all the species due to anatomical differences of the thorax and even of the lung airways. Alveolar collapse has been measured for to take place at depth of 30 msw (Falke et al., 1985) in the Weddell seals and 70 msw in the bottlenose dolphins (Ridgway and Howard, 1979). Gas exchange should occur up to this depth.

In human breath-hold divers nitrogen is hypothesized to accumulate in tissues because PN_2 increases at depth in the alveoli and nitrogen is taken up by the blood and tissues. During ascent, nitrogen diffusion from tissues to blood and alveolus is more slowly, thus nitrogen can build up in tissues (Ferrigno and Lundgren, 2003). The Decompression sickness described in Ama divers (women that do repetitive, shallow breath-hold dives for fishing pearls) has been attributed to a progressive nitrogen accumulation in tissues (Cross, 1965). There is a growing number of cases reported with symptoms of decompression sickness in breath hold diving (Schipke et al., 2006). Decompression sickness has also been reported (although unusual) in 2 cases of 192 deep single breath-hold dives, since they both required hyperbaric treatment to recover (Fitz-Clarke, 2009).

There are evidences of intramuscular nitrogen accumulation of two to three times the normal surface levels in bottlenose dolphin after repetitive short duration dives to

100 m depth (Ridgway and Howard, 1979), and several models have predicted a potential accumulation of nitrogen (even greater than 300%) in marine mammals under certain circumstances, thus DCS risk (Hooker et al., 2009; Houser et al., 2001; Zimmer and Tyack, 2007).

In the last 8 years, bubbles and lesions related to *in vivo* bubbles have increasingly been reported. Systemic venous gas embolism was first described in an atypical beaked whale mass stranding related to military maneuvers that occurred in the Canary Islands in 2002. Beaked whales (8 out of 8) presented acute lesions consistent with acute trauma due to *in vivo* bubble formation (Fernandez et al., 2005; Jepson et al., 2003). In addition chronic gas-bubble lesions were also reported in single strandings of Risso's dolphin (3 out of 24), common dolphins (3 out of 342), harbour porpoises (1 out of 1035) and in Blainville's beaked whale (1 out of 1) stranded in the United Kingdom (Jepson et al., 2003; Jepson et al., 2005) and dysbaric osteonecrosis (a chronic pathology of deep diving recognized in humans) has been described to occur in sperm whales (Moore and Early, 2004). Finally, Moore et al. (2009) described a high incidence of bubble lesions in bycaught seals and dolphins trapped at depth (15 out of 23) compared to stranded marine mammals (1 out of 41).

1.3 REFERENCES

2004. Policy on sound and marine mammals. In: Commission TMM, editor. Beaked whale technical workshop. Baltimore, Maryland.

Banks WH, Mill CC. 1953. TACKY ADHESION - A PRELIMINARY STUDY. Journal of Colloid Science 8(1):137-147.

Belanger LF. 1940. A study of the histological structure of the respiratory portion of the lungs of aquatic mammals. American Journal of Anatomy 67(3):437-469.

Bert P. 1870. Leçons sur la physiologie comparée de la respiration. Paris: J.B. Baillière.

Bert P. 1878. La Pression Barometrique: Recherches de Physiologie Expérimentale. Hitchcock MA, Hitchcock FA, translator. Paris: Masson.

Blatteau JE, Souraud JB, Gempp E, Boussuges A. 2006. Gas nuclei, their origin, and their role in bubble formation. Aviation Space and Environmental Medicine 77(10):1068-1076.

Boycott AE, Damant GCC, Haldane JS. 1908. The prevention of compressed air illness. Journal of Hygiene 8(3):342-443.

Boyle R. 1670. New pneumatical experiments about respiration. Philosophical transactions 5:2011-2058.

Butler PJ, Jones DR. 1997. Physiology of diving of birds and mammals. Physiological Reviews 77(3):837-899.

Campbell J. 1968. TRIBONUCLEATION OF BUBBLES. Journal of Physics D-Applied Physics 1(8):1085-&.

Cox TM, Ragen TJ, Read AJ, Vos E, Baird RW, Balcomb K, Barlow J, Caldwell JM, Cranford T, Crum LA, D'Amico A, D'Spain G, Fernandez A, Finneran JJ, Gentry R, Gerth WA, Gulland FMD, Hildebrand J, Houser D, Hullar T, Jepson PD, Ketten D, MacLeod CD, Miller P, Moore S, Mountain DC, Palka D, Ponganis PJ, Rommel S, Rowles T, Tyack PL, Wartzok D, Gisiner R, Mead J, Benner L. 2006. Understanding the impacts of anthropogenic sound on beaked whales. Journal of Cetacean Research and Management 7(3):117-187.

Cross ER. 1965. Taravana. Diving syndrome in the Tuamotu diver. In: Rahn H, Yokoyama T, editors. Physiology of breath-hold diving and the ama of Japan. Washington, DC.: National Academy of Science, National Research Council Publication. p 207-219.

Chappell MA, Payne SJ. 2006. A physiological model of gas pockets in crevices and their behavior under compression. Respiratory Physiology & Neurobiology 152(1):100-114.

Dean RB. 1944. The formation of bubbles. Journal of Applied Physics 15(5):446-451.

Denison DM, Kooyman GL. 1973. STRUCTURE AND FUNCTION OF SMALL AIRWAYS IN PINNIPED AND SEA OTTER LUNGS. Respiration Physiology 17(1):1-10.

Denison DM, Warrell DA, West JB. 1971. AIRWAY STRUCTURE AND ALVEOLAR EMPTYING IN LUNGS OF SEA LIONS AND DOGS. Respiration Physiology 13(3):253-&.

Drabek CM, Kooyman GL. 1983. TERMINAL AIRWAY EMBRYOLOGY OF THE DELPHINID PORPOISES, STENELLA-ATTENUATA AND STENELLA-LONGIROSTRIS. Journal of Morphology 175(1):65-72.

Eckenhoff RG, Olstad CS, Carrod G. 1990. HUMAN DOSE-RESPONSE RELATIONSHIP FOR DECOMPRESSION AND ENDOGENOUS BUBBLE FORMATION. Journal of Applied Physiology 69(3):914-918.

Elsner R. 1999. Living in water: solutions to physiological problems. In: Reynolds JE, III, Rommel S, editors. Biology of Marine Mammals. Washington, DC.: Smithsonian Institution Press. p 73-116.

European-Parliament. 2004. European Parliament resolution on the environment effects of high-intensity naval sonars.

Evans A, Walder DN. 1969. SIGNIFICANCE OF GAS MICRONUCLEI IN AETIOLOGY OF DECOMPRESSION SICKNESS. Nature 222(5190):251-&.

Falke KJ, Hill RD, Qvist J, Schneider RC, Guppy M, Liggins GC, Hochachka PW, Elliott RE, Zapol WM. 1985. SEAL LUNGS COLLAPSE DURING FREE DIVING - EVIDENCE FROM ARTERIAL NITROGEN TENSIONS. Science 229(4713):556-558.

Fernandez A, Edwards JF, Rodriguez F, de los Monteros AE, Herraez P, Castro P, Jaber JR, Martin V, Arbelo M. 2005. "Gas and fat embolic syndrome" involving a mass stranding of beaked whales (Family Ziphiidae) exposed to anthropogenic sonar signals. Veterinary Pathology 42(4):446-457.

Ferrigno M, Lundgren CEG. 2003. Breath-Hold Diving. In: Brubakk AO, Neuman TS, editors. Physiology and Medicine of Diving: Saunders. p 153-180.

Fick R. 1911. Zum Streit um dem Gelenkdruck. Anat Hefte 43(1).

Fitz-Clarke JR. 2009. Risk of decompression sickness in extreme human breath-hold diving. Undersea & Hyperbaric Medicine 36(2):83-91.

Fox FE, Herzfeld KF. 1954. GAS BUBBLES WITH ORGANIC SKIN AS CAVITATION NUCLEI. Journal of the Acoustical Society of America 26(6):984-989.

Francis TJR, Simon JM. 2003. Pathology of Decompression Sickness. In: Brubakk AO, Neuman TS, editors. Bennett and Elliott's Physiology and Medicing of Diving: Saunders. p 530-556.

Guyton AC. 1981. Physical principles of gaseous exchange; diffusion of oxygen and carbon dioxide through the respiratory membrane. Textbook of medical physiology. 6th Edition ed. Philadelphia: W.B. Saunders. p 491-503.

Hamilton RW, Thalmann ED. 2003. Decompression practice. In: Brubakk AO, Neuman TS, editors. Bennett and Elliott's Physiology and Medicing of Diving: Saunders. p 455-500.

Harris M, Berg WE, Whitaker DM, Twitty VC. 1945a. THE RELATION OF EXERCISE TO BUBBLE FORMATION IN ANIMALS DECOMPRESSED TO SEA LEVEL FROM HIGH BAROMETRIC PRESSURES. Journal of General Physiology 28(3):241-251.

Harris M, Berg WE, Whitaker DM, Twitty VC, Blinks LR. 1945b. Carbon dioxide as a facilitating agent in the initiation and growth of bubbles in animals decompressed to simulated altitudes. Journal of General Physiology 28(3):225-240.

Harvey EN. 1938. Some physical properties of protoplasm. Journal of Applied Physics 9(2):68-80.

Harvey EN. 1951. Physical factors in bubble formation. In: Fulton JF, editor. Decompression sickness. Philadelphia: Saunders. p 90-114.

Hayward ATJ. 1967. TRIBONUCLEATION OF BUBBLES. British Journal of Applied Physics 18(5):641-&.

Hennessy TR. On the site, origin, evolution and effects of decompression. In: Brubakk AO, Hemmingsen BB, Sundnes G, editors; 1989; Trondheim, Norway. Tapir.

Hills BA. 1977. Decompression sickness: The biophysical basis of prevention and treatment. Cichester, UK: Jhon Wiley.

Hooker SK, Baird RW, Fahlman A. 2009. Could beaked whales get the bends? Effect of diving behaviour and physiology on modelled gas exchange for three species: Ziphius cavirostris, Mesoplodon densirostris and Hyperoodon ampullatus. Respiratory Physiology & Neurobiology 167(3):235-246.

Houser DS, Howard R, Ridgway S. 2001. Can diving-induced tissue nitrogen supersaturation increase the chance of acoustically driven bubble growth in marine mammals? Journal of Theoretical Biology 213(2):183-195.

Ikels KG. 1970. PRODUCTION OF GAS BUBBLES IN FLUIDS BY TRIBONUCLEATION. Journal of Applied Physiology 28(4):524-&.

Ishiyama A. 1983. Analysis of gas composition of intra vascular bubbles produced by decompression. Bulletin of Tokyo Medical and Dental University 30(2):25-36.

Jepson PD, Arbelo M, Deaville R, Patterson IAP, Castro P, Baker JR, Degollada E, Ross HM, Herraez P, Pocknell AM, Rodriguez F, Howie FE, Espinosa A, Reid RJ, Jaber JR, Martin V, Cunningham AA, Fernandez A. 2003. Gas-bubble lesions in stranded cetaceans - Was sonar responsible for a spate of whale deaths after an Atlantic military exercise? Nature 425(6958):575-576.

Jepson PD, Deaville R, Patterson IAP, Pocknell AM, Ross HM, Baker JR, Howie FE, Reid RJ, Colloff A, Cunningham AA. 2005. Acute and chronic gas bubble lesions in cetaceans stranded in the United Kingdom. Veterinary Pathology 42(3):291-305.

Kooyman GL. 1973. RESPIRATORY ADAPTATIONS IN MARINE MAMMALS. American Zoologist 13(2):457-468.

Kooyman GL. 2009. Diving Physiology. In: Perrin WF, Würsig B, Thewissen JGM, editors. Encyclopedia of Marine Mammals. 2nd edition ed. San Diego, CA: Academic Press. p 327-332.

Kooyman GL, Hammond DD, Schroede.Jp. 1970. BRONCHOGRAMS AND TRACHEOGRAMS OF SEALS UNDER PRESSURE. Science 169(3940):82-&.

Kooyman GL, Kerem DH, Campbell WB, Wright JJ. 1973. PULMONARY GAS-EXCHANGE IN FREELY DIVING WEDDELL SEALS, LEPTONYCHOTES-WEDDELLI. Respiration Physiology 17(3):283-290.

Kooyman GL, Ponganis PJ. 1998. The physiological basis of diving to depth: Birds and mammals. Annual Review of Physiology 60:19-32.

McDonough PM, Hemmingsen BB. 1985a. A direct test for the survival of gaseous nuclei in vivo. Aviation Space and Environmental Medicine 56:54-56.

McDonough PM, Hemmingsen EA. 1984a. BUBBLE FORMATION IN CRABS INDUCED BY LIMB MOTIONS AFTER DECOMPRESSION. Journal of Applied Physiology 57(1):117-122.

McDonough PM, Hemmingsen EA. 1984b. BUBBLE FORMATION IN CRUSTACEANS FOLLOWING DECOMPRESSION FROM HYPERBARIC GAS EXPOSURES. Journal of Applied Physiology 56(2):513-519.

McDonough PM, Hemmingsen EA. 1985b. SWIMMING MOVEMENTS INITIATE BUBBLE FORMATION IN FISH DECOMPRESSED FROM ELEVATED GAS-PRESSURES. Comparative Biochemistry and Physiology a-Physiology 81(1):209-212.

Mollerlokken A, Gutvik C, Berge VJ, Jorgensen A, Loset A, Brubakk AO. 2007. Recompression during decompression and effects on bubble formation in the pig. Aviation Space and Environmental Medicine 78(6):557-560.

Moore MJ, Bogomolni AL, Dennison SE, Early G, Garner MM, Hayward BA, Lentell BJ, Rotstein DS. 2009. Gas Bubbles in Seals, Dolphins, and Porpoises Entangled and Drowned at Depth in Gillnets. Veterinary Pathology 46(3):536-547.

Moore MJ, Early GA. 2004. Cumulative sperm whale bone damage and the bends. Science 306(5705):2215-2215.

Pabst DA, Rommel S, McLellan WA. 1999. The functional morphology of marine mammals. In: Reynolds JE, III, Rommel S, editors. Biology of Marine Mammals. Washington, DC.: Smithsonian Institution Press. p 15-72.

Piantadosi CA, Thalmann ED. 2004. Pathology: whales, sonar and decompression sickness. Nature 428(6984):1 p following 716; discussion 712 p following 716.

Ponganis PJ, Kooyman GL, Ridgway S. 2003. Comparative diving physiology. In: Brubakk AO, Neuman TS, editors. Physiology and Medicine of Diving: Saunders. p 211-226.

Ridgway S. 1986. Diving by cetaceans. In: Brubakk AO, Kanwishe.J, Sundnes G, editors. Diving in animals and man. Trondheim: Royal Norwegian Society of Science and Letters. p 33-62.

Ridgway S, Johnston DG. 1966. Blood oxygen and ecology of porpoises of three genera. Science 151:1651-1654.

Ridgway SH, Howard R. 1979. DOLPHIN LUNG COLLAPSE AND INTRAMUSCULAR CIRCULATION DURING FREE DIVING - EVIDENCE FROM NITROGEN WASHOUT. Science 206(4423):1182-1183.

Satomura S. 1957. ULTRASONIC DOPPLER METHOD FOR THE INSPECTION OF CARDIAC FUNCTIONS. Journal of the Acoustical Society of America 29(11):1181-1185.

Sawatzky KD. 1991. The relationship between intravascular Doopler-detected gas bubbles and decompression sickness after bounce diving in humans [MSc thesis]. Toronto, Canada: York University.

Schipke JD, Gams E, Kallweit O. 2006. Decompression sickness following breath-hold diving. Research in sports medicine 14:163-178.

Scholander PF. 1940. Experimental investigations on the respiratory function in diving mammals and birds. Hvalradets Skrifter 22:1-131.

Scholander PF, Irving L, Grinnell SW. 1942. Aerobic and anaerobic changes in seal muscle during diving. Journal of Biological Chemistry 142:431-440.

Shaw LA, Behnke AR, Messer AC, Thomson RM, Motley EP. 1935. The equilibrium time of the gaseous nitrogen in the dog's body following changes of nitrogen tension in the lungs. American Journal of Physiology 112(3):545-553.

Tikuisis P. 1986. MODELING THE OBSERVATIONS OF INVIVO BUBBLE FORMATION WITH HYDROPHOBIC CREVICES. Undersea Biomedical Research 13(2):165-180.

Tikuisis P, Gerth WA. 2003. Decompression theory. In: Brubakk AO, Neuman TS, editors. Physiology and Medicine of Diving. Saunders ed: Saunders. p 419-454.

Vanliew HD, Burkard ME. 1995. BUBBLES IN CIRCULATING BLOOD - STABILIZATION AND SIMULATIONS OF CYCLIC CHANGES OF SIZE AND CONTENT. Journal of Applied Physiology 79(4):1379-1385.

VanLiew HD, Raychaudhuri S. 1997. Stabilized bubbles in the body: Pressure-radius relationships and the limits to stabilization. Journal of Applied Physiology 82(6):2045-2053.

Vann RD, Butler FK, Mitchell SJ, Moon RE. 2011. Decompression illness. The Lancet 377(9760):153-164.

Vernon HM. 1907. The solubility of air in fats, and its relation to caisson disease. Proceedings of the Royal Society of London Series B-Containing Papers of a Biological Character 79(533):366-371.

Wallwork SC, Grant DJ. 1977. Physical chemistry for students of pharmacy and biology. 3rd edition ed. London: Longman.

Whitaker DM, Blinks LR, Berg WE, Twitty VC, Harris M. 1945. MUSCULAR ACTIVITY AND BUBBLE FORMATION IN ANIMALS DECOMPRESSED TO SIMULATED ALTITUDES. Journal of General Physiology 28(3):213-223.

Wikipedia tfe. 2011. Henry's law.

Williams TM, Worthy GAJ. 2002. Anatomy and physiology: the challenge of aquatic living. In: Hoelzel AR, editor. Marine Mammal Biology. Oxford: Blackwell Science.

Yount DE. 1979. SKINS OF VARYING PERMEABILITY - STABILIZATION MECHANISM FOR GAS CAVITATION NUCLEI. Journal of the Acoustical Society of America 65(6):1429-1439.

Zimmer WMX, Tyack PL. 2007. Repetitive shallow dives pose decompression risk in deep-diving beaked whales. Marine Mammal Science 23:888-925.

TABLA DE CONTENIDO

2 CHAPTER II: DEVELOPMENT OF A METHODOLOGY FOR GAS EMBOLISM STUDIES

2.1 INTRODUCTION

Gas-bubble lesions have been described in cetaceans stranded in spatio-temporal concordance with military maneuvers (Fernandez et al., 2005; Jepson et al., 2003). Authors have suggested a decompression-like disease as a plausible mechanism to explain the observed lesions. These findings have been widely discussed since then and have become scientifically controversial. Further investigations, including gas analysis of bubbles have been claimed (Piantadosi and Thalmann, 2004).

Gas chromatography has been demonstrated as a valid method to distinguish between putrefaction gases and air embolism(Pierucci and Gherson, 1968; Pierucci and Gherson, 1969) and has been used as a forensic tool in humans for this purpose (Bajanowski et al., 1998). Attempts have been made to analyze the gas produced during decompression using a wide variety of methods (Armstrong, 1939; Bert, 1878; Harris et al., 1945; Ishiyama, 1983; Lillo et al., 1992; Smith-Sivertsen, 1976). However, appropriate and accurate measurements of respiratory gases while avoiding atmospheric air is difficult; with the development and sophistication of new Doppler and imaging techniques in the 1970s and 1980s, less attention was paid to gas composition.

Gas chromatography technology allows us to analyze permanent gases at the same time as hydrocarbons in a single injection; however, avoidance of atmospheric air is still a problem. Additionally, cetaceans might strand on beaches that are not easily accessible and might require execution of the necropsy *in situ.* To our knowledge it does not exist today a transportable apparatus that can measure respiratory gases as well as hydrocarbons produced by microorganism's metabolism simultaneously. For instance, analysis of hydrocarbons requires hydrogen, which is not allowed to be transport without special security measures. Although, gas extraction may occasionally

be performed at the stranding site, gas analysis must take place in a laboratory. Therefore, storage and transportation of gas samples are needed.

Fig. 2.1: Pictures showing a typical non-easy accessible stranding localization. Looking for a stranded cetacean on a beach down a cliff (A). Transporting the necropsy material through the same beach until the stranding site for in situ necropsy performance (B).

The main objective of this thesis is therefore to develop a methodology that enables *in situ* gas sampling from stranded cetaceans and the corresponding transport to the laboratory. Thus, methodology should remain as simple as possible to be included in the stranded cetaceans necropsy protocol and with non-breakable materials whenever possible.

2.2 MATERIAL AND METHODS

2.2.1 MATERIAL

Material used were cetaceans stranded in the Canary Islands coast between 2006-2009 with different decomposition status. Sampling of gas from different organs requires the use of different techniques. Therefore, different tools were tested for sample collection and storage. The gases likely to be of scientific interest are found in organ cavities (such as intestine or air sinuses), inside vessels (emboli), or mixed with blood in the heart. The tools that we have tested are vacutainers, insulin syringes and an aspirometer.

2.2.1.1 Vacuum tubes

The most delicate part of gas study is the storage. Vacutainers are glass tubes (not easily breakable) sealed with a partial vacuum inside using rubber stoppers (Fig. 2.2). They are normally used for blood extraction. Suction of blood is produced by the pressure difference between the inside of the tube and the environment. If this system is applied to gas-filled cavities rather than blood-filled vessels, gas will be suctioned. Vacutainers were studied for their suitability for the conservation of gas samples due to their industrial vacuum and special sealed.

Fig. 2.2: Vacuum tubes.

Air (1mL) was injected into twenty 3.5mL with additive vacutainers, and into twenty 5mL additive-free vacutainers. Vacutainers were kept upside-down at room temperature for 21 days, and the evolution of air content was analyzed on storage days 1, 7, 14 and 21 (Fig. 2.7).

In addition, the background of the 5 mL additive-free vacutainer was compared to that of manually helium purged 2 mL container and the glass block-pressure syringe used for manual injection into the gas chromatograph for observational studies (Fig. 2.8).

The best storage temperature was determined by the injection of a fixed amount of air (vacutainers were allowed to equilibrate with atmospheric air using an open needle) into 60 vacutainers, which were stored at different temperatures: room temperature (20-24˚C), refrigerator (4˚C) and freezer (-80˚C). Air content was analyzed at days 1, 7, 14, and 21 after injection, with five replicates for each time and treatment (Fig. 2.9). Values of area for air content (oxygen and nitrogen) of vacutainers stored at different temperatures and observed on a specific date were analyzed using a model of analysis of variance with two factors of variation (temperature and day) and interactions between both factors. Multiple comparisons were carried out by means of the corresponding linear test.

Additionally, some vacutainers were sampled at two different times to observe whether puncturing through the rubber affects later gas conservation inside the vacutainer. This content was compared with vacutainers content exposed to the same temperature and the same time but without previous puncturing (Fig. 2.10).

Diffusion of the different gases through the 5 mL additive-free vacutainer at room temperature (21˚C) was studied. Thirty vacutainers were completely filled with atmospheric air, and five replicates were analyzed each day from the same day of injection until the 5^{th} day (Fig. 2.11). This procedure was repeated with pure hydrogen (Fig. 2.12) and pure CO_2 (Fig. 2.13). Since oxygen and nitrogen were measured from the

same tubes previously filled with atmospheric air, their ratio was treated in the same manner as each gas alone (Fig. 2.14). Average gas values for each day were also used to simulate a mixture of these gases (Fig. 2.15).

Finally, to test whether vacutainers were resistant to pressure changes and therefore suitable for transportation by airplane, 30 vacutainers were completely filled with atmospheric air and 15 were transported (round trip) in the passenger cabin of an airplane. Previous experiences led us to the observation that the vacutainers were squeezed if they were transported within an airplane's cargo hold.

2.2.1.2 Insulin syringe

To sample bubbles, disposable insulin syringes (BD Plastipak U-100 insulin) were tested (Fig. 2.3). Because insulin syringes are designed for liquid volume measurements, their accuracy for gas volume measurements was studied by injecting different atmospheric air volumes promptly into vacutainers. The air content injected from the insulin syringe into the vacutainer was later analyzed by gas chromatography and statistical regression studies were performed (Fig. 2.16).

Fig. 2.3: Insulin syringe.

The atmospheric air background of the syringe was also analyzed. Syringes were used for the extraction of pure helium, which was then injected into the vacutainers. Air content was analyzed and compared to that of intact vacutainers. The levels of oxygen and nitrogen in two experimental conditions were compared using the Wilcoxon test for independent samples.

2.2.1.3 Aspirometer

If the carcass is fresh or very fresh (decomposition code 2 or 1 respectively, see grading systems used, chapter 9.2.1) (Kuiken and García-Hartmann, 1991), then an aspirometer will be necessary to separate the gas from the blood found in the heart.

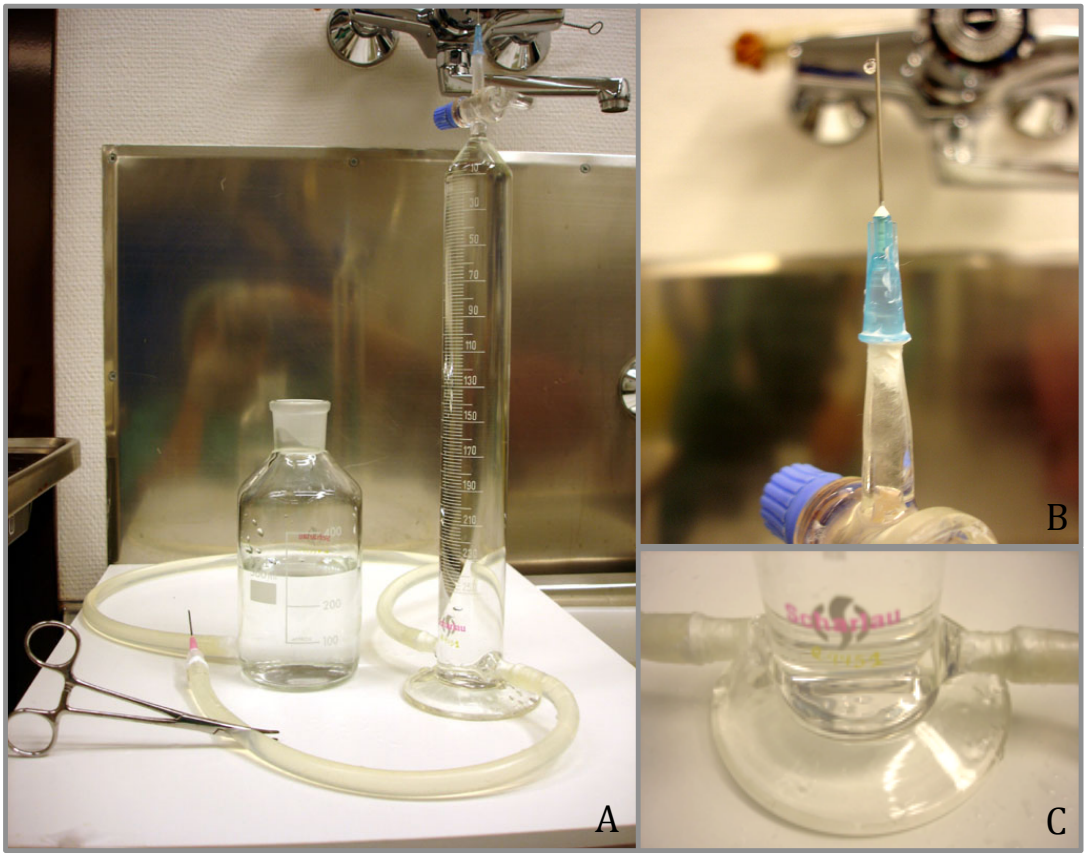

Fig. 2.4: Aspirometer (A), detail of the stopcock and the needle sealed and completely filled with water, detailed of the joints with the rubber tubes sealed.

Basically the aspirometer consists of two glass flasks connected to each other by a rubber tube, and an extra tube with a free end where the needle for puncture is placed (Fig. 2.4). The flasks differ in shape and functionality. One flask is actually a reverse gas burette with a hexagonal base similar to those of graduated cylinders for easy handling and better support. The burette has a glass stopcock in the upper part and two tubes at the bottom. The burette is scaled for the measurement of the gas volume beginning

from the most upper part where the gas will be collected. The stopcock is directly connected to a needle. The tubes at the bottom are made to connect with the other flask and with the needle to puncture the heart, through the rubber tubes. The remaining flask is a normal glass flask but with a tube in the bottom to connect with the reverse burette through the rubber tube. The complete system must be filled with distilled water, including the needle connected to the burette's stopcock, and air bubbles must be removed.

The aspirometer works by differences in pressure created by the vertical displacement of the simple gas flask. If this flask is moved upwards the water will move from this flask to the burette and from here all along the free rubber tube and the puncturing needle. This is the position in which the user must puncture the heart, since the entire system is filled with distilled water and atmospheric air pollution is not possible. It is also necessary in this case to fill in the pericardial cavity with distilled water for the same purpose. Moving down the flask creates a negative pressure in the burette and in the free rubber tube, suctioning whatever is found inside the heart. On this position the user should clamp the free rubber tube. Gas will ascend to the upper part of the burette and then the two physical phases will be separated. To collect the sample, it is only necessary to apply a vacutainer and to open the stopcock.

The aspirometer was first designed by Dyrenfurth, but we and many other authors have introduced modifications. We first reproduced the aspirometer described by Bajanowski et al. (1998) and later modified some observational defaults. Instead of having a glass flask joined to a gas burette, we designed a reverse gas burette with a hexagonal base similar to those of graduated cylinders for easier handling and better support. This simple modification eliminates one possible entrance of atmospheric air and at the same time reduces slopes or surface contact where small bubbles sometimes become attached, maximizing gas sample size recovery. The new design makes handling easier, while the hexagonal base gives stability to the tool.

Regarding liquid as a gas barrier, distilled water was tested versus an aqueous solution of NaCl. For this purpose, 1 mL of hydrogen and CO_2 was introduced ten times each through the rubber tubes and recovered with a 5-mL additive-free vacutainer at the top of the gas burette with the aspirometer filled with distilled water. Air content was compared with 10 vacutainers, into which 1 mL of the corresponding gas had previously been injected. Both experiments were conducted in the same laboratory conditions. The same procedure was repeated for CO_2 alone with an aqueous NaCl solution at $20\%_{wt}$ NaCl and pH 4 lowered by the addition of 1 M HCl droplets.

2.2.2 METHODS

2.2.2.1 Gas analysis

Gas analysis was conducted by gas chromatography. Samples were injected manually into the analyzer (Varian 450-GC) with the use of a block-pressure syringe (Supelco A-2 series). The temperature of the injector was set at 230˚C. This analyzer was equipped with a Varian CP7430 column composed of two different sub-columns in tandem: a (Q) PoraBOND Q column, for separation of CO_2 and hydrocarbon compounds up to 4 carbons, and a (M) Molsieve 5 A column, for separation of permanent gases (such as oxygen, nitrogen, argon, etc). To detect these compounds, it is necessary to have both a thermal-conductivity detector (TCD) and a flame-ionization detector (FID) disposed one after the other. The TCD is a universal detector for permanent gases. Its temperature was fixed at 80°C, while the temperature filament was 160°C. The FID is a selective hydrocarbon destructive detector. Because of its destructive nature, the FID must always be placed after the TCD. The temperature for the FID was fixed at 230°C. Samples were run for 25 minutes with an isothermal temperature of 45°C and electronically controlled flux with a fixed pressure of 13.1 psi on the head column. Helium was used as the carrier gas.

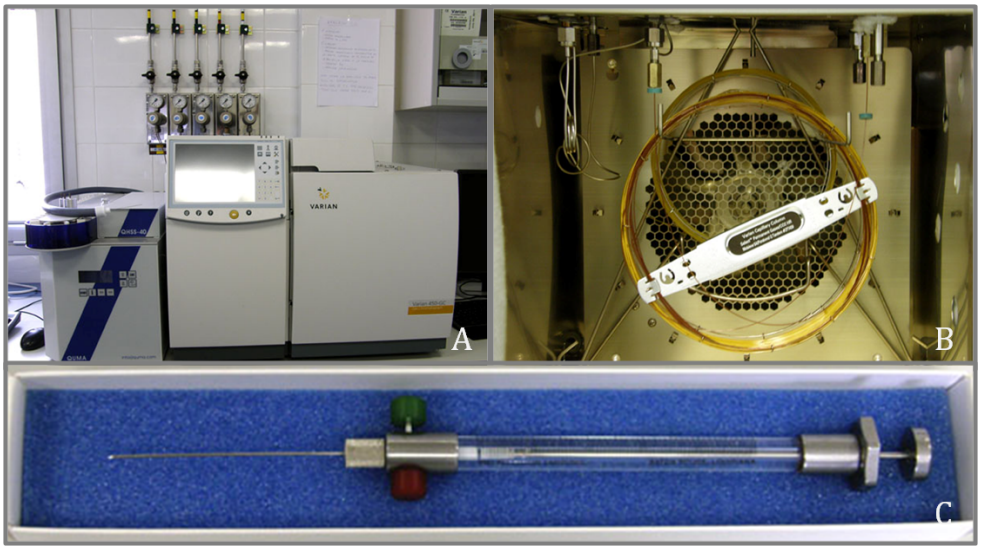

Fig. 2.5: Gas chromatograph (A), tandem column (B), block-pressure syringe (C).

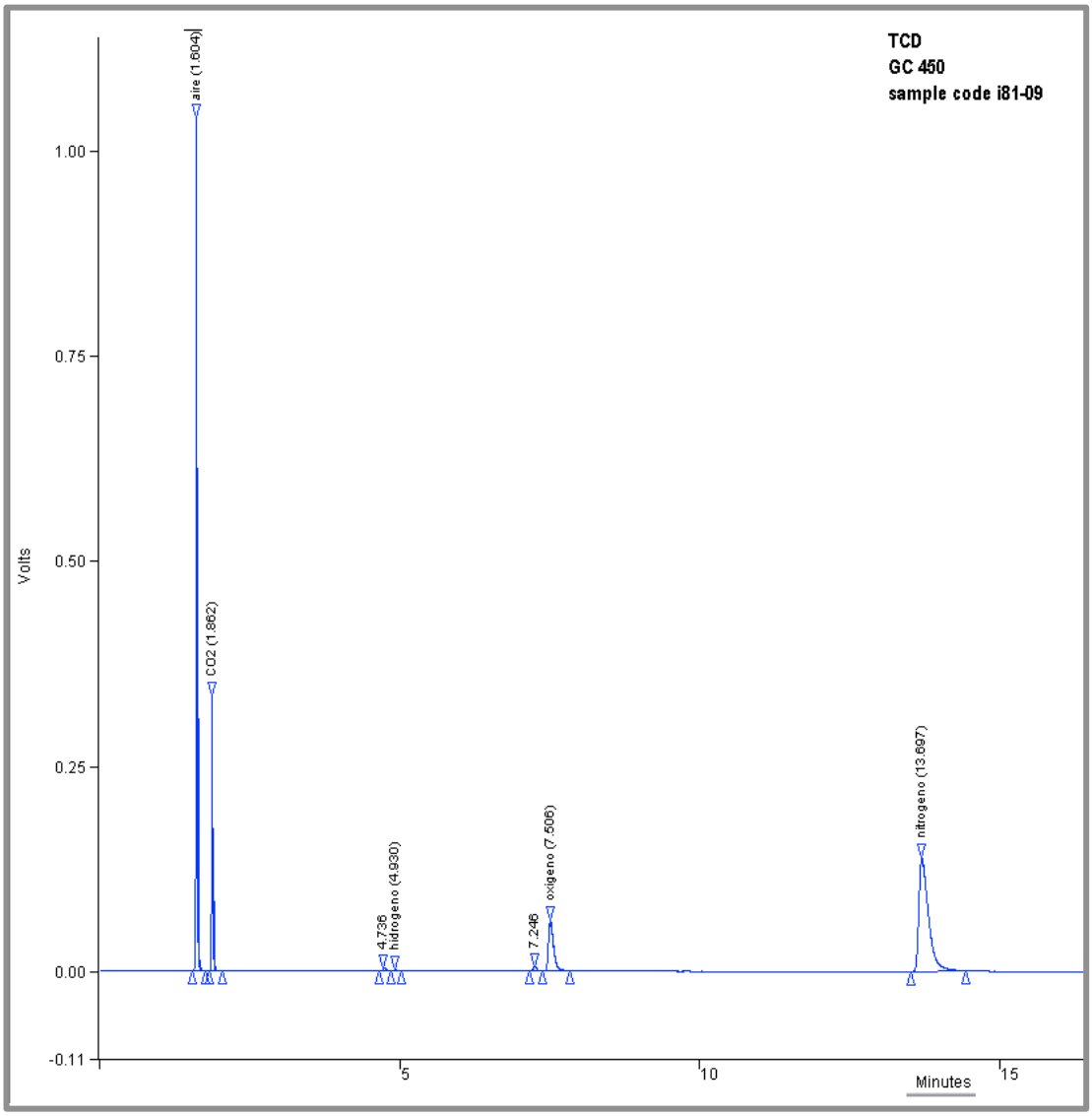

Fig. 2.6: Chromatogram view from TCD detectors showing peaks of air (oxygen and nitrogen together) hydrogen, oxygen and nitrogen.

2.2.2.2 Gas calculations

Since gases are temperature- and pressure-dependent, calibration curves were frequently recalculated for every gas involved. Calibration curves were made using pure gases, except for oxygen and nitrogen, for which atmospheric air was used.

When samples were studied, the vacutainer's background was corrected for by measuring it on blanks which were always exposed to the same pressure, temperature, and storage time conditions as the samples. The detection limit was set at $S_{\min} = \overline{S}_{blank} + 3s_{blank}$, where $S_{\min}$ is the minimum detectable signal, $\overline{S}_{blank}$, is the average signal for a given gas in the blanks, and s_{blank} is the associated standard deviation (Kaiser, 1947).

2.2.2.3 Statistics analysis

All data were analyzed using the 'R' data analysis software, version 2.11.1 (R Development Core Team, 2010). The numerical variables were summarized as means and standard deviations. Regression models were evaluated with the R^2 coefficient. The most parsimonious model was chosen. Hypothesis testing was considered significant when the corresponding *P*-value was less than 0.05. The same consideration was taken for analysis of variance studies and comparisons of two means. For small samples, the Wilcoxon test was applied.

2.3 RESULTS

2.3.1 VACUUM TUBES

For the evolution of the air content on storage days 1, 7, 14, and 21 in two different vacutainer types, we considered the following log-linear model (equation 2.1) with an adjustment of R^2 = 0.944. All estimated parameters had a *P*-value less than 0.001 (Table 2.1; Fig. 2.6).

$$Ln(air) = q + a \cdot (type) + b \cdot (day) \tag{2.1}$$

$$Ln(air) = 10.7 + 0.453 \cdot (type) - 0.009 \cdot (day) \tag{2.2}$$

where *type* = 1 or 0 according to whether the vacutainer type is with or without air. The diffusion rate was obtained from the model as *exp(β)*, see equations (2.3) and (2.4).

Table 2.1: Estimation of parameters for model of diffusion rate and its associated P values:

Parameter	Estimation (SE)	P value	Adjusted R^2
q	10.7 (0.011)	< 0.001	0.944
a (type)	0.453 (0.011)	< 0.001	
b (day)	- 0.009 (0.001)	< 0.001	

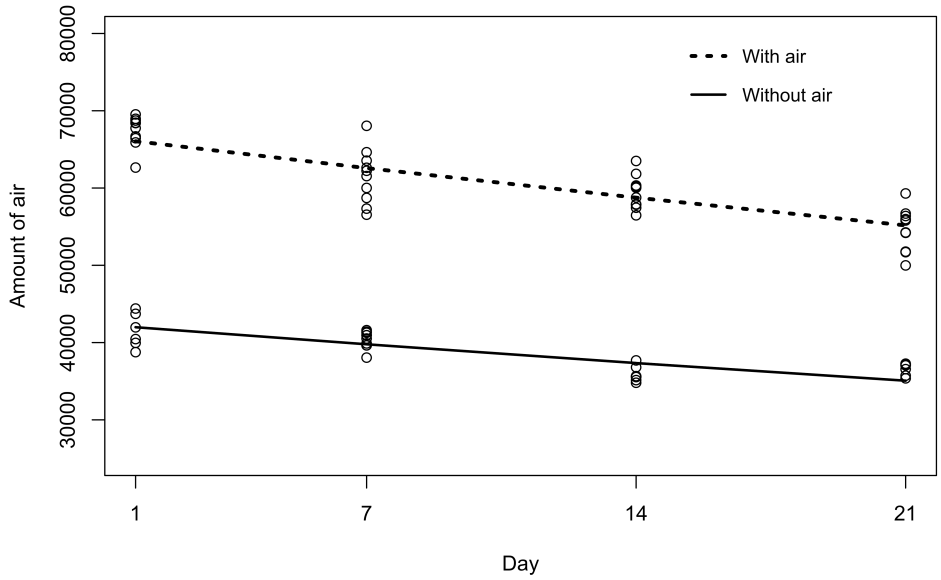

Fig. 2.7: Diffusion rate from vacutainers. Evolution of air content with time in two different vacutainer types: 3.5 mL with additives (discontinuous lines) and 5mL without additives (continuous lines) are represented with its regression lines.

Estimated air value as a function of vacutainer type and observation day can be expressed as:

$$air\left(type,\ day\right) \ = \ \exp\left[q + a\cdot\left(type\right) \ + b\cdot\left(day\right)\right] \tag{2.3}$$

Diffusion rate is calculated based on the model as follows:

$$\frac{air\left(type, day+1\right)}{air\left(type, day\right)} = \frac{\exp\left[\theta + \alpha\cdot\left(type\right) + \beta\cdot\left(day+1\right)\right]}{\exp\left[\theta + \alpha\cdot\left(type\right) + \beta\cdot\left(day\right)\right]} \tag{2.4}$$

Therefore, diffusion rate was the same in both vacutainer types. Loss of sample occurred at a rate of 0.99% (95% CI = 0.989%, 0.992%) per day.

Air background of vacutainers and helium containers was found to be very similar (Fig. 2.7). The background of the block pressure syringe is also included in the containers, and will always be included in the gas samples, as well. It represents almost half percent of the total air background measured in a container. With this in mind, the

background of the containers was found only slightly higher. Differences in the mean values of air background between both container types were very small, but standard deviation was much smaller in the vacutainers than in the helium container.

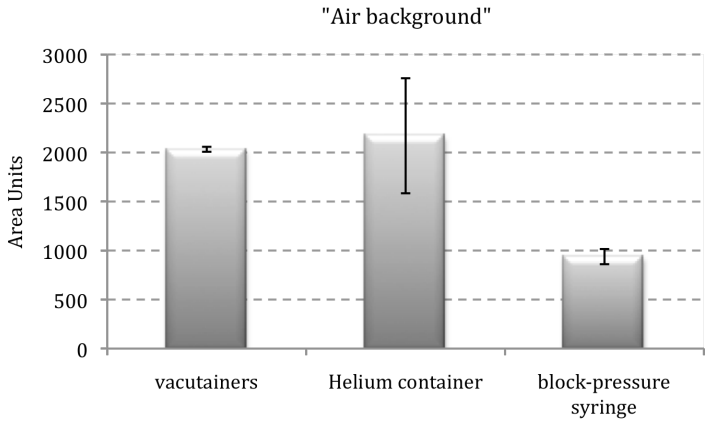

Fig. 2.8: Comparison of the mean and standard deviations values of the atmospheric air background from the 5ml additive-free vacutainers, the helium container and the block-pressure syringe.

Regarding storage temperature, mean values were found to be similar within the same temperature through time, except for day 14 where an interaction was found for all temperatures (Fig. 2.8). Differences were found between temperatures. Room and refrigerator average values were similar, but clearly differed from freezer values (Table 2.2).

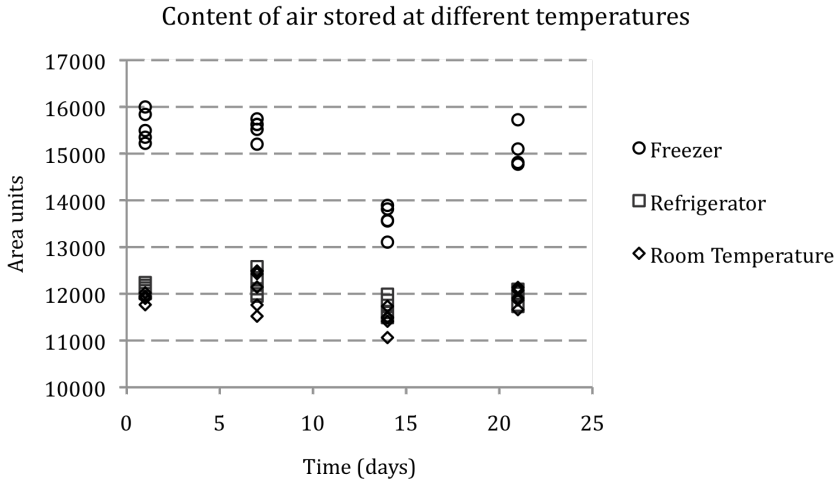

Fig. 2.9: Air content (oxygen in the right side and nitrogen in the left side) on the same days but stored at different temperatures (room , fridge and freezer temperature).

Table 2.2: Average values of air content (oxygen and nitrogen) of vacutainers stored at different temperatures and analyzed in a determine date. Different letters indicates significant differences of average values.

	Temperature	1 day	7 days	14 days	21 days
O_2	Room (20-24ºC)	11910 ^{a}	12069 ^{a}	11438 ^{b}	11929 ^{a}
	Refrigerator (4ºC)	12122 ^{a}	12187 ^{a}	11694 ^{b}	11933 ^{a}
	Freezer (-80ºC)	15581 ^{c}	15542 ^{c}	13589 ^{d}	14966 ^{e}
N_2	Room (20-24ºC)	45712 ^{a}	46459 ^{a}	44012 ^{b}	45573 ^{a}
	Refrigerator (4ºC)	46557 ^{a}	46889 ^{a}	45076 ^{b}	46012 ^{a}
	Freezer (-80ºC)	61119 ^{c}	60848 ^{c}	53217 ^{d}	58526 ^{e}

Additionally, when repetitive punctures were done an increase in content was found in all temperatures, with the refrigerator samples being the most affected and the room temperature samples being the least affected (Fig. 2.9).

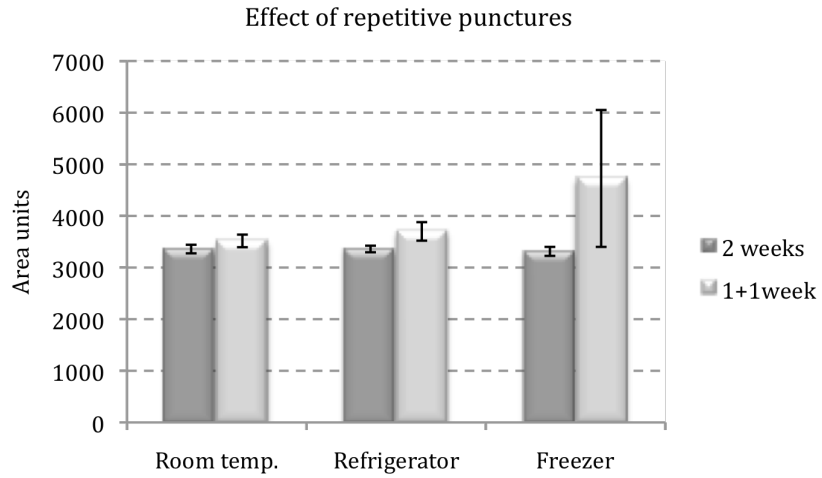

Fig. 2.10: Effect of repetitive punctures in air content of samples stored at different temperatures. Error bars represent the standard deviation.

Diffusion rate for the different gases during the first five days was found to be very small and no relevant differences were found among the different gases. Central values for each day where always within the range of 0.95 to 1.05, considering gas content from day zero as one (Fig. 2.11-2.14). Hydrogen was the gas with more disperses data, even though the central value for day five was within the stated range (Fig. 2.12).

Variability of the ratio data was much lower and the resulting composition was very stable, (Y axe scale had to be minimized in this graph to observe bar error data) (Fig. 2.14).

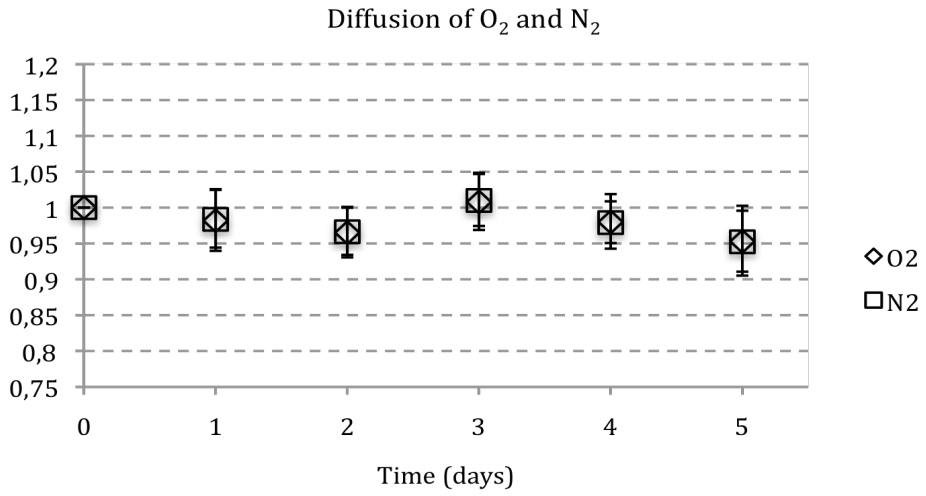

Fig. 2.11: Atmospheric air diffusion from the vacutainer represented by oxygen and nitrogen.

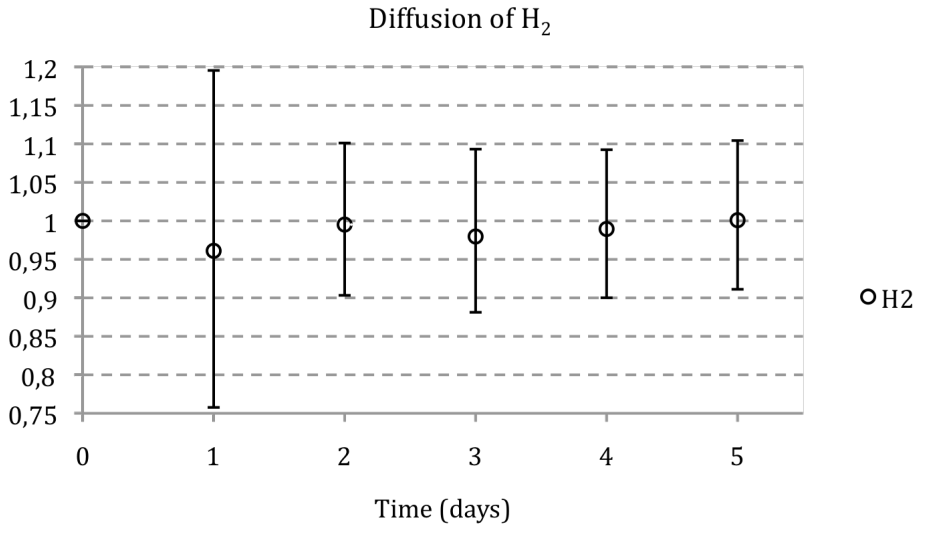

Fig. 2.12: Hydrogen diffusion from the vacutainer.

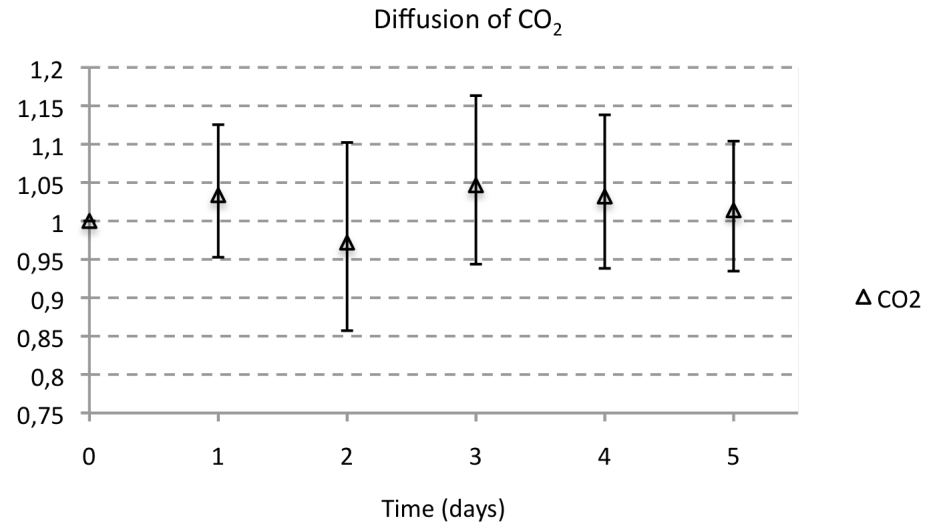

Fig. 2.13: Carbon dioxide diffusion from the vacutainer.

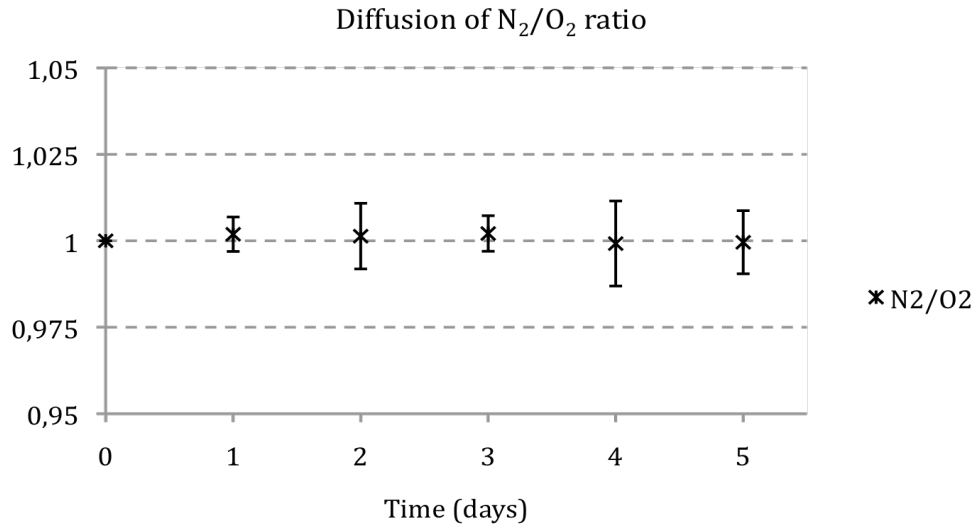

Fig. 2.14: Diffusion of N_2/O_2 ratio from the vacutainer.

No tendencies were found for relative composition of the mixture expressed in percentages (Fig. 2.15) in contrast with absolute values (Fig. 2.5).

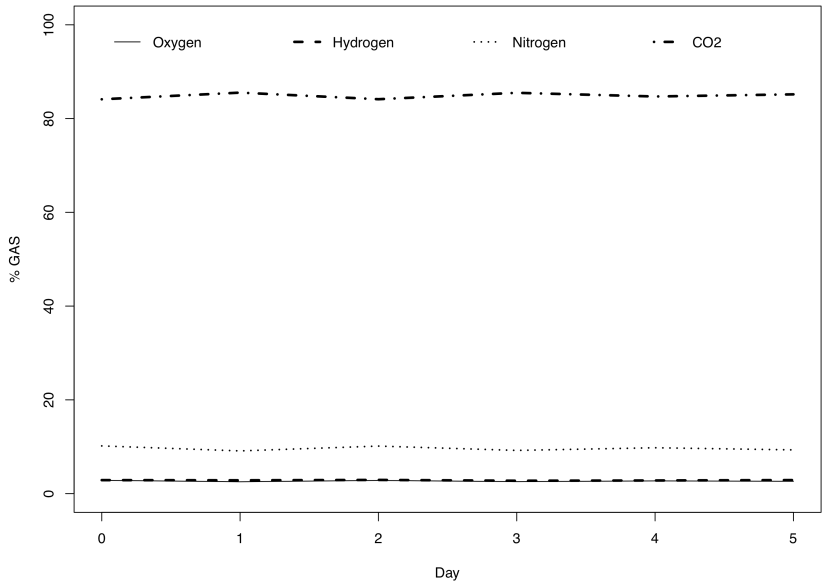

Fig. 2.15: Relative amount of gases expressed in percentages and its variation along time.

Finally, no significant differences were found for either oxygen (P= 0.137) or nitrogen (P= 0.056) area units when samples were exposed to a flight round-trip.

2.3.2 INSULIN SYRINGE

The Insulin syringe demonstrated to be very accurate for gas volumes measurements demonstrated by a good linear adjustment (R^2= 0.9959) to different volumes sampled (Fig. 2.16).

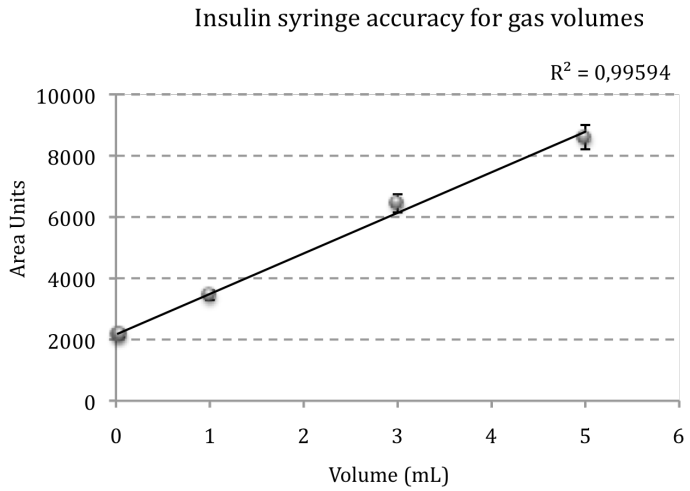

Fig. 2.16: Regression adjustment of gas volume measurements done with the insulin syringe. Error bars represent %RSD.

Additionally, no significant differences were found for either oxygen (P = 0.336) or nitrogen (P= 0.337) when analyzing the atmospheric air background of the syringe. This means that the syringe does not implement atmospheric air background on the methodology.

2.3.3 ASPIROMETER

Gas barrier liquid resulted to be important from gas composition point of view. Differences were found showing an increase in oxygen and nitrogen and a marked decrease in CO_2 carbon dioxide when the gas was forced to cross through the distilled water of the aspirometer. Hydrogen was always fully recovered. These differences were greatly reduced when using an aqueous 20%$_{wt}$ NaCl solution (Table 2.3).

Table 2.3: milliliters and area units of hydrogen and CO_2 together with its residual oxygen and nitrogen contents recovered from the aspirometer when forcing 1 mL of pure hydrogen or CO_2 to pass through the aspirometer filled with a barrier liquid and compared to a direct injection of 1 mL of the same gas in the vacuum tubes.

H_2 distilled water	ml recovered	H_2 (a.u.)	O_2 (H_2) (a.u.)	N_2 (H_2) (a.u.)
med_{asp}	1.1 (2.5E-08)	293,10	4338,80	14982,70
med_{ctrl}	1	245,50	3042,40	11193,90
med_{asp} - med_{ctrl}	+ 0.1	47,60	1296,40	3788,80
med_{ctrl} / med_{asp}	0.91	0,84	0,70	0,75
CO_2 distilled water	ml recovered	CO_2 (a.u.)	O_2 (CO_2) (a.u.)	N_2 (CO_2) (a.u.)
medasp	0,64	2688,20	3924,20	14163,70
medctrl (SE)	1	6505,95	2881,40	10347,05
medasp - medctrl	-0,36	-3817,75	1042,80	3816,65
medctrl / medasp	1,56	2,42	0,73	0,73
CO_2 saline water	ml recovered	CO_2 (a.u.)	O_2 (CO_2) (a.u.)	N_2 (CO_2) (a.u.)
medasp	1	5868,7	3308,45	11646,6
medctrl (SE)	1	6505,95	2881,40	10347,05
medasp - medctrl	0,00	-637,25	427,05	1299,55
medctrl / medasp	1,00	1,11	0,87	0,89

2.4 DISCUSSION

2.4.1 VACUUM TUBES

Cetaceans might strand on beaches that are not easily accessible, and may require that the necropsy be executed *in situ*. To our knowledge, no transportable apparatus exists that can simultaneously measure respiratory gases as well as hydrocarbons produced by the metabolism of microorganisms. Pierucci & Gherson used an aspirometer that was directly connected to a gas chromatograph (Pierucci and Gherson, 1968). More accurate analysis of hydrocarbons requires the use of a flame-ionization detector, which needs hydrogen to function, and the transportation of requires special safety measures. Therefore, although gas extraction can sometimes be performed at the stranding site, gas analysis must always take place in a laboratory, a situation that requires proper storage and transportation of gas samples.

Glass vacutainers were explored as candidates for gas storage because they are gas sealed by rubber stoppers, and are made of non-breakable glass that makes them suitable to perform for *in situ* necropsies. Keil (1979) compared different stoppers materials and studied the possible interactions of these materials with the gas against time, and found no appreciable differences(Keil et al., 1980). The presence of oxygen and nitrogen in the vacuum tubes has been described previously, and presents a problem for blood gas determinations(Lang et al., 1973; Mueller and Lang, 1973). Based on our results, vacutainers have similar air background that purged vials but with the advantage of having much lower variability (Fig. 2.7), probably because their vacuum is industrially in contrast with the manually procedure for purging. Since oxygen and nitrogen levels are very important from the diagnostic point of view of gas embolism (Bajanowski et al., 1998; Pierucci and Gherson, 1968), it is crucial to calculate the background and to correct for it using calculations. For this purpose, we propose to carry one blank (a vacutainer into which nothing has been injected) with each sample through the entire process, which experiences the same changes in temperature and pressure as the samples do. Then, a correction factor proposed by

Kaiser et al. (1947) should be introduced into the samples calculations for each gas. It would be given by its determination on the blanks as follows: $S_{\min} = \overline{S}_{blank} + 3s_{blank}$, where $S_{\min}$ is the minimum detectable signal, $\overline{S}_{blank}$, is the average signal for a given gas in the blanks, and s_{blank} is the associated standard deviation. Thus, a lower air background gives higher resolution for analyzing small samples. According to our model, the 5 mL additive-free vacutainer has the smallest background and both vacutainer types exhibit the same diffusion rate; therefore, we recommend using the 5-mL additive-free vacutainer. As a guideline we have observed that bubbles larger than 0.5 mL usually give good signals when using this vacutainer type, although smaller volumes have been analyzed successfully. It is important to note that when measuring the blanks, we are also correcting the air background from the gas-tight syringe that is used for manual injection into the gas chromatography. We haven't found any correction for the gas-tight syringe on previous papers.

Regarding temperature storage, since average values from day 21 were similar to those from day 1, the interaction found on day 14 was considered as incidental. Some fluctuation in the equipment may have happened that day. Room temperature was fixed to standardize the methodology for greater stability under the different circumstances tested (Fig. 2.9 and 2.10). The increase in oxygen and nitrogen content found on vacutainers which were puncture twice compared with those analyzed only once (Fig. 2.10) could only be explained by an atmospheric air entrance. Thus repetitive punctures or analyses should be avoided in the same tube. This might be because vacutainer's rubber stoppers are not done for this purpose. Rubber material seems to suffer the most if frozen.

Concerning the length of time spent in storage, the diffusion rate has been observed to be similar for the different gases. The diffusion rate calculated from our model at room temperature was 0.9%. Molloy (1973) described a similar value (1%) for gas-tight bottles kept at room temperature. This low diffusion rate offers the possibility that samples may be stored for several days without appreciable loss of gas and

without affecting the accuracy of the analysis. However, to achieve more accurate results it is highly recommended that the analysis be performed as soon as possible, and that relative quantities be calculated instead of absolute values (Fig. 2.11, 2.14). Based on our results diffusion rate is the same for the different gases at least for the first 5 days (Fig. 2.15).

Results on samples transported by plane indicate that there were no statistical differences and thus they can be transported by plane. Nitrogen P value (P= 0.056) is *quasi*-significant; therefore it would be preferable to transport the samples inside some pressure resistance cage to ensure no changes in gas composition.

2.4.2 INSULIN SYRINGE

Ferretti et al. collected expired air in an anesthesia bag and gas samples were drawn into glass syringes sealed with rubber stoppers and transported to the laboratory for analysis. Knowles (2006) studied the effects of syringe material, storage time, and storage temperature on normal arterialized blood gas values (Knowles et al., 2006). They concluded that for accurate results, samples drawn in plastic syringes should be analyzed immediately and that if storage is required, samples should be kept in glass.

Glass syringes are not suitable for fieldwork. They are very fragile and easily blocked, and it would be necessary to have one glass syringe per sample or to transport inert gas with which to purge the syringe between samplings and then store the sample elsewhere.

On the other hand, insulin syringes are made of plastic, making them disposable and very cheap. Handling of plastic material is always preferred versus glass during fieldwork. If a new syringe can be used for each bubble, purging is no longer necessary. In addition, our results show that the insulin syringe does not implement atmospheric air significantly, is very accurate for gas sampling (Fig. 2.16), and is compatible with storage in glass material (vacutainers) in accordance with the findings of Knowles (2006).

2.4.3 ASPIROMETER

The aspirometer should be made of some transparent material with few surface cracks to avoid bubble attachment. The use of glass was unavoidable for the aspirometer. Modifications of the aspirometer design include slope avoidance, one joint elimination, and easier and safer handling.

A barrier gas liquid is necessary to separate the free gas from the blood and to avoid atmospheric air pollution of the sample. Although the Van-Slyke method uses mercury for the same purpose, mercury is not an option for security reasons during transport. We have used either distilled water or an aqueous $20\%_{wt}$ NaCl solution in the aspirometer. Erben and Nadvornik (1963), as well as Pierucci & Gherson (1969), used an aqueous $20\%_{wt}$ solution and considered the dilution of the gases into the solution to be negligible. Keil et al. (1979) compared the use of distilled water with the use of saline-saturated dilution as liquid barriers and found no appreciable differences. Bajanowsky et al. (1998) used distilled water following the conclusion by Keil et al. (1979) that there were no differences for either liquid barrier.

We have found differences to be considered in both solutions. It is important to highlight that our NaCl solution was also an acid solution, and that we did observe differences between this solution and distilled water. Table 2.3 depicts a marked decrease in CO_2 signal, and an increase in nitrogen and oxygen, when the aspirometer is used. These differences may be explained by two simultaneous processes: solubilization of the gas compounds in the liquid barrier according to Henry's Law; and dragging of the inherent gas (mainly nitrogen and oxygen) previously dissolved in the distilled water.

Among the analyzed gases, only CO_2 was noted to be significantly dissolved, with a scale change of 2.42. According to Henry's Law and applying a mass balance, its diffusion coefficient in distilled water at 24˚C is 1.82. In fact, according to the Henry's

Law expressions seen in the Introduction Chapter, (see equations 1.4-6), it is possible to relate both scales of Henry constanst as follows:

$$K^{i}_{H,cc} = K^{i}_{H,c} \cdot RT \tag{2.5}$$

Henry's Law in terms of the ratio of concentration of gaseous component *i* in both phases (aqueous and gaseous), would be expressed by:

$$K^{i}_{H,cc} = \frac{C^{aq}_{i}}{C^{g}_{i}} = K^{i}_{H,c} \cdot RT \tag{2.6}$$

Equation (2.6) allows us to evaluate the distribution of component *I* between two phases, by simply knowing the value of Henry's constant in molar concentration scale and the absolute temperature of the water in the aspirometer during the sampling procedure.

Applying the equation (2.6) to the case of Oxygen at 25°C (298.15 K), its distribution between phases would be:

$$\frac{C^{aq}_{O_2}}{C^{g}_{O_2}} = K^{O_2}_{H,c} \cdot RT$$

$$\frac{C^{aq}_{O_2}}{C^{g}_{O_2}} = 0.0013\left(\frac{mol}{atm \cdot L}\right) \cdot 0.082\left(\frac{atm \cdot L}{K \cdot mol}\right) \cdot 298.15(K) = 0.0318 \tag{2.7}$$

Through this example, shown in equation (2.7), it could be say that for every 100 moles of oxygen found in the gas phase there is only 3 moles in aqueous phase at 298.15 K.

The first member of equation (2.7) is the ratio of *i* concentration in both phases, so that could be applied the mass balance of component *i* during collection with the aspirometer:

$$\text{Concentration "i" } (\text{sample, gas}) = \text{Concentration "i" } (\text{aspirometer, aqueous}) + \text{Concentration "i" } (\text{top-aspirometer, gas}).$$

$$C^{g}_{i,input} = C^{aq}_{i} + C^{g}_{i,output} \tag{2.8}$$

Applying Henry's law to equation (2.8) is obtained:

$$C^{g}_{i,input} = C^{aq}_{i} + C^{g}_{i,output} = K^{i}_{H,c} \cdot RT \cdot C^{g}_{i,output} + C^{g}_{i,output}$$
$$C^{g}_{i,input} = \left(1 + K^{i}_{H,c} \cdot RT\right) \cdot C^{g}_{i,output} \tag{2.9}$$

It should be noted that equation (2.9) represents the mass ratio (molar) of gas *i* between the input and output of the aspirometer. It can be clearly seen that the concentration of component *i* in the colected gas phase at the top of the aspirometer, is reduced by the partial solubilization in the liquid barrier. It should be noted as well that the bracketed term form equation (2.9) is the correction factor applied to the concentration of component *i* in the output in order to obtain the concentration at the entrance of the aspirometer, or what is the same, to get the concentration value of *i* in the gas bubble without going through the barrier liquid of the aspirometer. That concentration should be the same as if the gas could be directly collected with the vacutainer.

However, this value explains 75% of CO_2 behaviour. The remaining scale change might be explain by the chemical reaction of CO_2, which is an acidic gas, with the distilled water:

$$CO_2(g) + H_2O \rightleftharpoons H_2CO_3(aq)$$
$$H_2CO_3(aq) + H_2O \rightleftharpoons HCO_3^-(aq) + H_3O^+(aq) \tag{2.10}$$

On the other hand, incorporation of the inherent liquid barrier gases could happen by dragging simultaneously to dilution. Therefore, instead of observing a slight decrease in nitrogen and oxygen signals according to Henry's Law, an increase was recorded. Nitrogen and oxygen are incorporated from the liquid barrier to the gas sample. Keil et al. (1979) also noted an incorporation of oxygen when storing gas samples in flasks with a liquid barrier. Pulling of these gasses could be due to molecular collisions between the gas sample and the inherent dissolved gas into solution. Thus, this phenomenon is molar fraction dependent. According to table 2.3, the chemical nature of the gas is not a factor since CO_2 and hydrogen moved similar quantities of nitrogen and oxygen. Dyrenfurth (1928) proposed to boil distilled water just before its use. Thermal and vacuum treatments were considered to diminish the amounts of nitrogen and oxygen diluted in the barrier liquid, but were excluded. It is not possible to transport the aspirometer filled with any liquid. Purring from the flask to the aspirometer at the stranding place will counteract this kind of treatments.

Additionally, correction factors may change depending on which solution is used, water temperature, and pH according to Henry's Law. In the Canary Islands, the ambient temperature is very constant during the year (20-24ºC). Due to the high heat capacity of the water, this variation is even lower for the water temperature. These special climate circumstances allowed us to calculate a unique correction factor, but other researchers should consider the termperature range of the water in which they are working. We used a correction factor of 0.73 for nitrogen and oxygen, and 2.42 for CO_2 when distilled water was used as barrier liquid (Table 2.3). For $20\%_{wt}$ NaCl aqueous solution we used a correction factor of 0.89 for nitrogen, 0,87 for oxygen, and 1.11 for CO_2. Recovery signals were therefore improved when an aqueous $20\%_{wt}$ NaCl solution was used and we strongly recommend this solution under normal circumstances, but not for cetaceans. Assays on the carcasses of deep diving cetaceans were unsuccessful when an aqueous $20\%_{wt}$ NaCl solution was used. Gas bubbles did not move freely through the aspirometer due to viscosity and drag effects. For comparison reasons, we decided to use always distilled water.

2.5 STANDARDIZED METHODOLOGY

According to the results, the methodology to be applied remains as follows:

2.5.1 GAS SAMPLING FROM CAVITIES

The 5-mL additive-free vacutainer (BD Vacutainer® Z. ref: 367624) is directly applied to cavities with its appropriate plastic holder or adapter and a double-pointed needle. To avoid atmospheric air, the needle must first be inserted into the cavity for purging; second, the vacutainer must be pushed against the double-pointed needle; and finally, the vacutainer must be removed, always before the needle is released from the cavity. This method allows adequate sampling from sinuses, the digestive tract, and even from heart ventricles if the putrefaction of the carcass ranges from grade three to grade five. Filling the pericardial sac with distilled water is always necessary to avoid atmospheric air in cetaceans.

2.5.2 GAS SAMPLING FROM THE HEART CAVITIES

If the decomposition status is fresh or very fresh (decomposition code 2 or 1, respectively), then an aspirometer will be necessary to separate the gas from the blood found in the heart. The aspirometer works by differences in pressure created by the vertical displacement of the simple gas flask. If this flask is moved upwards, the water will move from this flask to the burette and from here all along the free rubber tube and the puncturing needle. This is the position in which the user must puncture the heart, since the entire system is filled with distilled water and atmospheric air pollution is not possible. It is also necessary in this case to fill the pericardial cavity with distilled water for the same purpose. Moving down the flask creates a negative pressure in the burette and in the free rubber tube, suctioning whatever is found inside the heart. Clamp the free rubber tube in this position. Gas will ascend to the upper part of the burette and then the two physical phases will be separated. To collect the sample, it is only necessary to apply a vacutainer and to open the stopcock.

2.5.3 GAS SAMPLING FROM BUBBLES

Disposable insulin syringes (BD Plastipak U-100 insulin) are used and their contents are promptly injected into a vacutainer. One new syringe and one new vacutainer are used for each bubble.

2.5.4 TRANSPORT AND STORAGE OF GAS SAMPLES

Vacutainers are kept upside-down at room temperature with one blank per sample, or a total of at least 3 blanks.

2.5.5 GAS ANALYSIS

Gas analysis is conducted by gas chromatography. Samples are injected manually into the analyzer (Varian 450-GC) with the use of a block-pressure syringe (Supelco A-2 series). The temperature of the injector is set at 230˚C. This analyzer is equipped with a Varian CP7430 column composed of two different sub-columns in tandem: a (Q) PoraBOND Q column, for separation of CO2 and hydrocarbon compounds up to 4 carbons, and a (M) Molsieve 5 A column, for separation of permanent gases (such as oxygen, nitrogen, argon, etc). To detect these compounds, it is necessary to have both a thermal-conductivity detector (TCD) and a flame-ionization detector (FID) disposed one after the other. The TCD is a universal detector for permanent gases. Its temperature is fixed at 80°C, while the temperature filament is 160°C. The FID is a selective hydrocarbon destructive detector. Because of its destructive nature, the FID must always be placed after the TCD. The temperature for the FID is fixed at 230°C. Samples are run for 25 minutes with an isothermal temperature of 45°C and electronically controlled flux with a fixed pressure of 13.1 psi on the head column. Helium is used as the carrier gas.

2.5.6 GAS CALCULATIONS

Since gases are temperature- and pressure-dependent, calibration curves should be recalculated frequently. Calibration curves are made using pure gases, except for oxygen and nitrogen, for which atmospheric air is used.

When samples are studied, the vacutainer's background is corrected for by measuring it on blanks, which are always exposed to the same pressure, temperature, and storage time conditions as the samples. The detection limit is set at $S_{\min} = \overline{S}_{blank} + 3s_{blank}$, where $S_{\min}$ is the minimum detectable signal, $\overline{S}_{blank}$, is the average signal for a given gas in the blanks, and s_{blank} is the associated standard deviation (Kaiser, 1947).

2.6 REFERENCES

Armstrong HG. 1939. Analyisi of gas emboli. Engineering Section Memorandum Report. Wright Field, Ohio.

Bajanowski T, Kohler H, DuChesne A, Koops E, Brinkmann B. 1998. Proof of air embolism after exhumation. International Journal of Legal Medicine 112(1):2-7.

Bert P. 1878. La Pression Barometrique: Recherches de Physiologie Expérimentale. Hitchcock MA, Hitchcock FA, translator. Paris: Masson.

Fernandez A, Edwards JF, Rodriguez F, de los Monteros AE, Herraez P, Castro P, Jaber JR, Martin V, Arbelo M. 2005. "Gas and fat embolic syndrome" involving a mass stranding of beaked whales (Family Ziphiidae) exposed to anthropogenic sonar signals. Veterinary Pathology 42(4):446-457.

Harris M, Berg WE, Whitaker DM, Twitty VC, Blinks LR. 1945. Carbon dioxide as a facilitating agent in the initiation and growth of bubbles in animals decompressed to simulated altitudes. Journal of General Physiology 28(3):225-240.

Ishiyama A. 1983. Analysis of gas composition of intra vascular bubbles produced by decompression. Bulletin of Tokyo Medical and Dental University 30(2):25-36.

Jepson PD, Arbelo M, Deaville R, Patterson IAP, Castro P, Baker JR, Degollada E, Ross HM, Herraez P, Pocknell AM, Rodriguez F, Howie FE, Espinosa A, Reid RJ, Jaber JR, Martin V, Cunningham AA, Fernandez A. 2003. Gas-bubble lesions in stranded cetaceans - Was sonar responsible for a spate of whale deaths after an Atlantic military exercise? Nature 425(6958):575-576.

Kaiser H. 1947. Die berechnung der nachweisempfindlichkeit. Spectrochimica Acta 3(1):40-67.

Keil W, Bretsxhneider K, Patzelt D, Behning I, Lignitz E, Matz J. 1980. Luftembolie oder Fäulnisgas? Zur Dianostik der cardialen Luftembolie an der Leiche. Beiträge zur Gerichtlichen Medizin 38:395-408.

Knowles TP, Mullin RA, Hunter JA, Douce FH. 2006. Effects of syringe material, sample storage time, and temperature on blood gases and oxygen saturation in arterialized human blood samples. Respiratory Care 51(7):732-736.

Kuiken T, García-Hartmann M. Dissection techniques and tissues sampling. In: Newsletter, editor; 1991; Leiden, Netherlands.

Lang GE, Mueller RG, Hunt PK. 1973. Posible error resulting from use of "Nitrogen-filled" Vacutainers for blood-gas determinations. Clin Chem 19(5):559-563.

Lillo RS, Maccallum ME, Caldwell JM. 1992. Intravascular bubble composition in guinea-pigs a possible explanation for differences in decompression risk among different gases. Undersea Biomedical Research 19(5):375-386.

Mueller RG, Lang GE. 1973. Phase equilibrium of oxygen in nitrogen-filled vacutainers. Clinical Chemistry 19(10):1198-1200.

Piantadosi CA, Thalmann ED. 2004. Pathology: whales, sonar and decompression sickness. Nature 428(6984):1 p following 716; discussion 712 p following 716.

Pierucci G, Gherson G. 1968. Experimental study on gas embolism with special reference to the differentiation between embolic gas and putrefaction gas. Zacchia 4(3):347-373.

Pierucci G, Gherson G. 1969. Further contribution to the chemical diagnosis of gas embolism. The demonstration of hydrogen as an expression of "putrefactive component". Zacchia 5(4):595-603.

Smith-Sivertsen J. The origin of intravascular bubbles produced by decompression of rats killed prior to hypebaric exposure. In: Lambertsen CJ, editor; 1976; Washington, DC. Bethesda MD. p 303-309.

Tabla de contenido

3 CHAPTER III: EXPERIMENTAL MODELS OF GAS EMBOLISM

3.1 INTRODUCTION

The presence of bubbles on the venous side of the circulatory system is called Venous Gas Emboli (VGE). VGE can occur due to different causes such as accidents related to surgical procedures (Muth and Shank, 2000), trauma, criminal intervention, barotraumas (Knight, 1996) or gas-phase separation in the body after decompression (Hamilton and Thalmann, 2003). VGE has been shown to be statistically correlated with Decompression Sickness (DCS) by means of ultrasound (Sawatzky, 1991).

In the atypical beaked whale stranding in Canaries 2002 and Almeria 2006, massive gas emboli was observed grossly in the venous circulation, and more important, similar lesions to those described for human fatal diving accidents were observed (Arbelo et al., 2008; Fernandez et al., 2005; Jepson et al., 2003). Massive VGE in dead cetaceans was a new finding that needed further research. But, VGE has also been little studied in forensic science.

Gas analysis of bubbles were claimed in response to the report on gas and fat syndrome in beaked whales atypically stranded (Piantadosi and Thalmann, 2004), although there is very few empirical data on composition of gas emboli produced by decompression(Armstrong, 1939; Bert, 1878; Harris et al., 1945b; Ishiyama, 1983; Lillo et al., 1992; Smith-Sivertsen, 1976). There is even less information on gas composition related to post-mortem time. There are few more studies of air embolism applied to forensic science (Bajanowski et al., 1998a; Bajanowski et al., 1998b; Dyrenfurth, 1928; Erben and Nádvornik, 1963; Keil et al., 1980; Pedal et al., 1987; Pierucci, 1985; Pierucci and Gherson, 1968; Pierucci and Gherson, 1969; Richter, 1905).

Therefore we decided to set up three animal models with New Zeeland White Rabbits (NZWR) in which control of different variables was established in order to use as a reference of data found in stranded cetaceans. In these models we have evaluated *post-mortem* (PM) the presence of free gas employing a semi-quantitative score and gas samples were taken and analyzed by means of the methodology described on chapter II. These models consisted on:

1. Putrefaction study; where healthy animals were euthanized and allowed to decompose under control circumstances.
2. Induced air embolism study; where atmospheric air was infused into the venous circulatory system until dead of the animal.
3. Compression/decompression model; where animals were exposed to an extreme diving profile. Additionally to PM exploration of free gas, VGE was monitored by ultrasound just after surfacing and prior to death.

3.1.1 GASES AND PUTREFACTION

Decomposition is the continual process of gradual decay and disorganization of organic tissues and structures after death. It is composed of two processes: autolysis and putrefaction. Autolysis consists of the fast and intense spontaneous self-destruction of tissues by the body enzymes present in the cells, without any bacterial interference (Lerner and Lerner, 2006).

Putrefaction is the breakdown by microorganisms such as bacteria, fungi and protozoa (from the intestine and the environment) and follows autolysis (Knight, 1996). This results in the production of gases, liquids and simple molecules. Various gases (CO_2, H_2S, CH_4, NH_3, SO_2, H_2) produced in the process distend the tissues (Vass et al., 2002). Along with these, a variety of volatile organic compounds (VOCs) are liberated. These volatile substances are intermediate products of decomposition while the large biological macromolecules such as proteins, nucleic acids, carbohydrates and

lipids are broken down into their building block components (C, H, O, N, P and S) (Statheropoulos et al., 2005).

Many bacteria involved in putrefaction processes (*proteus* and *coli* species and *bacillus subtilis*) are components of the physiological flora of the intestine, that after death, reach the organs mainly via the vessels(Jackowski et al., 2005). Tissues rich in blood vessels (more dependent on oxygen and energy) are the first ones to suffer autolysis, whereas those poorly irrigated or deprived from blood vessels, like the ocular corneas, are not immediately affected by decomposition(Lerner and Lerner, 2006).

In forensic science, postmortem formation of intracardial gas has been reported using Computed Tomography (CT) and Magnetic Resonance Imaging (MRI) (Jackowski et al., 2005). Additionally gas analyses have been performed in human corpses (Bajanowski et al., 1998a; Pierucci and Gherson, 1968; Pierucci and Gherson, 1969; Statheropoulos et al., 2005) and in rabbits (Pierucci and Gherson, 1968; Pierucci and Gherson, 1969). But we haven't found any report about the amount of free gas found in veins or tissues during autopsy or necropsy and how these are form during the first PM hours.

We considered necessary to develop a semi-quantitative grading system of gas putrefaction production on the different tissues with post-mortem time using macroscopic observations during necropsies. This approach to evaluate the gas produced because of putrefaction might be of importance as well for forensic science. If there are suspicious of possible air embolism, chest radiography (or other imagine technique) is recommended in forensic science as well as explorations of veins and puncture under water of the right and left ventricles (Knight, 1996). But it is important to distinguish how much gas is because of putrefaction, how much is because of dissection and how much is because of other possible causes such as gas embolism.

3.1.2 AIR EMBOLISM

Air embolism (AE) is the entry of atmospheric or alveolar air into the vascular system and is mainly a iatrogenic problem (Muth and Shank, 2000). Depending the anatomical entry and presence of the air two broad categories can be distinguished:

Venous air embolism. Atmospheric air enters the systemic venous system and reaches the lungs, causing interference with gas exchange, cardiac arrhythmias, pulmonary hypertension, right ventricular strain, and eventually cardiac failure. Air may enter the venous systems in accidents related to surgical procedures, criminal interventions or even during pregnancy and after delivery through the veins of the myometrium (Knight, 1996; Muth and Shank, 2000; Weissman et al., 1996)

Arterial air embolism. Atmospheric air enters the pulmonary veins or directly into the arteries of the systemic circulation. The entry of gas into the aorta causes the distribution of gas bubbles into nearly all organs. Small emboli in skeletal muscles or viscera are well tolerated but the obstruction of the functional end of coronary arteries or the nutritive arteries of the brain result in severe morbidity or death. Air may enter the arteries as a result of overexpansion of the lung by decompression barotraumas (alveolar air) or as a result of paradoxical embolism. A paradoxical embolism occurs when air or gas that has entered the venous circulation manages to enter the systemic arterial circulation (Muth and Shank, 2000).

Air embolism is of growing interest since in many cases it resulted as a complication of numerous invasive medical procedures thus there are few more studies of air embolism compared to putrefaction alone, applied to forensic science. Pierucci & Gherson, (1969) carried out the largest data set on air embolism under control circumstances and versus post-mortem time, on New Zeeland White Rabbits and did some measurements in humans. Bajanowski et al. (1998) applied the parameters defined by Pierucci & Gherson (1969) to humans.

3.1.3 GASES AND DECOMPRESSION

Decompression illness is a term used to describe diseases caused by intravascular or extravascular bubbles that are formed as a result of reduction in environmental pressure (decompression). The term covers both arterial gas embolism and Decompression Sickness (DCS) (Vann et al., 2011).

In diving, arterial gas embolism usually occurs during the ascent when expanding gas stretches and ruptures alveolar capillaries (pulmonary barotraumas) allowing alveolar gas to enter the arterial circulation (Vann et al., 2011). As explained above, if breathing air, this would be arterial air embolism.

DCS alone is the disease caused by bubble formation due to gas phase separation in the body. Gas phase may arise from supersaturated gas tissues after decompression (Hamilton and Thalmann, 2003) this is when the sum of the dissolved gas tensions (oxygen, carbon dioxide, nitrogen, helium) and water vapour exceeds the local absolute pressure (Vann et al., 2011).

It is important to remind that both arterial AE and DCS can result from decompression and that they can occur simultaneously.

Nowadays, the ultrasound or Doppler is becoming widely used for evaluation of VGE after decompressions as an objective and quantitative measure of decompression stress. This method does not allow for measurement of the entire bubble population in a body, but does provide a method for detecting bubbles in the vascular system in a living organism.

There were some previous studies that had examined for macroscopic intravascular bubbles before (Harris et al., 1945b; Smith-Sivertsen, 1976) and there were as well some attempts of analyzing the gas (Armstrong, 1939; Bert, 1878; Harris et al., 1945b; Ishiyama, 1983; Lillo et al., 1992; Smith-Sivertsen, 1976). These studies

consist in different models, with different methodologies and exposures. None of them have taken into account the gases and effects produced by putrefaction together with decompression.

These models will provided us objective data about the differences in free-gas presence and abundance between the three processes if they would exist. Additionally, in the compression/decompression model, we might observe if there is any relationship between VGE monitored alive with ultrasound (which has been shown to be statistically correlated with DCS), and bubbles observed grossly PM. Thus, the animal experimental models were performed also in order to contribute to the little knowledge that there is on gas composition in the three processes, and once more, to try to find differences between them.

.

3.2 MATERIAL AND METHODS

3.2.1 ANIMALS

41 New Zeeland White Rabbits (Animal Supply Center of the Negrin Hospital, Spain and NTNU, Norway) of 2.5-3.8 kg were used split in three groups for different experimental methods: induced air embolism, control or gas putrefaction studies and compression/decompression treatment. All experiments were conducted in accordance with the European Union regulations for laboratory animals. Experimental protocols for induced air embolism and putrefaction models were approved by the Ethical Committee for Animal Experiments of the University of Las Palmas de Gran Canaria (Spain) and the Norwegian Committee for Animal Experiments approved the protocol for the compression/decompression model. 21 animals were provided by the Unit of Animal experiments of the Negrín hospital (Las Palmas de Gran Canaria, Spain) and 20 more were provided by the Unit of Comparative Medicine, St Olav University Hospital (Trondheim, Norway).

3.2.2 PRETREATMENT

All experiments were conducted under surgical anesthesia. Anesthesia used was Medetomidine (0.5 mg/kg) and Ketamine (25 mg/kg) subcutaneously. Surgical anesthesia was reached in few minutes. On the compression/decompression model an extra dose of anesthesia was given after surfacing of animals to ensure surgical anesthesia through all the experiment.

3.2.3 EXPERIMENTAL MODELS

3.2.3.1 Putrefaction gas study

10 NWZR of 2729 ± 168 g weigh were first anaesthetized and later euthanized with an injection of 200mg/ kg diluted pentobarbital intraperitoneally. Euthanized animals were kept in hermetic closed plastic boxes for biological material at room temperature (22.9-24.6°C). Complete necropsies, including gas sampling protocol described in chapter II, were carried out in each animal at different *post mortem* (PM) time. Necropsies were performed at 1, 3, 6, 12, 27, 42, 47, 53 (one animal at each PM examination time) and 67 (two animals) PM hours. Animals were identified with its PM examination time followed by a P (Putrefaction).

Fig. 3.1: Hermetic closed plastic boxes for storage of dead animals (A) and display for underwater sampling and necropsy table with time board schedule and clock for controlling PM intervals (B).

3.2.3.2 Induced Air embolism

Air embolism was induced to 11 NZWR, by venous injection of atmospheric air on previously anaesthetized rabbits. A catheter (0.36 mm I.D.) was placed in the central vein of the ear and moved centrally. Atmospheric air was infused with the use of a pump at 2.2mL/min rate until death of animal. The amount of air infused varied between 4.5 and 13mL. This experiment was performed on 11 NZWR with an average weight of 2875.55g ± 184. Dead animals were kept on hermetic closed plastic boxes for biological material at room temperature (23-25.3°C). Complete necropsies, including gas sampling protocol described in chapter II, were carried out for each animal at different PM time. Necropsies were performed at 0, 20 and 40 minutes, and 1, 3, 6, 12, 27, 42, 53 and 67 PM hours (one animal at each PM examination time). Animals were named with its PM examination time followed by AE (Air Embolism).

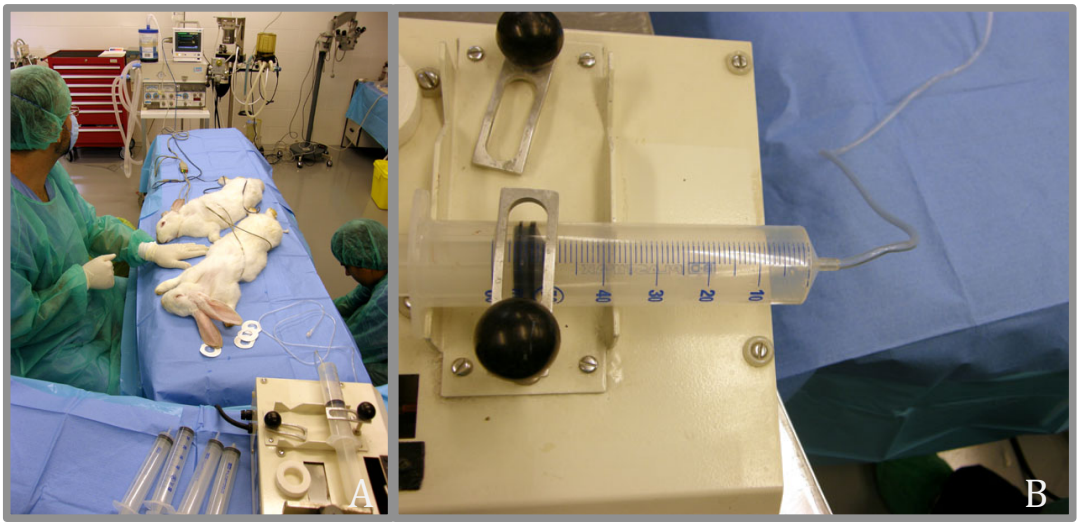

Fig. 3.2: Display for vital signs monitoring, pump and catheters for atmospheric air infusion at a control rate and anaesthetized rabbits (A). Detailed picture of the air pump(B).

3.2.3.3 Compression/decompression model

20 Anesthetized rabbits of 3570 ± 165 g weight were compressed in pairs to 8 absolute atmospheres (ATA) breathing air. They stayed there for 45 minutes followed by a fast decompression. Compression and decompression was done at a rate of 0.33m/s in a dry, hyperbaric chamber (Animal Chamber System, NUT, Haugesund, Norway). Diving profile was selected for explosive decompression induction. After decompression, the pulmonary artery and the aorta of the rabbits were monitored with the use of ultrasound for *in vivo* bubble detection. For this purpose a 10 MHz transducer connected to a FiVe ultrasound scanner (GE Vingmed Ultrasound AS, Norway) was used.

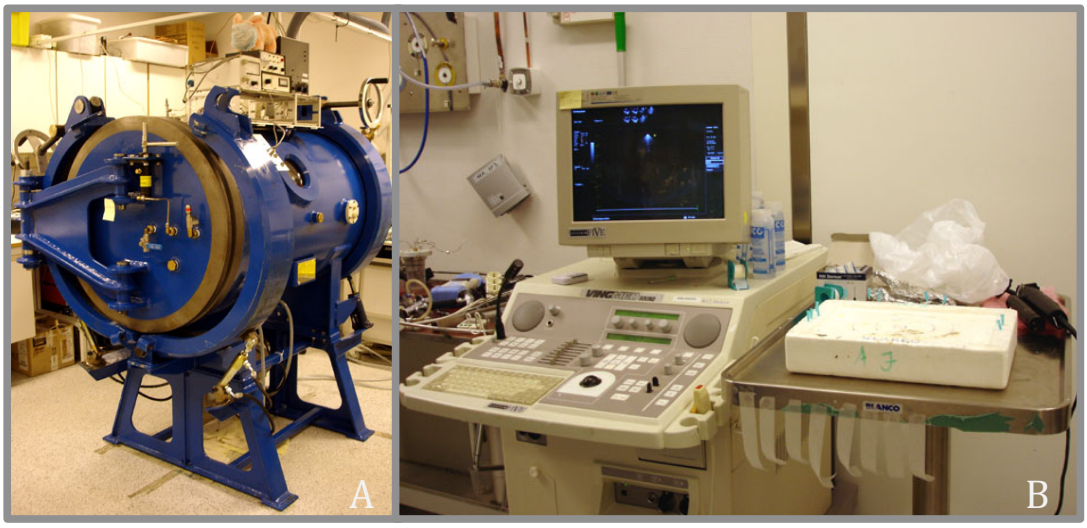

Fig. 3.3: Hyperbaric chamber (A). Ultrasound (B).

Bubbles were detected as bright spots, the number of gas bubbles was evaluated using a grading scale from 0 to 5 (Eftedal and Brubakk, 1997): grade 0 is no bubbles, 1 represents an occasional bubble, 2 represents at least one bubble every fourth heart cycle, 3 is at last one bubble every heart cycle, 4 is continuous bubbling, and 5 is massive bubbling (see appendix 9.1).

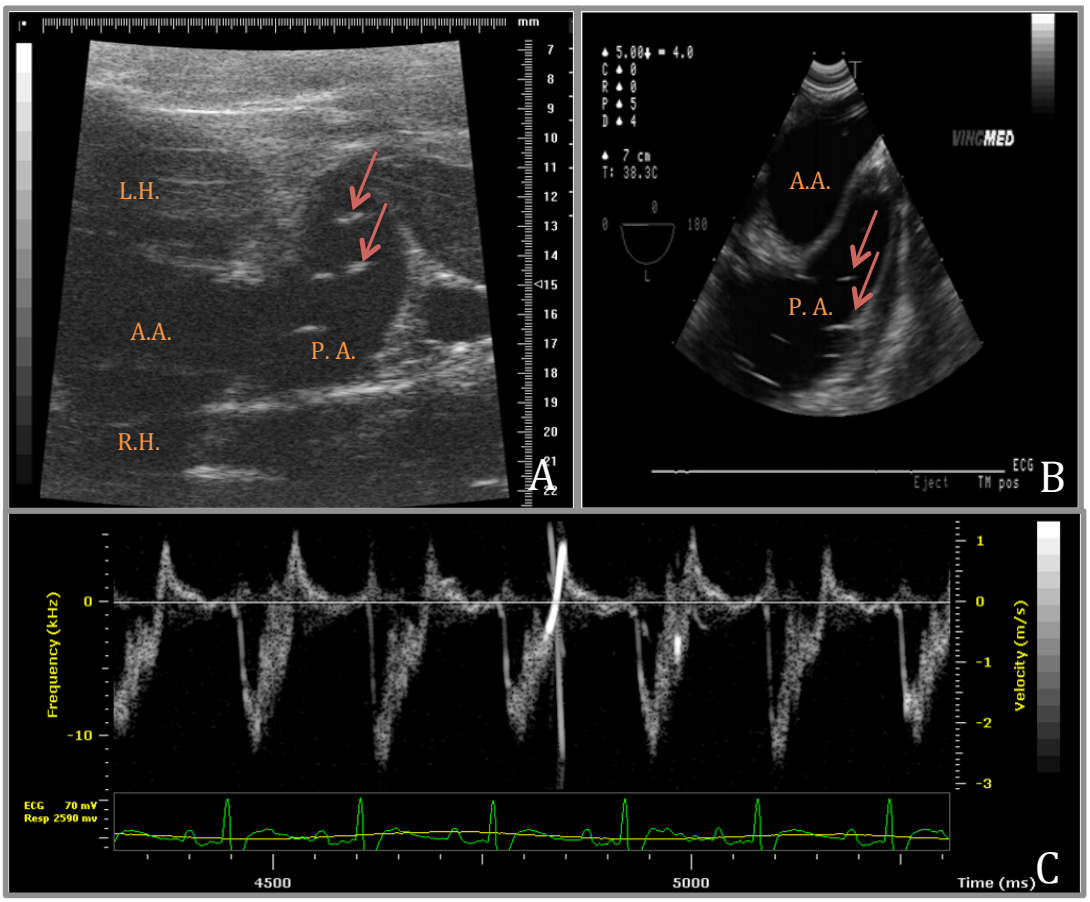

Fig. 3.4: Ultrasound images of rat hearts with bubble score 3 (A) and 4 (B). Red arrows are indicating bubbles. Anatomic features on these images are left heart (L.H.), right heart (R.H.), aortic arch (A.A.) and pulmonary artery (P.A.). Dopler image (C) where heart bytes can be observed in green, in light gray is represented the noise caused by the blood flow with each byte and in bright white is the high intensity noise reflected by the surface of the bubble. These images are used with permission of the NTNU.

Monitoring was repeated every 15 minutes. If the rabbit survived for 1 hour, it was euthanized with an intraperitoneal injection of 200mg/ kg diluted pentobarbital. Each pair of animals was examined at 0, 20 and 40 minutes, and 1, 3, 6, 12, 27, 42, 53 and 67 PM hours. Animals were named with its PM examination time followed by DCS (Decompression Sickness) and A or B to distinguish between animals.

3.2.4 NECROPSY

Tools and methods for gas sampling and analyses were discussed in chapter II, here we summarized the methodology applied to rabbits:

3.2.4.1 Dissection and external exploration

Necropsy protocols for different animals are very similar. We did use the same protocol in the rabbits that we normally use for cetaceans, except for animal position. Necropsy protocol is based on a standard procedure for cetaceans published by Kuiken and Harman (1991), the field guide for strandings of marine mammals by Geraci and Lounsbury (2005) and the domestic animal necropsy book by King et al. (1989). To these procedures some technical innovations have been added, including those reported here related to gas sampling.

For comparison reasons with cetaceans a decomposition code based on the state of conservation of the body was additionally given to each animal. The decomposition code of the body was determined following the parameters and classifications established in the protocol of necropsies of cetaceans of the European Cetacean Society (Kuiken and García-Hartmann, 1991): level 1-very fresh, level 2-fresh, level 3-moderate autolysis, level 4-advanced autolysis and level 5-very advanced autolysis. This code is as well described in appendix 9.2.1.

Rabbits were positioned in dorsal *decubitus* for the necropsy performance. Initially, the animal was explored externally in order to assure that non-perforate lesions were not present. Secondly, skin was removed. When removing the skin, we looked for bubbles on the subcutaneous vessels. If bubbles were seen, vessels were explored to confirm that they had not been cut during dissection. Then, the abdominal cavity was opened. Mesenteric and renal veins were screened for bubbles. After this

was done, the thoracic cavity was opened to have access to the heart. As soon as bubbles were detected, a photo was taken.

To evaluate bubbles abundancy found during dissection, a grading system from 0 to VI was stablished and observed in different vessels. Grade 0 is no bubbles or congestive veins, grade I is an occasional and small bubble, gradeII represents few bubbles and small discontinuities on blood flow, III is more abundant and larger discontinuities but nof filled with gas, while IV represents moderate presence of gas bubbles within an specific vein, V is abundant presence of bubbles and VI is when complete sections of the veins were filled with gas. When evaluating gas within fat tissues or subcapsular gas presence, a simpler grading from 0 to 3 was used. 0 is the absence of emphysema, 1 is scarce presence (afecting only a target organ), 2 is moderate (affecting more than one organ) and 3 is abundant (afecting many different organs). The spleen was sometimes observed to be filled with free gas. Therefore it is been recorded as 0 with no gas and 1 with gas (See appendix 9.2. Grading systems used).

After vessels exploration for bubbles, the animals were completely submerged in water for gas sampling. For gas extraction, it is important to avoid cutting large vessels during dissection of the animal. Only after bubble exploration and extraction of gas from cavities, large vessels can be cut and normal necropsy protocol can be followed.

3.2.4.1.1 Gas sampling from intestines

5mL vacutainer with no additives (BD Vacutainer® Z. ref: 367624) is directly applied to cavities with its appropriate plastic holder or adapter and a double-pointed needle. To avoid atmospheric air contamination, the needle was first inserted into the cavity for purging. Secondly the vacutainer was pushed against the double-pointed needle, and then the vacutainer was removed before the needle is released from the cavity.

3.2.4.1.2 Gas sampling from the heart cavities

Gas bubbles are separated from blood with the use of an aspirometer. For collecting the sample we only had to use a vacutainer and to open the stopcock.

3.2.4.1.3 Gas sampling from bubbles

Disposable insulin syringes (BD Plastipak U-100 insulin) were used and its content was promptly injected into a vacutainer. A new insulin syringe is used for each bubble and one new vacutainer tube was used per bubble.

Sampling was performed down the water. Bubbles were sampled only from Vena cava because here found the largest bubbles.

3.2.5 TRANSPORT AND STORAGE OF GAS SAMPLES

Vacutainers are kept upside-down at room temperature. Single samples are transported and stored together with one intact vacutainer (*blank*) per sample or a minimum of 3 blanks per samples set.

3.2.6 GAS ANALYSIS

Gas analysis was done by gas chromatography. Samples were injected manually into the gas chromatographer (Varian 450-GC) with the use of a block-pressure syringe (Supelco A-2 serie). The temperature of injector was set at 230˚C. This chromatographer was equipped with a Varian CP7430 column composed of two different sub-columns in tandem: a (Q) PoraBOND Q column, for separation of CO2 and hydrocarbons compounds up to four carbons, and a (M) Molsieve 5 A column, for

separation of permanent gases such as oxygen, nitrogen, argon, etc… For detection of these compounds it is necessary to have both; a thermal-conductivity detector (TCD), and a Flame-Ionization detector (FID), disposed one after each other. The TCD is a universal detector for permanent gases. Its temperature was fixed at 80˚C while the temperature filament was 160˚C. The FID is a selective hydrocarbons destructive detector. Because of its destructive feature, the FID must be always placed after the TCD. The temperature for the FID was fixed at 230˚C. Samples were running during 25 minutes with isotherm temperature of 45˚C and electronic controlled flux with fixed pressure of 13.1 psi on the head column. Helium was used as carrier gas.

3.2.7 GAS CALCULATIONS

Since gases are temperature and pressure dependent, calibration curves were done for every gas involved in each season. Calibration curves were done using pure gases except for oxygen and nitrogen were atmospheric air was used. Gas composition of samples was calculated in µL and µmoles from the calibration curves. To normalize samples in order to compare results, composition percentages were calculated from the µmoles.

When samples were studied, vacutainer's background was corrected by measuring it on blanks, which were always exposed to the same pressure, temperature and storage time conditions as the samples. The detection limit was set at $S_{\min} = \overline{S}_{blank} + 3s_{blank}$, where $S_{\min}$ is the minimum detectable signal, $\overline{S}_{blank}$, is the average signal for a given gas in the blanks, and s_{blank} is the associated standard deviation (Kaiser, 1947).

3.3 RESULTS

3.3.1 PUTREFACTION GAS STUDY

3.3.1.1 Free gas in tissues and/or veins

Presence and abundance of free gas in tissues and veins was evaluated with the grading systems described in the material and methods section as well as in the appendix 9.2. On the following table the different scale scores for each organ is shown. Every line represents a single animal at at each PM time.

Table 3.1: Decomposition code and PM gas bubble score in several organs for animals necropsied at different PM time

PM time (hours)	Decomposition code	Subcutaneous v.	Mesenteric v.	Femoral v.	Vena cava	Right atrium	Coronary v.	Spleen	Interstitial emphysema in fatty tissue	Subcapsular emphysema
1	1	0	0	0	0	0	0	0	*0*	*0*
3	1	0	0	0	0	0	0	0	*0*	*0*
6	2	0	1	0	0	0	0	0	*0*	*0*
12	2,5	I	II	0	0	0	0	0	*1*	*0*
27	3	II	II	II	II	0	0	0	*2*	*1*
42	4,5	III	III	III	III	IV	0	0	*2*	*1*
47	4	IV	IV	IV	IV	IV	0	0	*2*	*1*
53	4	II	II	II	II	0	0	0	*2*	*0*
67	4,5	III	IV	IV	VI	IV	0	0	*3*	*3*
67	5	V	IV	IV	VI	IV	0	0	*3*	*3*

As expected, decomposition code was observed to increase with PM time, although small inter-animal varitions were present. There was a clear tendency of increased gas production with PM time. At 6 and 12 hours PM, single or scarce bubbles

were found in some veins. At 27 hours PM, scarce to few bubbles could be find disseminated as well as some evidences of gas putrefaction (such as subcapsular gas). This PM time was coincident with decompostion code 3.

Gas from the heart was recovered only after 42 hours PM, corresponding to decomposition code IV or higher. Interindivdual variations were very evident between rabbits necropsied at 42 and 53 hours PM. The animal done at 42 hours PM was more decomposed that the animals of 53 hours PM, and more gas was found on the first animal than in the later. Median and interquartil range values for animals in which gas was recovered from the right heart was of 0.7±1.1 mL.

Subcapsular emphysema start to appear after 27 hours PM.

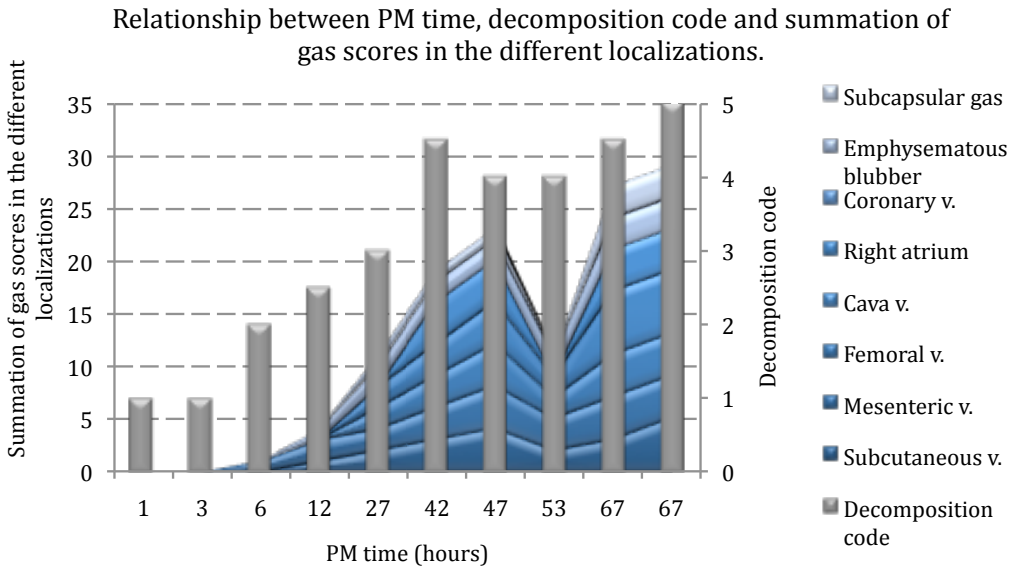

Fig. 3.5: Cumulative gas score in the different localizations along PM time and its relationship to decomposition code.

According to the above figure, animal necropsied at 53 hours PM seemed to be an outlier. If we removed this animal from the graph, the tendency of gas appearance with PM time becomes more evident.

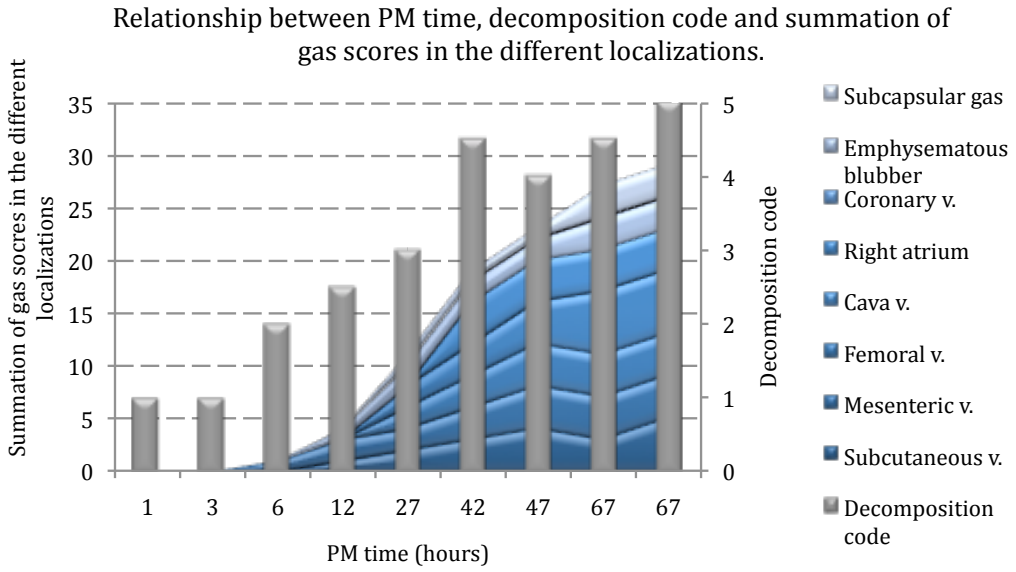

Fig. 3.6: Cumulative gas score in the different localizations along PM time and its relationship to decomposition code without animal necropsied at 53 hours PM.

Spleen morphology was found to be normal regardless decomposition code; no evidences of gas accumulation were seen in any of the ten rabbits.

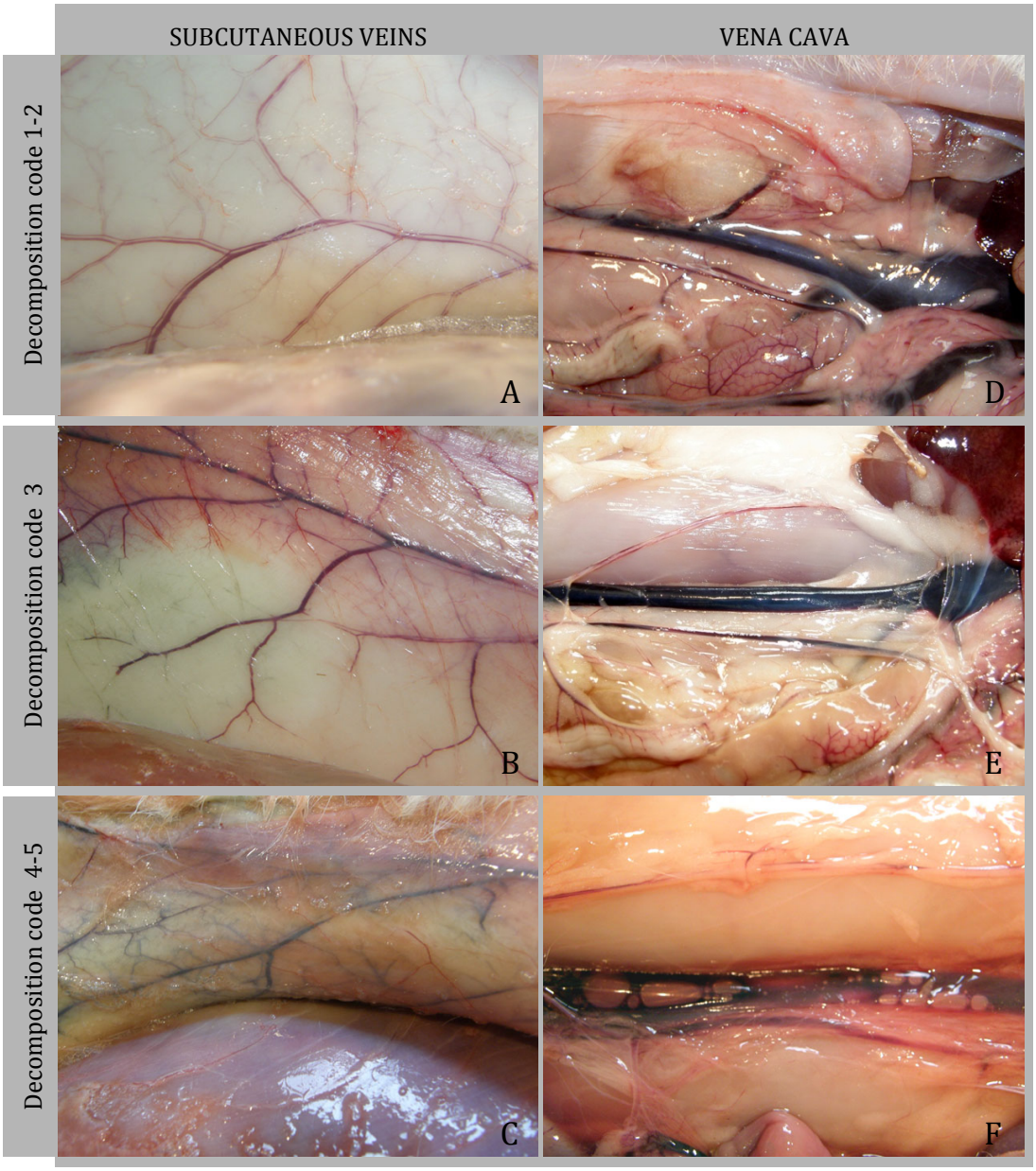

Fig 3.7: Pictures showing putrefaction evolution in organs with different decomposition codes and gas due to putrefaction. Subcutaneous veins with decomposition code 1-2 (A), 3 (B) and 4-5 (C). Vena cava with decomposition code 1-2 (D), 3 (E) and 4-5 (F).

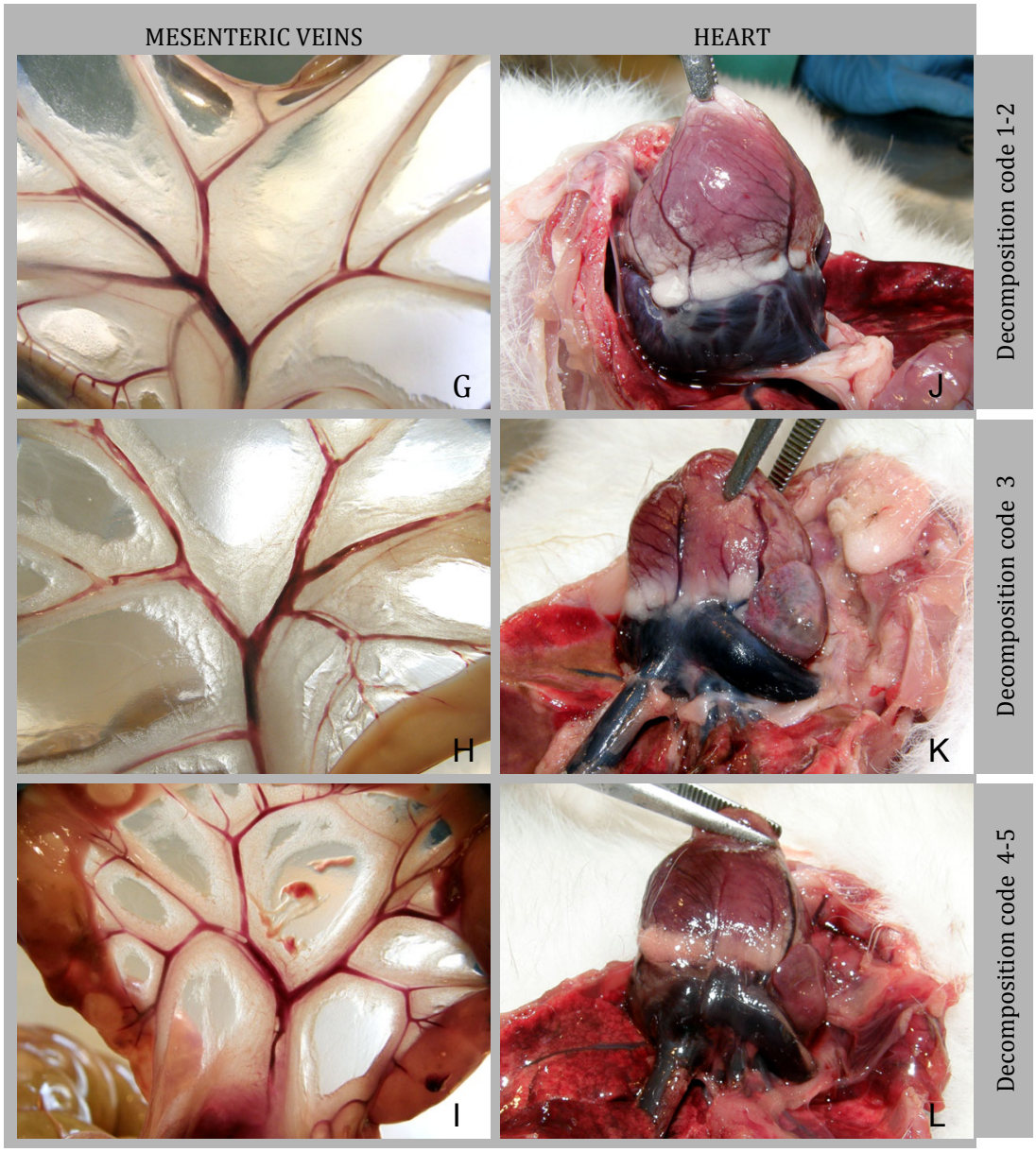

(Follow up) Fig 3.7: Pictures showing putrefaction evolution in organs with different decomposition codes and gas due to putrefaction. Mesenteric veins with decomposition code 1-2 (G), 3 (H) and 4-5 (I). Heart with decomposition code 1-2 (J), 3 (K) and 4-5 (L).

3.3.1.2 Gas composition

41 gas samples were obtained. A summary of average mole fraction expressed as a percentage of gas composition of samples of each animal can be observed in appendix 10.1.1.

Regarding gas composition of the intestine, there was a large variation between animals. However, some slight trends could be observed. Before 27 hours PM nitrogen and CO_2 percentages alternated, but after this time, CO_2 was always the main compound. The highest values for nitrogen and CO_2 were of 61.55% and 81.13% respectively. Except for one case (Intestine 1, 3h PM) contribution of methane to total percentage became relevant only after 27 hours PM. Appearance of H_2 in intestine was random and did not seem to have any relationship to PM time or decomposition code (Fig. 3.8).

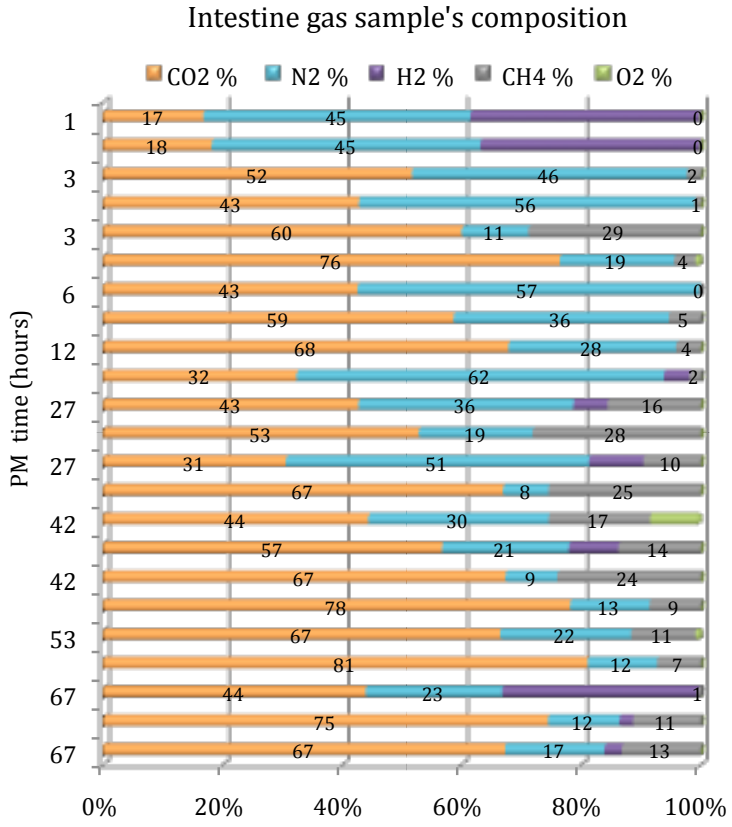

Fig. 3.8: Intestinal gas sample composition of each animal *vs.* PM time illustrating the contribution of each gas to the total amount in µmol percentage.

Abundant subcapsular emphysema was only observed after 67 hours PM. In the rabbit necropsied at 27 hours PM, gas was found inside the pericardial sac with atmospheric air like composition. Regarding the other subcapsular gas samples, similar compositions were found besides they belong to two animals and were found within different organs. Gas was composed of a mixture of CO_2, nitrogen and hydrogen in similar proportions. Only in one animal this composition was similar to that found in the intestine.

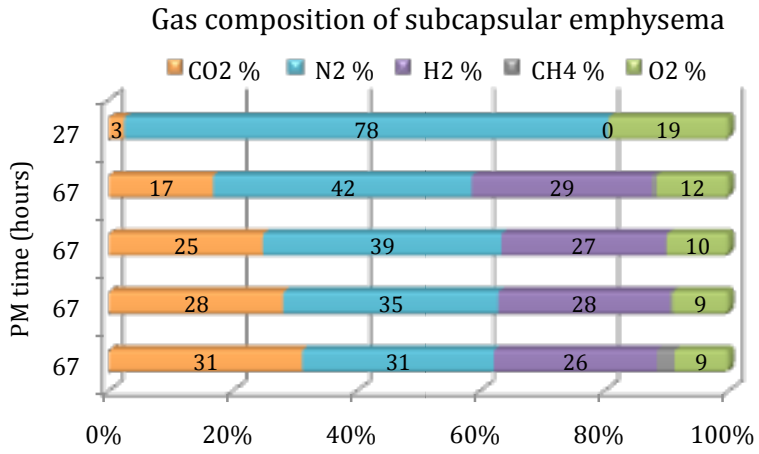

Fig. 3.9: Gas composition of subcapsular emphysema samples *vs.* PM time illustrating the contribution of each gas to the total amount in µmol percentage.

Heart gas samples were only recovered after 42 hours PM as previously mentioned. Gas in the left heart was exclusively found in the most decomposed rabbit (67PM h B) with a decomposition code of 5. Gas composition of the left heart was almost identical to the one of the right heart. Gas composition was not similar to that of the intestine, but similar to the subcapsular gas samples. Right heart gas composition at 42 hours PM was identical to atmospheric air and therefore considered as air pollution and eliminated from further studies. In all the rest samples, hydrogen was the dominant gas, similar to what was seen in subcapsular gas samples. The highest values for nitrogen and CO_2 were 63.71% and 43.41% respectively. Oxygen was always present but in variable quantities in both, subcapsular and heart gas samples.

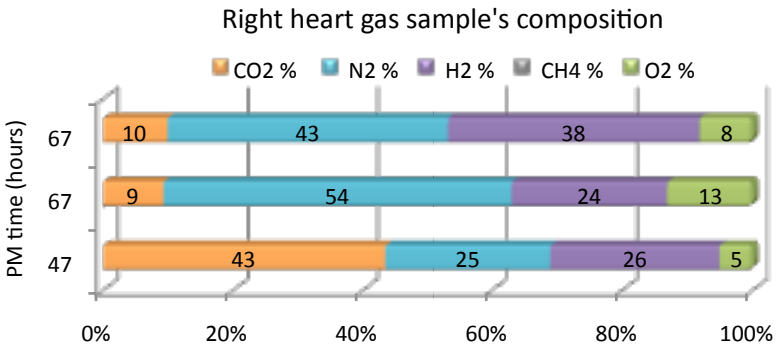

Fig. 3.10: Right heart gas composition of each animal *vs.* PM time, illustrating the contribution of each gas to the total amount in µmol percentage.

3.3.2 INDUCED AIR EMBOLISM

3.3.2.1 Free gas in tissues and/or veins.

Rabbits survived for various times. Thus, since air infusion rate was the same for all of them (x minutes), total injected volume was different.

Evaluation of the amount of gas bubble was done using the same grading system described for the putrefaction gas study and summarized in the appendix 9.2.

In the following table is represented the different bubble scores for each organ. Total injected air volume (mL) is noted in the third column. Every line represents a single animal. Peripheral veins were not always affected. Subcapsular gas start to appear after 27 PM hours which corresponds to decomposition code 3 or slightly higher. In addition emphysema in the fatty tissues started to be apearant at this PM time.

Decomposition code was observed to increase with PM time, with smaller inter-animal varitions than in the putrefaction model.

Table 3.2: .Decomposition code and gas abundancy score in several organs for animals necropsied at different PM time.

PM time (hours)	Decomposition code	Injected air (mL)	Subcutaneous v.	Mesenteric v.	Femoral v.	Vena cava	Right atrium	Coronary v.	Spleen	Interstitial emphysema in fatty tissues	Subcapsular emphysema
0	1	13	0	0	0	0	IV	IV	0	*0*	*0*
0,3	1	9	0	I	0	0	IV	0	0	*0*	*0*
0,6	1	5	0	0	0	V	V	V	0	*0*	*0*
1	1	13	I	V	IV	IV	IV	IV	0	*0*	*0*
3	1	6	I	V	IV	IV	V	IV	0	*0*	*0*
6	2	9	0	V	V	V	VI	I	0	*0*	*0*
12	2	8	V	VI	V	VI	VI	V	0	*1*	*0*
27	3,5	7	III	VI	V	V	VI	V	1	*2*	*1*
42	4,5	4,5	IV	VI	V	VI	V	V	0	*2*	*1*
53	5	6,5	V	VI	V	VI	V	V	1	*3*	*2*
67	5	8	IV	VI	IV	VI	V	0	0	*3*	*3*

Although infused air volume was not the same in all the animals, still a tendency for increasing gas production with PM time was observed. Main difference respecting putrefaction model was gas the higher starting level of gas. Median and interquartil range values for mL recovered from the right heart were of 2.2±3.

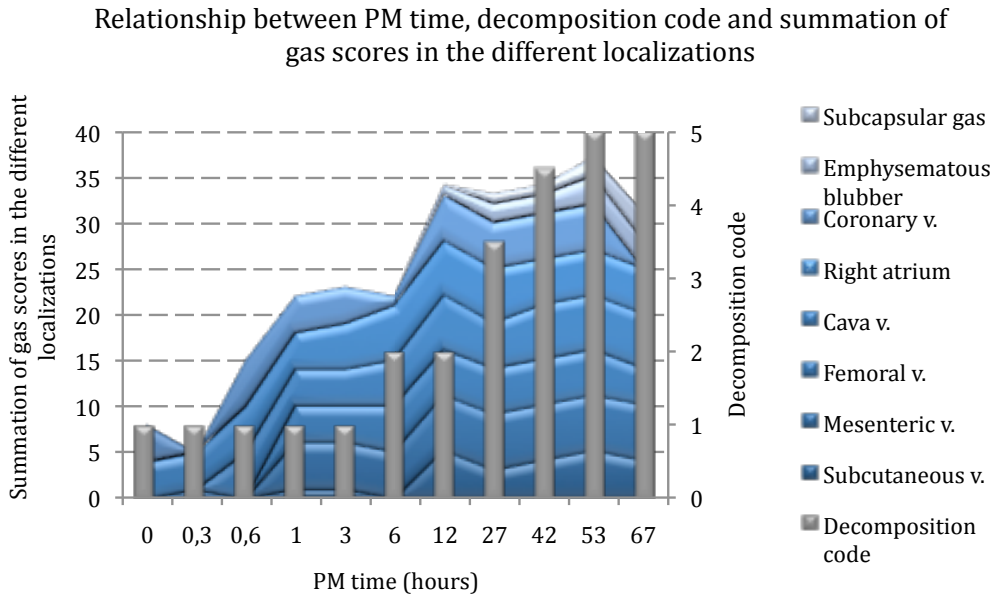

Fig. 3.11: Cumulative gas score in the different localizations at different PM time and its relationship with decomposition code.

Spleen was filled with free gas in two of eleven rabbits (18%). The 9 remaining rabbits had normal morphologies, without evidences of gas accumulation.

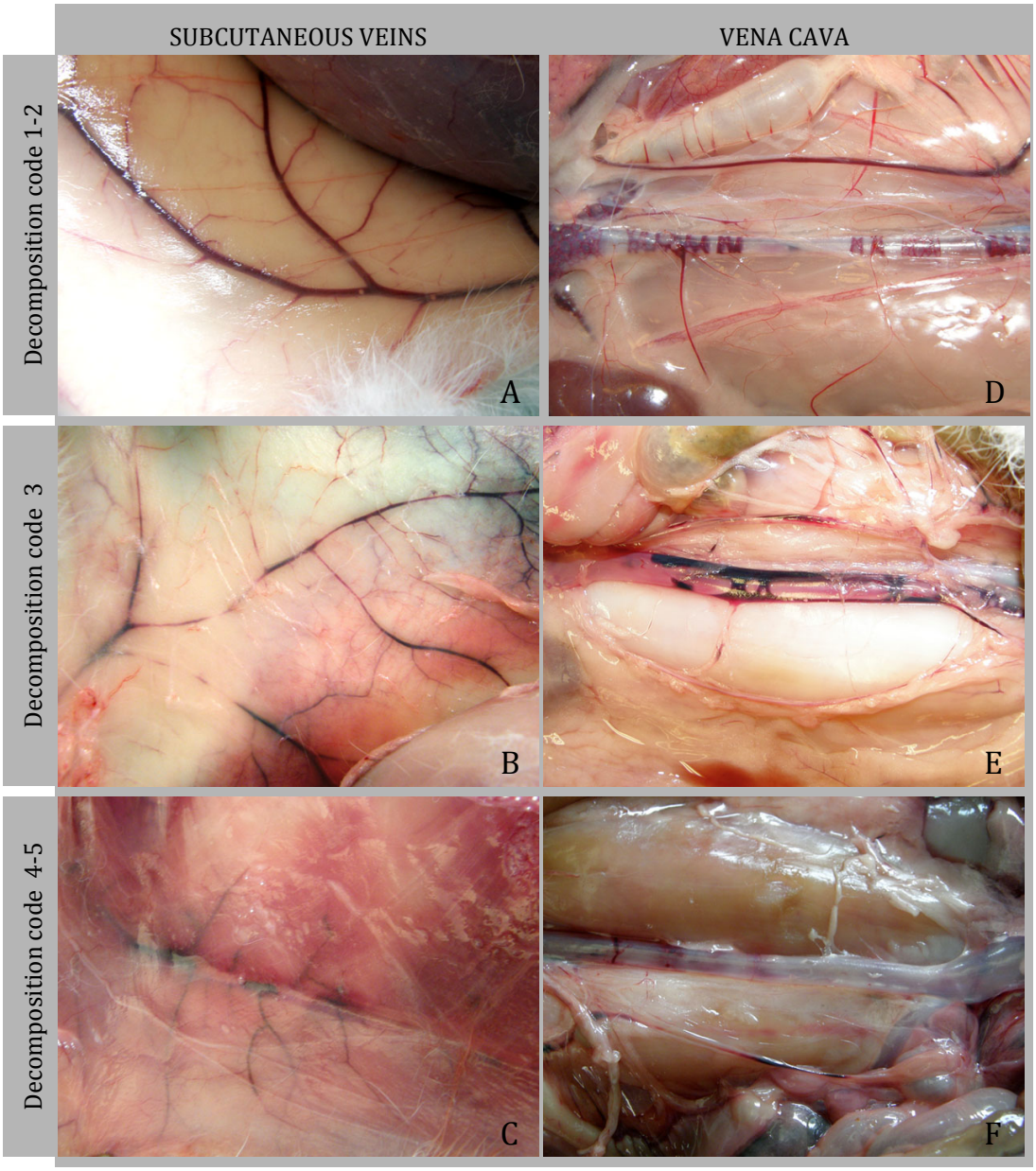

Fig 3.12: Pictures showing putrefaction evolution in organs with decomposition codes and summation of gas from air embolism and gas due to putrefaction. Subcutaneous veins with decomposition code 1-2 (A), 3 (B) and 4-5 (C). Vena cava with decomposition code 1-2 (D), 3 (E) and 4-5 (F).

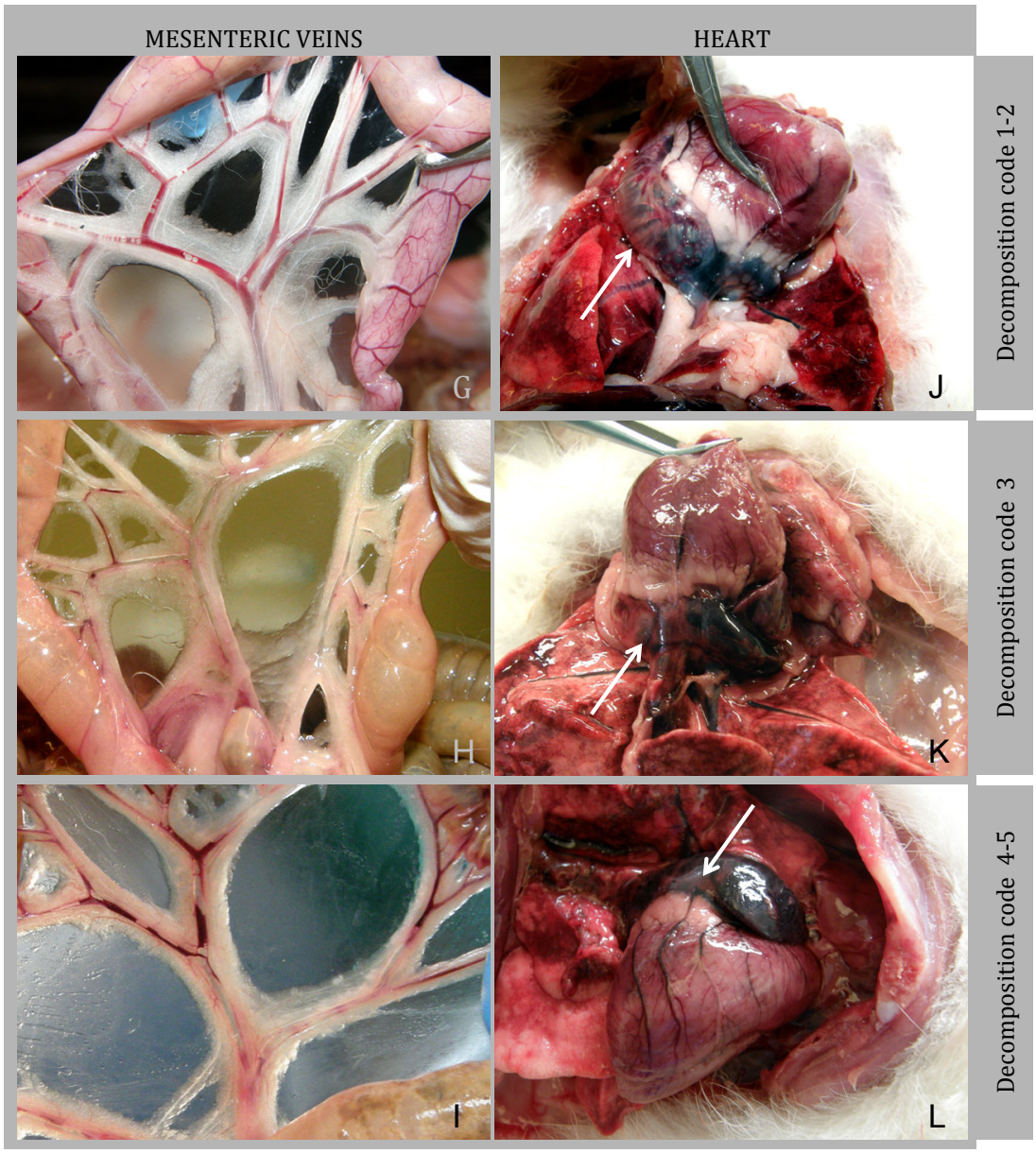

(Follow up) Fig 3.12: Pictures showing putrefaction evolution in organs with decomposition codes and summation of gas from air embolism and gas due to putrefaction. Mesenteric veins with decomposition code 1-2 (G), 3 (H) and 4-5 (I). Heart with decomposition code 1-2 (J), 3 (K) and 4-5 (L).

3.3.2.2 Gas composition

56 gas samples were obtained. A summary of average mole fraction expressed as a percentage of gas composition of samples of each animal can be observed in appendix 9.3.

Regarding intestine gas composition, except for three cases, CO_2 was always the major compound reaching values as high as 100%. On the same rare cases, nitrogen levels were about 70% while on the rest of the sample nitrogen levels were always lower than 25%. Although hydrogen and methane seemed to have a random appearance, they appear more frequently and in higher concentration in the most decomposed samples. After 12 hours PM, the summation of hydrogen and methane reached values close to the 50% of the sample composition.

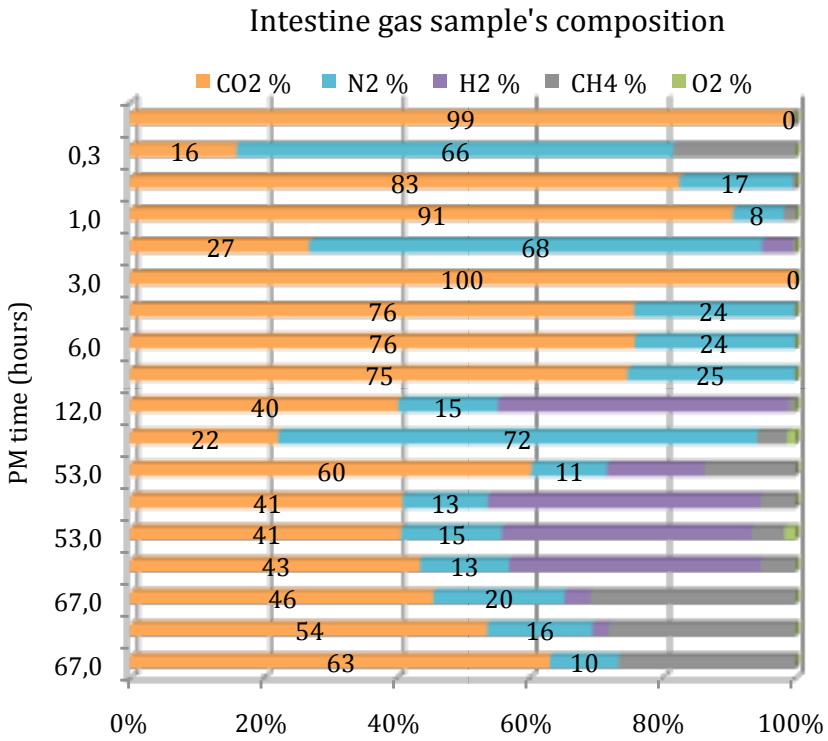

Fig. 3.13: Intestinal gas sample composition *vs* PM time illustrating the contribution of each gas to the total amount in percentage µmol.

Gas emboli sample composition from different localizations seemed to be very similar for each animal. N_2 started with high values of around 80% and decreased fast after the first 12 PM hours. CO_2 increased more linearly to reach similar or higher values than nitrogen after 42 PM hours. Hydrogen appeared mainly after 42 PM hours that corresponds to decomposition code 4.5. Methane was almost always present but in concentrations lower than 5%, while oxygen presence was very rare.

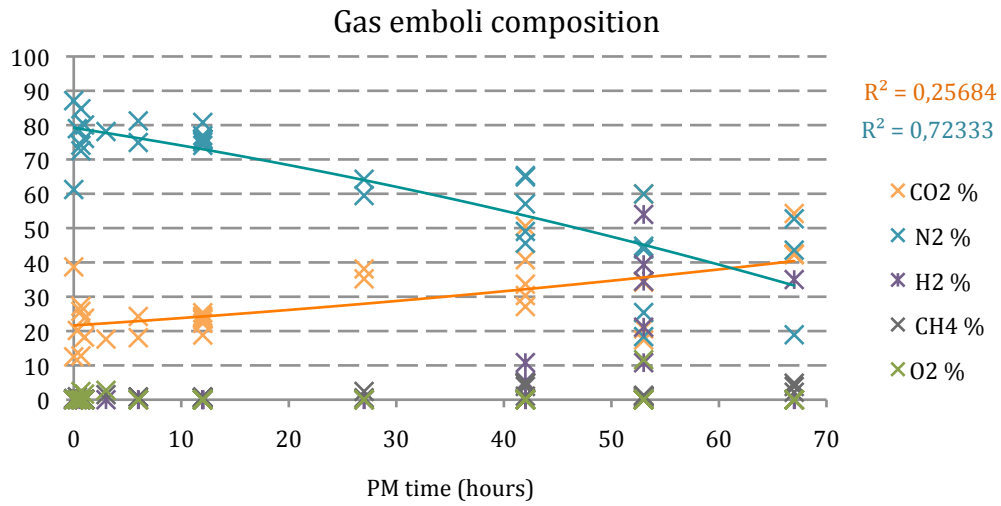

Fig. 3.14: Gas emboli composition from different localizations (heart, vena cava and aorta) taken at a given PM time. Regression line for nitrogen is in blue and for CO_2 in orange color.

Although the similarities of gas emboli components found in different localizations, gas sample composition after some hours PM appeared to be more disperse (Table 3.3).

Table 3.3: Percentage average of gas samples composition (µmol) and its standard deviation for each range time and decomposition code. In the last column it is represented the contribution of each gas to the total composition.

PM time	Decomposition code	% H_2	% O_2	% N_2	% CH_4	% CO_2	
0-12 h	1-2	0	0.4(0.8)	77(5.5)	0.5(0.4)	22.2(5.9)	N_2>> CO_2
27 h	3.5	0	0	61.9(3.4)	1.5(1.3)	36.6(2)	N_2> CO_2
42 h	4.5	3.2(4.3)	0	56.4(8)	3.9(1.5)	36.5(8.4)	N_2>CO_2>H2
53 h	5	32(16.7)	2.3(5.2)	38.5(16.6)	0.8(0.4)	20.4(22.3)	N_2>H2>CO_2
67 h	5	14.67(20.2)	0	38.4(17.5)	3.61(1.3)	46.3(6.9)	CO_2>H2>N_2

Therefore dataset was divided in two time ranges: before and after 12 hours PM. Before 12 hours PM dataset was very homogenous regardless sample localization (Fig: 3.15). Gas composition was mainly nitrogen (76.93%) and CO_2 (22.17%) (Table: 3.3).

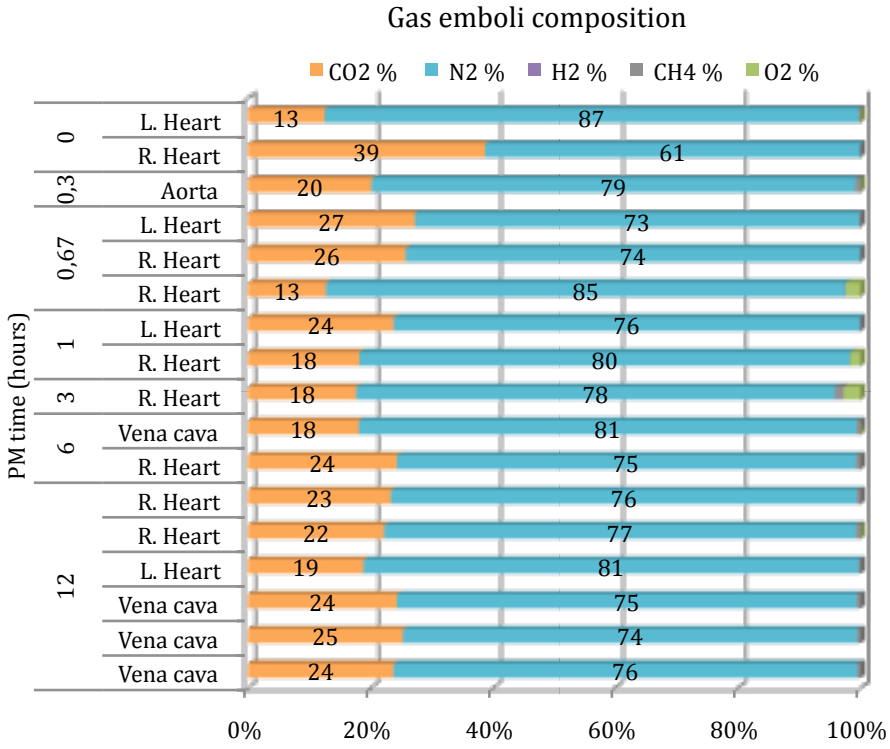

Fig. 3.15: Gas emboli composition from different localizations (heart, Vena cava and Aorta) *vs.* PM time illustrating the contribution of each gas to the total amount in percentage µmol for the first 12 PM hours.

At 27 hours PM (decomposition code 3.5), gas sample composition was still very similar between the different tissues but nitrogen levels started to decrease. After 42 hours PM, (decomposition code 4 or higher), variability between samples started to increase at the same time as hydrogen contribution to total composition became important.

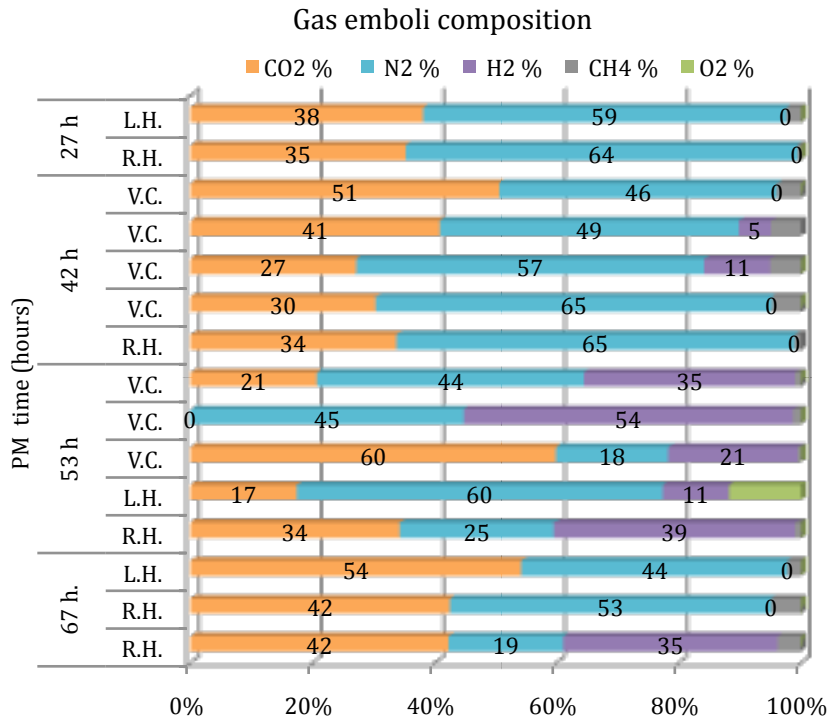

Fig. 3.16: Gas emboli composition from different localizations (heart, vena cava and aorta) *vs.* PM time illustrating the contribution of each gas to the total amount in percentage µmol for the first 12 PM hours.

Higher variability was found in the vena cava; therefore right heart and vena cava gas composition were explored again separately. By doing this, tendencies described above were confirmed in the right heart but with better adjustment, especially for CO_2, to the regression line.

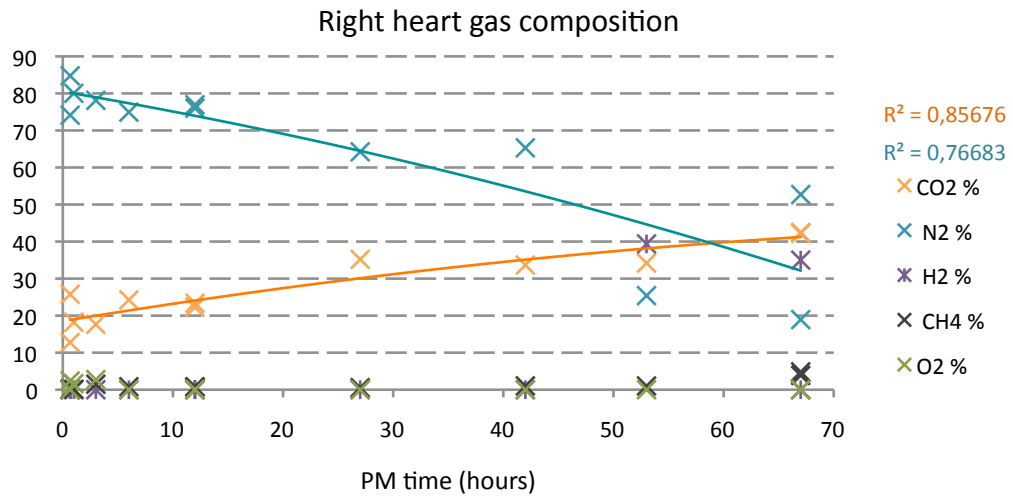

Fig. 3.17: Gas emboli composition from different localizations (heart, Vena cava and Aorta) taken at a given PM time. Regression line for nitrogen is in blue and for CO_2 in orange color.

Regarding vena cava, variability for CO_2% µmol was very high and no good adjustment was found. Additionally hydrogen was of higher importance in vena cava gas samples.

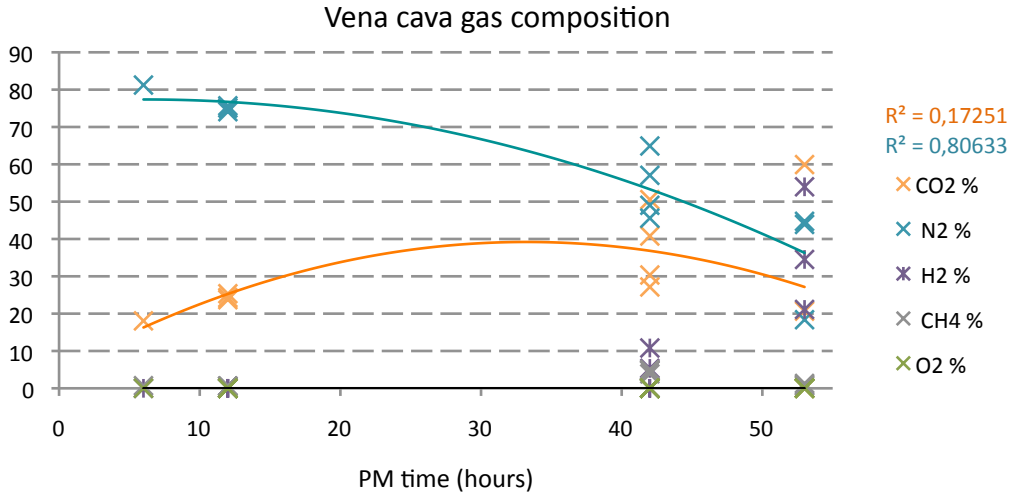

Fig. 3.18: Gas emboli composition from different localizations (heart, vena cava and aorta) taken at a given PM time. Regression line for nitrogen is in blue and for CO_2 in orange color.

When comparing both regression lines of CO_2 and nitrogen in right heart versus vena cava gas samples, higher stability and better regression adjustments in gas composition were found in the right heart.

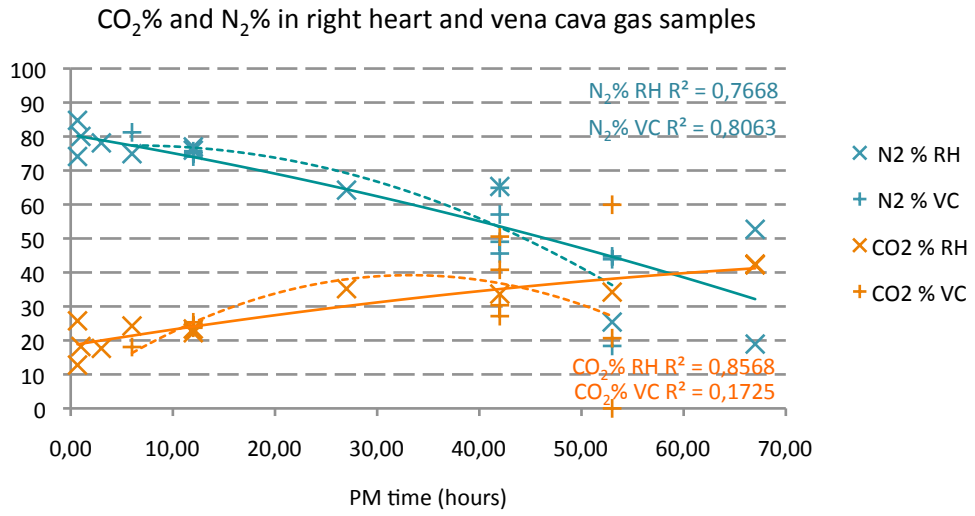

Fig. 3.19: Evolution of CO_2% (in orange) and N_2% (in blue) from heart and vena cava gas samples with PM time. Continuous lines represent regression lines for right heart, while discontinuous lines are regression curves for vena cava gas samples. The percentages are expressed in molar scale.

3.3.3 COMPRESSION/DECOMPRESSION MODEL

3.3.3.1 Free gas in tissues and/or veins

The response to the extreme diving profile was very heterogeneous, even in the same animal specie with similar sex, weigh and experimental protocol. There were several animal with none (bubble grade 0) or occasional bubbles (bubble grade 1). More than half of the animals had bubble grade 4 or higher.

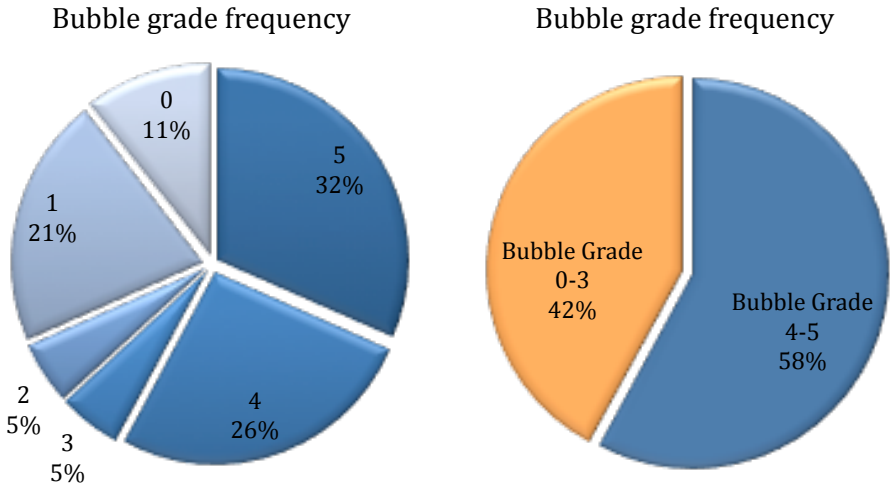

Fig. 3.20: On the left side, it is shown the frequency found for each bubble grade (0-5). On the right side bubble grades are grouped from 0-3 (orange color) and from 4-5 (blue color) to illustrate the percentage of animals that might have severe DCS against those with a lower response to the same diving profile.

This high variability was reflected in all studied parameters. One parameter specially affected was the total amount of gas recovered from the Heart with the aspirometer. The highest amount of gas recovered from the right heart in animals with bubble grade ranging 0-3 (represented in orange) was 0.35 mL, while the minimum values for rabbits with bubble grade 4-5 (represented in blue) were 2 mL and the maximum of 12mL. Median and interquartil range for both of groups are of 0.17±0.3 mL and 4±3.5mL respectively.

The following graph shows de amount of gas recovered after death from the R.H. expressed in mL of each animal. Colors referred to the bubble grade measure by means of ultrasound *in vivo*. Animals are grouped in pairs as they were dived. First bar of each pair represents animal named *A*, and the second one represents animal *B*.

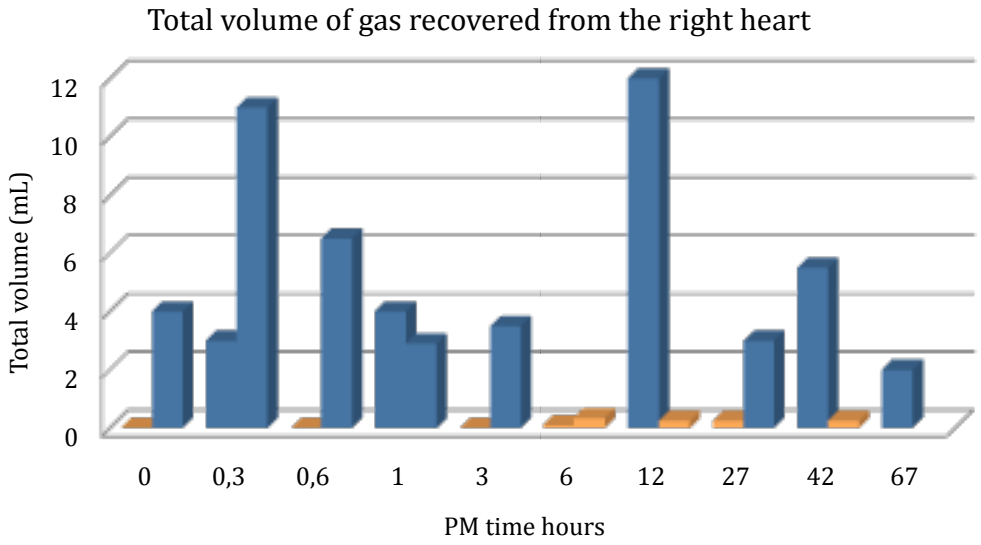

Fig. 3.21: Each bar represents total volume (mL) recovered from the right heart of each animal. Animals are grouped in pairs and associated with their PM examination time. Orange bars indicate the animals that had bubble grade 0-3, and blue bars are bubble grade 4 or higher.

All the animals with bubble grade 0-3 measured by means of ultrasound survived for at least one hour and were therefore euthanized. Animals with bubble grade 4-5 survived for very different times but all of them died within few minutes after surfacing (5-35 minutes).

Because of the high disparity in the data, affected parameters from animals with bubble grade 3 or lower will be represented separately from those with bubble grade 4 or higher.

3.3.3.1.1 Bubble grades 1-3

In animals within this bubble grade range, very few or none bubbles were observed during PM examination. The following table represents the different PM bubble scale scores for each organ (See tables in 6. Grading systems used) of animals that had bubble grade 0-3 measured by means of ultrasound. Every line represents a single animal. Missing PM examination times corresponds to animals that had bubble grade 4 or higher and are therefore considered a part on chapter 3.3.2.1.2.

Table 3.4: Decomposition code and gas abundancy score in several organs for animals that had bubble score 4 and 5 and were necropsied at different PM time.

PM time (hours)	*Decomposition code*	Bubble grade	Subcutaneous v.	Mesenteric v.	Femoral v.	Vena cava	Right atrium	Coronary v.	Spleen	Gas within fatty tissue	Subcapsular gas
0	1	1	0	0	0	0	0	0	0	*0*	*0*
0,4	1	0	0	0	0	0	0	0	0	*0*	*0*
3	1	3	0	0	0	0	0	0	0	*0*	*0*
6	2,5	0	0	0	0	0	0	0	0	*0*	*0*
6	2,5	1	0	0	0	0	0	0	0	*0*	*0*
12	2,5	2	0	0	0	0	0	0	0	*0*	*0*
27	3	1	0	II	0	0	IV	IV	0	*2*	*1*
42	4	1	0	III	0	0	IV	0	0	*2*	*1*

Only small amount of gas was found after 27 PM hours, which corresponds with decomposition code 3.

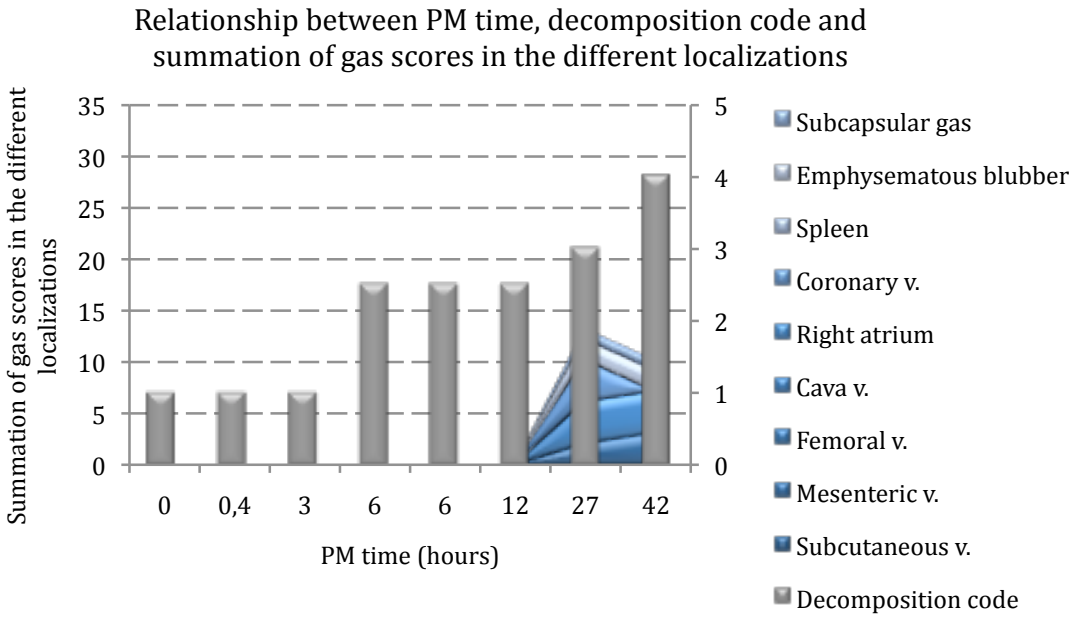

Fig. 3.22: Cumulative gas appearance in different tissues at different PM time and its relationship with decomposition code.

Spleen morphology was found to be normal according to its decomposition code, without evidences of gas accumulation in any of the 8 rabbits.

3.3.3.1.2 Bubble grades 4-5

In animals that had bubble grade 4 or 5, gas was abundant and disseminated in the entire organism independently of PM time or decomposition code. The only parameter that had a tendency being related to PM time was subcapsular gas. It started to appear at 12 hours PM with a decomposition code of 2.5.

In the following table the different scale scores for each organ of animals (See tables in 6. Grading systems used) with bubble grade 4 and 5 is shown. Every line represents a single animal. Missing PM examination times corresponds to animals that had bubble grade 3 or lower and were previously considered on chapter 3.3.2.1.1.

The Spleen was found filled with gas in three of eleven rabbits (27%). The eight remaining rabbits had normal morphologies, without evidences of gas accumulation.

Table 3.5: Decomposition code and gas abundancy score in several organs for animals that had bubble score 4 and 5 and were necropsied at different PM time.

PM time (hours)	Decomposition code	Bubble grade	Subcutaneous v.	Mesenteric v.	Femoral v.	Vena cava	Right atrium	Coronary v.	Spleen	Gas within fatty tissue	Subcapsular gas
0	1	4	V	V	V	V	IV	V	0	*2*	*0*
0,3	1	5	VI	V	V	V	V	V	0	*2*	*0*
0,3	1	4	VI	V	VI	VI	VI	V	0	*2*	*0*
0,6	1	5	V	VI	VI	V	V	V	0	*2*	*0*
1	1	4	VI	V	V	VI	V	I	0	*1*	*0*
1	1	5	VI	V	VI	VI	VI	IV	0	*1*	*0*
3	1	4	VI	V	VI	VI	V	I	1	*1*	*0*
12	2,5	5	VI	VI	VI	VI	VI	VI	1	*2*	*1*
27	3,5	4	VI	VI	VI	V	V	V	1	*3*	*1*
42	3,5	5	VI	VI	V	V	V	IV	0	*3*	*2*
67	4,5	5	VI	V	V	V	IV	IV	0	*3*	*3*

In the following graph the amount of gas found disseminated in the organs related to PM time can be seen (Fig: 3.23).

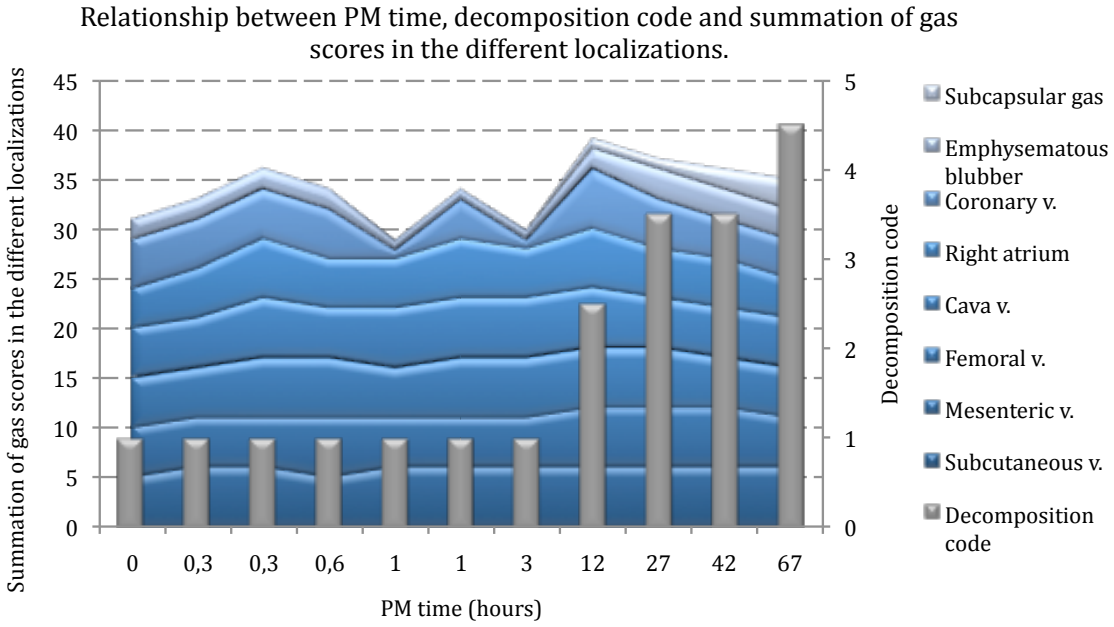

Fig. 3.23: Cumulative gas appearance on different tissues along PM time and its relation ship to decomposition code

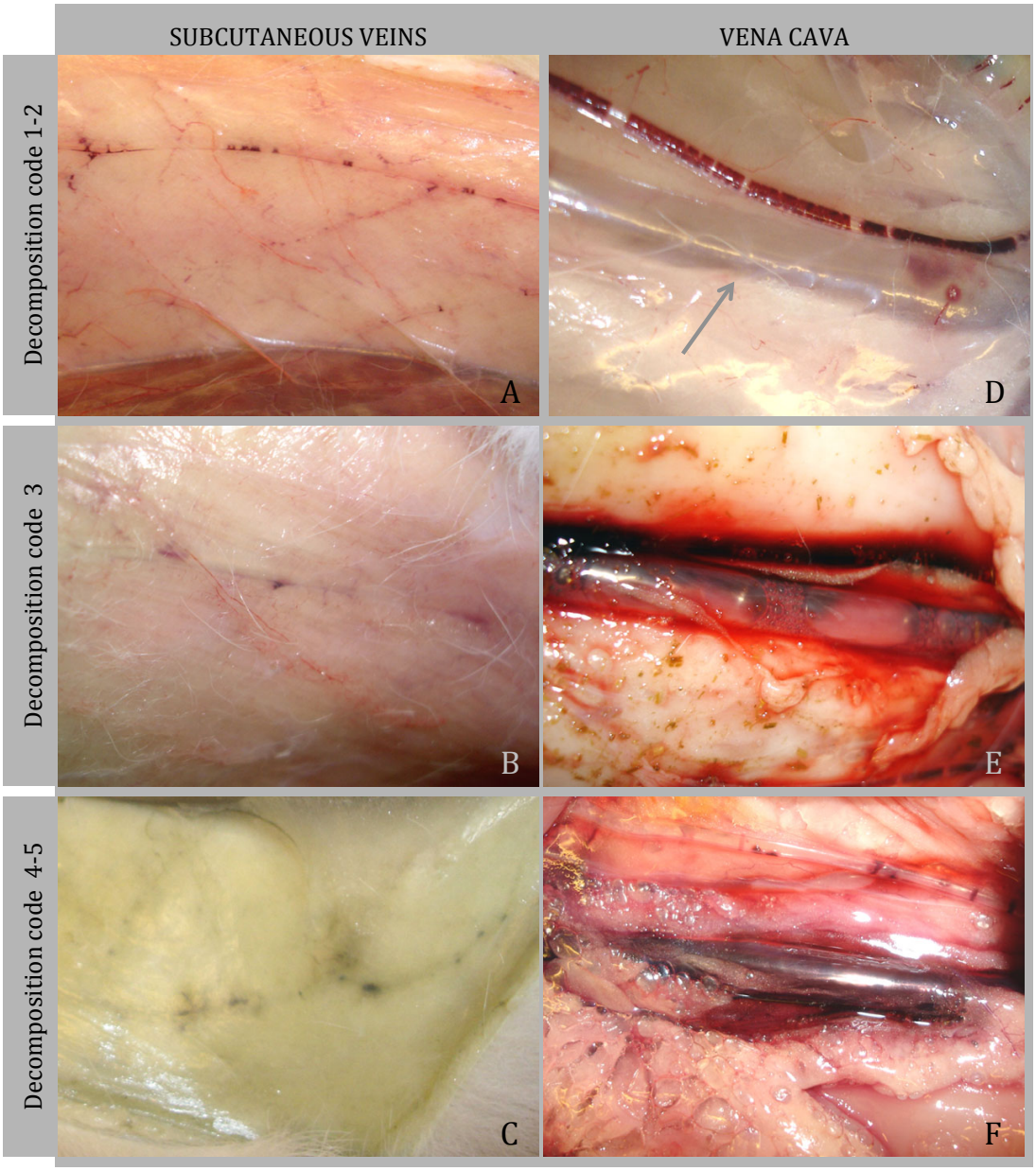

Fig 3.24: Pictures showing putrefaction evolution in organs with decomposition codes and summation of gas formed by decompression and gas due to putrefaction. Subcutaneous veins with decomposition code 1-2 (A), 3 (B) and 4-5 (C). Vena cava with decomposition code 1-2 (D), 3 (E) and 4-5 (F).

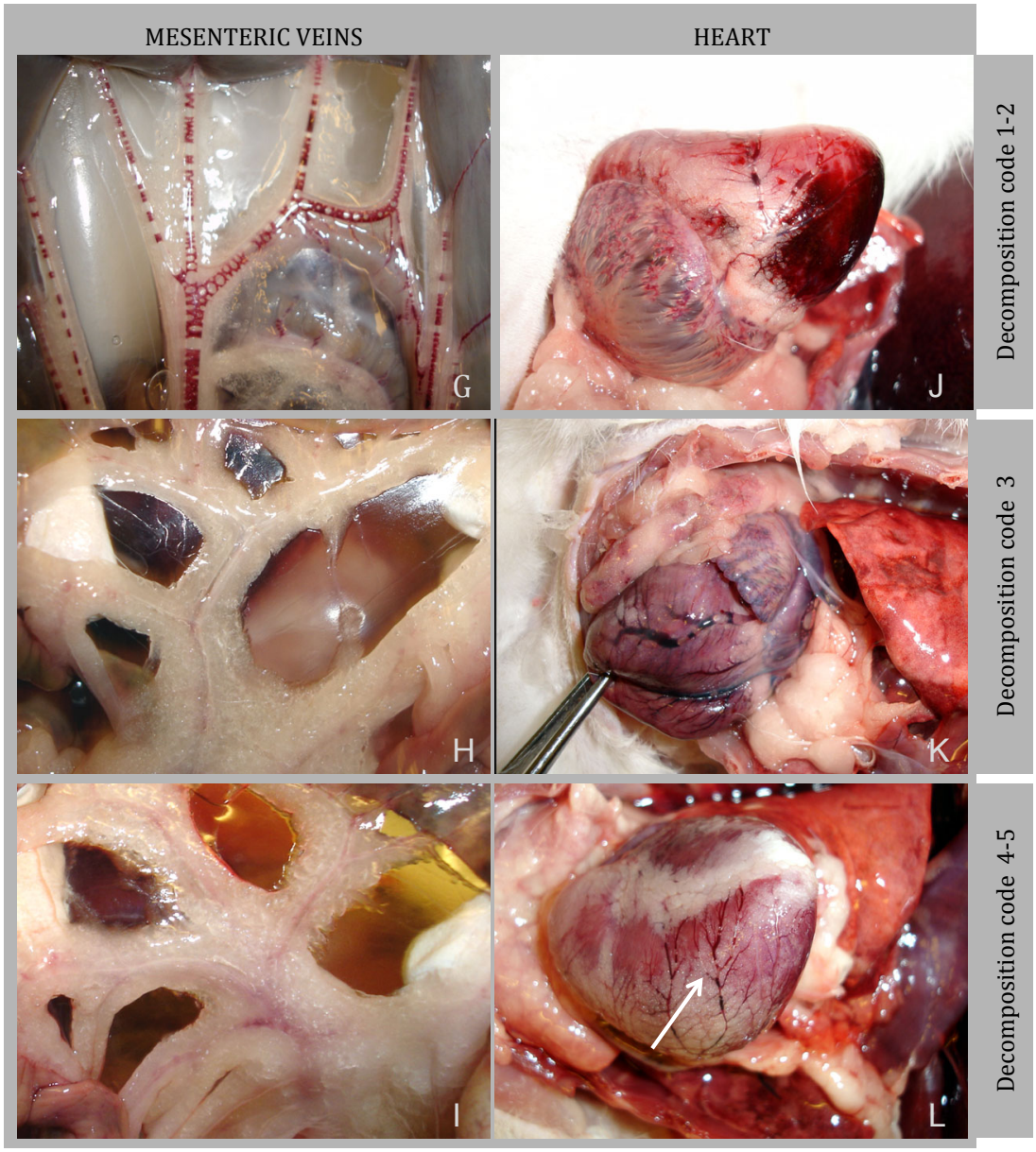

(Follow up) Fig 3.24: Pictures showing putrefaction evolution in organs with decomposition codes and summation of gas formed by decompression and gas due to putrefaction. Mesenteric veins with decomposition code 1-2 (G), 3 (H) and 4-5 (I). Heart with decomposition code 1-2 (J), 3 (K) and 4-5 (L).

3.3.3.2 Gas composition

71 gas samples were obtained. A summary of average mole fraction expressed as a percentage of gas composition of samples for each animal can be observed in appendix 9.3. Animals not represented here had no gas samples recovered successfully.

On this model, gas composition of intestine had a more stable composition between animals and PM time. Major compound in all the samples (except for the 20 min DCSA sample) was CO_2, reaching values as high as 91.56%. Correspondingly N_2 values were lower than on the previous models, having a maximum value of 38.94%. Most samples had a composition with values of 45-70 % CO_2, 10-30% N_2, and 8-15% of CH_4 (Fig. 3.25).

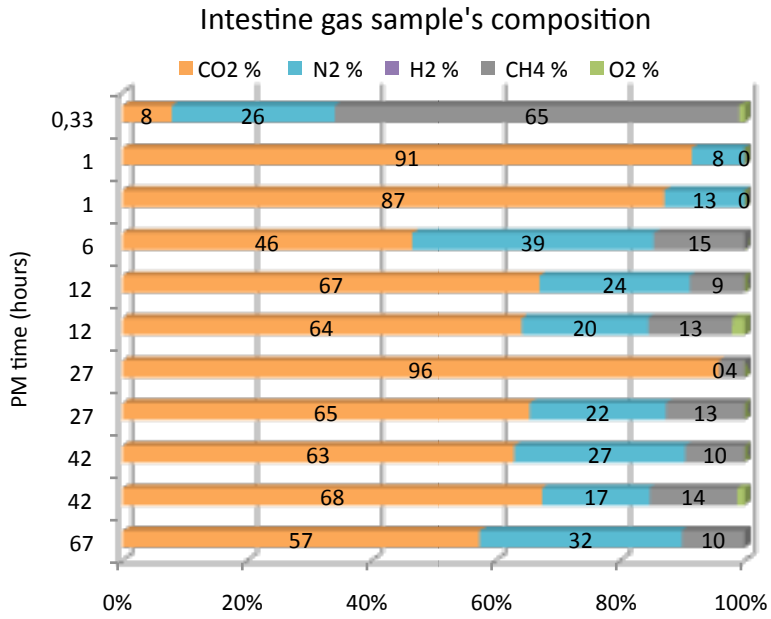

Fig. 3.25: Intestine gas sample composition of each animal *vs.* PM time illustrating the contribution of each gas to the total amount in µmol percentage.

Regarding gas volume and composition from Heart and Vena cava, rabbits with bubble grade ranging from 0-3 were treated separately from those with bubble grade 4 or higher.

3.3.3.2.1 Bubble grade 0-3

As described previously, very small gas volumes were recovered from the right heart of this group of rabbits (See Fig: 3.21). The highest gas volume recovered was 0.35mL.

Gas composition was found to remain constant with increasing PM time. Gas samples from the left heart were mainly recovered from rabbits with bubble grade 4-5. There was a single case within bubble grade range 0-3 from which gas was recovered from the left ventricle. This sample was taken at 42 PM hours. The sample volume was very small (smaller than 0.1mL). Gas composition was found to be the same as from the Right Heart. Except for one rabbit with PM examination at 6 hours, all the rest had a similar composition with mean values and standard deviations of 74.7±1.2 % of N_2, 15.1 ±2.3 % of O_2 and 10.1± 2.7 % of CO_2.

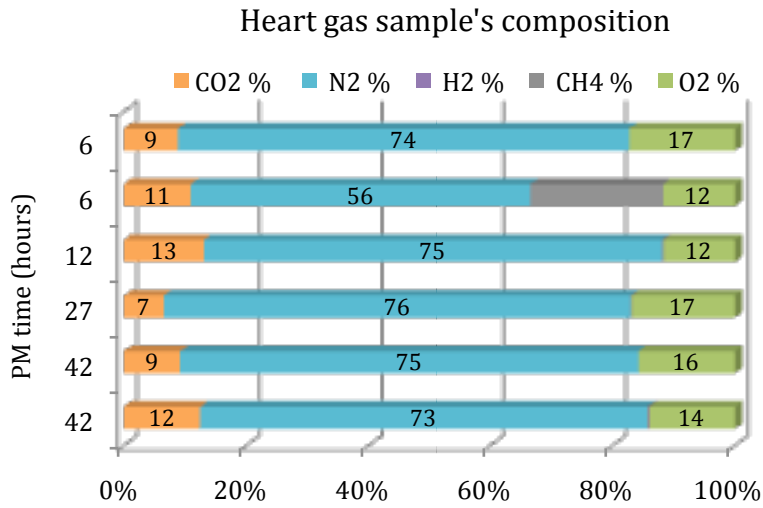

Fig. 3.26: Heart gas sample composition of each animal *vs.* PM time illustrating the contribution of each gas to the total amount in percentage.

3.3.3.2.2 Bubble grade 4-5

In this first group, nitrogen and CO_2 were again the main compounds. Nitrogen was always higher than CO_2 content except for the 12 hours PM sample. The highest values for nitrogen and CO_2 were of 85.62% and 58.65% respectively. Oxygen and methane presence was random and with values lower than 5% in most cases. Hydrogen appeared only after 42 hours PM. It was not possible to find a clear tendency with increasing PM time. The next figure shows lines linking the average value of each gas at a given PM time.

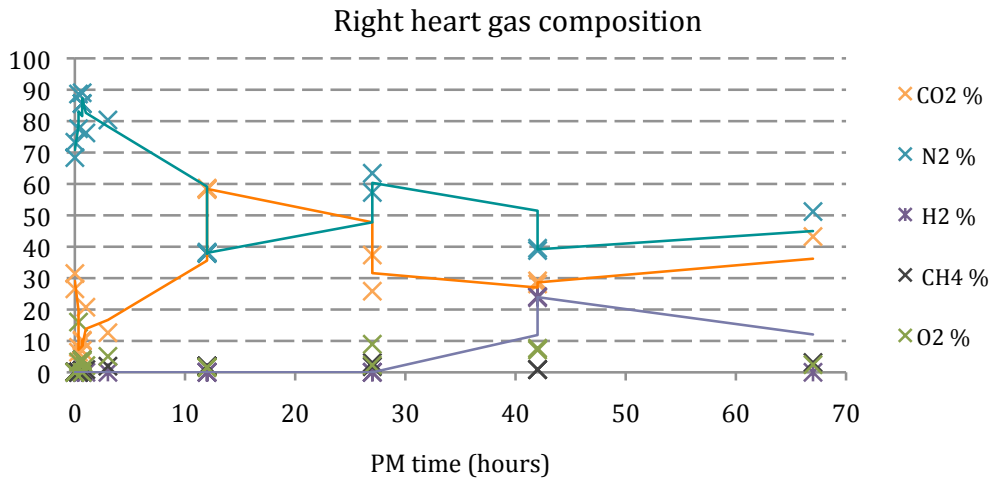

Fig. 3.27: Right heart samples composition taken at a given PM time. Lines are joining the average values for nitrogen in blue, for CO_2 in orange and for hydrogen in purple.

Although the variability was considerable, there were some indication of the occurrence of two different processes; one on the first hours when differences in nitrogen and CO_2 percentages were large, and a second one after three hours when nitrogen and CO_2 seemed to converge to a similar number of around 40-50%. Heart gas composition at 12 hours PM was clearly different from the rest. Thus, nitrogen and CO_2 were first explored without the interference of the 12 hours PM sample, and then in more detailed looking only to the first three hours PM. When studying the complete time range but without the 12 hours PM, tendencies of nitrogen and CO_2 became clear. Nitrogen levels decreased first fast and after slower until stabilize around 50%. In

contrast, CO_2 percentage increased linearly to meet nitrogen values after 67 hours PM (Fig. 3.27).

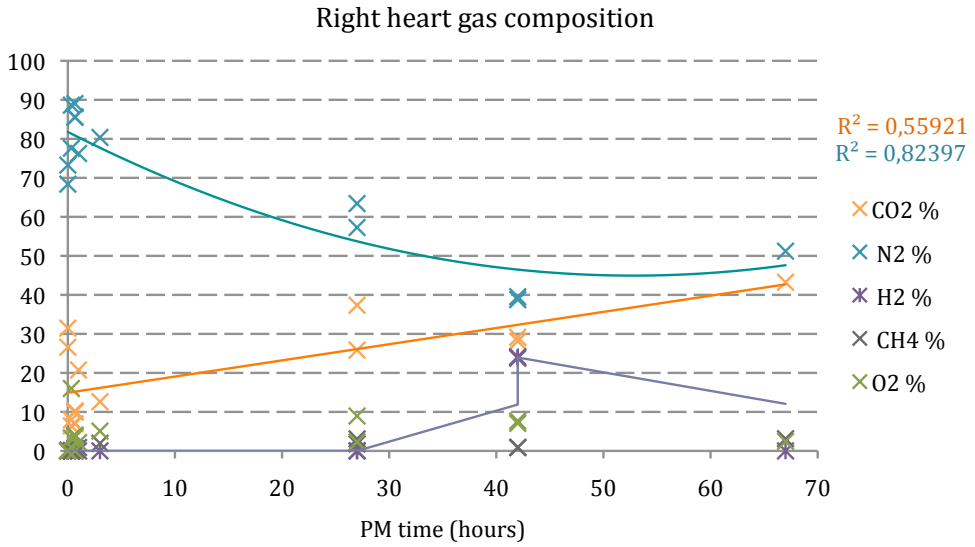

Fig. 3.28: Right heart samples composition taken at a given PM time excluding samples taken at 12 PM hours. Regression line for nitrogen is in blue and for CO_2 in orange color. Purple line joins average values for hydrogen.

When exploring the first three hours, no clear differences or tendencies were found for nitrogen or CO_2 percentages. Rabbits necropsied immediately after death, had higher CO_2 content, thus lower nitrogen in percentage.

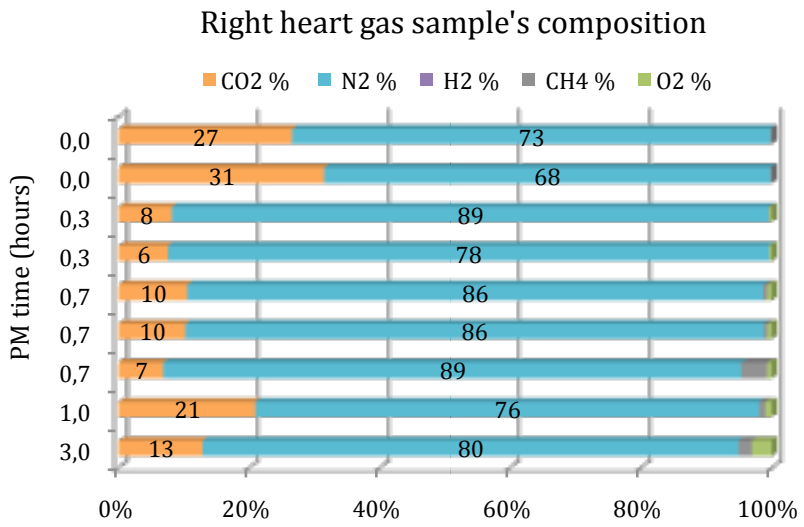

Fig. 3.29: Right heart gas sample composition of each animal *vs* PM time illustrating the contribution of each gas to the total amount in µmol percentage.

From the left heart, gas samples from 9 of 11 rabbits with bubble grade 4-5 were obtained. Gas composition from the left heart was found to be similar but more stable than right heart composition.

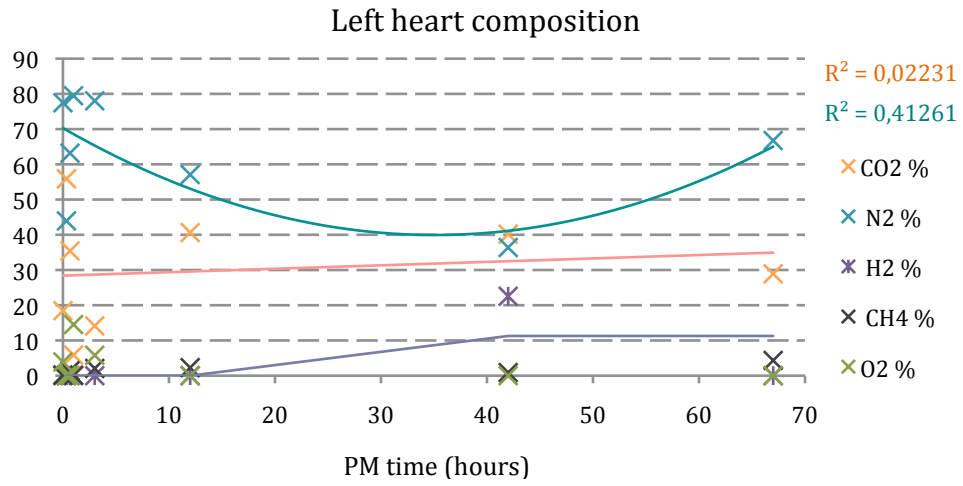

Fig. 3.30: Left heart gas sample composition taken at a given PM time. Regression line for nitrogen is in blue and for CO_2 in orange colour. Purple line joins average values for hydrogen.

In the Vena cava gas samples, once more a larger variability on the data was observed (Fig: 3.31).

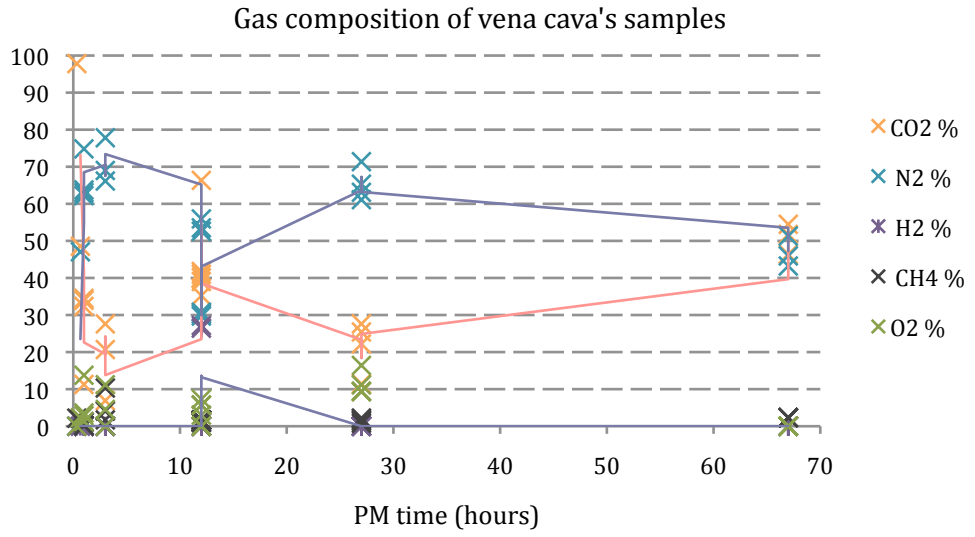

Fig. 3.31: Vena cava gas sample composition taken at a given PM time. Lines are joining the average values for nitrogen in blue, for CO_2 in orange and for hydrogen in purple.

Apparently, larger variability was present during the first hours; therefore we looked into this time range with more detail. During the first hours CO_2 was found to be even higher than nitrogen. After three hours, nitrogen and CO_2 content reached similar values as those observed in the induce air embolism study.

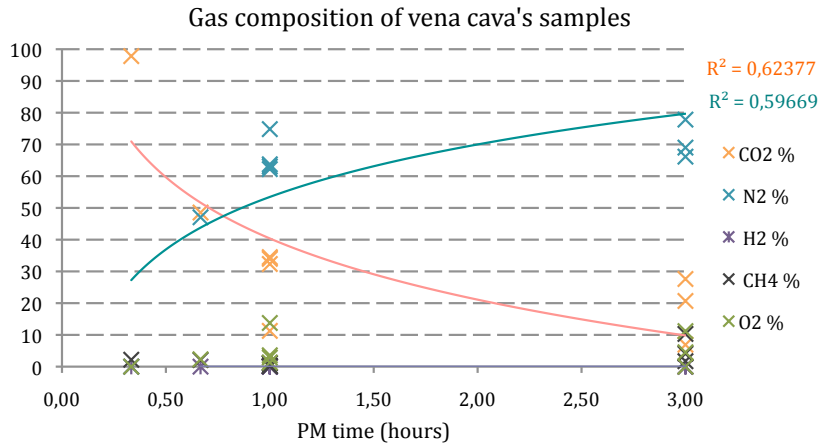

Fig. 3.32: Vena cava gas sample composition taken at a given *PM* time. Regression line for N_2 is in blue and for CO_2 in orange colour.

Finally, CO_2 and nitrogen content from the right and left Heart as well as from Vena cava gas samples were compared. Considering the complete time range, CO_2 and nitrogen had distant values that came closer after a few hours to meet at 67 hours PM.

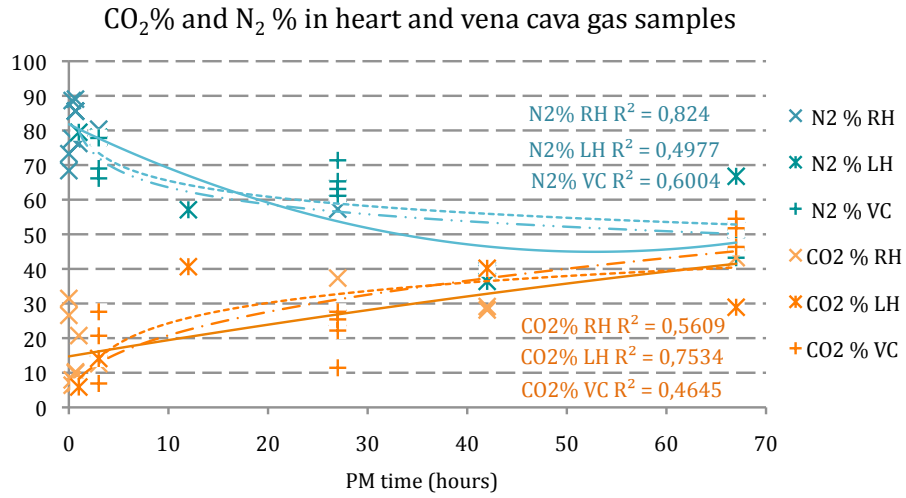

Fig. 3.33: Evolution of CO2% (in orange) and N2% (in blue) from heart and Vena cava gas samples with PM time. Continuous lines represent regression lines for right heart, discontinuous points and lines represent the left heart regression curves and discontinuous points are regression curves for Vena cava gas samples.

Regarding the first hours, it was notice a clear difference in gas composition between Heart and Vena cava gas samples. Gas from Vena cava had at first high levels of CO_2, and in a short time nitrogen and CO_2 met heart values. These values were the same of those found in the induce air embolism model. An interesting observation is that samples recovered from the right heart immediately after death, had also lower nitrogen and higher CO_2 values compared to other fresh right heart samples and similarly to Vena cava gas sample composition.

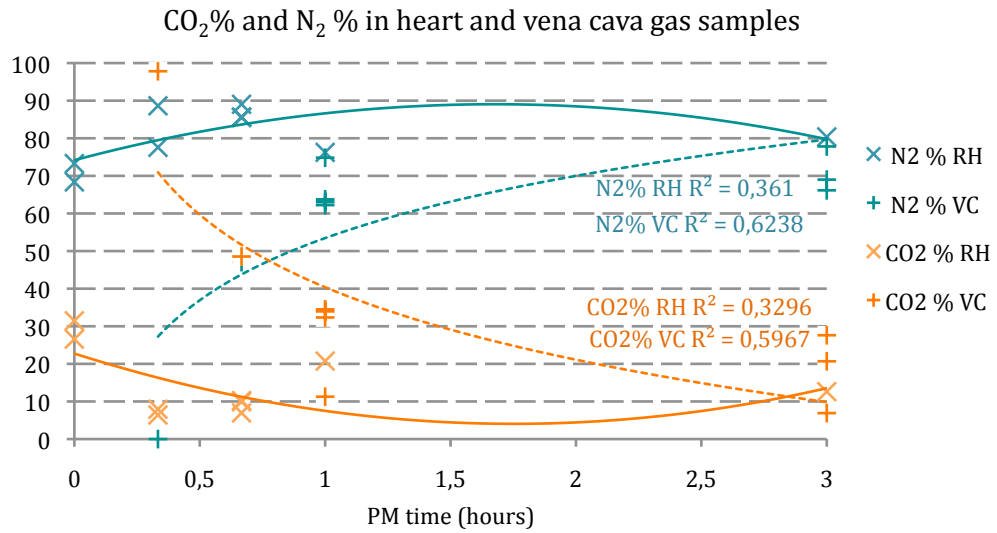

Fig. 3.34: Evolution of CO_2% (in orange) and N_2% (in blue) from heart and Vena cava gas samples with PM time. Continuous lines represent regression lines for right heart, while discontinuous lines are regression curves for Vena cava gas samples.

3.3.4 COMPARISON OF THE THREE MODELS

3.3.4.1 Gas abundance in tissues/veins

Initial gas abundance was clearly different in the three models. Gas abundance became more or less similar only in a very advance decomposition code (after 67 hours PM). Gas produced by putrefaction started to appear with decomposition code 2 (12 hours PM) but in a very scarce amount. It did not become relevant until decomposition code 4 was reached (42 hours PM). Even with decomposition code 4, amount of gas found only from decomposition was much lower from either air embolism or compression/decompression models (Fig: 3.31). Differences from the air embolism induced model and compression/decompression model were found mainly during the first hours PM (Fig: 3.35). Presence, abundance and dissemination degree was always higher in the compression/decompression model independently of PM time or decomposition code.

Main difference between the three models was found before 27 hours PM.

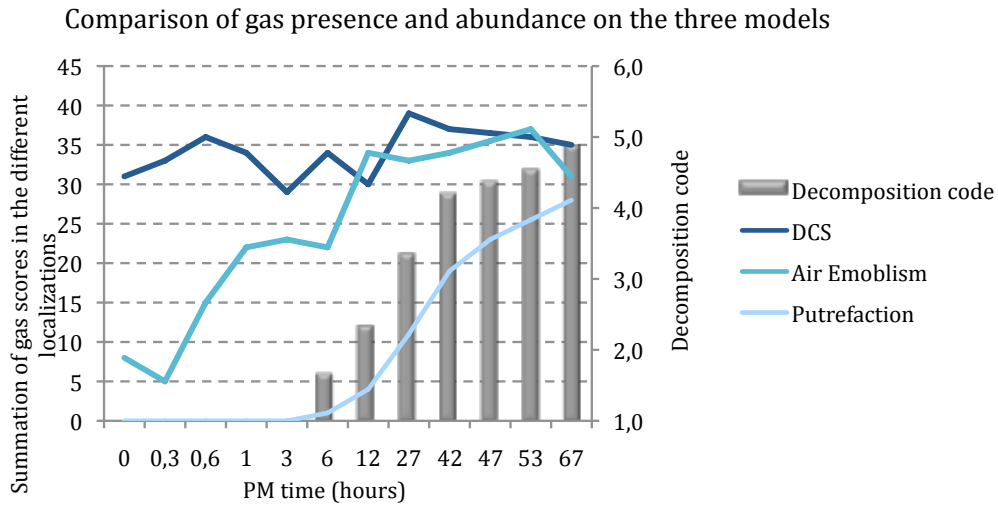

Fig. 3.35: Summation of gas scores in the different experimental models along PM time and its relationship with decomposition code.

Taken all the animals PM time and they respective decomposition codes, a strong correlation was found (r=0.9591; P<0.001). Thus, both factors have the same predictive value for summation of gas scores in the different localizations attending to treatment.

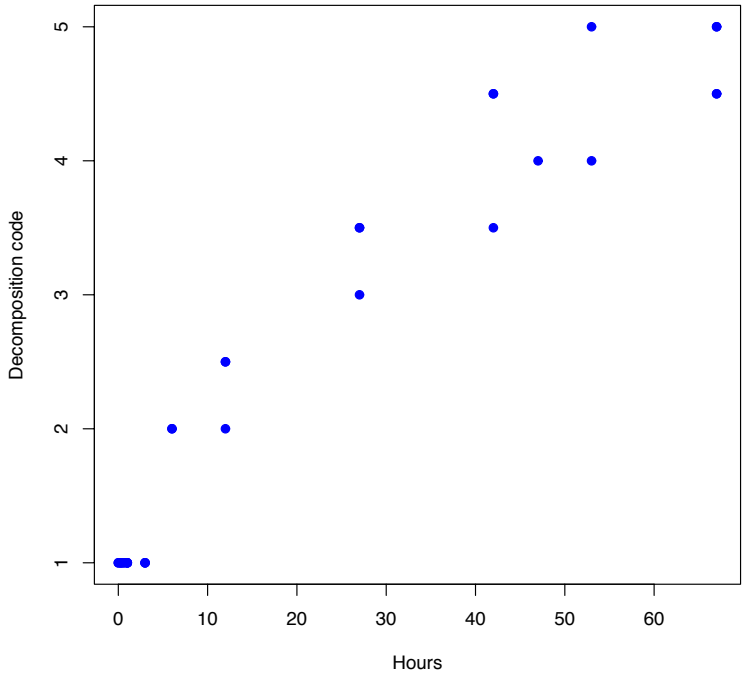

Fig. 3.36: Correlation between PM time (hours) and decomposition codes with a Pearson coefficient correlation value of 0.9591 (P<0.001).

A model for evolution of summation of gas scores in the different localizations along time (which is the same as decomposition codes attending to the results showed above) for the treatments: Putrefaction (treatment 1), induced AE (treatment 2) and compression/decompression (treatment 3).

Treatments resulted to be clearly different. The summation of gas score in the putrefaction model increases linearly with time while in the AE and in the compression/decompression model the best fit was a logarithmic model. The model obtained has and adjusted R^2 of 0,8982 remained as follows:

$$E\left[Gas\right] = \alpha + \tau_2 T_2 + \tau_3 T_3 + \beta_1 T_1 HOURS + \beta_2 T_2 \log\left(1 + HOURS\right) + \beta_3 T_3 \log\left(1 + HOURS\right)$$

Where T is kind of treatment and τ_2 y τ_3 expressed the differente starting levels for treatments 2 and 3.

Table 3.5: Estimated parameters for the model of evolution of the summation scores in the different tissues with PM time, with an adjusted R_2 of 0.8982

Parameter	*Estimation (SE)*	*P-value*
α	-0.797 (2.090)	0.7061 (NS)
τ_2 (effect of T_2 compared to T_1 at time 0)	11.986 (2.913)	< .001
τ_3 (effect of T_3 compared to T_1 at time 0)	33.112 (2.739)	< .001
β_1 (growing rate T_1 *in log-hours*)	0.409 (0.051)	< .001
β_2 (growing rate T_2 *in log-hours*)	6.228 (0.793)	< .001
β_3 (growing rate T_2 *in log-hours*)	1.051 (0.808)	0.2047 (NS)

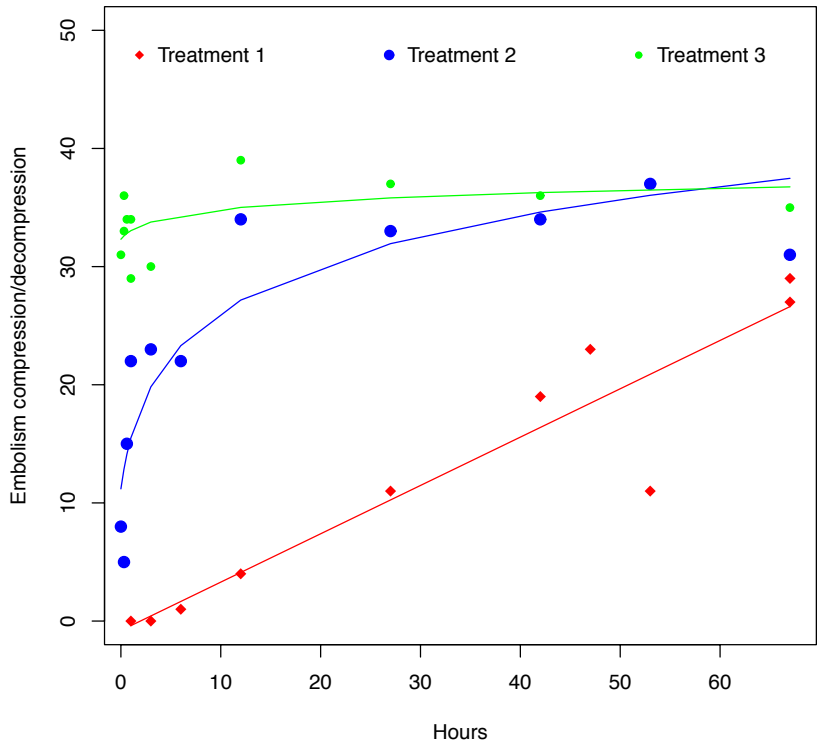

Fig. 3.37: Correlation between PM time (hours) and decomposition codes with a Pearson coefficient correlation value of 0.9591 (P<0.001).

From this model we can conclude that there were statistical differences between the treatments upto day one.

Putrefaction processes produce gases linearly at a rate of 0.409±0.051 gas scores per day. There is as well a significant growing rate for the air embolism treatment but there is not for the compression/decompression treatment since starting values are similar to end values.

Although the variability of gas recovered with PM time, absolute volume of gas-recovered form the right heart was markedly different between the three models. The highest volumes were always recovered from rabbits of the compression/decompression model with bubble grade 4-5 represented in the following graph as "DCS". Rabbits from the same model but with bubble grade 3 or lower were named as "non-DCS" in the figure. These animals had lower volumes than rabbits from the putrefaction model. This is because in the putrefaction model gas was recovered only after 42 hours PM, while rabbits with bubble grade 3 or lower were all examined before this time and the summation of both processes (air embolism and putrefaction) might not occurred yet attending to the results.

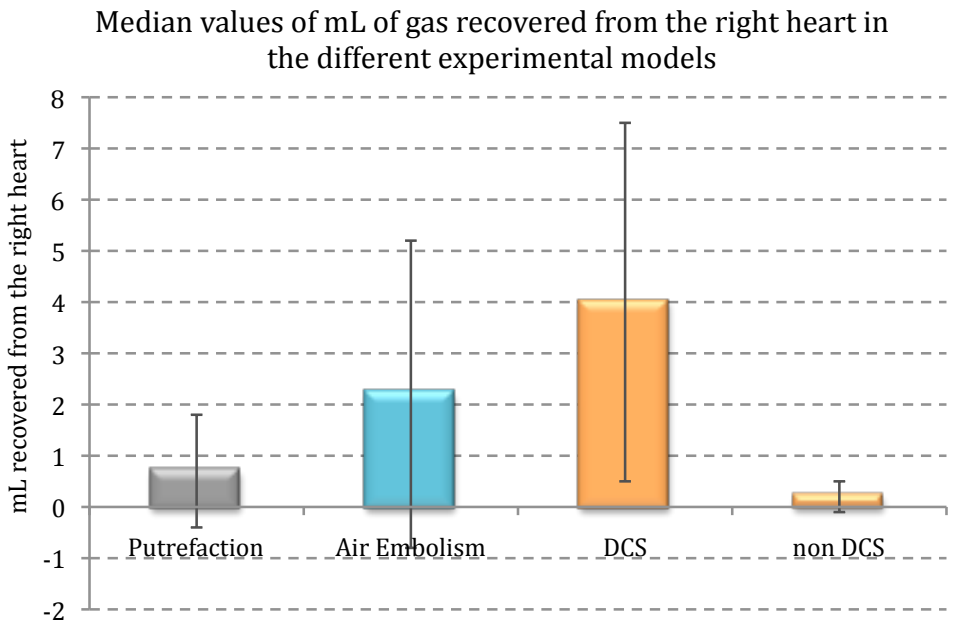

Fig. 3.38: Mean and standard deviation values of mL of gas recovered from the right heart in the three experimental models. The compression/decompression model has been divided in two subgroups according to bubble grades as "DCS" group and "non-DCS" group.

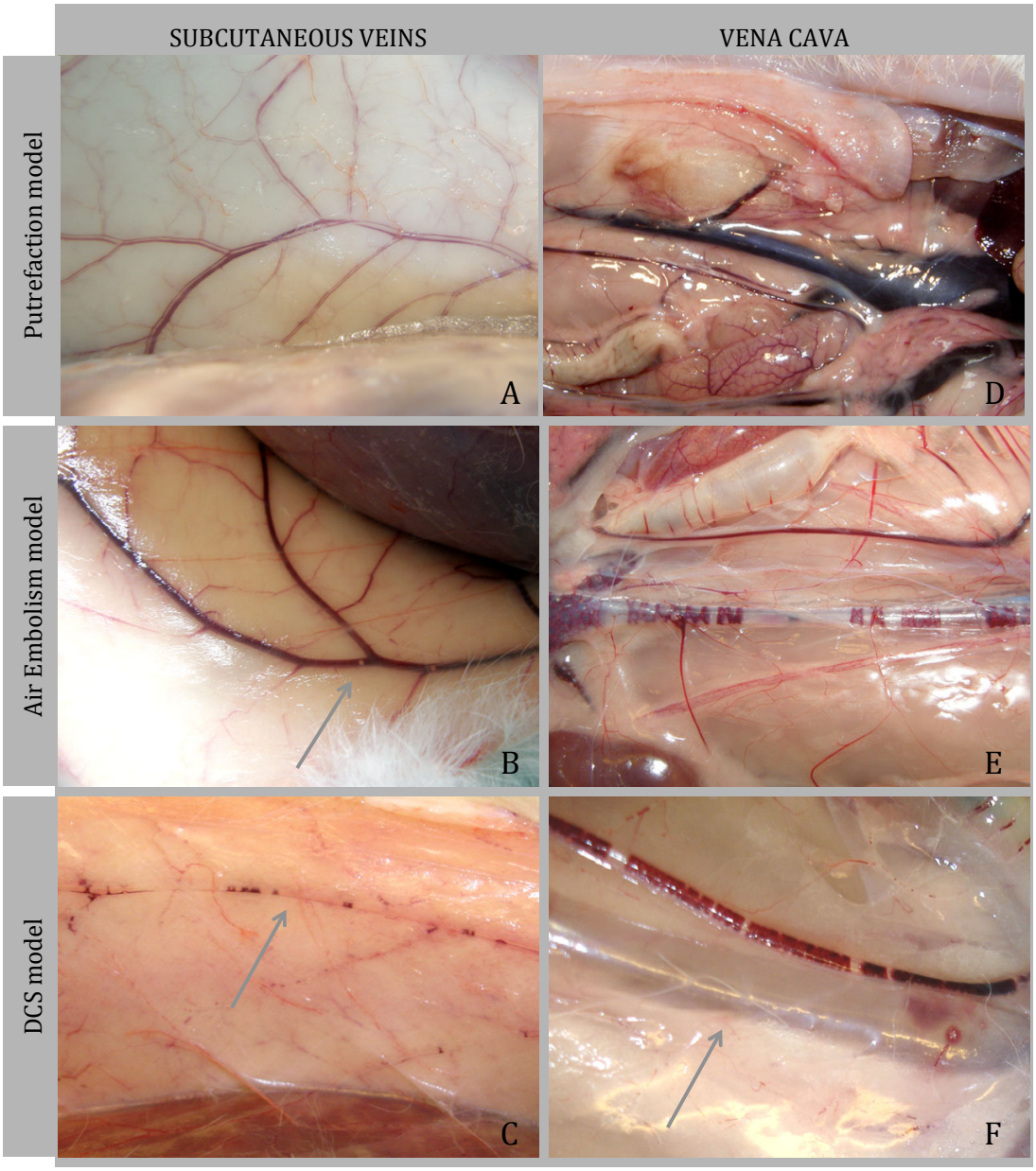

Fig 3.39: Pictures showing different gas abundance in the same tissues, with same decomposition code (1-2), but with different treatments. Subcutaneous veins with decomposition code 1-2 from the putrefaction model (A), induced air embolism model (B) and compression/decompression model (C). Vena cava with decomposition code 1-2 from the putrefaction model (A), induced air embolism model (B) and compression/decompression model (C).

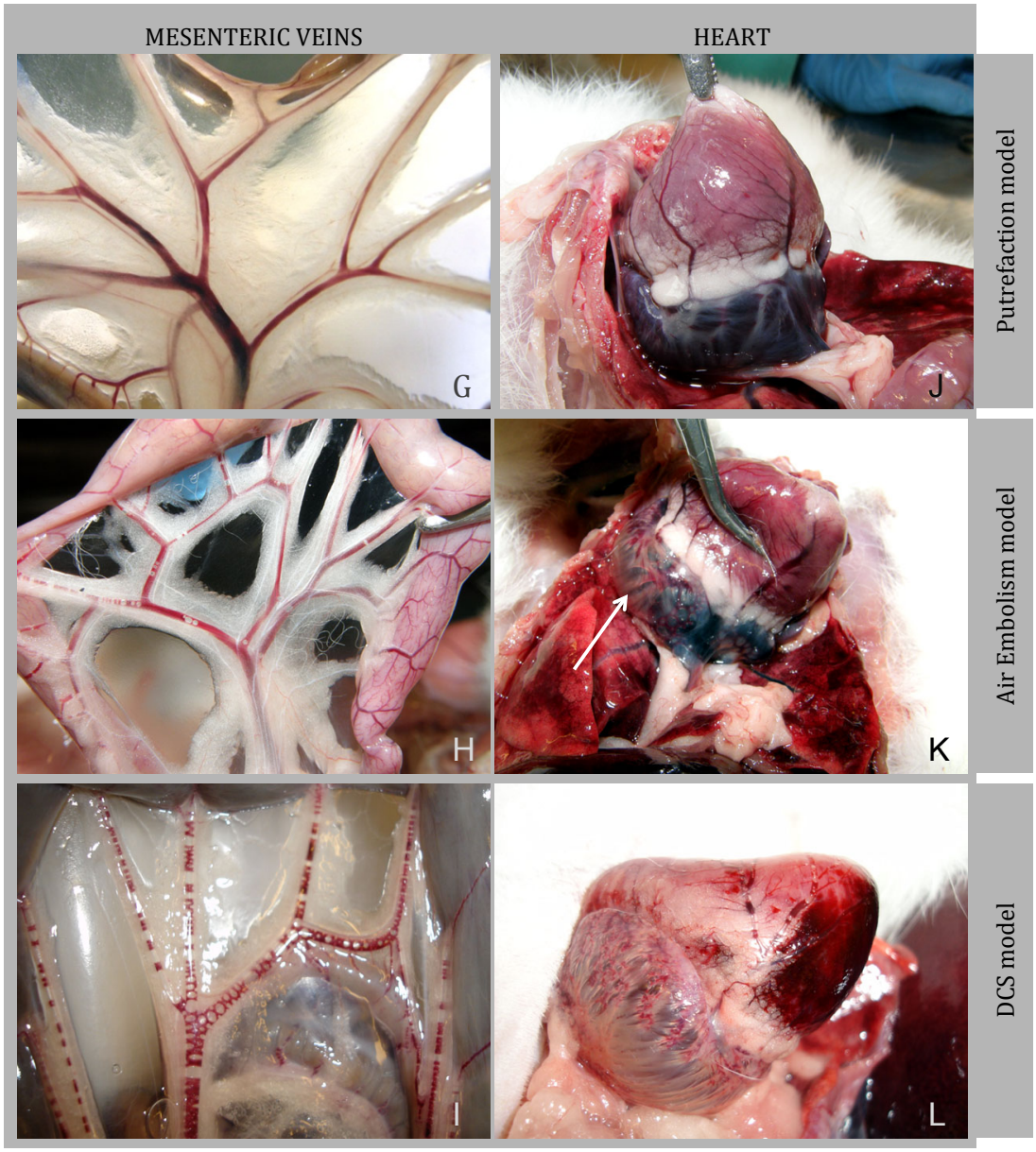

(Follow up) Fig 3.39: Pictures showing different gas abundance in the same tissues, with same decomposition code (1-2), but with different treatments. Mesenteric veins with decomposition code 1-2 from the putrefaction model (G), induced air embolism model (H) and compression/decompression model (I). Vena cava with decomposition code 1-2 from the putrefaction model (J), induced air embolism model (L) and compression/decompression model (M).

Additional differences between models were the presence of emphysema in fat in the compression/decompression model alone even immediately after dead and the

inflation of some spleens in both experimental models: induced air embolism (2/11) and compression/decompression model (3/11), but never in the putrefaction model (Fig. 3.40).

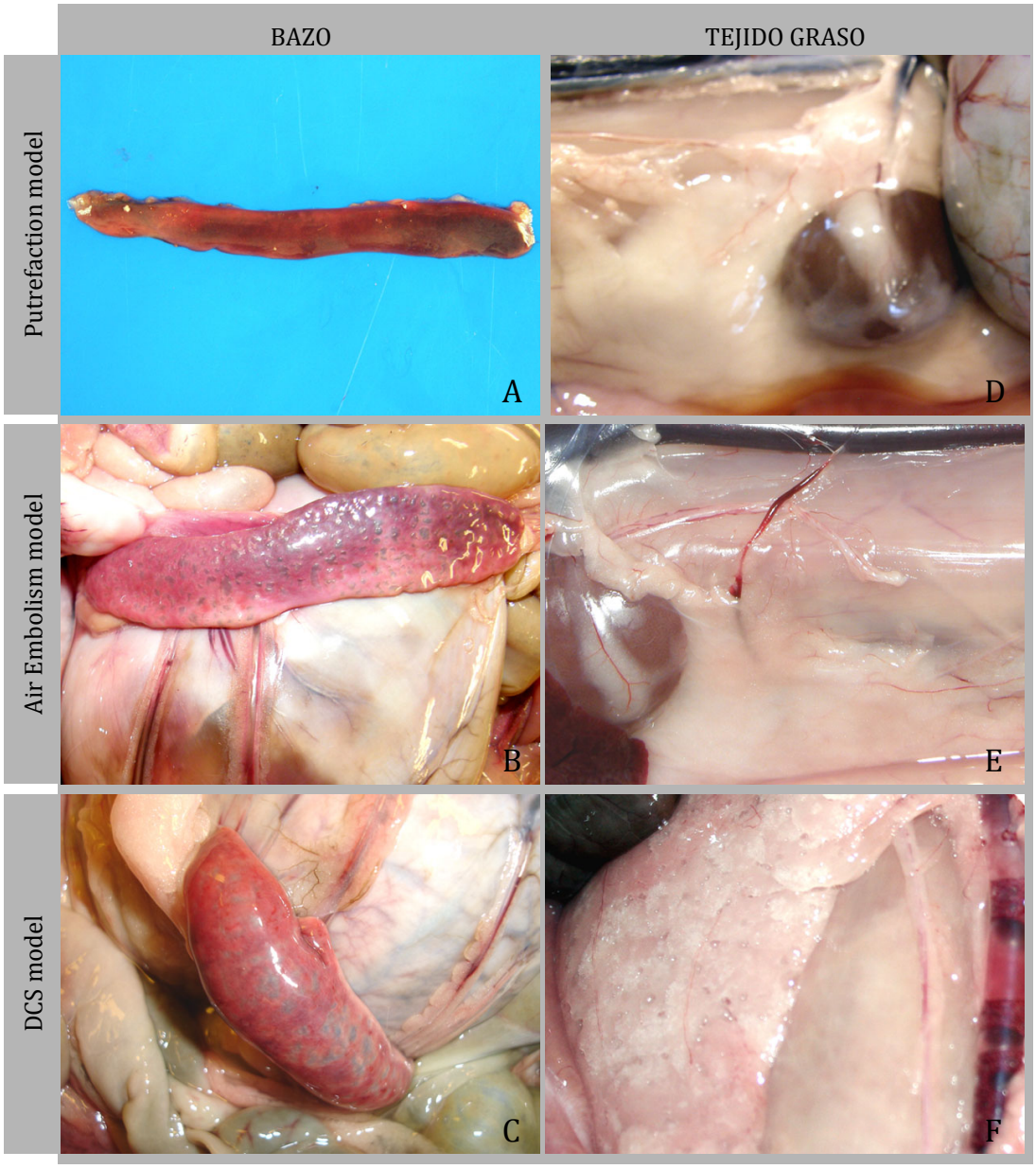

Fig. 3.40: Pictures showing normal spleen appearance with decomposition code 3 (A), an inflated spleen with same decomposition code (B), and inflated spleen with decomposition code 1 (C). Emphysematous appearance of fat with decomposition code 1 on the DCS model (F) compared to normal putrefaction (D) and air embolism (E) model with same decomposition code.

3.3.4.2 Gas composition

A total of 168 samples were obtained from the three models and analyzed. Based on results, samples obtained from the right heart were chosen for comparative studies since its composition resembled to be the most stable within each method.

Best regression adjustment for each model was selected. When comparing the induced air embolism and the compression/decompression gas composition, very similar tendencies were observed if samples taken at PM time 0 and 12 hours were removed from the study. Best regression adjustment (R^2= 0.91) for DCS was a logarithmic model (continuous purple line), but if a linear model was applied instead (discontinuous purple line), still a good fit was found (R^2=0.78) and more interestingly, regression line was then almost the same as for the AE (blue line). N_2 content in putrefaction gas samples was more or less similar to that found in either DCS either AE embolism after 42 PM hours.

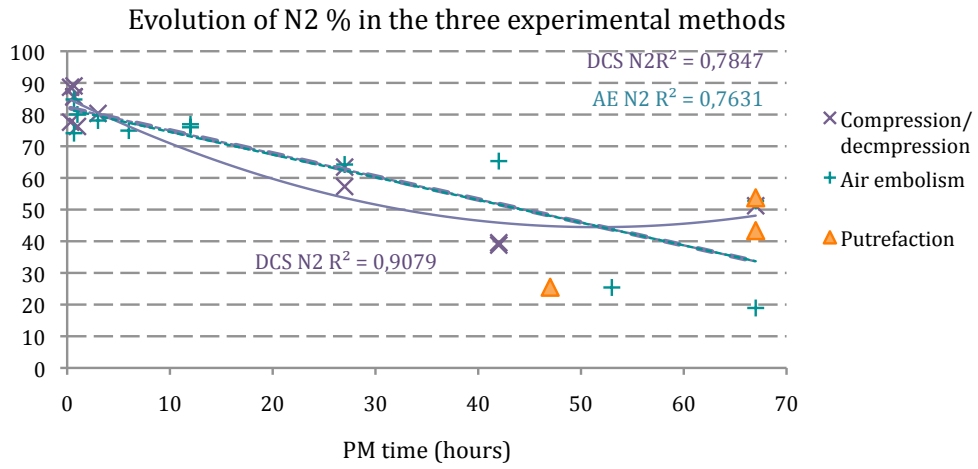

Fig. 3.41: Evolution of N_2 content in gas samples form right heart obtained in the putrefaction model (orange), induced air embolism model (blue) and compression/decompression model (purple). Regression lines represent best adjustments found for each model.

Similar behavior was observed with CO_2. Higher variability than with nitrogen was found. If zero and twelve *PM* time hours were not removed from the study, it was not possible to find a good regression adjustment (see Fig 3.34 and 3.35). If removed, good adjustment was found (R^2=0.84) and model behaves similarly to the CO_2 air embolism study. CO_2 content in putrefaction models is similar at 42 PM hours but different at 67 PM hours.

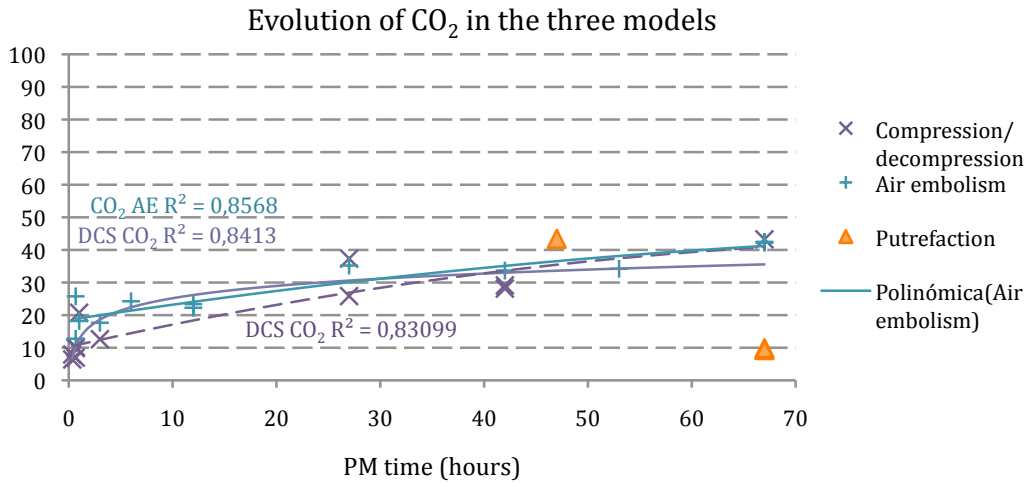

Fig. 3.42: Evolution of CO_2 content in gas samples form right heart obtained in the putrefaction model (orange), induced air embolism model (blue) and compression/decompression model (purple). Regression lines represent best adjustments found for each model.

When comparing gas samples that could be produced or mixed with putrefaction gases (after 42 PM hours according to the putrefaction model), hydrogen was found to be always present except in two of ten samples. Hydrogen values varies between 23-40 % affecting CO_2 and nitrogen content. Oxygen and methane were randomly present.

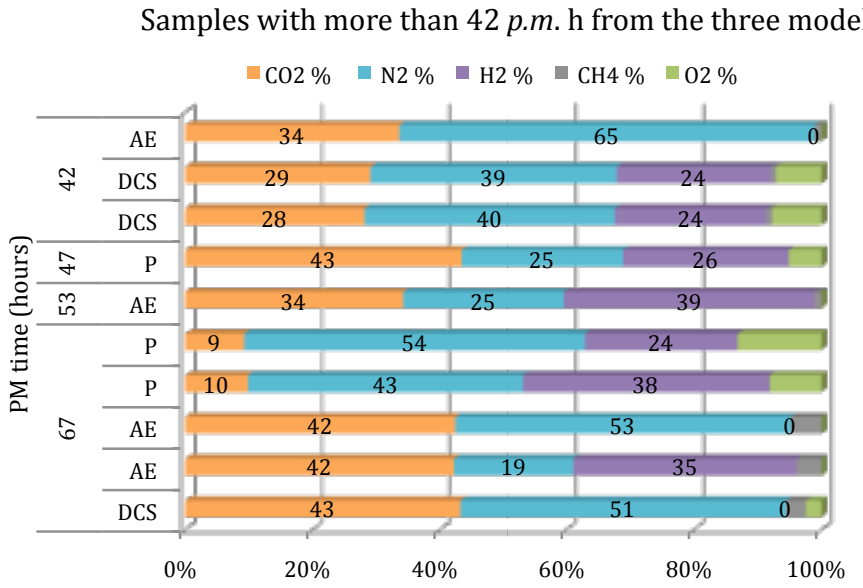

Fig. 3.43: Right Heart gas sample composition taken after more than 42 PM hours in the three models. Right heart gas sample composition of each animal *vs.* PM time illustrating the contribution of each gas to the total amount in percentage.

Samples from right heart taken at PM time zero and twelve hours were considered separately but together with other samples from Vena cava and left heart that didn't follow the same tendencies as the rest of samples obtained with the compression/decompression model. These samples have all in common a higher relative abundance of CO_2 that implies corresponding lower values of nitrogen compare to the rest of DCS samples and air embolism model. Similarly composition on the air embolism model is only found after 42 hours and in a single sample taken at zero PM hours. In contrast, the samples that did not match with the rest were recovered with very little PM time.

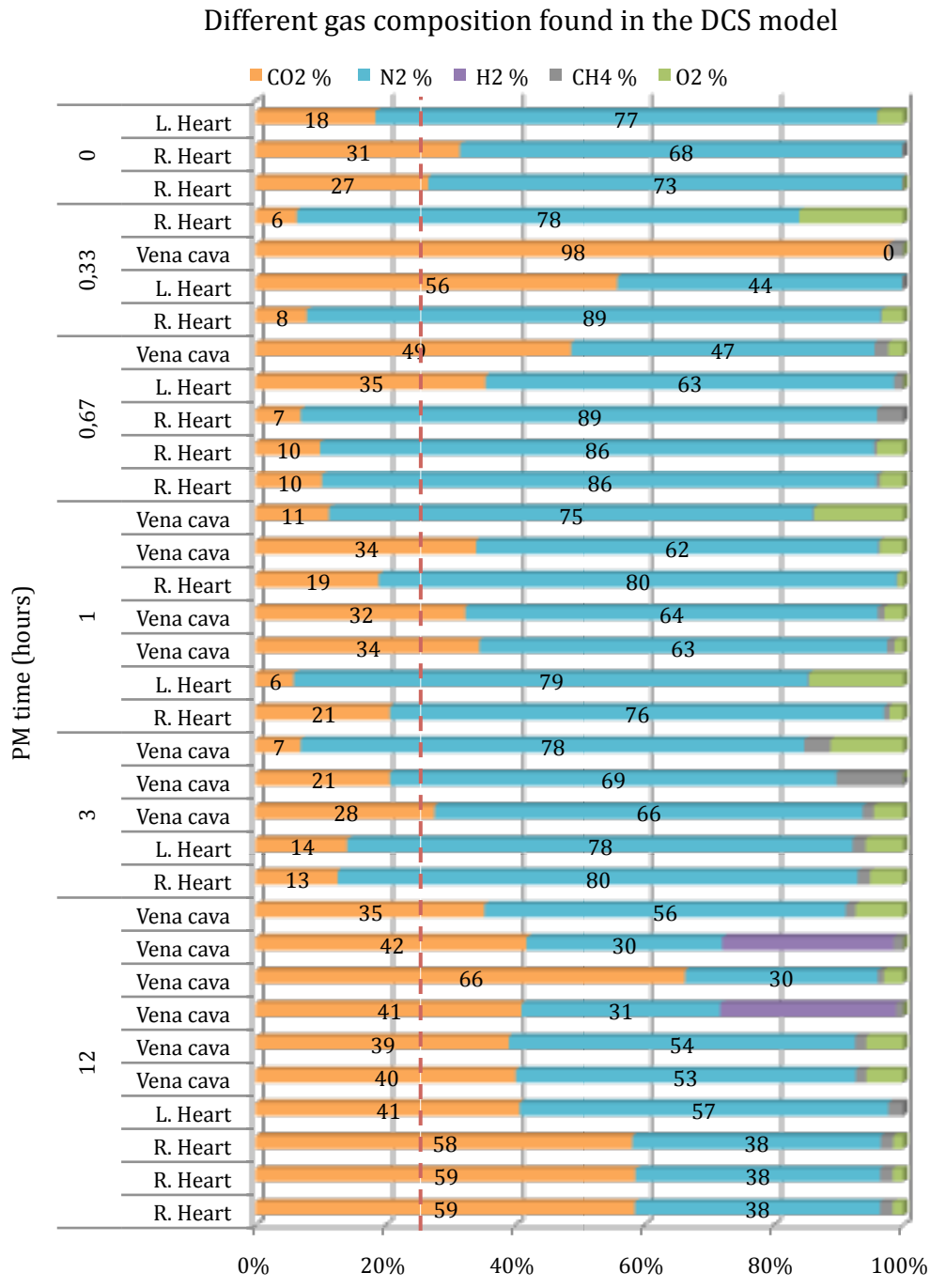

Fig. 3.44: Gas sample composition of samples from the DCS model that did not match with the observed tendencies. Gas composition is illustrated with the contribution of each gas to the total amount in percentage.

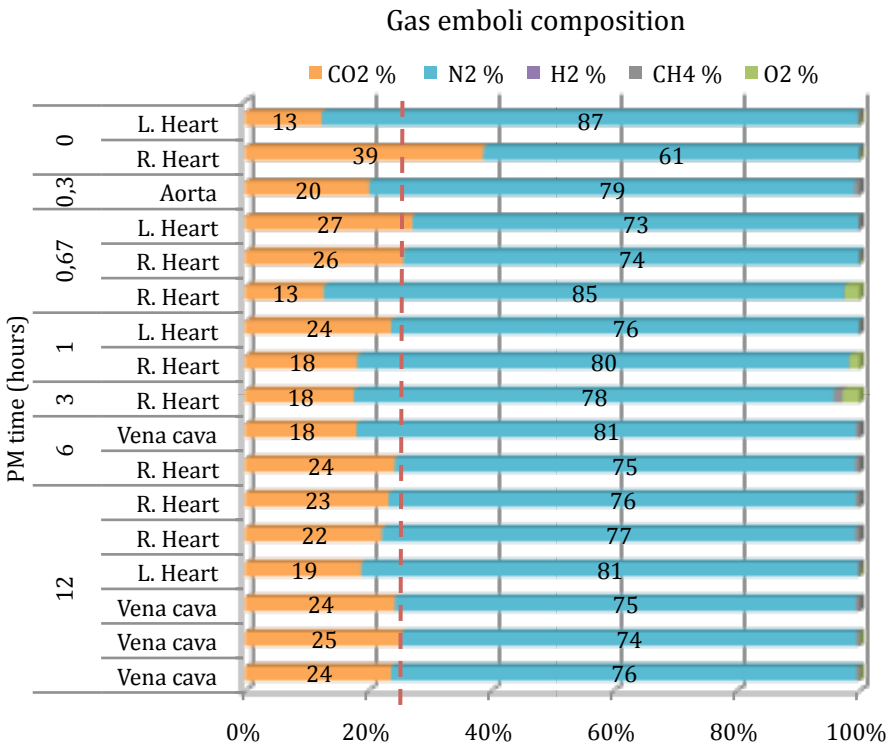

Fig. 3.45: Gas emboli composition from different localizations (heart, Vena cava and Aorta) *vs.* PM time illustrating the contribution of each gas to the total amount in percentage for the first 12 PM hours

3.4 DISCUSSION

3.4.1 PUTREFACTION GAS STUDY

Both after decompression caused by pressure reduction and following death, tissue gas can be released from solution and it will appear as free gas. The difference between the two processes is important, both for evaluating the effects of decompression on the organism and for forensic evaluation. Furthermore, the effect of the dissection process itself is important to evaluate.

Dissection technique was evaluated in our study since no gas was expected to be present during the first post-mortem hours. Our results were conclusive with this matter: no bubbles were found immediately or within few hours after death. Thus, it can be conclude that if dissection is properly done, it does not introduce perceptible amounts of gas during cutting. This result is consistent with Richter reports (Richter, 1905). Additionally, recovery of gas from right and left heart by puncture under the water had only one positive result from 20000 autopsies where this technique was applied (Knight, 1996) suggesting strongly that air recovered is not a dissection artifact.

The complete absence of gas bubbles in rabbits necropsied immediately or within few PM hours (decomposition code 1 and 2) is the most important result from this model. It indicates as expected, that a certain level of putrefaction must be reached in order to produce enough gas to favor gas phase separation from fluids or at least to be large enough to be macroscopically detected. Evidences of autolysis (discontinuities in the blood) were found with decomposition code 3, but very few or none gas bubbles were observed before decomposition code 4. Therefore, if large amounts of bubbles are found grossly within decomposition code 1-3, this is most likely due to gas embolism.

Another expected but not less interesting result is the high correlation between decomposition code and post-mortem time. This is of special interest when time of

death is unknown as it uses to happen with stranded cetaceans. This is why we have tried to refer to decomposition code instead of post-mortem time through the study, since weather conditions, death circumstances, species differentiations and inter-individual variations are expected to alter decomposition processes. A clear example of inter-individual variations was found on animal examined after 53 PM hours. Gas content and decomposition code was lower than expected.

Similar gas composition was found between free subcapsular gas and free gas inside the heart, but they were not clearly related to intestine gas composition. In the first ones, gas composition was a mixture of CO_2, nitrogen, hydrogen, with small quantities of oxygen and trace levels of methane. There was some variation among samples, and in one of them, methane levels were of importance. SH_2 was not detected. Hydrogen seemed to be a clear indicator of putrefaction gases, although its absence cannot be interpreted as absence of putrefaction gases. Nitrogen levels were rarely higher than 50%. In contraposition intestine gas samples had quite frequently important amount of methane and hydrogen appear randomly. Our results are in accordance with Pierucci and Gherson 1968 and 1969 experiences regarding putrefaction gases. They used similar methodology and animal models.

In these analyses we did not detect any VOC. It is reported that routine methods as GC may not detect them at their low concentration (Zumwalt et al., 1982). For detecting VOC in human corpses, a Gas Chromatograph/ Mass Spectrum with high resolution chromatographic separation was used (Statheropoulos et al., 2005). Our column allows us to separate compounds up to five carbons. The TCD is a universal detector, and the FID is a more sensible detector for hydrocarbons. With this combination of column and detectors, hydrocarbons (most VOC are hydrocarbons) smaller than five carbons should have been detected if present in higher weight than 100 pg. So small concentrations do not affect overall gas composition and our results are similar to the previous studies using the same animal model and similar methodology (Pierucci and Gherson, 1968; Pierucci and Gherson, 1969).

3.4.2 INDUCED AIR EMBOLISM

In the air embolism study rabbits survived for various times showing high differences in gas volume tolerance among the animals. When doing the necropsy, it could be seen that not the same organs were affected to the same extend on the different animals although air infusion was performed in the same localization in all of them (ear central vein). From the clinical point of view, it would be interesting to do a complete pathology study on these animals and to determine which organs were the most affected in each case.

Although the large variation in infused air volume, a trend of gases production with PM time could be seen. Main difference from this model to the putrefaction one, was the starting level of free gas found in veins. Bubbles were mostly found in the large veins. There was a marked increase during the first 12 PM hours. Infused volumes of air were random and did not follow any time sequence; therefore, this increase cannot be explained by the differences in air volume infusion. Gases produced by putrefaction alone cannot justify either this increase, since very few gases were produced on this time and decomposition code in the experimental putrefaction model. A reasonable explanation could be that small bubbles keep growing after death of the animal by incorporation of dissolved gases of the surroundings, as the same time as bubbles coalescence and become large enough to be macroscopically observed.

Gas embolism produced by direct entrance of atmospheric air was consistently composed of 77±5.5% of N_2 and 22.2±5.9% of CO_2 up to decomposition code 2. In decomposition code 3, levels of nitrogen started to decrease slowly at the same time as CO_2 levels increased. With decomposition code 4, hydrogen started to appear and there was a mix with putrefaction gas. Here differences in composition between different bubbles were high. Some still maintained a gas embolism composition, while others had a composition most similar to putrefaction gases. With decomposition code 5, most of the samples had clearly a typical gas putrefaction composition. It could be clearly

seen how gas bubbles change composition as putrefaction processes advance. This is very important since it is confirming that with this methodology it is possible to distinguish between putrefaction gases and gas embolism although VOC are not detected.

It is also important to notice that having a clear gas putrefaction composition does not rule out the possibility of having previously a gas embolism. In the rabbit with decomposition code 5, we know for sure that it suffered and died because of gas embolism because we have caused it but gas analyses show a "*typical*" gas putrefaction composition. With decomposition code 4 it cannot be done either any statement about gas embolism occurrence. To sum up, values of nitrogen close to 70% and absence of putrefaction gases are indicators of gas embolism, but putrefaction gases does not exclude the possibility of having a venous gas embolism because gas bubble composition changes as the putrefaction advances.

These results are very similar to those presented by Pierucci and Gherson (1968) and (1969) and they reached the same conclusions. Our results in nitrogen levels are very similar to those found by these authors through all time range, but we did find higher values of CO_2 and lower values of oxygen than they did. These differences might be explained partially by differences in the methodology. They injected air into the femoral vein of several rabbits and gas samples were recovered with its own aspirometer at different PM intervals. They used an aqueous solution of NaCl but they did not use a correction factor. (Although the correction factor for this solution is much smaller than for the distilled water as discussed previously in chapter III). They did realize however that they had some extra oxygen and nitrogen, because when they injected helium instead of air they did recovered these gases as well. Therefore, this might be a reasonable explanation for small differences.

Pierucci and Gherson (1968) reported relatively high concentrations of oxygen immediately after death (around 10%) and low levels of CO_2 (around 5%). Then oxygen dropped quickly in the first hour to reach very low values (1-3%) and CO_2

increased to concentrations higher than 10%. Our results for the same PM time is 77% of N_2, 22% of CO_2 and 1% O_2. These differences cannot be explained alone for the absence of the correction factor discussed before. May be, this difference is because of the anesthetics. Pierucci and Gherson (1968) do not describe any anesthetics used. We have used medetomidine/ketamin. This anesthesic is reported to reduce heart and respiration rate, a significant drop in arterial pO_2 and an increase in arterial pCO_2 in NZWR (Hellebrekers et al., 1997).

3.4.3 COMPRESSION/DECOMPRESSION MODEL

The aim of this model was to obtain a volume of bubbles large enough to cause the death of the animal. Large volumes of gas were desired for accurate gas analyses and for future comparison studies with cetaceans in which we have observed massive bubbling. Thus, a very extreme diving profile was chosen.

Besides having done a very homogenous model (same specie, gender, similar weight, same anesthetic dose, same diving profile…) the response to the extreme diving profile was very heterogeneous. There were clearly two different groups. A first group with low bubble grade (1-3), which survived for at least one hour (attending to the protocol, animals that survived for one hour were euthanized), with low bubble score when examined PM and from which very little gas volume was recovered from the heart; and a second group with high bubble grade (4-5), which died within few minutes (5-35 minutes), that had high bubble score when examined PM and from which significant larger gas volume were recovered. Individual differences, physiological pre-conditions, and in-dive conditions have been known to influence bubble formation and risk of DCS (Tikuisis and Gerth, 2003).

Since we did a very homogenous model and in-dive conditions were the same for all of them, individual differences seemed to be the main responsible for the heterogeneity of the response. This is not a surprising finding, Eckenhoff (1990)

reported a considerable inter and intra-individual variability in bubble formation at any level of exposure. Differences between both groups were so extreme that we considered necessary to do the analysis of the data separately for each group.

Up to bubble grade 3, none to few bubbles were observed grossly during necropsy. In all the cases with bubble grade 4 or higher bubbles were observed dispersed through all the veins. In many cases, lesions such as hemorrhages were observed in association with bubbles. Localization and distribution of bubbles might be of importance for a better understanding of where bubble forms and the physiopathology related to them.

There are some previous studies that had examined for macroscopic intravascular bubbles. Smith-Sivertsen (1976) compressed and decompressed dead rats. They presumed that since circulation is not having place in dead animals, localization of bubbles in this particular study might be close to their site of origin. Bubbles were found most frequently in the left ventricle and aorta (95%), followed by peripheral vessels (58%) and central veins (10%) (Smith-Sivertsen, 1976). Harris et al. (1945), followed similar protocol and performed the necropsy under a dissecting binocular. They found large numbers of bubbles in the heart, veins, arteries and often in the lymphatic system.

To find out if bubbles found at autopsy were introduced during the decompression through rupture of capillaries, either by expanding intestinal gases or in the lungs, some dead animals were dissected with minimal damage to blood vessels and placed in a decompression chamber with a plate glass in the top to permit direct observations of the animals during the exposure. They observed a sudden stream of bubbles appearing in the small branches that coalescence in the larger vessels. The gas expanded soon through the vascular systems, in arteries as well as in veins.

They got the same result when they repeated the experiment clamping the postcava and dorsal aorta either just anterior to the diaphragm either posterior to vessels supplying the digestive tract.

They concluded that the primary source of the bubbles that they were observing was not the vessels from the lungs or the digestive tract derived by leaking but instead, it was the small vein branches were bubbles came from, deep within the tissues and most commonly from muscular regions (Harris et al., 1945b).

This results is in concordance with physics theories; the venous end of capillary beds have low pressure and high gas tension as nitrogen diffuses out of tissues into the blood (Francis and Simon, 2003). Both studies (Harris et al., 1945b; Smith-Sivertsen, 1976) had experienced similar results as ours: they found two distinctive groups with animals that had profusely bubbling spreading throughout the body, or not at all. Our study might be the first one in relating this phenomenon with grading code for ultrasonic images.

One of the differences found between bubble grade measured by ultrasound and post-mortem bubble score examination could be due to different resolution limits of both methods. Ultrasound has higher resolution, thus smaller single bubbles can be detected with this method rather than visually observed. On the other hand, small bubbles are more susceptible to be trapped and excreted in the pulmonary capillaries (Francis and Simon, 2003) or simply get diluted. According to LaPlace equation, smaller bubbles have larger inner pressure, thus dissolve more quickly than large bubbles (Hrncir, 1996). If there are many small bubbles they might coalescence and form a larger bubble that can be visually observed. Large bubbles are more stable. Our results show that bubbles can last at least for 67 hours.

In addition, gas bubbles are formed in nearly all decompressions. Gas bubbles, in the absence of clinical manifestations of DCS, have been introduced as "*silent bubbles*" (Nishi et al., 2003). It seems like few gas bubbles are well tolerated. Animals with

bubble grade 3 or lower survived at least for one hour (after one hour animals were euthanized), while animals with bubble grade 4 or higher died before 35 minutes. This is also in accordance with the statistical correlation found between intravascular Doppler-detected gas bubbles and decompression sickness after bounce diving in humans (Sawatzky, 1991). Although our results shouldn't be directly extrapolated to humans because there might exit differences in gas volume tolerance among species (since there are differences even between individuals of the same specie as discussed previously), they suggest that dives resulting in bubble grade higher than 3 should be avoided for the safety of the diver.

Regarding gas composition, gas produced by compression and decompression has a composition similar to infused air embolism, but variability was always higher especially for CO_2. Composition on fresh samples consisted in 70-90% of N_2, 6-30% of CO_2 and 0-10% of O_2. These results are very similar to those described by previous authors (Armstrong, 1939; Bert, 1878; Ishiyama, 1983; Smith-Sivertsen, 1976). Although differences in animal models, experimental procedure and gas analyses methodology, they all report values of nitrogen between 79-86 % (Armstrong reported values of 60-65% of N_2), levels of CO_2 of 11-22% (Armstrong reported values around 28% of CO_2) and of levels of oxygen between 0-4% (Armstrong reported values of 6-11% of O_2).

These results are slightly different from those reported by Harris et al. (1945) and Lillo et al. (1992) with even higher levels of nitrogen and very low content of either CO_2 either oxygen. Differences between studies are so big, that it is senseless try to explain the possible reasons for differences in gas composition. Chappell et al (2006), found that although the metabolic gases may only represent a small amount of the gas in the bubble, their presence has a significant effect on the behavior of the bubble under decompression due to the high diffusivity of these gases.

3.4.4 COMPARISON OF THE THREE MODELS

Decompression is likely to allow bubble formation even after death. This is an insurmountable difficulty for pathologist and it is generally assumed that at least some bubbles could be artifacts. Thus, part of the differentiation is quantitative (Knight, 1996) but also qualitative, since there could be some pathological evidences indicating in vivo bubble formation such as hemorrhages associated with the bubbles. Therefore, a complete pathological study should be always performed.

Regarding the quantitative differentiation of venous gas emboli, we consider that our grading system to evaluate the presence and abundance of bubbles in several veins at different PM times is an important contribution to this problematic and that the putrefaction study could be used as a guideline for distinguishing how much gas can be expected at different PM times. Indeed, this is the first systematic study performed at different PM times to study gas evolution (both abundance and composition) and comparing three different situations: putrefaction alone, infused air embolism and gas produced by compression/decompression.

We have found statistical differences regarding gas abundance between the three models up to decomposition code 3 (day one). Mainly, there is almost no gas or very few bubbles produced by putrefaction at this point. In contrast there was a moderate to large amount of gas in the air embolism model and always-tremendous large quantities of bubbles in the compression/decompression model (Fig. 3.35 and 3.37). From these results we can conclude that if large amounts of bubbles are present within decomposition code 1-3, putrefaction gases are not the source, thus there is a venous gas embolism. Therefore presence of large amount of gas within decomposition code 1-3 is determinant from the diagnostic point of view, independently of gas composition.

Variability in gas amount in the air embolism model could be due to the different air volumes infused. This should be always kept in mind when analyzing this model.

Anyhow there were some constant differences found within this PM time between the air embolism model and the compression/decompression model. Amount of gas become similar only around decomposition code 3. With decomposition code 1 and 2, larger amounts of gas was always found in the decompression model.

In addition, gas embolism was not as widely distributed in the first as in the later. In both cases, large veins were affected, but only in the compression/decompression model peripheral veins were as well severely affected. This could be clearly seen in the subcutaneous veins (see Fig. 3.39). This difference might be due to how bubbles grow in the compression/decompression model in contrast with a concrete entrance of gas in a given localization as in the induced air embolism.

During decompression, bubbles are hypothesized to grow from pre-existing gas nuclei (Harvey, 1945). Although where and how these nuclei are formed and stabilized is unknown, it is generally acknowledge that gas nuclei might be attached to the endothelial layer. Bubbles from the vascular periphery would be dislodge occasionally from the vessel walls and washed out into the central venous vessels, where bubbles would coalescence and increase in size. It has been reported that in the periphery of the body, small intravascular bubbles may grow into sufficient size to occlude small vessels and as such give rise to stationary intravascular bubbles (Daniels, 1984). Bubbles in the peripheral veins have been described grossly as well in compressed/decompressed animals as discussed before (Harris et al., 1945b; Smith-Sivertsen, 1976), but we haven't found any report about this observation in induced air embolism.

On the other hand, in the induced air embolism, air is entering into the venous circulation through a single point. This process is similar to a lung related trauma where air enters the circulation via the pulmonary vein and from there, left heart, aorta and the arterial circulatory system.

Another interesting observation was the finding of some spleens completely filled with free gas. This was observed in 2/11 animals (18%) in the air embolism model and in 3/11 animals (27%) in the compression/decompression model, but never in the putrefaction one 0/10. It is important to highlight that the observation of the spleen filled with gas is a gross observation, where changes in spleen morphology are only noticeable in extreme cases where large amounts of gas were present. Thus, it is a yes or no observation. Mild to moderate gas accumulation in the spleen require further studies through histology in order to see if more spleens were affected in a moderate scale.

Jepson (2005), found macroscopically gas filled cavities in the liver of 10/2376 (0.4%) cetaceans and only 2/2376 (0.08%) had microscopic cavities in the spleen (Jepson et al., 2005). From these numbers, it can be deduced that free gas within the spleen is not a common finding. Because gas in the spleen was found both, in the induced air embolism and in the compression/decompression model, it seems more likely to be a phenomenon related to gas accumulation rather than *in situ* bubble formation.

The spleen has open and closed circulation, but 90% of the blood has been calculated to take the open route. We consider that in order to get gas accumulated in the spleen, the open route is the most likely one. Arterial capillaries open directly into the cordal meshwork of the red pulp and the blood is forced into the venous sinuses through the pores or interendothelial spaces of the sinus wall. These pores measure between 0.5 and 2.5 μm. If gas bubbles reach the pulp via the open circulation, some (the smallest) might be forced to pass through the pores, others might expand either because of lower pressure in the open circulation than in the veins either because of incorporation of diluted gases from the surroundings and others might coalescence with other bubbles. If bubbles increase in size because any of the previous or some other reasons, it would become harder to force the bubbles to pass through the pores, and gas might accumulate in the spleen. This scenario would only be then possible if bubbles get arterialized by way of transpulmonary passage (if for example the lung is overloaded with gas) or cardiac defects such as a patent foramen oval or atria septal

defect. This might explain why this phenomenon has been only observed in a few cases, although a detailed microscopic examination is pending.

A distinguishing parameter was found on the compression/decompression model compared to the others: the presence of free gas within the fat tissue. This was not observed either in the putrefaction model, either in the induce air embolism model before decomposition code 4. Thus, the presence of free gas within fat tissue with decomposition code 1-3 should be considered as an indicator of severe decompression.

Bubbles in the abdominal tissue of decompressed rats have been studied before with a stereosmicroscope and were interpreted as diagnostic for decompression sickness. Furthermore, they were used as an approaching model to CNS since bubbles during decompression from saturation are most likely to be formed in tissues with a high lipid content and a poor perfusion (Hyldegaard and Madsen, 1989).

This might be related to fat embolism that has been described to occur in decompression. There is a controversy over the origin of fat emboli in decompression states whether it is caused by air-bubble disruption of fat depot tissues whether it involves a much more complicated biochemical reactions involving lipids in blood (Knight, 1996). Although we cannot exclude biochemical reactions because we haven't done any study on this matter, our observations suggest that air bubbles are present within fat tissues in decompression. Bubbles might disrupt the fatty tissue and enter into circulation reaching target organs such as the lungs.

Regarding gas composition, composition of gases and its evolution is much clear in the putrefaction model and in the induced air embolism than in the compression/decompression model. There is a much larger variation in the later model than in the previous that makes difficult to interpret the results.

In the putrefaction model hydrogen was present in all samples recovered from the heart and Vena cava (except for the one considered as atmospheric air pollution)

while in the air embolism hydrogen starts to appear after 42 PM hours (decomposition code 4), but it was not always present. On the other hand it was never present in a fresh sample, thus hydrogen was considered as an indicator of putrefaction. Previous authors had the same results regarding experimental putrefaction, induced air embolism and hydrogen incidence (Pierucci and Gherson, 1969).

The composition of air embolism and its evolution in composition with putrefaction processes is more or less clear since very similar results to ours has been previously reported (Pierucci and Gherson, 1968): starting values of nitrogen are around 70-80% while there are some discrepancies between our results and previous studies regarding how the remaining 20% is distributed between oxygen and CO_2. In any case, CO_2 reaches values close to 20% within one PM hour (Pierucci and Gherson, 1968). Both studies agree as well in how around 24 PM hours, which corresponds to decomposition code 3 in our study, levels of nitrogen started to decrease slowly at the same time as CO_2 levels increased and how after 42 PM hours (decomposition code 4), hydrogen started to appear and there was a mix with putrefaction gas.

All this process is unclear in the compression/decompression model. Some samples had a similar composition to the induced air embolism for the same PM time, but others did not. When there was putrefaction (decomposition 4 or higher), composition samples from all the models were very similar (Fig. 3.43), but it did not happen the same with the fresh samples. Higher CO_2 concentrations were found in fresh samples, mainly in samples recovered from the Vena Cana (Fig. 3.44; 3.45). If the samples that are out of the red line for CO_2 concentrations in figure 3.45, were not considered for regression curves, then very similar tendencies were found for both models: induced air embolism model and compression/decompression model (Fig 3.41; 3.42). But, these samples are not a few. We cannot just exclude them. The first impulse might be to question the accuracy of the method. This was ruled out because the same methodology was applied to the air embolism model and this variability on CO_2 content was not found. Then, why are these samples different? Why do they have

higher CO_2 content? Why CO_2 content is always higher in the Vena cava samples compared to the heart samples of the same animal?

One possible explanation is that this variability has to be with bubble formation, since it is seen mostly in the fresh samples and Vena cava is expected to be closer to the site of bubble formation than the heart. There are large evidences suggesting a role of CO_2 in bubble formation from empirical to theoretical data.

Behnke stated that empirical evidences points to a higher incidence of bends in association with a rise in the CO_2 level respecting to work in compressed air (Behnke, 1951). Bullfrogs exposed to atmospheres of 60-70% of CO_2 and then rapidly decompressed (hypobaric treatment), had in the majority of the cases massive bubbling, while only 3 of 18 in the control group (with no CO_2 pretreatment but with the same decompression profile) presented bubbles (Harris et al., 1945b). These authors report additionally gas analyses with CO_2 contents ranging from 60 to 80 % in bubbles formed in dead rats. Additionally, they injected a mixture of gas with 50% of CO_2 into the blood stream of a frog and they found that the bubbles equilibrate with the blood in a few seconds. Berghage (1978) reported statistically significant rise in decompression sickness when the animals breathed elevated levels of CO_2 in either He-O_2, or N_2-O_2 mixtures and were compressed and decompressed (hyperbaric treatment) (Berghage et al., 1978).

Physical models have shown how CO_2 diffuses rapidly into existing bubbles, like the one performed by Harvey (1945) consisted on layers of water alternately saturated with air and CO_2. Bubbles were moving vertically crossing the different water layers. They increased in size in the CO_2 saturated water and decreased in the air-saturated layer. These changes in volume were very fast, indicating an immediate equilibrium with the surroundings. Other model consisted in tubes with saturated water with nitrogen or CO_2 that were decompressed. Bubbles form with less mechanical agitation in the CO_2 water and grow in size at a higher relative rate (Harris et al., 1945b).

An explanation for this phenomenon is that CO_2 diffusion coefficient is 20 times higher than oxygen and 60 times higher than nitrogen (Guyton, 1981). Based on this, it is hypothesized that CO_2 availability near a newly formed cavity is very high and that consequently there are great probabilities that the pressure in the bubble built up high enough to overcome the surface tension (Dean, 1944), thus yielding an important role to CO_2 in bubble formation. Also in a mathematical model of gas pockets in crevices, it was reported that although metabolic gases might represent a small amount of the gas in the bubble, their presence has a significant effect on the behavior of the bubble under decompression due to the high diffusivity of these gases (Chappell and Payne, 2006).

Although there is not a definite knowledge about which tissues the vascular bubbles originate from, it is generally assumed that they likely form on the venous end of capillary beds or venous sinusoids because inert gas tensions are higher and because the blood pressure is lower (Francis and Simon, 2003). In addition, bubbles have been observed to appear first in the small branches, predominantly from muscles of the legs and back (Harris et al., 1945a). Harris (1945) proposed that at these localizations, CO_2 tension might reach high levels locally in the muscles, reducing the magnitude of mechanical disturbance necessary for creating bubbles and acting therefore as a facilitator in bubble formation. They also suggested that bubbles at their point of origin might contain large levels of CO_2 because of its high availability and diffusion rate, but its composition would change to predominantly nitrogen as bubbles move out into the larger veins and heart where nitrogen would be responsible for further growth and maintenance of the bubble.

Our results are in accordance with this hypothesis. CO_2 levels were usually higher in the Vena cava than they were in the heart and variabilities in CO_2 got smaller at the same time as nitrogen increased in relevance and gas bubble composition was consistently composed of around 80% of nitrogen and 20% of oxygen (except for rabbit studied at twelve PM hours).

Other factors that we considered to enhance this phenomenon are the blocking of the microcirculation and surface area. Blocking of the microcirculation causes not only tissue ischemia but also retards the elimination of dissolved gas and so produces local areas with gas tensions higher than the surrounding tissue (Davies, 1983). Under these special circumstances CO_2 tensions are expecting to increase. The rate of bubble growth is largely determined by gas diffusion that depends on pressure difference, surface area, diffusion constants and gas solubility (Blatteau et al., 2006).

Surface area for gaseous exchange is very reduced in large bubbles occupying an entire section of a vein compare to smaller bubbles surrounded blood. Thus, original composition would remain longer, at the same time as this bubble is blocking the circulation and altering the overall gaseous exchange between tissues and the alveoli. Furthermore, when there is massive bubbling, lungs can become over helmed and gaseous exchange be compromised. All these factors will increase gas tensions locally in tissues and peripheral veins due to gas accumulation of both nitrogen and CO_2 enhancing bubble growth.

The rabbit to which necropsy was performed after 12 PM hours had the highest gas volume score. Almost 12 mL were recovered from the right heart using the aspirometer (the aspirometer might suction blood and gas from the Vena cava as well when placed on the right heart). There was no more capacity for gas occupancy in the heart (Fig. 3.20), vena cava was completely filled with gas, and the blood was pushed away by the gas. Several hemorrhages were observed dispersed in the body. We consider that this animal is a good example for gaseous exchange jeopardized by lung over helmed because of massive bubbling, with low bubble surface for gaseous exchange, and high gas tensions locally in tissues and veins because of the deficient washout of gases. This might explain the high concentrations of CO_2 found (40-60%) in the vena cava, right heart and left heart.

All these factors vary greatly locally such as bubble size, localization of the bubble, gases dissolved in the surroundings or the surrounding's metabolism. Bubbles

are gas phase systems in contact with a liquid phase where a continuous dynamic equilibrium is taking place. Since the surrounding of the bubble is changing continuously, we cannot expect to have the same composition for different bubbles size, localization and so on.

Composition of bubbles produced because of decompression were found to be highly variable although they tend to become similar to air embolism composition bubbles and will vary as putrefaction process advances. Thus, composition of bubbles was not found to be diagnostic of decompression sickness, although it can help to exclude other causes. On the other hand amount and distribution of bubbles, together with the presence of bubbles in the adipose tissue was found to be diagnostic of decompression sickness, although this should be always be interpreted together with a complete pathological study to confirm in vivo bubble formation.

Finally, it is important to keep mind that barotrauma and air embolism can occur simultaneously to decompression sickness, and that these two processes might overlap in many cases. In these cases pathological studies are of even more importance.

3.5 REFERENCES

Arbelo M, Bernaldo de Quirós Y, Sierra E, Méndez M, Godinho A, Ramírez G, Caballero MJ, Fernandez A. 2008. Atypical beaked whale mass stranding in Almeria's coast: Pathological study. The International Journal of Animal Sound and its Recording 17:293-323.

Armstrong HG. 1939. Analyisi of gas emboli. Engineering Section Memorandum Report. Wright Field, Ohio.

Bajanowski T, Kohler H, DuChesne A, Koops E, Brinkmann B. 1998a. Proof of air embolism after exhumation. International Journal of Legal Medicine 112(1):2-7.

Bajanowski T, West A, Brinkmann B. 1998b. Proof of fatal air embolism. International Journal of Legal Medicine 111(4):208-211.

Behnke AR. 1951. Decompression sickness following exposure to high pressures. In: Fulton JF, editor. Decompression sickness. Phyladelphia: Saunders. p 53-89.

Berghage TE, Keating LJ, Wooley JM. Decompression sickness in rats and mice rapidly decompressed after breathing various concentrations of carbon dioxide. In: Lambertsen CJ, editor. Underwater Physiology; 1978. Bethesda. p 485-496.

Bert P. 1878. La Pression Barometrique: Recherches de Physiologie Expérimentale. Hitchcock MA, Hitchcock FA, translator. Paris: Masson.

Blatteau JE, Souraud JB, Gempp E, Boussuges A. 2006. Gas nuclei, their origin, and their role in bubble formation. Aviation Space and Environmental Medicine 77(10):1068-1076.

Chappell MA, Payne SJ. 2006. A physiological model of gas pockets in crevices and their behavior under compression. Respiratory Physiology & Neurobiology 152(1):100-114.

Daniels S. 1984. ULTRASONIC MONITORING OF DECOMPRESSION PROCEDURES. Philosophical Transactions of the Royal Society of London Series B-Biological Sciences 304(1118):153-175.

Davies JM. 1983. Studies on bubble formation after decompression: with special reference to the development and testing of the integrating ultrasonic pulse-echo imaging system for bubble detection. Oxford: University of Oxford.

Dean RB. 1944. The formation of bubbles. Journal of Applied Physics 15(5):446-451.

Dyrenfurth F. 1928. Über den qualitativen und quantitativen nachweis von sauerstoff in lungenund darmgasen von leichen und seine anwendung bei der gerischtsärztlichen feststellung der atmung neugeborener. Dtsch Z ges gerichtl Med 12:23-29.

Eckenhoff RG, Olstad CS, Carrod G. 1990. HUMAN DOSE-RESPONSE RELATIONSHIP FOR DECOMPRESSION AND ENDOGENOUS BUBBLE FORMATION. Journal of Applied Physiology 69(3):914-918.

Eftedal O, Brubakk AO. 1997. Agreement between trained and untrained observers in grading intravascular bubble signals in ultrasonic images. Undersea & Hyperbaric Medicine 24(4):293-299.

Erben JU, Nádvornik F. 1963. The quantitative demonstration of air embolism: in certain cases of fatal trauma. Journal of Forensic Medicine 10(2).

Fernandez A, Edwards JF, Rodriguez F, de los Monteros AE, Herraez P, Castro P, Jaber JR, Martin V, Arbelo M. 2005. "Gas and fat embolic syndrome" involving a mass stranding of beaked whales (Family Ziphiidae) exposed to anthropogenic sonar signals. Veterinary Pathology 42(4):446-457.

Francis TJR, Simon JM. 2003. Pathology of Decompression Sickness. In: Brubakk AO, Neuman TS, editors. Bennett and Elliott's Physiology and Medicing of Diving: Saunders. p 530-556.

Geraci JR, Lounsbury VJ. 2005. Marine Mammals Ashore: a Fiel Guide for Strandings. Second ed. Baltimore, MD: National Aquarium in Baltimore.

Guyton AC. 1981. Physical principles of gaseous exchange; diffusion of oxygen and carbon dioxide through the respiratory membrane. Textbook of medical physiology. 6th Edition ed. Philadelphia: W.B. Saunders. p 491-503.

Hamilton RW, Thalmann ED. 2003. Decompression practice. In: Brubakk AO, Neuman TS, editors. Bennett and Elliott's Physiology and Medicing of Diving: Saunders. p 455-500.

Harris M, Berg WE, Whitaker DM, Twitty VC. 1945a. THE RELATION OF EXERCISE TO BUBBLE FORMATION IN ANIMALS DECOMPRESSED TO SEA LEVEL FROM HIGH BAROMETRIC PRESSURES. Journal of General Physiology 28(3):241-251.

Harris M, Berg WE, Whitaker DM, Twitty VC, Blinks LR. 1945b. Carbon dioxide as a facilitating agent in the initiation and growth of bubbles in animals decompressed to simulated altitudes. Journal of General Physiology 28(3):225-240.

Harvey EN. 1945. DECOMPRESSION SICKNESS AND BUBBLE FORMATION IN BLOOD AND TISSUES - HARVEY LECTURE, OCTOBER 26, 1944. Bulletin of the New York Academy of Medicine 21(10):505-536.

Hellebrekers LJ, deBoer EJW, vanZuylen MA, Vosmeer H. 1997. A comparison between medetomidine-ketamine and medetomidine-propofol anaesthesia in rabbits. Laboratory Animals 31(1):58-69.

Hrncir E. 1996. Importance of surface tension in therapeutic compression in decompression sickness. Physiological Research 45(6):467-470.

Hyldegaard O, Madsen J. 1989. INFLUENCE OF HELIOX, OXYGEN, AND N2O-O2 BREATHING ON N-2 BUBBLES IN ADIPOSE-TISSUE. Undersea Biomedical Research 16(3):185-193.

Ishiyama A. 1983. Analysis of gas composition of intra vascular bubbles produced by decompression. Bulletin of Tokyo Medical and Dental University 30(2):25-36.

Jackowski C, Schweitzer W, Thali M, Yen K, Aghayev E, Sonnenschein M, Vock P, Dirnhofer R. 2005. Virtopsy: postmortem imaging of the human heart in situ using MSCT and MRI. Forensic Science International 149(1):11-23.

Jepson PD, Arbelo M, Deaville R, Patterson IAP, Castro P, Baker JR, Degollada E, Ross HM, Herraez P, Pocknell AM, Rodriguez F, Howie FE, Espinosa A, Reid RJ, Jaber JR, Martin V, Cunningham AA, Fernandez A. 2003. Gas-bubble lesions in stranded cetaceans - Was sonar responsible for a spate of whale deaths after an Atlantic military exercise? Nature 425(6958):575-576.

Jepson PD, Deaville R, Patterson IAP, Pocknell AM, Ross HM, Baker JR, Howie FE, Reid RJ, Colloff A, Cunningham AA. 2005. Acute and chronic gas bubble lesions in cetaceans stranded in the United Kingdom. Veterinary Pathology 42(3):291-305.

Kaiser H. 1947. Die berechnung der nachweisempfindlichkeit. Spectrochimica Acta 3(1):40-67.

Keil W, Bretsxhneider K, Patzelt D, Behning I, Lignitz E, Matz J. 1980. Luftembolie oder Fäulnisgas? Zur Dianostik der cardialen Luftembolie an der Leiche. Beiträge zur Gerichtlichen Medizin 38:395-408.

King JM, Dodd DC, Newson ME, Roth L. 1989. The Necropsy Book. New York State College of Veterinary Medicine CU, editor. Ithaca, E.E.U.U.: Charles Louis Davis, D.V.M. Foundation.

Knight B. 1996. Forensic Pathology. Arnold, editor. London.

Kuiken T, García-Hartmann M. Dissection techniques and tissues sampling. In: Newsletter, editor; 1991; Leiden, Netherlands.

Lerner L, Lerner BW. 2006. Decomposition. World of Forensic Science: eNotes.com.

Lillo RS, Maccallum ME, Caldwell JM. 1992. Intravascular bubble composition in guinea-pigs a possible explanation for differences in decompression risk among different gases. Undersea Biomedical Research 19(5):375-386.

Muth CM, Shank ES. 2000. Primary care: Gas embolism. N Engl J Med 342(7):476-482.

Nishi RY, Brubakk AO, Eftedal O. 2003. Bubble detection. In: Brubakk AO, Neuman TS, editors. Bennett and Elliott's Physiology and Medicine of Diving. 5th Edition ed: Saunders. p 501-529.

Pedal I, Moosmayer A, Mallach HJ, Oehmichen M. 1987. AIR-EMBOLISM OR PUTREFACTION - RESULTS OF GAS-ANALYSIS AND THEIR INTERPRETATION. Zeitschrift Fur Rechtsmedizin-Journal of Legal Medicine 99(3):151-167.

Piantadosi CA, Thalmann ED. 2004. Pathology: whales, sonar and decompression sickness. Nature 428(6984):1 p following 716; discussion 712 p following 716.

Pierucci G. 1985. THE POST-MORTEM DIAGNOSIS OF GAS EMBOLISM. Pathologica (Genoa) 77(1048):145-156.

Pierucci G, Gherson G. 1968. Experimental study on gas embolism with special reference to the differentiation between embolic gas and putrefaction gas. Zacchia 4(3):347-373.

Pierucci G, Gherson G. 1969. Further contribution to the chemical diagnosis of gas embolism. The demonstration of hydrogen as an expression of "putrefactive component". Zacchia 5(4):595-603.

Richter M. 1905. Gerichtsärztliche Diagnostik und Technik.: S. Hirzel, Leipzig.

Sawatzky KD. 1991. The relationship between intravascular Doopler-detected gas bubbles and decompression sickness after bounce diving in humans [MSc thesis]. Toronto, Canada: York University.

Smith-Sivertsen J. The origin of intravascular bubbles produced by decompression of rats killed prior to hypebaric exposure. In: Lambertsen CJ, editor; 1976; Washington, DC. Bethesda MD. p 303-309.

Statheropoulos M, Spiliopoulou C, Agapiou A. 2005. A study of volatile organic compounds evolved from the decaying human body. Forensic Science International 153(2-3):147-155.

Tikuisis P, Gerth WA. 2003. Decompression theory. In: Brubakk AO, Neuman TS, editors. Physiology and Medicine of Diving. Saunders ed: Saunders. p 419-454.

Vann RD, Butler FK, Mitchell SJ, Moon RE. 2011. Decompression illness. The Lancet 377(9760):153-164.

Vass AA, Barshick SA, Sega G, Caton J, Skeen JT, Love JC, Synstelien JA. 2002. Decomposition chemistry of human remains: A new methodology for determining the postmortem interval. Journal of Forensic Sciences 47(3):542-553.

Weissman A, Kol S, Peretz BA. 1996. Gas embolism in obstetrics and gynecology - A review. Journal of Reproductive Medicine 41(2):103-111.

Zumwalt RE, Bost RO, Sunshine I. 1982. EVALUATION OF ETHANOL CONCENTRATIONS IN DECOMPOSED BODIES. Journal of Forensic Sciences 27(3):549-554.

TABLA DE CONTENIDO

4 CHAPTER IV: GAS EMBOLISM IN STRANDED CETACEANS

4.1 INTRODUCTION

Gas-bubble lesions have been described in cetaceans stranded in spatiotemporal concordance with military maneuvers (Fernandez et al., 2005; Jepson et al., 2003). Authors suggested a decompression-like disease as a plausible mechanism for explaining the observed lesions. These findings have been largely discussed since then and have become a scientific controversy. Further investigations, including gas analysis of bubbles have been claimed (Piantadosi and Thalmann, 2004).

The new pathological entity named "Gas Bubble Disease" or " Decompression like Sickness" in cetaceans was deeply discussed in a specific Workshop Marine Mammal Commission of the United States (2004) with the participation of international experts and one of its main conclusions was that: " induced Gas-bubble disease, is a plausible pathologic mechanism for the morbidity and mortality seen in cetaceans associated with sonar and merits further investigations"

Several mechanisms were proposed (Cox et al., 2006), most of them related to a disturbance caused by an acoustic signal that could:

A. Affect normal diving behavior leading to increased supersaturation, thus increasing DCS risk.
B. Activate gas nuclei allowing them to grow by passive diffusion.
C. Favor gas nuclei growth by rectified diffusion.

One of these mechanisms was considered particularly feasible: an acoustically induced behavioral change (dive response) that leads to formation of significant gas bubbles, which damage multiple organs or interfere with normal physiology function (Cox et al., 2006).

Some species of BWs have dive profiles not previously observed in other marine mammals such as very deep foraging dives (up to 2000 msw and as long as 90 min), relatively slow controlled ascents followed by a series of bounce dives of 100-400 msw (Hooker and Baird, 1999; Tyack et al., 2006). These diving profiles are considered as extreme dives and alterations of this dive sequences by a behavioral response might induce excessive nitrogen supersaturation driving growth of bubbles in a manner similar to decompression sickness in humans (Cox et al., 2006).

The waters of the Canary Islands make up one of the richest and most diverse areas in the Northeast Atlantic, with 28 different species reported, 21 of the Odontocete group and 7 of the Mysticete group. Of these 28 species, at least 26 have been found stranded on the coasts of the Canary Islands (Martin et al., 2009).

It is an area of extremely high natural value due to its strategic position on the migratory path of many species and to its oceanographic characteristics (temperature, deep and steep bathymetry close to shore because of the lack of a continental shelf, abundant cephalopods and areas of calm waters in the South-Southwest of the island). This has given rise to the establishment of year round resident populations of cetaceans, such as the bottlenose dolphin (*Tursiops truncatus*), short-finned pilot whale (*Globicephala macrorhynchus*), Risso's dolphin (*Grampus griseus*), sperm whale (*Physeter macrocephalus*), Cuvier's beaked whale (*Ziphius cavirostris*) and Blainville's beaked whale (*Mesoplodon densirostris*). The Canary Islands archipelago is the only place in Europe where it is possible to observe species such as short-finned pilot whale (*Globicephala macrorhynchus*), rough-toothed dolphin (*Steno bredanensis*), Atlantic spotted dolphin (*Stenella frontalis*) and Bryde's whale (*Balaenoptera edeni*) all year round (Martin et al., 2009).

This high biodiversity including both shallow and deep diving species, make the Canary Islands an excellent natural laboratory for the study of gas embolism in cetaceans with different diving behaviors. We have decided to make the segregation of

deep and non-deep diving species depending whether they do foraging dives usually deeper than 500 m depth or not.

Unfortunately, time-depth recorders have only been used in some cetaceans' species. While in others, foraging depths are deduced from observational studies of ecosystem use, bathymetry of their habitats and stomach content.

Mysticets are not known to do deep foraging dives. As an example, Fin whales (*Balaenoptera physalus*) usually dive to around 98 m depth with 6 min of duration when foraging (Croll et al., 2001).

Among odontocetes the small dolphins perform the shallower dives. Common dolphins (*Delphinus delphis*) forage at depths of 90 m for 3 min and pantropical spotted dolphins (*Stenella attenuata*) usually dive to 50-100 m depth for 2-4 min (Stewart, 2009).

On the other hand there are also deep divers of the *Delphinidae* family that we can find in the Canary Islands waters: the short-finned pilot whale (*Globicephala macrorhynchus*) and the Risso's dolphin (*Grampus griseus*). Pilot whales from Canary Islands have been extensively studied. They have been reported to perform both shallow and deep dives (deeper than 500 m). Mean values for both dive types were of 90 m versus 723 m depth and duration types of 3 and 15 min respectively (Aguilar de Soto, 2006). No diving behavior studies have been carried out in Risso's dolphin but habitat preferences (steep slopes from 500 to 1000 m depth) and diet (principal prey are bathypelagic cephalopods) suggest deep diving foraging (Astruc and Beaubrun, 2005; Gannier, 1998).

Very little is known about pigmy and dwarf sperm whales (SWs) (*Kogia breviceps* and *Kogia sima*), but they frequently strand in the Canary Islands' coasts. The diet of the pigmy SW is composed of bathypelagic cephalopods, some of them found at depths of 800 to 1200 m depth, suggests once more deep diving behavior (West et al., 2009).

The sperm whale is resident specie in the Canary Islands. It is well known for its very deep dives, reaching up to 2035 m depth (Kooyman, 2009). Routine foraging dives have been reported from 643 to 985 and 45 min duration (Watwood et al., 2006).

Sightings and strandings of BWs in the Canary Islands are very frequent. Five species have been reported so far: Cuviers', Blainville's, Gervais', Sowerby's and Bottlenose BW (Martin et al., 2009). In this family (*Ziphiidae*) we find the deepest and longest foraging dives ever reported for any other air-breathing specie correspond to those performed by Cuvier's BW and Blainville's BW with 1070m and 58 min, and 835 and 47 min respectively (Tyack et al., 2006). The bottlenose BW (*Hyperodoon ampullatus*), has been recorded to dive every 80 minutes to over 800 m depth with durations as long as 70 min (Hooker and Baird, 1999). Depths of foraging dives for Sowerby's BW or Gervais' BW are unknown.

4.2 MATERIAL AND METHODS

4.2.1 MATERIAL

Animals used for the study were cetaceans stranded in the Canary Islands between 2006 and 2010, BW mass stranded in Azores in 2009, SW mass stranded in Italy in 2009, and two sea lions (*Otaria byronia*) from aquatic-parks of Canary Islands remitted for necropsy to our institution. In total, 93 marine mammals belonging to 18 different species were necropsied and 496 gas samples analyzed. Except for the sea lions (pinnipeds of the family *Otariidae*) all the rest were stranded cetaceans (Fig. 5.1). Few were mysticets, all of them belonging to the family *Balaenopteridae* (rorquals). Among odontocetes, most of the animals were of the family *Delphinidae* (dolphins) but *Kogiidae* (pygmy and dwarf sperm whales), *Physeteridae* (sperm whales) and *Ziphiidae* (beaked whales) were also present in the study.

Animals were identified by its stranding number, which is represented as CET ("cetacean") followed by the stranding number. Animals not stranded in the Canary Islands are identified by its investigation number, which is represented by I ("investigation") followed by its corresponding number and the year when it was studied.

Cetaceans that had been observed to strand alive were considered as "active strandings", all the rest were considered as "passive strandings". Cases with signs of "active stranding" were noted with a question mark. Additionally it was indicated when the cetaceans were involved either in a single stranding or in a "typical mass stranding" refering to two or more cetaceans, other than a female and her calf, coming ashore at the same time and location (Geraci and Lounsbury, 2005).

Pathological studies were conducted by the Division of Histology and Animal Pathology of the Institute for Animal Health (University of Las Palmas de Gran

Canaria), in order to identify lesions and to determine a morphological diagnosis, identify aetiological agents and, ultimately, to reach a final diagnosis. As a result of these processes, cause(s) of death (defined as pathological entities) were identified whenever possible (Arbelo, 2007; Unit of Cetaceans Research, 2006; 2007; 2008; 2009; 2010).

The data was first segregated in two broad groups: deep divers and non-deep divers, considering as deep divers as those species supposed to dive usually deeper than 500m for foraging (*Kogia*, *Physeter*, *Ziphius*, *Mesoplodon*, *Globicephala* and *Grampus*). These genera were further studied alone except for *Ziphius* and *Mesoplodon* that were studied together as the family *Ziphiidae*.

Table 4.1: Identification number of the marine mammals included in the study, biological information, stranding circumstances, storing conditions, decomposition code and most likely (*) cause of dead established by individual pathological studies.

Identification number	Specie	Deep diver	Gender	Age	Active stranding	Mass stranding	Frozen	Decomposition code	Cause of dead*
CET 339	*Globicephala macrorhynchus*	yes	F	adult	yes	no	no	2	Septicaemia
CET 360	*Globicephala macrorhynchus*	yes	M	calve	yes	no	no	1	Infectious meningitis
CET 361	*Globicephala macrorhynchus*	yes	ND	adult	no	no	no	5	Trauma
CET 362	*Stenella frontalis*	no	F	adult	yes	no	no	1	Septicaemia
CET 363	*Stenella frontalis*	no	F	Subadult	?	no	yes	2	Obstruction by foreign body.
CET 364	*Delphinus delphis*	no	M	Subadult	no	no	yes	3	Infectious meningoencephalitis
CET 367	*Stenella coeruleoalba*	no	M	calve	no	no	yes	5	Abnormal development
CET 368	*Stenella frontalis*	no	M	juvenile	?	no	yes	3	Trauma
CET 369	*Balaenoptera physalus*	no	F	adult	no	no	no	4	Trauma
CET 370	*Stenella coeruleoalba*	no	M	adult	yes	no	no	3	Septicaemia
CET 371	*Stenella frontalis*	no	F	adult	?	no	no	2	Trauma
CET 372	*Balaenoptera borealis*	no	F	Subadult	no	no	no	5	not determined
CET 373	*Delphinus delphis*	no	F	adult	yes	no	no	2	Septicaemia
CET 374	*Stenella coeruleoalba*	no	M	adult	no	no	no	3	Trauma
CET 375	*Stenella coeruleoalba*	no	M	neonate	no	no	yes	3	Neonatal weakness
CET 376	*Stenella coeruleoalba*	no	F	adult	no	no	yes	2	Neoplasia
CET 379	*Mesoplodon bidens*	yes	M	adult	?	no	no	2	Trauma Septicaemia
CET 380	*Stenella coeruleoalba*	no	M	Subadult	?	no	no	2	Infectious encephalitis
CET 381	*Delphinus delphis*	no	M	Subadult	no	no	yes	4	Infectious encephalitis
CET 382	*Delphinus delphis*	no	M	adult	?	no	no	3	Sinusitis and meningoencefalitis by *Nasitrema* sp.
CET 384	*Stenella frontalis*	no	M	adult	no	no	yes	3	Toxoplasmosis
CET 390	*Globicephala macrorhynchus*	yes	M	calve	?	no	no	3	Septicaemia

(Follow-up) Table 4.1: Identification number of the marine mammals included in the study, biological information, stranding circumstances, storing conditions, decomposition code and most likely (*) cause of dead established by individual pathological studies.

Identification number	Specie	Deep diver	Gender	Age	Active stranding	Mass stranding	Frozen	Decomposition code	Cause of dead*
CET 393	*Stenella frontalis*	no	F	adult	?	no	no	2	Neoplasia
CET 395	*Stenella frontalis*	no	M	adult	no	no	yes	2	Neoplasia
CET 397	*Kogia breviceps*	yes	F	adult	no	no	no	3	Trauma Septicaemia
CET 399	*Globicephala macrorhynchus*	yes	M	neonate	no	no	no	5	Trauma
CET 400	*Stenella coeruleoalba*	no	M	adult	no	no	no	2	Parasitoses Senile disease
CET 402	*Stenella coeruleoalba*	no	F	adult	no	no	no	5	Septicaemia Senile disease
CET 404	*Kogia breviceps*	yes	M	adult	yes	no	no	1	Encephalopathy of unknown etiology
CET 409	*Stenella coeruleoalba*	no	F	Subadult	no	no	yes	3	Infectious encephalitis Parasitoses
CET 413	*Pseudorca crassidens*	no	M	juvenile	yes	no	no	2	Trauma Septicaemia
CET 418	*Stenella frontalis*	no	F	adult	?	no	yes	2	Heart failure
CET 419	*Steno bredanensis*	no	F	juvenile	no	no	yes	2	Septicaemia
CET 421	*Stenella frontalis*	no	M	calve	no	no	yes	2	not determined
CET 425	*Delphinus delphis*	no	F	juvenile	no	no	yes	4	Parasitoses
CET 430	*Steno bredanensis*	no	F	Subadult	no	no	no	4	not determined
CET 431	*Grampus griseus*	yes	M	juvenile	yes	no	no	2	Infectious meningitis
CET 434	*Steno bredanensis*	no	M	adult	no	yes	no	5	Not determined
CET 435	*Stenella frontalis*	no	F	adult	no	no	no	5	Trauma
CET 437	*Steno bredanensis*	no	F	adult	no	yes	no	5	Not determined
CET 438	*Steno bredanensis*	no	F	Subadult	no	no	no	5	Not determined
CET 456	*Grampus griseus*	yes	F	adult	yes	no	yes	2	Infectious meningoencephalitis
CET 459	*Kogia breviceps*	yes	M	adult		no	no	3	Trauma Bycatch?
CET 460	*Stenella coeruleoalba*	no	M	calve	no	no	no	4	Trauma

(Follow-up) Table 4.1: Identification number of the marine mammals included in the study, biological information, stranding circumstances, storing conditions, decomposition code and most likely (*) cause of dead established by individual pathological studies.

Identification number	Specie	Deep diver	Gender	Age	Active stranding	Mass stranding	Frozen	Decomposition code	Cause of dead*
CET 462	*Stenella frontalis*	no	F	calve	no	no	yes	5	not determined
CET 463	*Physeter macrocephalus*	yes	F	neonate	yes	no	no	1	Parental segregation
CET 464	*Globicephala macrorhynchus*	yes	M	juvenile	no	no	no	4	Enterotoxaemia Septicaemia
CET 469	*Stenella coeruleoalba*	no	F	adult	?	no	no	3	Parasitoses Senile disease
CET 471	*Ziphius cavirostris*	yes	F	calve	?	no	no	2	Chronic renal failure
CET 472	*Grampus griseus*	yes	F	Subadult	no	no	no	2	Trauma
CET 473	*Steno bredanensis*	no	F	juvenile	yes	no	no	2	Septicaemia
CET 474	*Stenella coeruleoalba*	no	M	adult	no	no	yes	2	Septicaemia
CET 476	*Stenella coeruleoalba*	no	F	calve	no	no	no	2	Chronic renal failure
CET 482	*Delphinus delphis*	no	F	adult	no	no	yes	3	Bacterial broncopneumonia
CET 483	*Grampus griseus*	yes	M	adult	yes	no	no	2	Venous gas embolism
CET 487	*Stenella coeruleoalba*	no	F	juvenile	no	no	no	5	not determined
CET 504	*Globicephala macrorhynchus*	yes	M	adult	no	no	no	4	Meningitis Septicaemia
CET 505	*Tursiops truncatus*	no	M	juvenile	no	no	no	5	not determined
CET 506	*Stenella coeruleoalba*	no	F	neonate	no	no	yes	4	not determined
CET 509	*Tursiops truncatus*	no	M	Subadult	no	no	no	4	not determined
CET 510	*Mesoplodon europaeus*	yes	M	adult	?	no	no	3	Trauma Possible viral disease
CET 512	*Globicephala macrorhynchus*	yes	M	adult	no	no	no	3	Septicaemia
CET 515	*Stenella frontalis*	no	M	adult	no	no	yes	2	Toxoplasmosis
CET 517	*Delphinus delphis*	no	M	adult	no	no	no	2	Chronic renal failure
CET 520	*Physeter macrocephalus*	yes	F	calve	no	no	no	4	Trauma
CET 521	*Delphinus delphis*	no	ND	juvenile	no	no	yes	5	not determined

(Follow-up) Table 4.1: Identification number of the marine mammals included in the study, biological information, stranding circumstances, storing conditions, decomposition code and most likely (*) cause of dead established by individual pathological studies.

Identification number	Specie	Deep diver	Gender	Age	Active stranding	Mass stranding	Frozen	Decomposition code	Cause of dead*
CET 522	*Stenella frontalis*	no	M	adult	no	no	yes	3	Toxoplasmosis
CET 523	*Balaenoptera acutorostrata*	no	M	calve	no	no	no	2	Parental segregation
CET 526	*Tursiops truncatus*	no	F	adult	?	no	no	2	Septicaemia
CET 527	*Stenella coeruleoalba*	no	F	adult	yes	no	yes	3	Parasitoses Bacterial infection
CET 530	*Stenella frontalis*	no	F	adult	?	no	no	2	Trauma Toxoplasmosis
CET 531	*Stenella frontalis*	no	M	juvenile	?	no	no	2	Septicaemia
CET 533	*Grampus griseus*	yes	M	adult	no	no	no	4	Not determined Parasitoses
CET 534	*Grampus griseus*	yes	M	Subadult	yes	no	no	1	Viral disease Bacterial/Mycotic infection
CET 537	*Stenella coeruleoalba*	no	F	adult	no	no	no	2	Septicaemia
CET 542	*Kogia sima*	yes	ND	adult	no	no	no	4	Septicaemia
CET 543	*Tursiops truncatus*	no	M	adult	no	no	no	5	Senile disease Parasitoses
CET 544	*Physeter macrocephalus*	yes	M	juvenile	no	no	no	5	Trauma Ship collision
CET 546	*Stenella coeruleoalba*	no	M	adult	yes	no	no	3	Trauma Stranding Stress Syndrome
CET 547	*Mesoplodon europaeus*	yes	M	adult	?	no	no	4	not determined
CET 548	*Stenella frontalis*	no	M	calve	no	no	no	2	Viral disease
CET 549	*Grampus griseus*	yes	F	adult	no	no	no	2	Venous gas embolism
CET 552	*Balaenoptera borealis*	no	M	juvenile	no	no	no	5	pending
I134/07	*Otaria byronia*	no	M	adult	no	no	no	3	not determined
I181/09	*Mesoplodon bidens*	yes	M	Juvenile	yes	yes	no	3	pending
I182/09	*Mesoplodon bidens*	yes	F	adult	no	yes	no	3	pending
I183/09	*Mesoplodon bidens*	yes	F	adult	?	yes	no	3	pending
I184/09	*Mesoplodon bidens*	yes	F	adult	?	yes	no	4	pending

(Follow-up) Table 4.1: Identification number of the marine mammals included in the study, biological information, stranding circumstances, storing conditions, decomposition code and most likely (*) cause of dead established by individual pathological studies.

Identification number	Specie	Deep diver	Gender	Age	Active stranding	Mass stranding	Frozen	Decomposition code	Cause of dead*
I185/09	*Mesoplodon bidens*	yes	F	adult	no	yes	no	5	pending
I344/07	*Otaria byronia*	no	*M*	*juvenile*	no	no	no	2	Iatrogenic pneumo-mediastinum
I298/09	*Physeter macrocephalus*	yes	*M*	*juvenile*	yes	yes	no	3	Not determined
I299/09	*Physeter macrocephalus*	yes	*M*	*juvenile*	yes	yes	no	2	Not determined
I300/09	*Physeter macrocephalus*	yes	*M*	*juvenile*	yes	yes	no	2	Not determined

4.2.2 METHODS

Necropsy and gas sampling have been fully described and discussed in detail previously on chapter III. Here is presented the final methodology and how it has been integrated in the necropsy protocol.

4.2.2.1 Dissection and external exploration

Necropsy protocol is based on a standard procedure for cetaceans published by Kuiken and Harman (1991), the field guide for strandings of marine mammals by Geraci and Lounsbury (2005) and the domestic animal necropsy book by King et al. (1989). To these procedures some technical innovations have been added, including those reported here related to gas sampling.

The decomposition code of the body was determined following the parameters and classifications established in the protocol of necropsies of cetaceans referenced by the European Cetacean Society (Kuiken and García-Hartmann, 1991): level 1-very fresh, level 2-fresh, level 3-moderate autolysis, level 4-advanced autolysis and level 5-very advanced autolysis. This code is as well described in appendix 9.2.1.

Cetaceans were positioned in right lateral *decubitus* for the performance of the necropsy. In first place, the animal was explored externally in order to assure that non-perforate lesions were not present. Secondly, skin and blubber was removed taking into account possible gas embolism within the subcutaneous vessels. If bubbles were seen, vessels were explored to confirm that they had not been cut during dissection. Then, the abdominal cavity was opened. Mesenteric and renal veins were screened for bubbles. After this was done, the thoracic cavity was opened to have access to the heart and pericardial sac. Once this was carefully open, pericardial veins were explored. As soon as bubbles were detected, a photo was taken.

Evaluation of emphysema and gas embolism in veins was done retrospectively in many cases, using photos and data written in the necropsy reports, thus a more simple grading system than that of the rabbits was used: grade 0 is no bubbles, grade I means few bubbles and grade II represents abundant presence of bubbles. Screened vessel for gas bubble's score were subcutaneous, mesenteric, coronary veins as well as the lumbo-caudal venous plexus. Subcapsular gas was evaluated with a similar grading system: grade 0 is no subcapular gas, grade I means presence of subcapsular gas in one or two organs and grade II represents wide distribution. Gas in spleen was not scored in cetaceans as it was never found in our study (See appendix 9.1. Grading systems used).

Since bubble score was done retrospectively using pictures, some information was missing in some animals. In these cases a question mark was written besides the bubble score. When only one question mark was present, the sumatory of the free gas in tissues/veins was done but an asterisk (*) was noted together with the result. Then the summation should be considered as the real measured score with potentially 0-2 unites more. On the other hand, if more than one question mark was present, the summation was not done, understanding that it won't be realistic, thus a question mark was noted besides the summation. If decomposition was so advance that veins could not be clearly distinguised from the rest of the tissues then an asterisk alone wa written in the summation box.

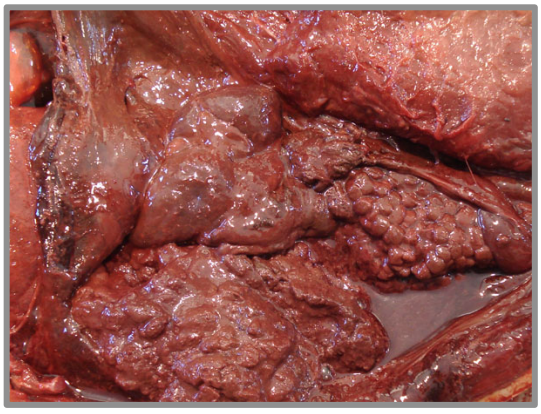

Fig. 4.1: Very advance autolysis (decomposition code 5). Veins cannot be distinguished or identified.

After vessels exploration for bubbles, the pericardial sac was filled in with distilled water and mesenteric veins were placed down the water when possible for gas sampling. For gas extraction, it is important to avoid cutting large vessels during dissection of the animal. Only after bubble exploration and extraction of gas from cavities, large vessels can be cut following a routine necropsy protocol.

4.2.2.1.1 Gas sampling

Gas sampling, analytical methodology was fully described in detailed in chapter III. Here it is presented the use of the methodology and how this was integrated in the necropsy protocol. Routine samples included at first right and left heart as well as the intestine. After 2008 this protocol was implemented to include gas sampling from aorta and pulmonary artery when blood was found inside the heart cavities trying therefore to get a clean gas sample (without blood). Pterygoid sinuses were also included to be sampled. From 2009 up to date, the aspirometer was used routinely for gas sampling in fresh animals.

4.2.2.1.2 Gas sampling from cavities

5mL vacutainer with no additives (BD Vacutainer® Z. ref: 367624) was directly applied to cavities with its appropriate plastic holder or adapter and a double-pointed needle. To avoid atmospheric air contamination, the needle was first inserted into the cavity for purging. Secondly the vacutainer was pushed against the double-pointed needle, and then the vacutainer was removed before the needle was released from the cavity. This method allows adequate sampling from sinuses, digestive tract, and even also from heart ventricles, if carcasses putrefaction ranges from grade three to five. Filling of the pericardium sac with distilled water is always necessary for atmospheric air avoidance in cetaceans.

4.2.2.1.3 Gas sampling from the heart cavities

When decomposition status was fresh or very fresh (putrefaction grade 2 or 1 respectively), then the aspirometer was used for the separation of gas from the blood found in the heart cavities. This apparatus was mainly used after 2009. Detailed description about how the aspirometer works was given in chapter II.

4.2.2.1.4 Gas sampling from bubbles

Disposable insulin syringes (BD Plastipak U-100 insulin) were used and its content was promptly injected into a vacutainer. A new insulin syringe is used for each bubble and one new vacutainer tube was used per bubble.

Although we strongly recommend sampling bubbles down the water, this procedure is not an easy task in cetaceans and under determined circumstances this becomes almost impossible. Thus, only mesenteric and coronary veins were sampled down the water whenever possible. Coronary veins were sampled down the water by filling the pericardium sac with distilled water, while mesenteric veins could be sample down the water by placing some intestine portions down the water in a tray. Filling the pericardium sac in large whales is not feasible and many times bubbles might be caudally located. These bubbles can only be reached after opening completely the pericardium sac. Other bubble's localizations were just not possible to place down the water without cutting a large vessel.

4.2.2.2 Transport and storage of gas samples

Vacutainers were kept upside-down at room temperature. Single samples were transported and stored together with one intact vacutainer (*blank*) per sample or a minimum of 3 blanks per samples set.

4.2.2.3 Gas analysis

Gas analysis was done by gas chromatography. Samples were injected manually into a gas chromatograph (Varian 450-GC) with the use of a block-pressure syringe (Supelco A-2 serie). Temperature of injector was set up at 230°C. This chromatograph was equipped with a Varian CP7430 column composed of two different sub-columns in tandem: a (Q) Porabond Q column, for separation of CO_2 and hydrocarbons compounds upto 4 carbons, and a (M) Molsieve 5 A column, for separation of permanent gases such as oxygen, nitrogen, argon, and so on. For detection of these compounds it was necessary to have both; a thermal-conductivity detector (TCD), and a Flame-Ionization detector (FID) disposed one after each other. The TCD is a universal detector for permanent gases. Its temperature was fixed at 80°C while the temperature filament was 160°C. The FID is a selective hydrocarbons destructive detector. Because of its destructive feature, the FID must be always placed after the TCD. The temperature for the FID was fixed at 230°C. Samples were running during 25 minutes with isotherm temperature of 45°C and electronic controlled flux with fixed pressure of 13.1 psi on the head column. Helium was used as carrier gas.

4.2.2.4 Gas calculations

Since gases are temperature and pressure dependent, calibration curves were frequently recalculated. They were performed using pure gases except for oxygen and nitrogen where atmospheric air was used. Gas composition of samples was calculated in µL and µmoles from the calibration curves. To normalize samples in order to compare results, composition percentages were calculated from the µmoles.

When samples were studied, vacutainer's background was corrected by measuring it on blanks, which were always exposed to the same pressure, temperature and storage time conditions as the samples. The detection limit is set at $S_{\min} = \overline{S}_{blank} + 3s_{blank}$, where $S_{\min}$ is the minimum detectable signal, $\overline{S}_{blank}$, is the

average signal for a given gas in the blanks, and s_{blank} is the associated standard deviation (Kaiser, 1947).

4.3 RESULTS

18 different species were studied for gas embolism. The most abundant species were *Stenella frontalis* (19%) and *Stenella coeruleoalba* (17%) followed by *Delphinus delphis* (9%), *Globicephala macrorhynchus* (9%) and *Grampus griseus* (8%). All of them belong to the family *Delphinidae* (dolphins). 34 out of 93 (37%) were deep divers but their number of samples taken comprised 55% of the total (274/496).

25% of the total of animals were frozen.

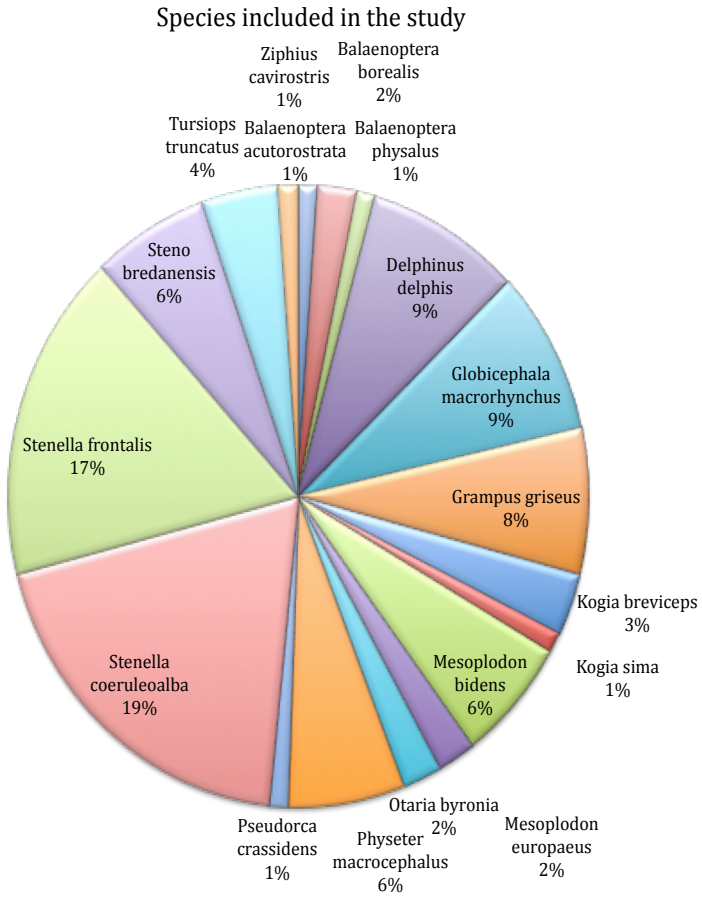

Fig. 4.2: Species of marine mammals sampled for this study.

With the 93 animals, all decomposition codes were covered. Decomposition code 1 comprised the least number of cases, but decomposition code 2 was the highest.

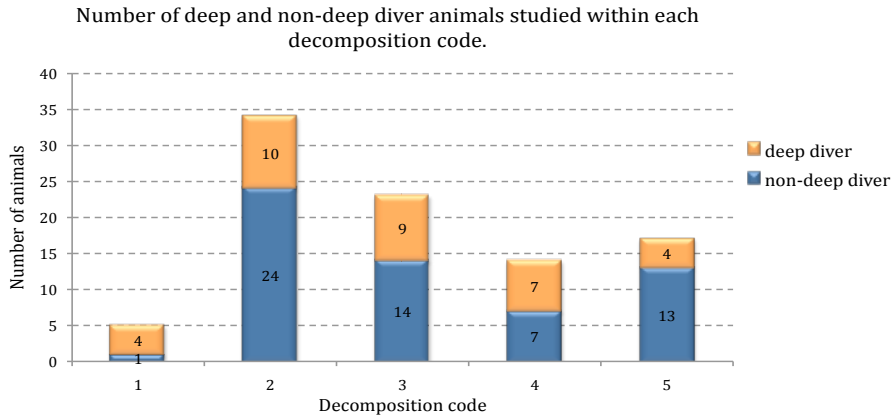

Fig. 4.3: Number of animals studied within each decomposition code.

In the experimental putrefaction model performed in rabbits very few if any differences were found between code 1 and 2, and between 4 and 5, thus these decomposition codes were sometimes explored together. When joining these groups, animals with decomposition code 1-2 represent 42% of the total, 25% presented decomposition code 3 and 33% had decomposition codes 4 or 5. This aggregation made the study of the decomposition codes to become more equilibrated. Deep and non-deep divers are well distributed through the different decomposition codes.

Bubbles were found in 56 out of 93 animals (60%) and they were absent in 33 out of 93 (36%) but the observation was not correctly done in 4 out of 93 animals (4%).

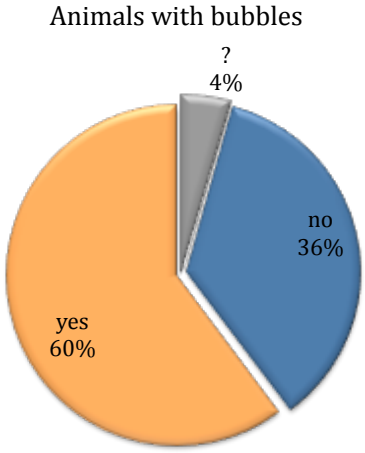

Fig. 4.4: Percentage of animals that presented bubbles in the veins. Positive results are shown in orange, negative in blue and observations not properly done are in grey represented by a question mark.

It was found a clear difference in the amount of carcasses presenting bubbles after segregating the data set into deep-diving and non-deep diving animals. There was an increase of 30% of bubbles prevalence in the deep diving group compare to non-deep divers.

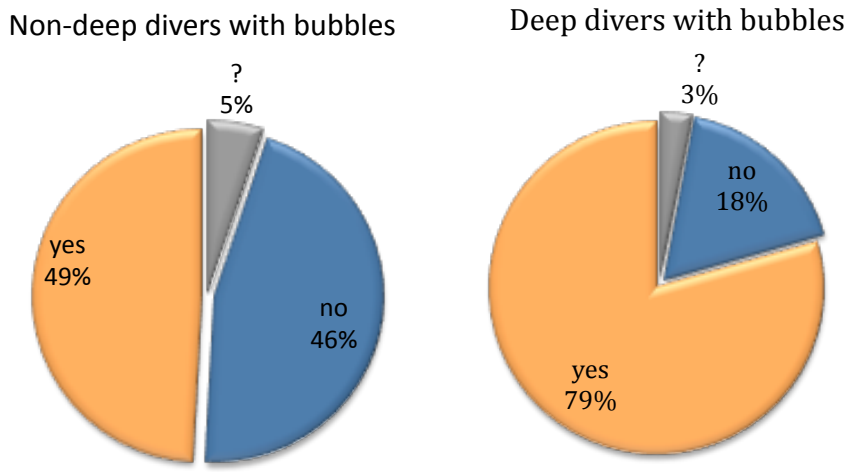

Fig. 4.5: Figures showing the relative percentage of animals that presented bubbles within the group of non-deep divers and the group of deep divers.

In addition, it was found a direct positive relationship between decomposition code and animals with bubbles.

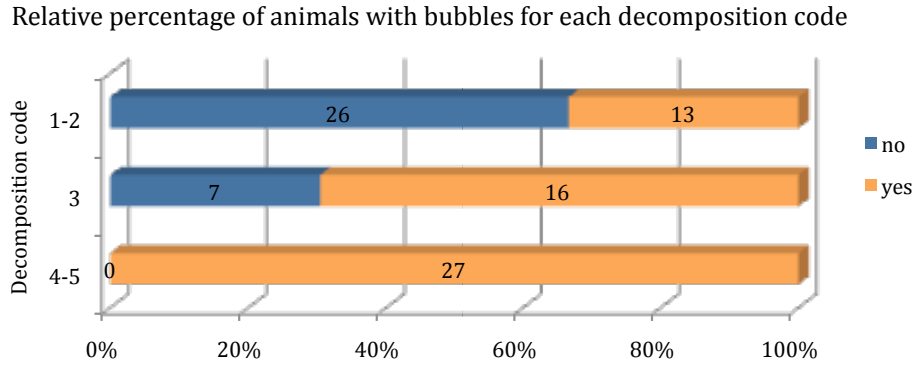

Fig. 4.36 Number and relative percentage of animals with bubbles (in orange) compared to those without bubbles (in blue) regarding to decomposition code.

After these results, we decided to take only fresh animals (decomposition codes 1 and 2) to look for relationships that might be related to the presence of bubbles like the kind of stranding (active or passive) or the carcass conservation mode (freezing)

before sampling. Results showed a direct positive relationship between active stranding and presence of bubbles, being found in a higher relative percentage (50%) in those active stranded compared to passive stranded animals (20%).

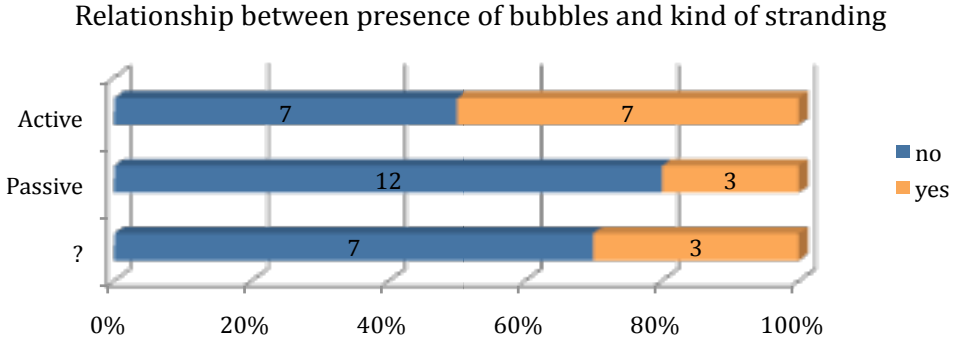

Fig. 4.7: Relationship between presence of bubbles (in orange) and stranding (active *vs* passive). The question marks represent animals found dead but with suspicious signs of active stranding.

On the other hand it was found a negative relationship with frozen animals, but the number of those frozen carcasses was very small (9) compared to the total number of total fresh animals (30).

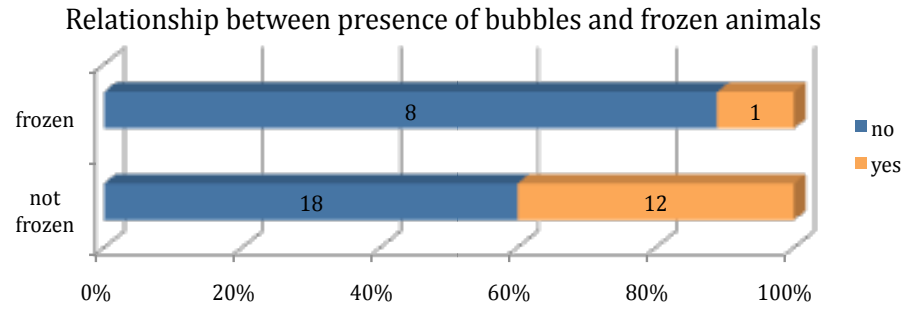

Fig. 4.8: Relationship between presence of bubbles (in orange) and the possible effect in frozen animals.

The proportion of animals that presented bubbles changed meaningfully if, in addition to the deep and non-deep diver's segregation we consider decomposition codes as we have done for active stranding and frozen animals. As expected, all the cases with an advance decomposition code showed bubbles, but the proportion of animals observed with bubbles with decomposition code 3 and decomposition codes 1-2 changed dramatically. While 50% of the non-deep divers remained free of bubbles with decomposition code 3, all the deep divers had bubbles. It was remarkable the high

prevalence of bubbles even in fresh deep-diving animals (57%) compared to non-deep divers (20%). Prevalence of bubbles was almost three times higher. These results showed us the importance of doing separate detailed analyses for each group.

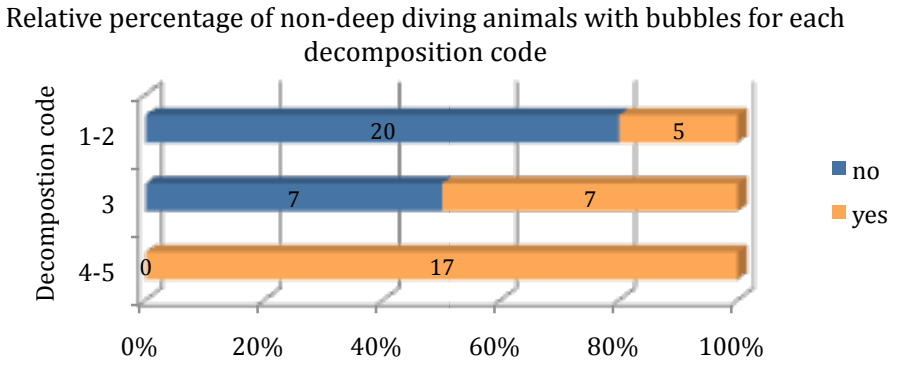

Fig. 4.9: Number and relative percentage of non-deep diving animals in which bubbles were observed (in orange) compare to those in which bubbles were absent (in blue) attending to decomposition code.

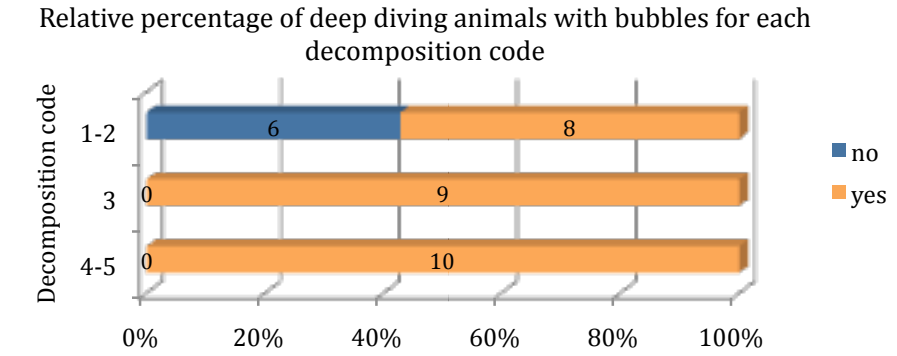

Fig. 4.10: Number and relative percentage of deep diving animals in which bubbles were observed (in orange) compare to those in which bubbles were absent (in blue) attending to decomposition code.

SEPARADOR NON DEEP DIVERS

4.3.1 NON-DEEP DIVERS

This group includes such diverse and different species as sea lions (pinnipeds of the family *Otariidae*), rorquals (mysticets of the family *Balaenopteridae*) and dolphins (odontocetes of the family *Delphinidae*).

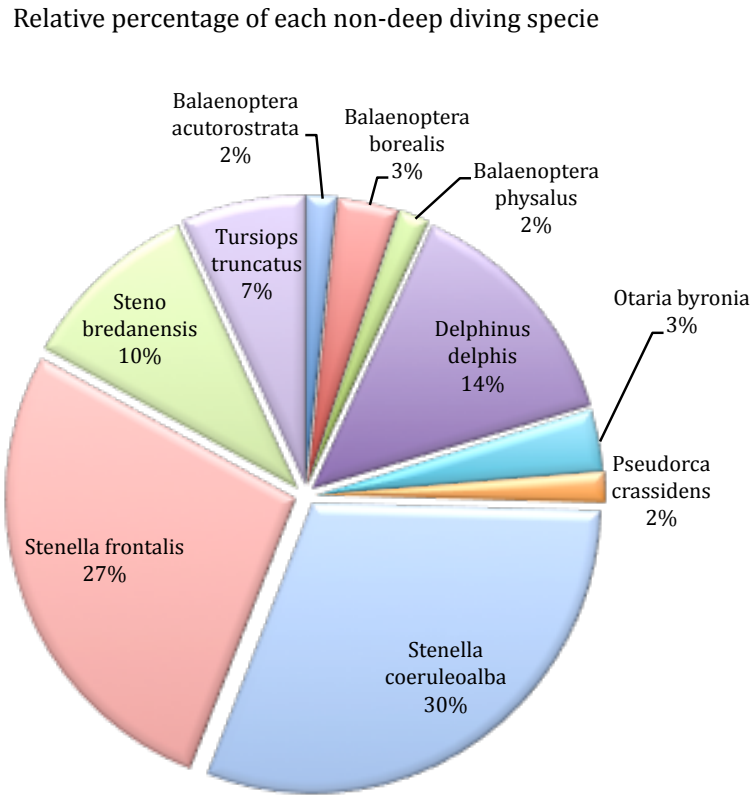

Fig. 4.11: Relative percentage of each deep diving specie included in the study.

Most of the non-deep divers were *Stenella* either frontalis or *coeruleoalba*, followed by *Delphinus delphis*, *Steno bredanensis* and *Tursios truncates*, all of them belong to the *Delphinidae* family. Other members of the Delphinidae family (*Pseudorca crassidens*), mysticets (*Balaenoptera acuturostrata*, *Balaenoptera borealis* and *Balaenoptera physalus*) and pinnipeds (Otaria byronia) were found in small numbers within the study.

4.3.1.1 Free gas in tissues and/or veins

Presence and abundance of free gas in tissues and veins was evaluated with the grading system described under material and methods section in this chapter as well as in appendix 9.2. Since PM time was unknown for most of the cases, animals were arranged first by decomposition code, and secondly in mounting order of the summation of free gas in the different tissues, in order to detect more clearly tendencies or disparities within the dataset. Some stranding circumstances that might be of relevance are described together with the cetacean number (for identification purposes) and gas bubble scores.

4.3.1.1.1 With decomposition code 1

Table 4.1: Cetacean number, specie, stranding circumstances and gas bubble score for non-deep diving animals with decomposition code 1.

Identification number	Specie	Active stranding	Mass stranding	Frozen	Bubbles	Subcutaneous v.	Mesenteric v.	Lumbo-caudal venous plexus	Coronary v.	Subcapsular emphysema	Summation	Diagnosis
CET 362	*Stenella frontalis*	yes	no	no	yes	0	0	I	?	1	2	Septicaemia

4.3.1.1.2 With decomposition code 2

Table 4.2: Cetacean number, specie, stranding circumstances and gas bubble score for non-deep diving animals with decomposition code 2.

Cetacean number	Specie	Active stranding	Mass stranding	Frozen	Bubbles	Subcutaneous v.	Mesenteric v.	Lumbo-caudal venous plexus	Coronary v.	Subcapsular emphysema	Summation	Diagnosis
CET 371	*Stenella frontalis*	yes	no	no	no	0	0	0	0	0	0	Trauma
CET 380	*Stenella coeruleoalba*	?	no	no	no	0	0	0	0	0	0	Infectious Encephalitis
CET 393	*Stenella frontalis*	?	no	no	no	0	0	0	0	0	0	Neoplasia
CET 413	*Pseudorca crassidens*	?	no	no	no	0	0	0	0	0	0	Trauma Septicaemia
CET 418	*Stenella frontalis*	yes	no	no	no	0	0	?	0	0	0*	Heart failure
CET 421	*Stenella frontalis*	?	no	yes	no	0	0	?	0	0	0*	not determined
CET 474	*Stenella coeruleoalba*	no	no	yes	no	0	0	0	0	0	0	Septicaemia
CET 523	*Balaenoptera acutorostrata*	no	no	yes	no	0	0	0	0	0	0	Parental segregation
CET 530	*Stenella frontalis*	no	no	no	no	0	0	0	0	0	0	Trauma. Toxoplasmosis.
CET 531	*Stenella frontalis*	?	no	no	no	0	0	0	0	0	0	Septicaemia
CET 548	*Stenella frontalis*	?	no	no	no	0	0	0	0	0	0	Viral disease
CET 363	*Stenella frontalis*	no	no	no	no	0	0	?	0	1	1*	Obstruction by foreign body
CET 373	*Delphinus delphis*	yes	no	no	no	0	0	0	0	1	1	Septicaemia
CET 376	*Stenella coeruleoalba*	no	no	yes	no	0	0	?	0	1	1*	Neoplasia
CET 395	*Stenella frontalis*	no	no	yes	no	0	0	?	0	1	1*	Neoplasia
CET 419	*Steno bredanensis*	no	no	yes	no	0	0	?	0	1	1*	Septicaemia
CET 476	*Stenella coeruleoalba*	no	no	no	no	0	0	0	0	1	1	Chronic renal failure
CET 515	*Stenella frontalis*	no	no	yes	yes	0	I	0	0	0	1	Toxoplasmosis
CET 400	*Stenella coeruleoalba*	no	no	no	no	0	0	?	0	2	2*	Parasitoses Senile disease
CET 517	*Delphinus delphis*	no	no	no	no	0	0	0	0	2	2	Chronic renal failure

(Follow-up) Table 4.2: Cetacean number, specie, stranding circumstances and gas bubble score for non-deep diving animals with decomposition code 2.

Cetacean number	Specie	Active stranding	Mass stranding	Frozen	Bubbles	Subcutaneous v.	Mesenteric v.	Lumbo-caudal venous plexus	Coronary v.	Subcapsular emphysema	Summation	Diagnosis
CET 526	*Tursiops truncatus*	?	no	no	yes	0	I	?	0	0	2*	Septicaemia
I344/07	*Otaria byronia*	no	no	no	no	0	0	0	0	2	2	Iatrogenic pneumomediastinum
CET 473	*Steno bredanensis*	yes	no	no	yes	0	I	0	0	2	3	Septicaemia
CET 537	*Stenella coeruleoalba*	no	no	no	yes	0	I	I	I	0	3*	Septicaemia

With decomposition code 3

Table 4.3: Cetacean number, specie, stranding circumstances and gas bubble score for non-deep diving animals with decomposition code 3.

Cetacean number	Specie	Active stranding	Mass stranding	Frozen	Bubbles	Subcutaneous v.	Mesenteric v.	Lumbo-caudal venous plexus	Coronary v.	Subcapsular empnysema	Summation	Diagnosis
CET 368	*Stenella frontalis*	?	no	yes	no	0	0	?	0	0	0*	Trauma
CET 384	*Stenella frontalis*	no	no	yes	no	0	0	?	0	?	0*	Toxoplasmosis
CET 522	*Stenella frontalis*	no	no	yes	no	0	0	0	0	0	0	Toxoplasmosis
CET 527	*Stenella coeruleoalba*	yes	no	yes	no	0	0	0	0	0	0	Parasitoses Bacterial infection
I134/07	*Otaria byronia*	no	no	no	no	0	0	0	0	0	0	Not determined
CET 375	*Stenella coeruleoalba*	no	no	yes	no	0	0	?	0	1	1*	Neonatal weakness
CET 409	*Stenella coeruleoalba*	no	no	yes	no	0	0	?	0	1	1*	Infectious encephalitis Parasitoses
CET 364	*Delphinus delphis*	no	no	yes	yes	0	0	I	0	1	2	Infectious meningoencephalitis
CET 374	*Stenella coeruleoalba*	no	no	no	yes	0	0	I	I	0	2	Trauma
CET 382	*Delphinus delphis*	?	no	no	yes	0	0	0	I	1	2	Sinusitis and meningoencephalitis by *Nasitrema* sp.
CET 370	*Stenella coeruleoalba*	yes	no	no	yes	I	0	I	0	1	3	Septicaemia
CET 469	*Stenella coeruleoalba*	?	no	no	yes	0	I	I	I	2	5	Parasitoses Senile disease
CET 546	*Stenella coeruleoalba*	yes	no	no	yes	0	I	II	II	1	6	Trauma Stranding stress syndrome
CET 482	*Delphinus delphis*	no	no	yes	yes	0	II	II	I	2	7	Bacterial broncopneumonia

4.3.1.1.3 With decomposition code 4

Table 4.4: Cetacean number, specie, stranding circumstances and gas bubble score for non-deep diving animals with decomposition code 4.

Cetacean number	Specie	Active stranding	Mass stranding	Frozen	Bubbles	Subcutaneous v.	Mesenteric v.	Lumbo-caudal venous plexus	Coronary v.	Subcapsular emphysema	Summation	Diagnosis
CET 509	*Tursiops truncatus*	no	no	no	yes	0	I	I	I	2	5	not determined
CET 506	*Stenella coeruleoalba*	no	no	yes	yes	I	II	I	I	2	7	not determined
CET 430	*Steno bredanensis*	no	no	no	yes	?	II	II	II	2	8*	not determined
CET 460	*Stenella coeruleoalba*	no	no	no	yes	II	II	II	?	2	8*	Trauma
CET 369	*Balaenoptera physalus*	no	no	no	?	?	?	?	?	1	?	Trauma
CET 381	*Delphinus delphis*	no	no	yes	yes	?	?	1	?	1	?	Infectious encephalitis
CET 425	*Delphinus delphis*	no	no	yes	?	?	?	?	?	?	?	Parasitoses.

4.3.1.1.4 With decomposition code 5

Table 4.5: Cetacean number, specie, stranding circumstances and gas bubble score for non-deep diving animals with decomposition code 5.

Cetacean number	Specie	Active stranding	Mass stranding	Frozen	Bubbles	Subcutaneous v.	Mesenteric v.	Lumbo-caudal venous plexus	Coronary v.	Subcapsular emphysema	Summatory	Diagnosis
CET 372	*Balaenoptera borealis*	no	no	no	yes	II	II	II	II	2	10	Not determined
CET 434	*Steno bredanensis*	no	yes	no	yes	II	II	II	II	2	10	Not determined
CET 435	*Stenella frontalis*	no	no	no	yes	II	II	II	II	2	10	Trauma
CET 437	*Steno bredanensis*	no	yes	no	yes	II	II	II	II	2	10	Not determined
CET 462	*Stenella frontalis*	no	no	yes	yes	II	II	II	II	2	10	Not determined
CET 487	*Stenella coeruleoalba*	no	no	no	yes	II	II	II	II	2	10	Not determined
CET 505	*Tursiops truncatus*	no	no	no	yes	II	II	II	II	2	10	Not determined
CET 367	*Stenella coeruleoalba*	no	no	yes	yes	*	*	*	*	2	*	Abnormal development
CET 402	*Stenella coeruleoalba*	no	no	no	yes	*	*	*	*	2	*	Septicaemia Senile disease
CET 438	*Steno bredanensis*	no	no	no	yes	*	*	*	*	*	*	Not determined
CET 543	*Tursiops truncatus*	no	no	no	yes	*	2	*	*	2	*	Parasitoses Senile disease
CET 552	*Balaneoptera borealis*	no	no	no	yes	*	2	*	2	2	*	Pending
CET 521	*Delphinus delphis*	no	no	yes	?	?	?	?	?	2	?	Not determined

On the following graph it is shown the cumulative gas appearance in different tissues for each decomposition code. Animals that were not correctly studied were not introduced in the graph. The asterisk in the top of some bars represent that that animal could have from 0 to 2 more score units since one location was not properly screened. A 5 bubble score for visual representation was given to animals in a very advance decomposition code where veins could not be clearly distinguised from the rest of the tissues. It should be remember that this value is not meaningful and its only given for visual representation, thus these animals are shown with a different colour.

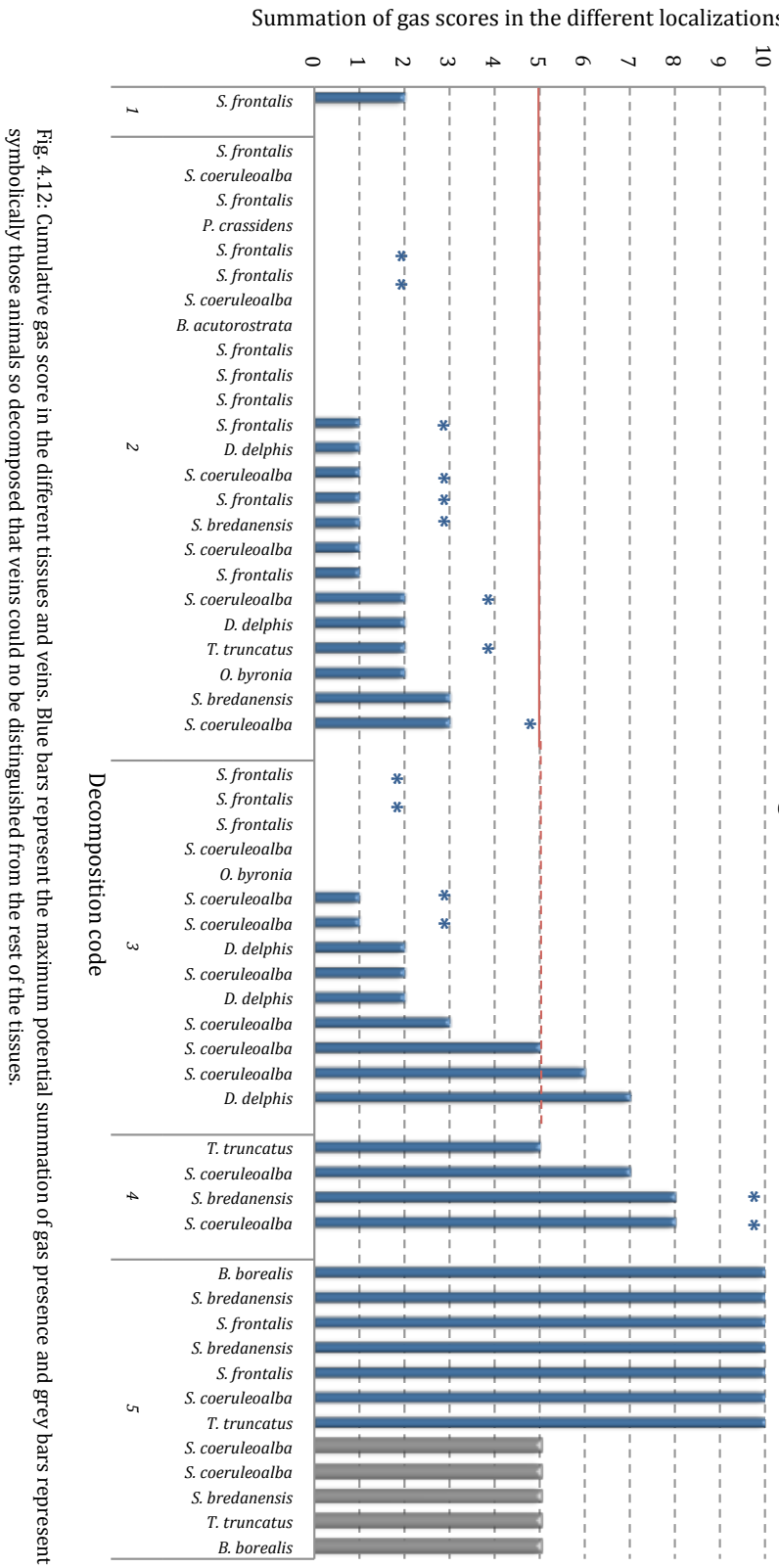

Fig. 4.12: Cumulative gas score in the different tissues and veins. Blue bars represent the maximum potential summation of gas presence and grey bars represent symbolically those animals so decomposed that veins could no be distinguished from the rest of the tissues.

The solid and discontinuous red line, represent the cut off selected as a guideline to distinguish animals that had higher summation of gas scores in tissues and veins in the different localizations. This line is solid up to decomposition code 2 and discontinuous in decomposition code three (explained in the discussion section).

There was not any animal with bubble score higher than 5 within decomposition codes 1-2. Few bubble scores were above 5 with decomposition code 3. Dolphins with advanced autolysis (decomposition code 4) had scores ranging from 5 to 8 and potentially 10; while all the animals in a very advanced autolysis (decomposition code 5) had the maximum gas score until certain decay state where integrity of the tissues was lost. It is important to notice that gas within tissues (emphysema) is included in the bubble score summation. Actually, most of the small bars within decomposition codes 1 and 2 correspond to emphysema. There was a high prevalence of emphysema with up to 44% of the fresh animals presenting emphysema in some organ. Most of the times it was peri-renal located.

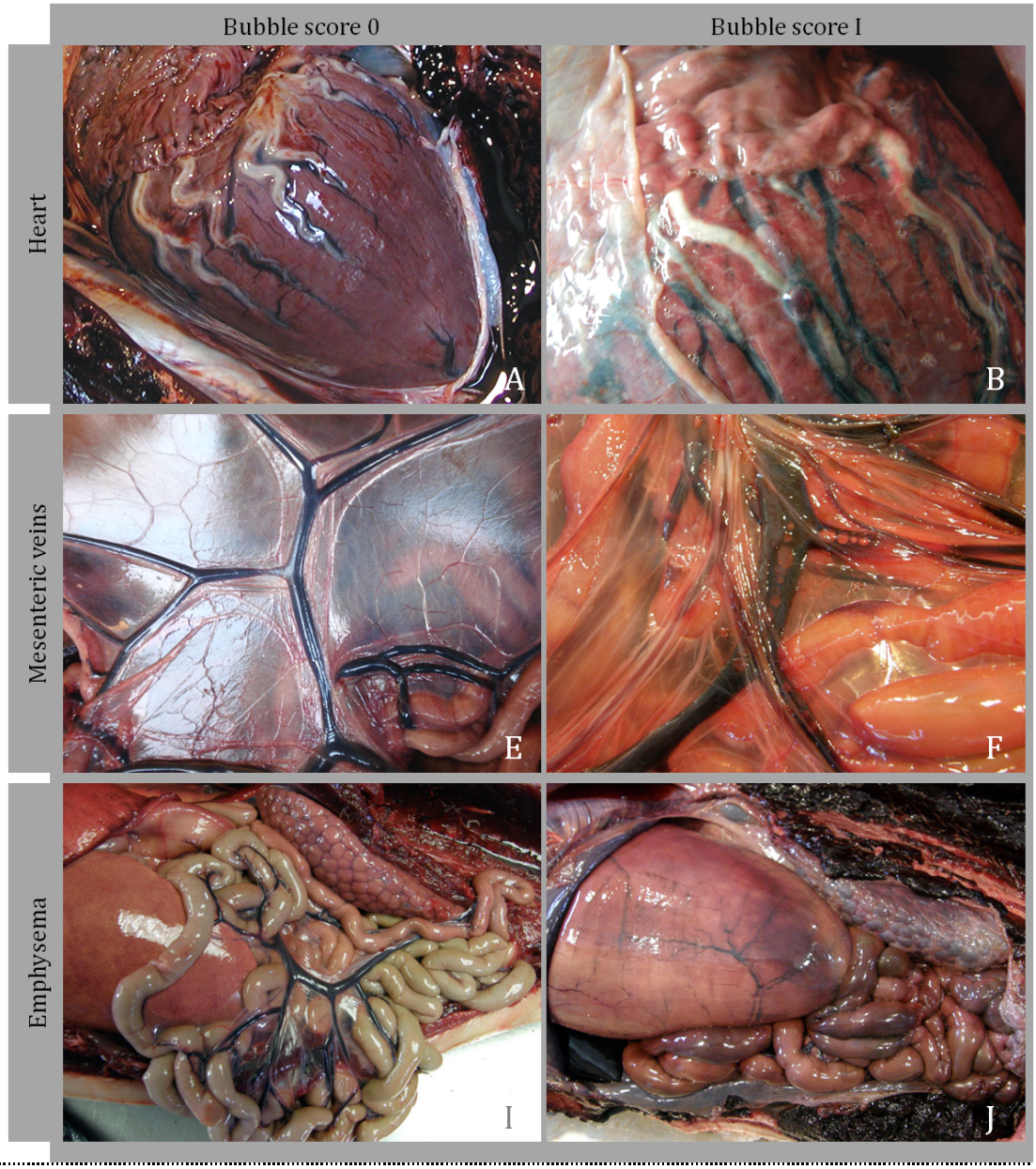

Fig. 4.13: Pictures showing different bubble and emphysema scores from animals with fresh to incipient autolysis (decomposition codes 1-3), as well as normal appearance in cases of advance autolysis where the putrefaction processes are evident in heart (A-D), mesenteric veins (E-H) and renal area (I-L).

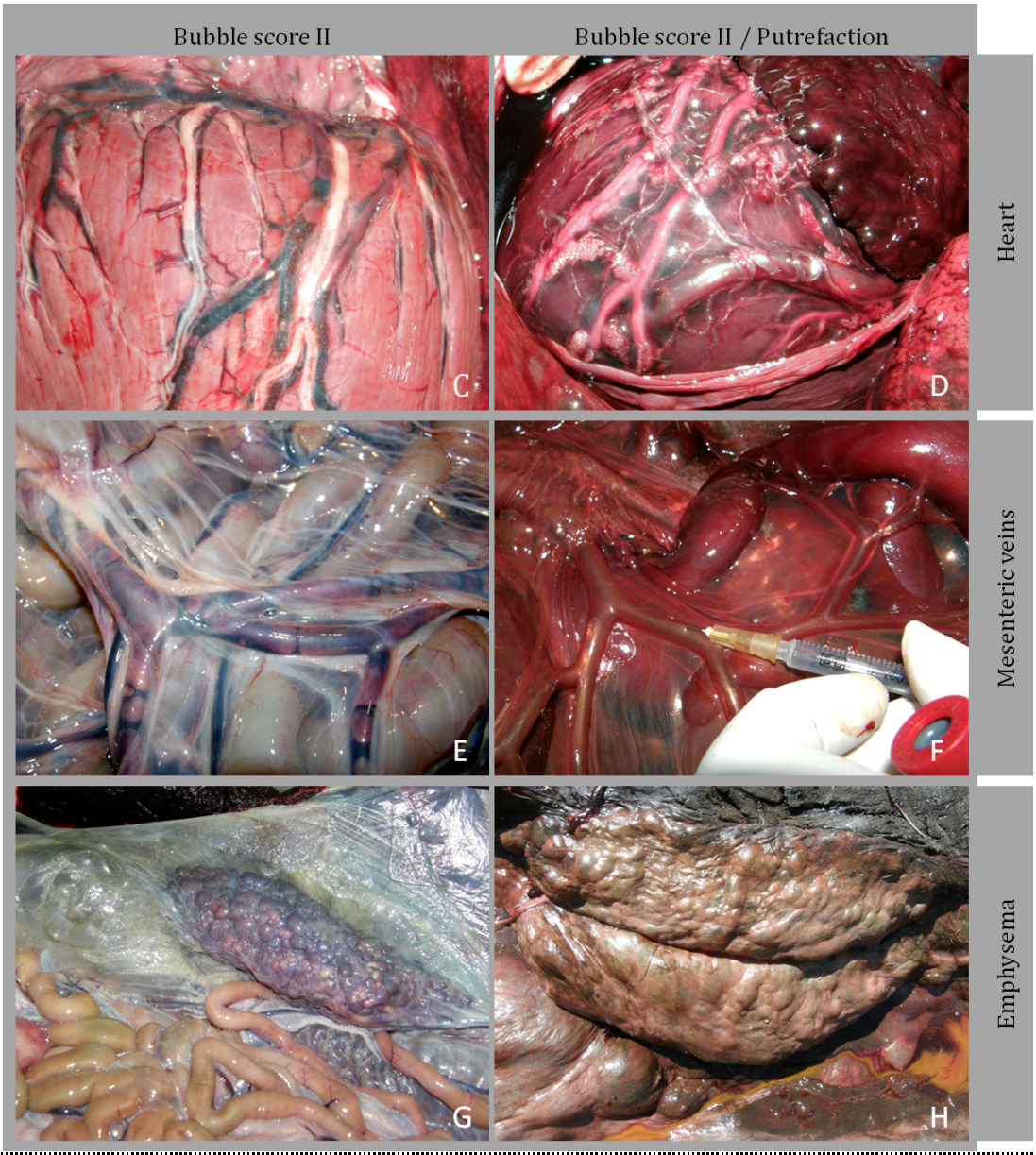

(Follow up) Fig. 4.13: Pictures showing the different bubble and emphysema scores from animals with fresh to incipient autolysis (decomposition codes 1-3), as well as normal appearance in cases of advance autolysis where the putrefaction processes are evident in heart (A-D), mesenteric veins (E-H) and renal area (I-L).

4.3.1.2 Gas composition

222 gas samples were obtained. Detailed gas composition of each analyzed sample expressed as percentage of average mole fraction is given in appendix 8.2.1. Samples were arranged following the same order as in the graphs of free gas abundance in tissues and veins: first by decomposition code and then by gas abundance in tissues.

A large variation in gas composition of the intestine was found once more. The only noticeable tendency is the increase of CO_2 % with decomposition codes up to 100% sometimes, and the simultaneous decrease of N_2%. Although some high values of N_2% were reported, usually nitrogen content was not higher than 50%. Hydrogen content seemed first to increase and then to decrease, but variability is too high to determine any tendency. On the other hand, oxygen and methane were randomly present and always in very low concentrations. Methane was not an important gas contrarily to what it could be expected.

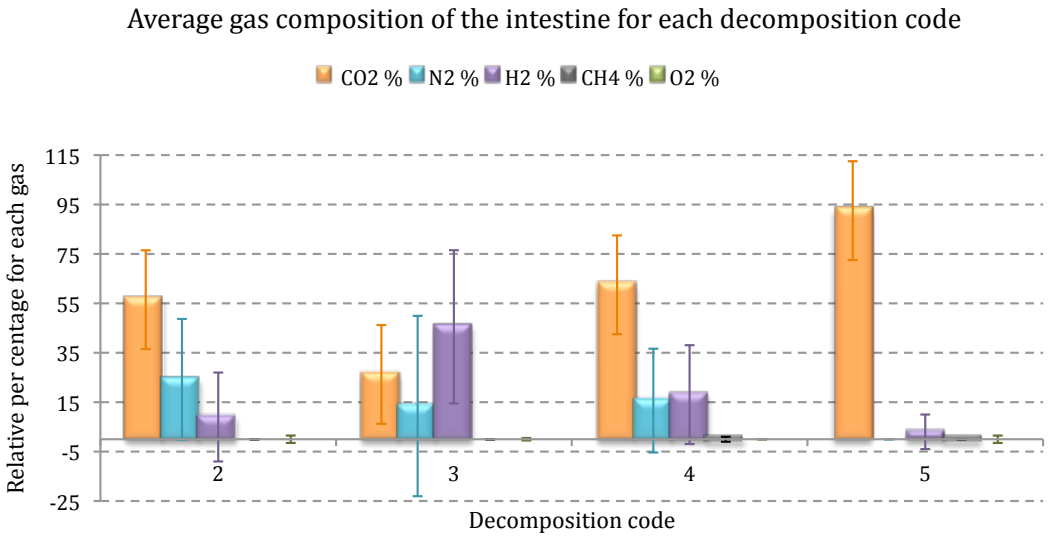

Fig. 4.14: Average and variability of the gas composition expressed with the median and the inter-quartile range for each compound for decomposition code 2 (n=20), decomposition code 3 (n=13), decomposition code 4 (n=5) and decomposition code 5 (n=10).

Not many samples were taken from putrefactive emphysemas, and some of them got air polluted. Nevertheless, gas composition was clearly identified by high levels of CO_2 and presence of hydrogen. Nitrogen could be also present in quantities lower than 45%. Samples circumscribed by a red circle and that one indicated with a red arrow, have a composition clearly different from the rest and merits a specific and individual analysis.

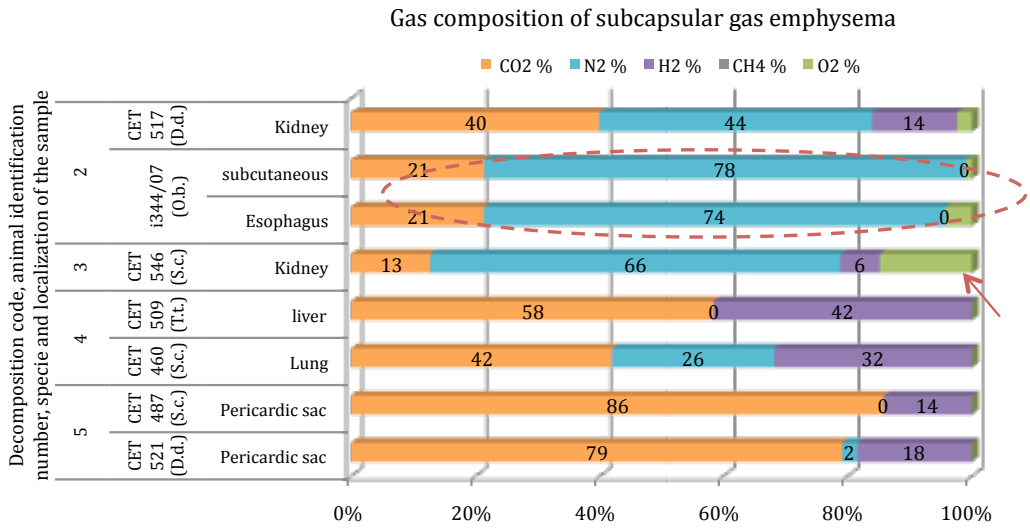

Fig. 4.15: Subcapsular gas composition of the samples taken from different localizations and within different decomposition codes illustrating the contribution of each gas to the total amount in µmol percentage.

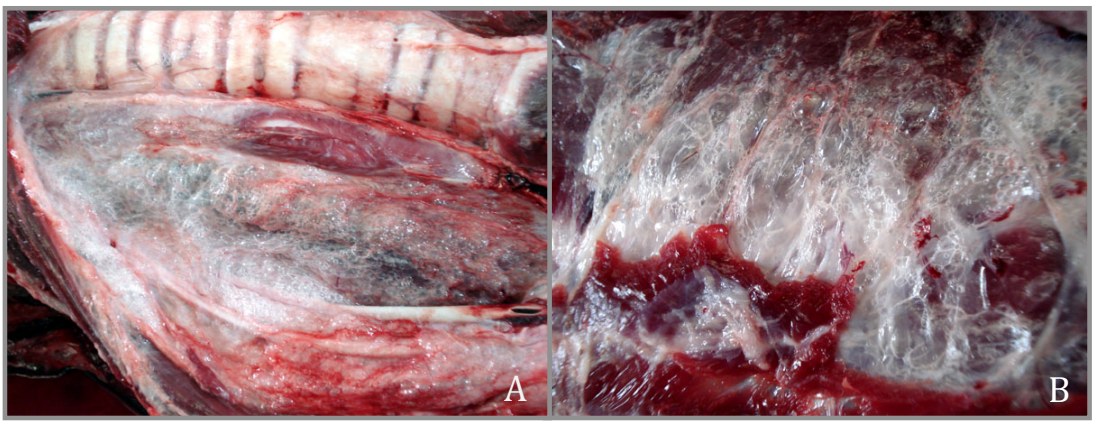

Fig. 4.16: Pneumomediastinum (A) and subcutaneous emphysema (B) from I344/07.

Few samples were taken from the sinuses of non-deep diving animals; but gas composition results were very similar for animals within decomposition codes (1-3) with mean values and standard deviations of 16 ± 2 % of CO_2 and 83 ± 2 % of N_2. We didn't take any sample from sinuses of animals with decomposition code 4. Although the small sample size there was a dramatic difference between fresh to incipient autolysis samples (decomposition codes 1-3) compare to samples from cases with very advance autolysis (decomposition code 5) in which CO_2 and N_2 were almost transposed (70 and 30% respectively).

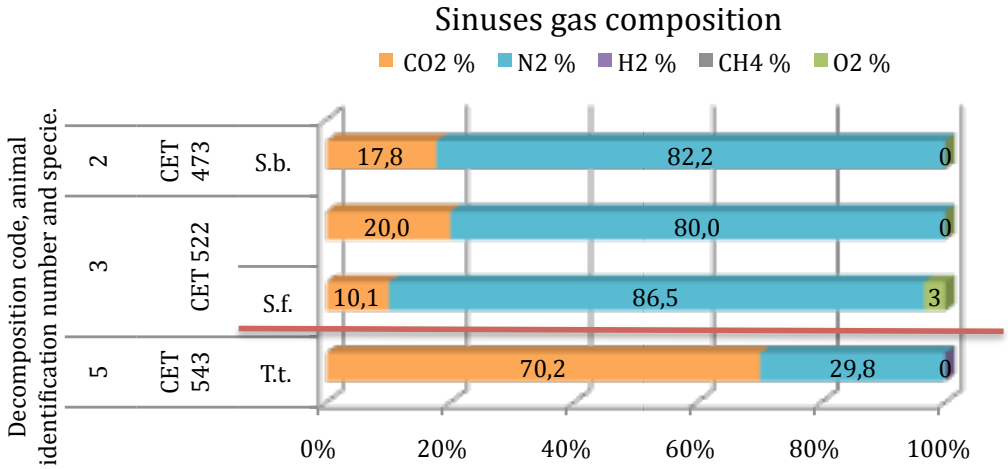

Fig. 4.17: Sinuses gas composition taken from animals with different decomposition codes illustrating the contribution of each gas to the total amount in µmol percentage. The solid red line is separating decomposition code 5 from the rest as it has a very different gas composition.

Regarding gas samples taken from the heart it is important to notice several things. In many cases blood was recovered from the heart. This was more frequent in fresh animals (decomposition code 1-2). When using the aspirometer, it could be clearly seen how only blood was being suctioned, thus no gas samples were obtained.

If the sample was taken directly with vacuum tubes and little blood entered into the tube, the headspace was analyzed, but considered as the headspace of the blood and not as free gas found inside the heart (although some free gas might have entered into the tube together with the blood).

When a considerable amount of blood entered into the tube, these samples were not analyzed for protecting the gas-tight syringes and the column of the gas chromatograph.

In other cases, when analyzing the gas content of the tubes, this was not higher than the quantification limit and it was therefore considered empty. On the other hand, if the heart was not sampled because of special circumstances, this was clearly stated in the corresponding table of the appendix. When an atmospheric air composition was found this was indicated in the appendix (10.2) besides the gas compounds.

Since atmospheric concentrations of CO_2 are too small to be detected by gas chromatography, it was used as an indicative of gases stem inside the carcass. But if it was found in very low concentrations and there was a very similar atmospheric air composition, air pollution was suggested as a plausible phenomenon.

Finally, there were some samples that contained one single gas compound in concentrations slightly higher than the established detection limit, typically CO_2 or hydrogen. Since the background of the vacuum tubes contains mainly oxygen and nitrogen, their detection limit is always higher than that for CO_2 and hydrogen. Thus, when these conditions were met, the sample was identified as very small and it was counted for gas found in the heart (Fig. 5.9) but it was not considered representative of its original composition. Thus, samples with blood, air polluted or identified with little gas were not included for gas composition characterization and are not illustrated in the following figure (Fig. 4.18).

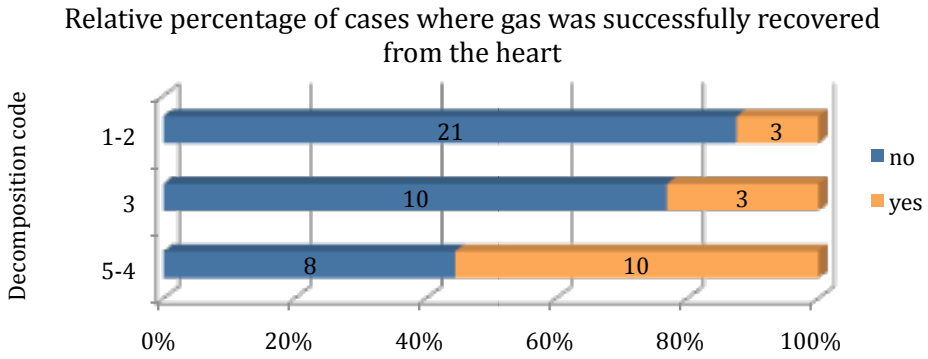

Fig. 4.18: Relative percentage and number of cases where gas was successfully recovered from the heart (in orange) related to decomposition code.

In this figure, it could be seen that only very few fresh animals (3/24; 12%) had free gas in the heart. The prevalence of gas with decomposition code 3 was still low (3/13; 23%) and strongly higher (10/18; 56%) in animals with a more advance decomposition code (4 and 5).

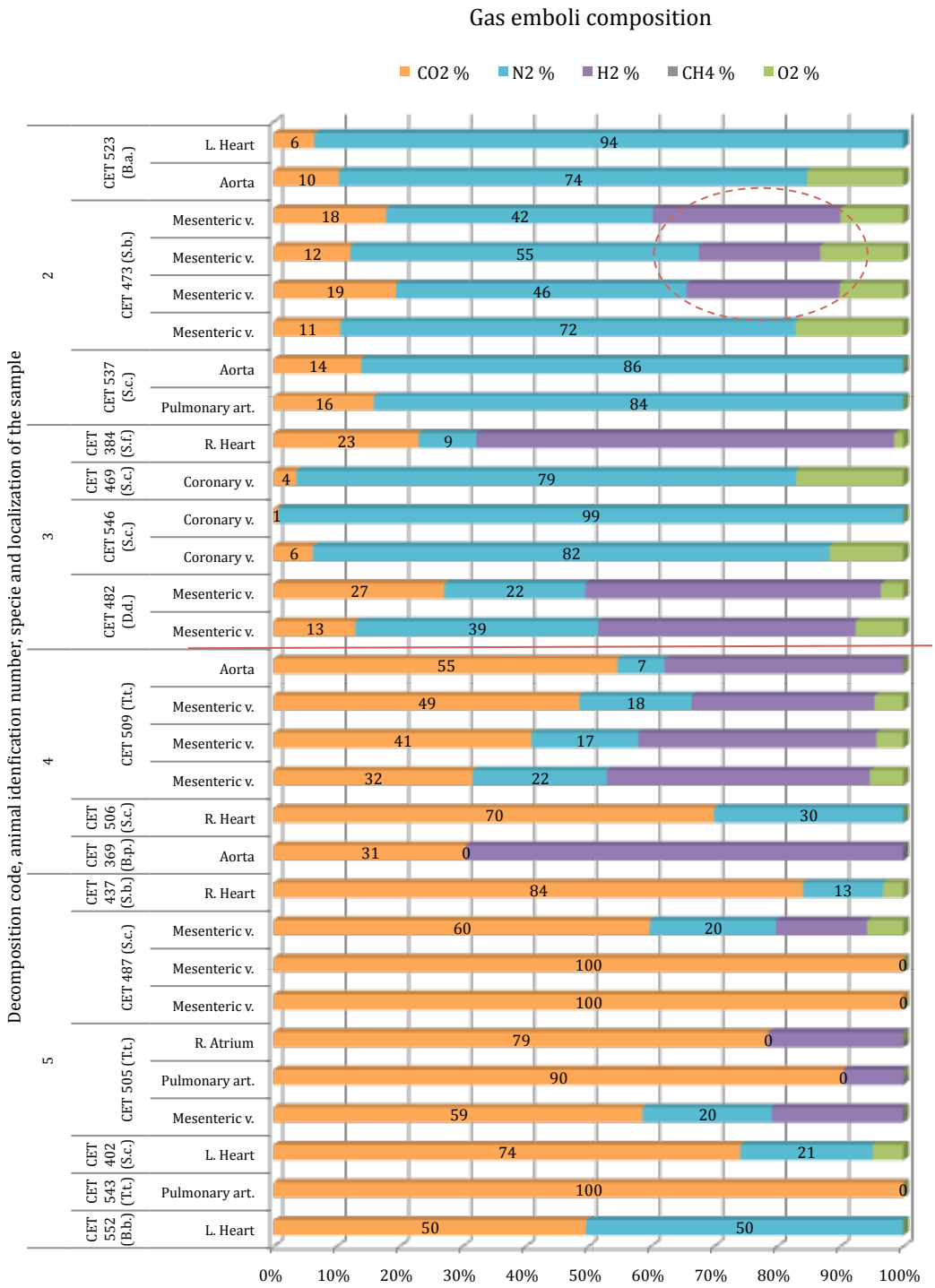

Fig. 4.19: Gas embolism composition sampled form different localizations and with different decomposition codes, illustrating the contribution of each gas to the total amount in percentage µmol. The solid red line is separating decomposition codes 4 and 5 from the rest since they have high amounts of CO_2 compare to samples from fresher decomposition codes where the main compound in nitrogen. The circle in enclosing samples with gas composition different from their group.

In this figure it could be observed a positive tendency of CO_2 % to increase with decomposition codes up to even 100%, at the same time as N_2% decreased. H_2 was found in most of the samples taken with decomposition code 4, and in few samples from fresher animals. In fresh animals, when H_2 was not present, very high contents of N_2 were found (70-90%). The leftovers of these samples were mainly composed of CO_2.

SEPARADOR DEEP DIVING ANIMALS

4.3.2 DEEP DIVERS

We have considered as deep divers those species supposed to dive usually deeper than 500m for foraging (*Kogia*, *Physeter*, *Ziphius*, *Mesoplodon*, *Globicephala* and *Grampus*). These genera were further studied alone except for *Ziphius* and *Mesoplodon* that were studied together as the family *Ziphiidae*. These subgroups were present in the study in similar proportions. The only group that had fewer representatives was the *Kogia*.

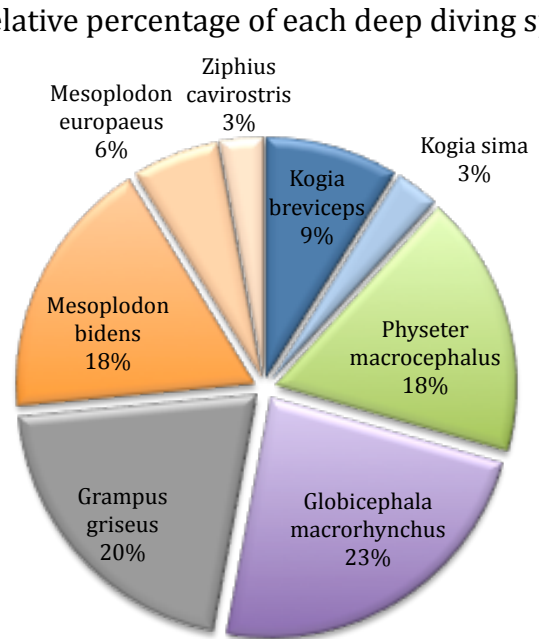

Fig. 4.20: Relative percentage of each deep diving specie included in the study. Different species belonging to the same subgroups are represented with the same colour but different tonality.

Before studying the subgroups we looked at the quantity of gas found in different tissues and veins in the deep divers group. Presence and abundance of free gas in tissues and veins was evaluated with the grading system described on material and methods from this chapter and in appendix 9.2.

Since exact PM time was unknown for most of the cases, animals were arranged first by decomposition code, and secondly in mounting order of the summation of free gas in the different tissues, in order to observe more clearly tendencies or disparities

within the dataset. Detailed information about each score assigned to a given vein or tissue as well as additional information about the animal and stranding circumstances that might be of relevance are described together with the cetacean number (for identification purposes) are given in the corresponding subgroup information.

We found that it was not only the number of animals that presented bubbles that increased compared to non-deep divers, but also the amount of gas found in tissues and veins. There were few fresh animals (decomposition code 2) above score 5. Among them, two were dramatically higher, as high as the very decomposed animals (decomposition code 5). With decomposition code 3, there was a group of animals with gas score slightly above 5. With decomposition codes 4 and 5, similar gas abundance was found than that of non-deep divers (Fig 4.21).

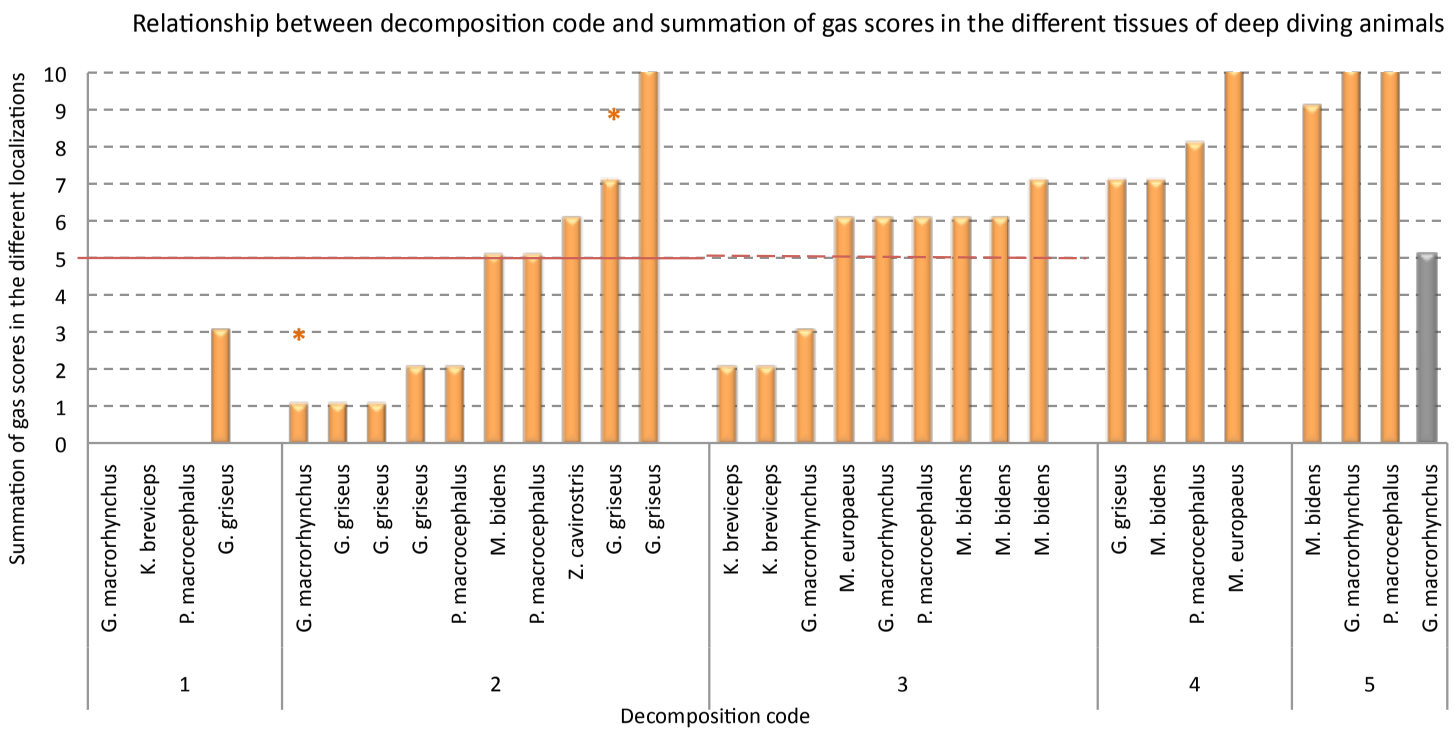

Fig. 4.21: Cumulative gas score in the different tissues and veins. Orange bars represent the maximum potential summation of gas presence and grey bars represent symbolically those animals so decomposed that veins could no be distinguished from the rest of the tissues.

SEPARADOR KOGIA

4.3.2.1 *Kogiidae*

4.3.2.1.1 Free gas in tissues and/or veins

Presence and abundance of free gas in tissues and veins was evaluated with the grading system described under material and methods section in this chapter as well as in appendix 9.2. Since PM time was unknown for most of the cases, animals were arranged first by decomposition code, and secondly in mounting order of the summation of free gas in the different tissues, in order to detect more clearly tendencies or disparities within the dataset. Some stranding circumstances that might be of relevance are described together with the cetacean number (for identification purposes) and gas bubble scores.

Table 4.6: Cetacean number, specie, decomposition code, stranding circumstances and gas bubble score for *Kogia*.

Cetacean number	Specie	Decomposition code	Active stranding	Mass stranding	Frozen	Bubbles	Subcutaneous v.	Mesenteric v.	Lumbo-caudal venous plexus	Coronary v.	Subcapsular emphysema	Summation	Diagnosis
CET 404	*Kogia breviceps*	1	yes	no	no	no	0	0	0	0	0	0	Emcephalopathy of unknown etilogy
CET 397	*Kogia breviceps*	3	no	no	no	yes	0	0	1	0	1	2	Trauma Septicaemia
CET 459	*Kogia breviceps*	3		no	no	yes	0	1	1	0	0	2	Trauma Bycatch?
CET 542	*Kogia sima*	4	no	no	no	?	?	?	?	?	?	?	Septicaemia

Four *Kogia* were studied with different decomposition codes. Unfortunately, gas abundance was not well observed for the most decomposed animals, but gas samples were taken and analyzed.

Any of the studied animals had gas bubble score higher than 5. Even with decomposition code 3, these *Kogia* presented only some scarce bubbles in the lumbo-caudal venous plexus and/or in the mesenteric veins.

Subcapsular emphysema was not present in important amounts.

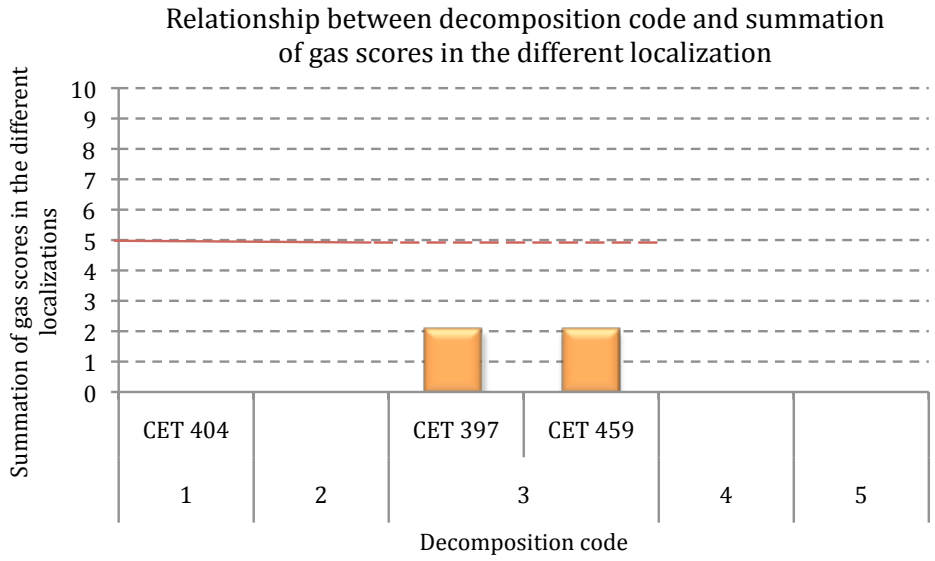

Fig. 4.22: Cumulative gas appearance in tissues and veins of each *Kogia* within its corresponding decomposition code.

4.3.2.1.2 Gas composition

13 gas samples were obtained from *Kogia*. Detailed gas composition of each analyzed sample expressed as percentage of average mole fraction is given in appendix 7.2.2. Samples were arranged following the same order as in the graphs of free gas abundance in tissues and veins: first by decomposition code and then by gas abundance in tissues.

Regarding gas composition of the intestine, the main compound was CO_2, nitrogen was found only in low concentrations, and in one of the samples methane was present in important quantities. Unfortunately there were not more samples with other decomposition code than three.

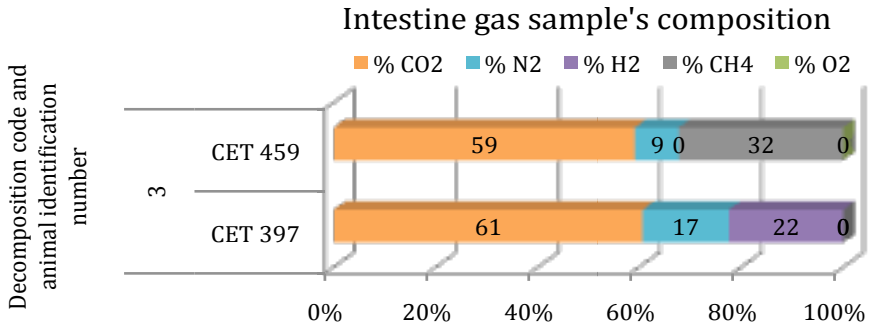

Fig. 4.23: Intestine gas composition from *Kogia* within decomposition code 3 illustrating the contribution of each gas to the total amount in µmol percentage

Few samples were obtained from the circulatory system. Nitrogen was found in high concentrations (higher than 70%) in all the samples. Hydrogen was present with decomposition code 4. In the sample from the right heart of the *Kogia* CET 542, oxygen was also found in levels of 16% suggesting possible air pollution.

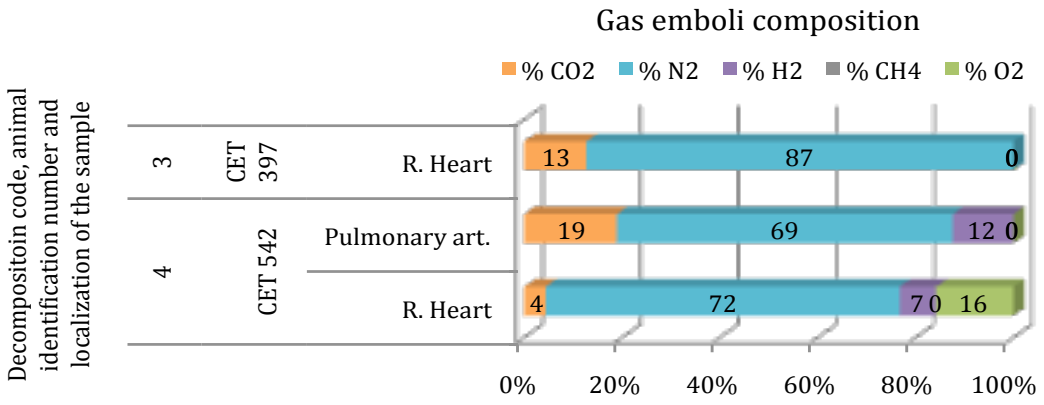

Fig. 4.24: Gas embolism composition sampled form different localizations and with different decomposition codes, illustrating the contribution of each gas to the total amount in percentage µmol.

SEPARADOR CACHALOTES

4.3.2.2 *Physeteridae*

4.3.2.2.1 Free gas in tissues and/or veins

Presence and abundance of free gas in tissues and veins was evaluated with the grading system described under material and methods section in this chapter as well as in appendix 9.2. Since PM time was unknown for most of the cases, animals were arranged first by decomposition code, and secondly in mounting order of the summation of free gas in the different tissues, in order to detect more clearly tendencies or disparities within the dataset. Some stranding circumstances that might be of relevance are described together with the cetacean number (for identification purposes) and gas bubble scores.

Table 4.7: Cetacean number, decomposition code, stranding circumstances and gas bubble score for *Physeter macrocephalus*.

Cetacean number	Decomposition code	Active stranding	Mass stranding	Frozen	Bubbles	Subcutaneous v.	Mesenteric v.	Lumbo-caudal venous plexus	Coronary v.	Subcapsular empysema	Summation	Diagnosis
CET 463	1	yes	no	no	no	0	0	0	0	0	0	Parental segregation
I298/09	2	yes	yes	no	yes	0	0	0	1	1	2	Not determined
I299/09	2	yes	yes	no	yes	1	0	0	2	2	5	Not determined
I300/09	3	yes	yes	no	yes	0	2	0	2	2	6	Not determined
CET 520	4	no	no	no	yes	2	2	2	2	0	8	Trauma
CET 544	5	no	no	no	yes	2	2	2	2	2	10	Trauma Ship collision

Six animals of this specie were included in the study. Fortunately with these six animals all decomposition codes were covered. A clear tendency of gas accumulation with decomposition codes was observed. The only animal on which no bubbles were observed was a newborn sperm whale. In all the rest of animals bubbles were observed, especially in the coronary veins.

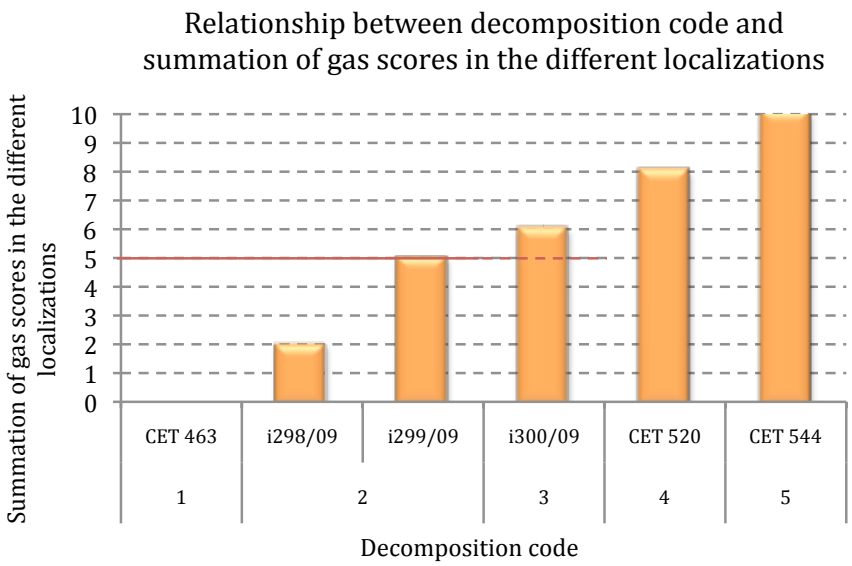

Fig. 4.24: Cumulative gas appearance in tissues and veins of each *Physeter macrocephalus* within its corresponding decomposition code.

It was found one fresh animal with summation of bubble score 5, and one animal with incipient autolysis with summation of bubble score higher than 5. These two animals stranded together in a mass stranding that occurred in Italy on December 2009. In these animals, large bubbles were observed mainly in the coronary veins but pneumomediastinum was additionally present.

Fig. 4.25: Alive sperm whale beached in the mass stranding of Italy.

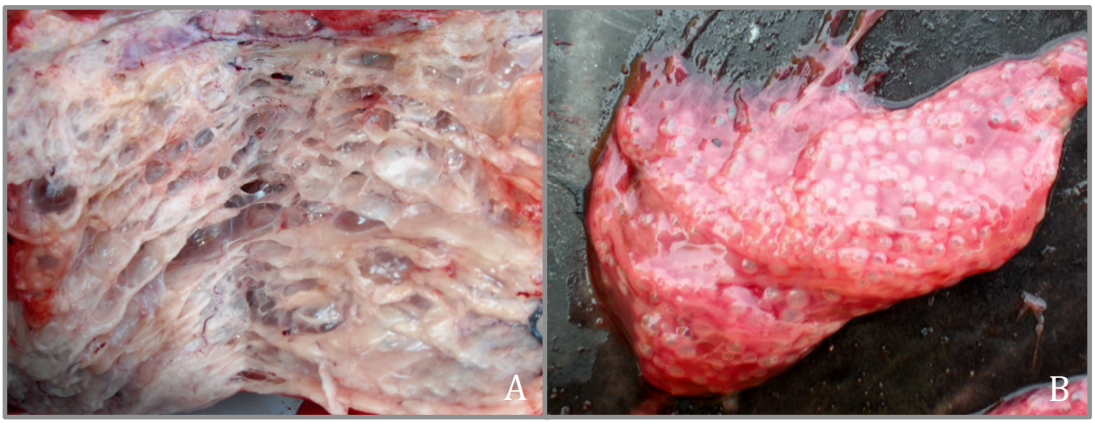

Fig. 4.26: Pneumomediastinum (A) and clot with gas bubbles (B) from a sperm whale mass stranded in Italy.

4.3.2.2.2 Gas composition

40 gas samples were obtained from *Physeter macrocephalus* carcasses. Detailed gas composition of each analyzed sample expressed as percentage of average mole fraction is given in appendix 7.2.2. Samples were arranged following the same order as in the graphs of free gas abundance in tissues and veins: first by decomposition code and then by gas abundance in tissues.

In the intestine a large variation in gas composition was found once more. No tendencies were observed. CO_2 was in most of the cases the main compound. Nitrogen was found in one sample in relatively high concentrations (68%). Hydrogen appeared randomly and as in the *Kogia*, methane was also of importance in some samples.

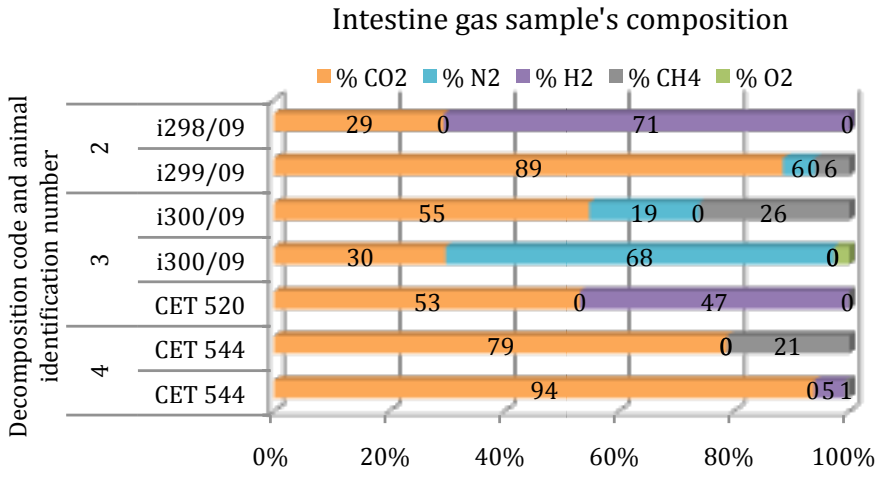

Fig. 4.27: Intestine gas composition from *Physeter macrocephalus* within different decomposition codes illustrating the contribution of each gas to the total amount in µmol percentage.

Regarding emphysema only two samples were taken from the same animal with decomposition code 3. Gas composition was mainly composed of hydrogen followed by CO_2 and small quantities of nitrogen and oxygen.

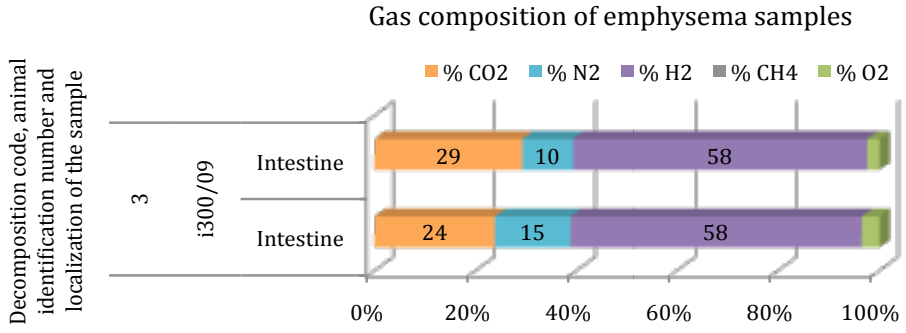

Fig. 4.28: gas composition of emphysema found in the intestinal serosa of *Physeter macrocephalus* with decomposition code 3 illustrating the contribution of each gas to the total amount in µmol percentage

Much more information was obtained from gas embolism. Gas was found in the left heart of a newborn calf composed mainly of nitrogen and CO_2. In the rest of the animals it was not possible to sample the heart because of the thick heart wall of juvenile or adult sperm whales, but bubbles were observed in coronary veins of all these analyzed animals. Oxygen was found in these bubbles of the coronary veins in contrast to the newborn heart sample. Oxygen levels decreased as autolysis advanced. Hydrogen

appeared with decomposition code 3. Methane was not present in of these samples cases.

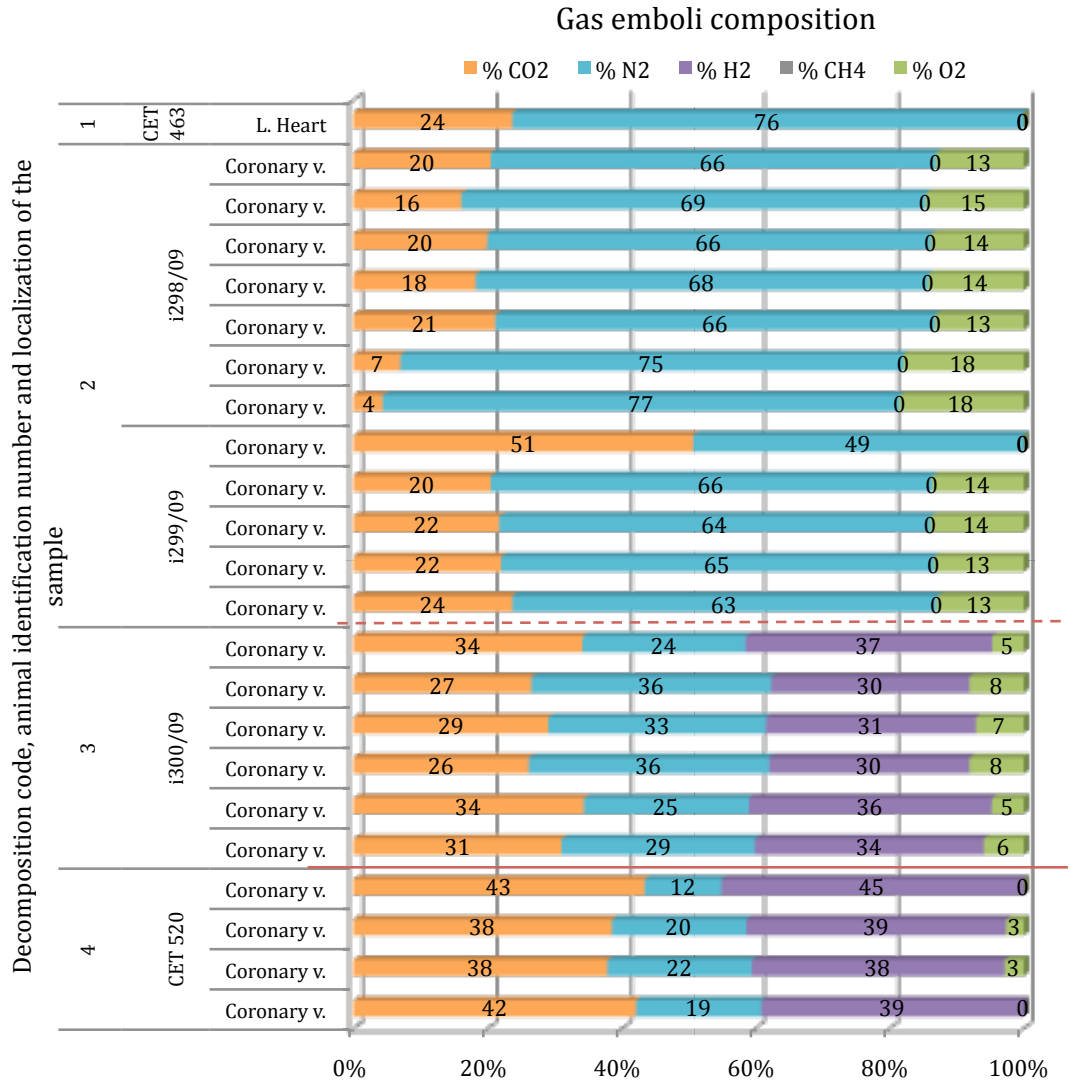

Fig. 4.29: Gas embolism composition sampled form different localizations and with different decomposition codes, illustrating the contribution of each gas to the total amount in percentage µmol. The solid red line is separating decomposition code 4 from the rest, and the continuous line is separating decomposition code 3 from 2.

Since gas composition was found to be so consistent for each animal and there were suspicious evidences of tendencies, mean gas values and standard deviations were calculated for each compound of the different carcasses and were organized maintaining the same criteria of decomposition code and gas abundance in tissues and veins. It was found a clear tendency of nitrogen to decrease with decomposition code (R^2=0.96). Similar trend could be observed for oxygen except for the very fresh sample where oxygen was absent.

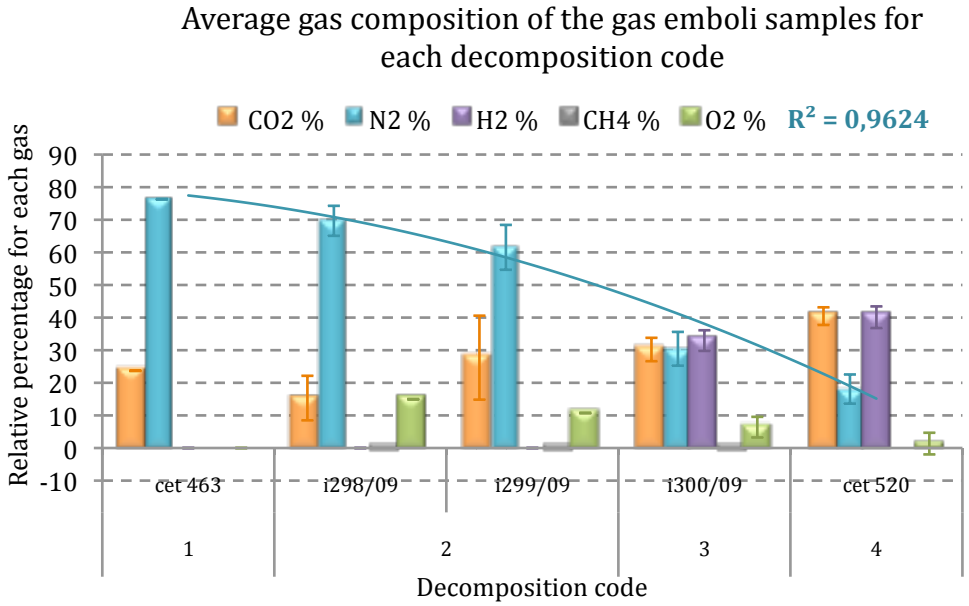

Fig. 4.30: Average and variability of the gas composition expressed with the mean and the standard deviation for each compound for decomposition code 1 (n=1), decomposition code 2 (n=7; n=5), decomposition code 3 (n=6) and decomposition code 4 (n=4).

SEPARADOR CALDERONES

4.3.2.3 *Globlicephala*

4.3.2.3.1 Free gas in tissues and/or veins

Presence and abundance of free gas in tissues and veins was evaluated with the grading system described under material and methods section in this chapter as well as in appendix 9.2. Since PM time was unknown for most of the cases, animals were arranged first by decomposition code, and secondly in mounting order of the summation of free gas in the different tissues, in order to detect more clearly tendencies or disparities within the dataset. Some stranding circumstances that might be of relevance are described together with the cetacean number (for identification purposes) and gas bubble scores.

Table 4.1: Cetacean number, decomposition code, stranding circumstances and gas bubble score for *Globicephala macrorhynchus.*

Cetacean number	Decomposition code	Active stranding	Mass stranding	Frozen	Bubbles	Subcutaneous v.	Mesenteric v.	Lumbo-caudal venous plexus	Coronary v.	Subcapsular gas emphysema	Summation	Diagnosis
CET 360	1	yes	no	no	no	0	0	0	0	0	0	Infectious meningitis
CET 339	2	yes	no	no	yes	0	1	?	0	0	1*	Septicaemia
CET 390	3	?	no	no	yes	0	0	1	1	1	3	Septicaemia
CET 512	3	no	no	no	yes	1	2	1	2	0	6	Septicaemia
CET 464	4	no	no	no	yes	?	1	2	?	2	?	Enterotoxemia Septicaemia
CET 504	4	no	no	no	yes	?	2	?	?	2	?	Meningitis Septicaemia
CET 399	5	no	no	no	yes	2	2	2	2	2	10	Trauma
CET 361	5	no	no	no	yes	*	*	*	*	2	*	Trauma

Bubbles were observed in all except one *Globicephala*, but the summation of the bubble score was only higher than 5 in one case (CET 512) with decomposition code 3. Unfortunately animals with advanced autolysis (decomposition code 4) were not well studied and therefore, they were not included in the following figure. The grey bar

represents *Globicephala* CET 361 with a very advanced autolysis in which veins could not be evaluated. A 5 bubble score for visual representation was given to this animal but it should be remember that this value is not meaningful and its only given for visual representation, thus this animal is shown with a different colour. The asterisk (*) in the top of CET 339 represent that that animal could have from 0 to 2 more score units since one location was not properly screened.

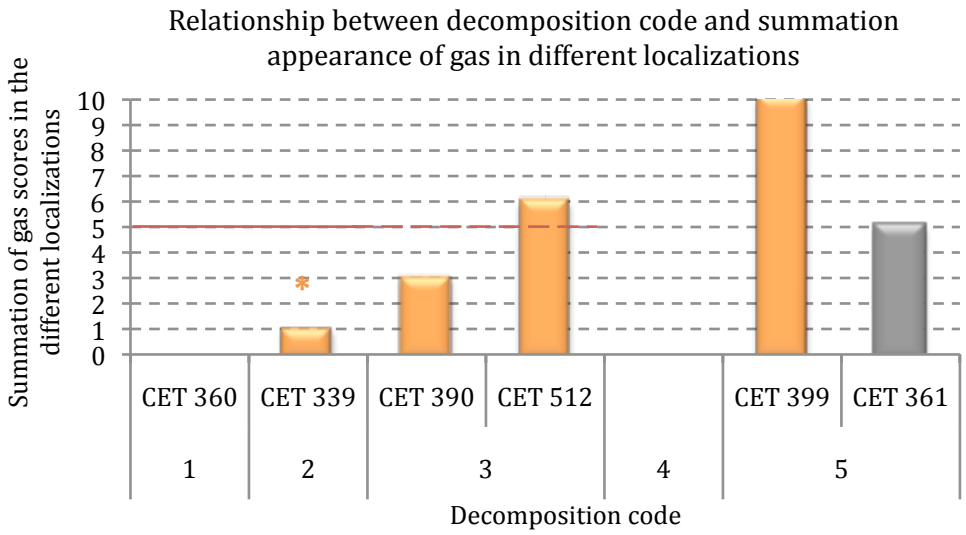

Fig. 4.31: Cumulative gas appearance in tissues and veins of each *Globicephala macrorhynchus* included in the study within its corresponding decomposition code.

4.3.2.3.2 Gas composition

42 gas samples were obtained from *Globicephala macrorhynchus* carcasses. Detailed gas composition of each analyzed sample expressed as percentage of average mole fraction is given in appendix 7.2.2. Samples were arranged following the same order as in the graphs of free gas abundance in tissues and veins: first by decomposition code and then by gas abundance in tissues.

In the intestine we found two different gas composition groups; the first one with decomposition code 1 composed of high nitrogen content followed by CO_2 and oxygen and a second one with decomposition codes 3 and 4 where gas composition consisted mainly in CO_2 and hydrogen. In these samples, there was not oxygen. Methane did not appear in any of both gas composition groups.

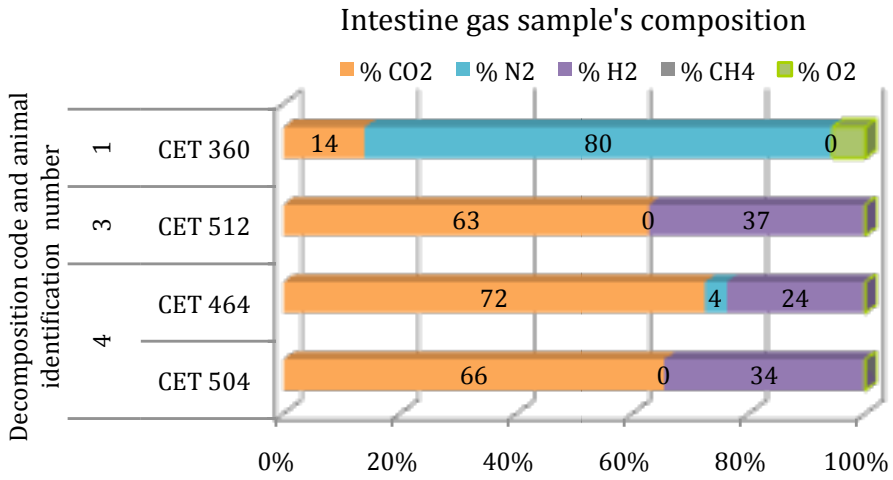

Fig. 4.32: Intestine gas composition from *Globicephala macrorhynchus* within different decomposition codes illustrating the contribution of each gas to the total amount in µmol percentage.

Only two samples were obtained from sinuses of *Globicephala* carcasses. These two samples had a very similar atmospheric air composition independently of decomposition code that suggests air pollution.

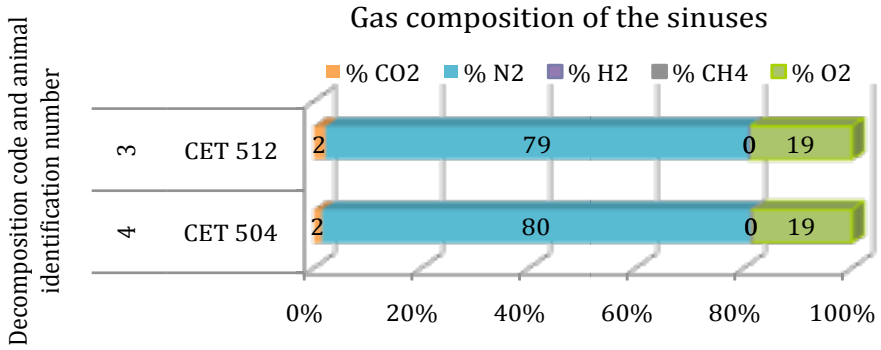

Fig. 4.33: Composition of gas taken from the sinuses of two *Globicephala macrorhynchus* with different decomposition codes illustrating the contribution of each gas to the total amount in µmol percentage.

Regarding gas composition of free gas found in the circulatory system, one single sample was obtained from a very fresh animal (CET 360). This sample was composed of high content of nitrogen (74%) followed by oxygen and CO_2. All the other samples were obtained from more decomposed animals.

Within decomposition code 3 there was one animal (CET 512) with a considerable amount of bubbles (bubble score higher than 5). Not all the bubbles had the same gas composition. Hydrogen was already present in most of them, even though there were some bubbles with high nitrogen content and oxygen was not present or in small concentrations. The rest of the bubbles were composed of a mixture of CO_2, hydrogen and nitrogen where any of them was present in significant higher quantities than the others.

Gas samples obtained from animals with decomposition code 4 were composed of CO_2, hydrogen and nitrogen, being CO_2 the major compound and nitrogen the smallest with concentrations lower than 30%. There was neither oxygen nor methane.

With decomposition code 5 nitrogen was not present any more. Gas composition was a mixture of CO_2 and hydrogen with similar concentrations but CO_2 was always found in slightly higher concentrations.

It was found a clear difference in gas composition with decomposition codes.

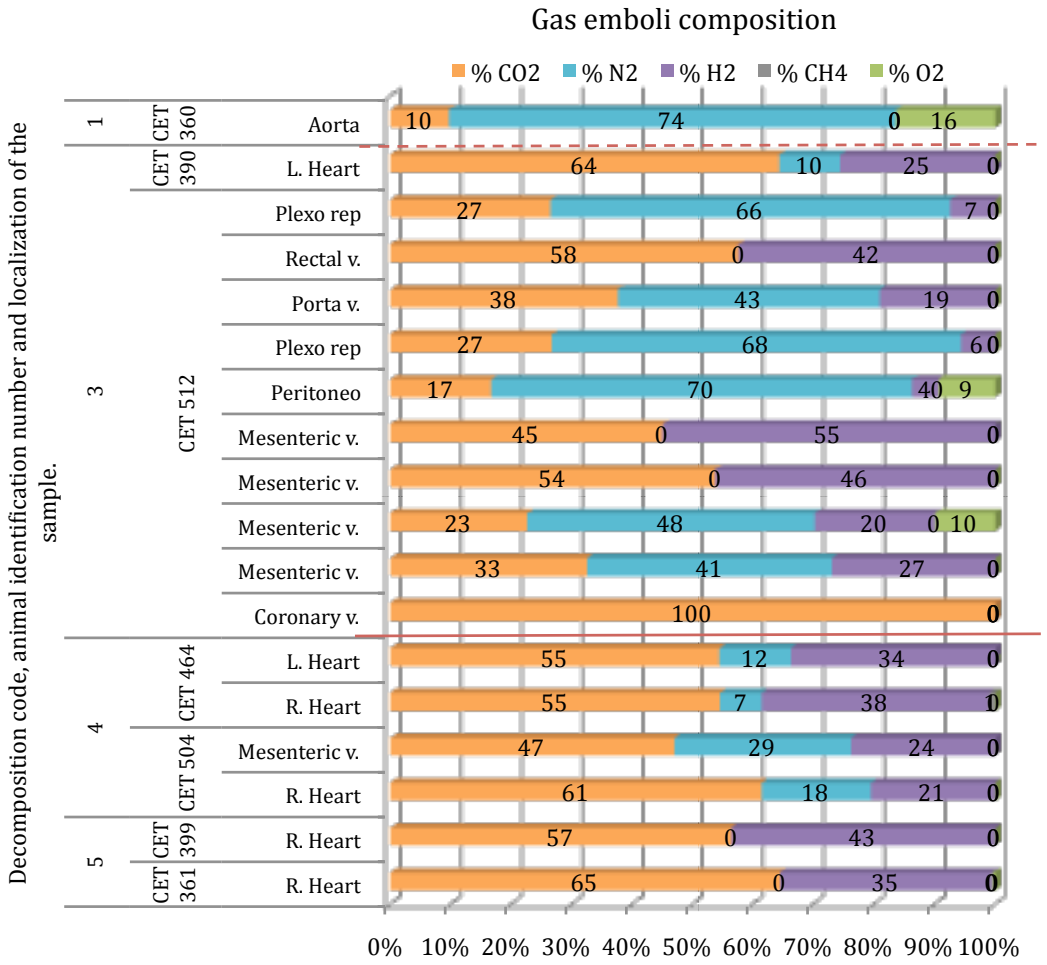

Fig. 4.34: Gas embolism composition sampled form different localizations and with different decomposition codes, illustrating the contribution of each gas to the total amount in percentage µmol. The discontinuous line is separating decomposition codes 4 and 5 from the fresher samples since these decomposition codes have a clear different gas composition. The discontinuous line is separating decomposition code 3 from 1 and 2.

SEPARADORES GRAMPUS

4.3.2.4 *Grampus*

4.3.2.4.1 Free gas in tissues and/or veins

Presence and abundance of free gas in tissues and veins was evaluated with the grading system described under material and methods section in this chapter as well as in appendix 9.2. Since PM time was unknown for most of the cases, animals were arranged first by decomposition code, and secondly in mounting order of the summation of free gas in the different tissues, in order to detect more clearly tendencies or disparities within the dataset. Some stranding circumstances that might be of relevance are described together with the cetacean number (for identification purposes) and gas bubble scores.

Table 4.8: Cetacean number, stranding circumstances and gas bubble score for *Grampus griseus* included in the study.

Cetacean number	Decomposition code	Active stranding	Mass stranding	Frozen	Bubbles	Subcutaneous v.	Mesenteric v.	Lumbo-caudal venous plexus	Coronary v.	Subcapsular emphysema	Summation	Diagnosis
CET 534	1	yes	no	no	yes	0	0	I	II	0	3	Viral disease Bacterial/Mycotic infection
CET 431	2	yes	no	no	no	0	0	0	0	1	1	Infectious meningitis
CET 472	2	no	no	no	no	0	0	0	0	1	1	Trauma
CET 456	2	yes	no	yes	no	0	0	0	0	2	2	Infectious meningoencepalitis
CET 483	2	yes	no	no	yes	?	II	II	I	2	7	Venous gas embolism
CET 549	2	no	no	no	yes	II	II	II	II	2	10	Venous gas embolism
CET 533	4	no	no	no	yes	I	II	I	I	2	7	Not determined Parasitoses

Bubbles were observed in 3 out of 6 (50%) fresh animals. Two of these animals had a very large amount of gas although the fresh decomposition code. Their gas bubble score is even higher than that observed in an animal with advance autolysis from the same specie but it is also the highest score reported among the 94 animals studied. The

small bars within the decomposition code 2 represent the presence of subcapsular gas, but no bubbles were observed in the veins.

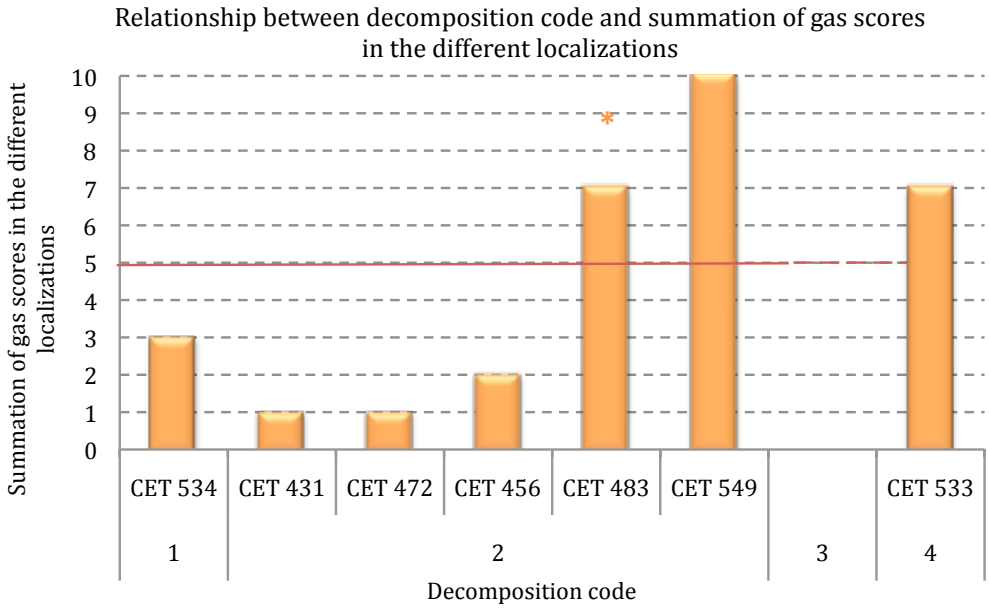

Fig. 4.35: Cumulative gas appearance in tissues and veins of each *Grampus griseus* within its corresponding decomposition code.

The animal with the highest summation of gas score had in addition pneumothorax (evident by the flattening of the aorta and the outcoming of gases when opening the thorax cavity), pneumodiastinum and a pleura lesion.

Fig. 4.36: Thoracic cavity of the Grampus CET 549 where the lesion in the pleura and the flattening of the aorta caused by the pneumothorax are shown.

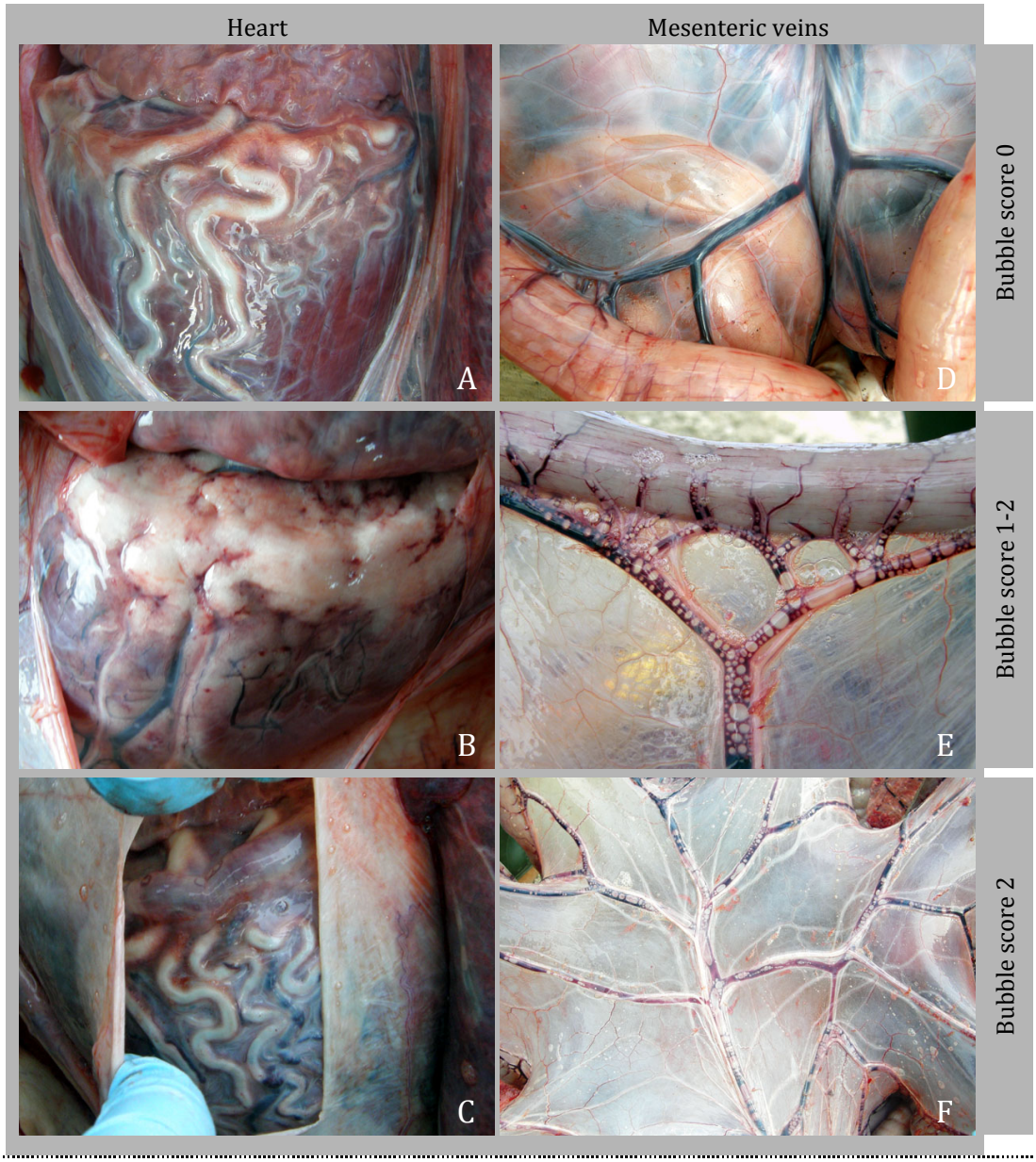

Fig. 4.37: Pictures showing the heart (A-C) and the mesenteric veins (D-F) with different bubble scores from fresh (decomposition codes 1-2) *Grampus*.

4.3.2.4.2 Gas composition

41 gas samples were obtained. Detailed gas composition of each analyzed sample expressed as percentage of average mole fraction is given in appendix 10.2.2 Samples were arranged following the same order as in the graphs of free gas abundance in tissues and veins: first by decomposition code and then by gas abundance in tissues.

In the intestine it was found a large variation from samples composed mainly by CO_2 to samples with high nitrogen contents (73-86%). This nitrogen contents are among the highest recorded for intestine gas sample's composition. Once more oxygen and methane did not play an important role in the gas composition and hydrogen appear again randomly.

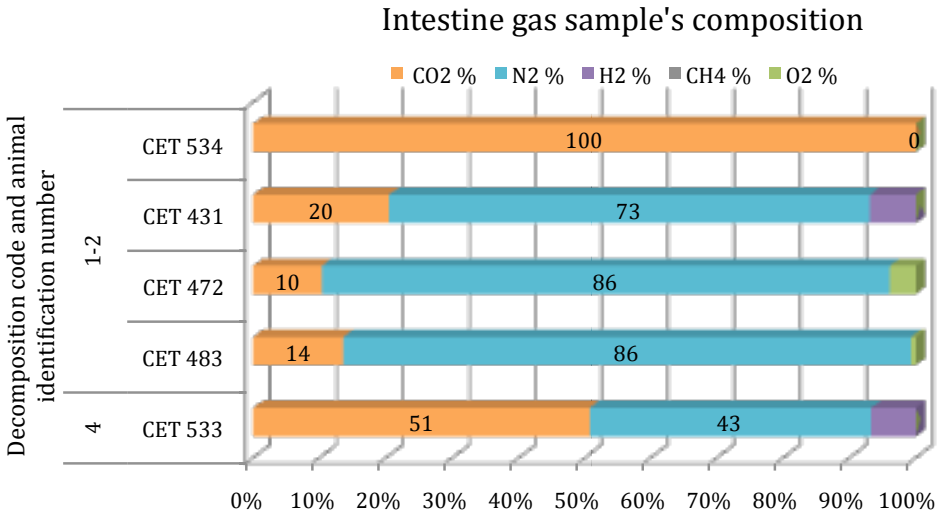

Fig. 4.38: Intestine gas composition from *Grampus griseus* within different decomposition codes illustrating the contribution of each gas to the total amount in µmol percentage

Regarding gas composition of the sinuses only two samples were successfully obtained; one from a very fresh animal and the other one from a carcass with advanced autolysis. Gas composition was clearly different. While in the fresh animal there was an important content of nitrogen (64%), in the more decomposed animal, the gas composition was mainly CO_2.

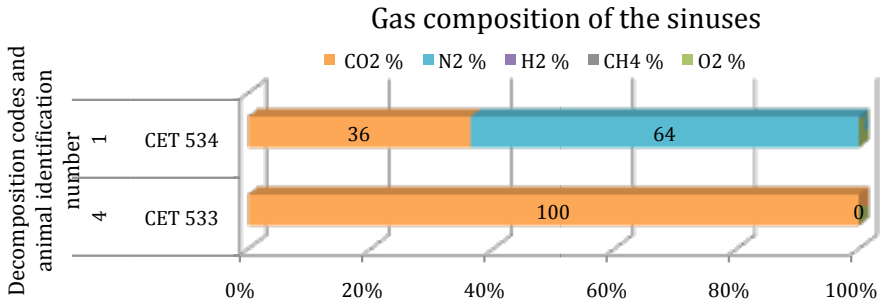

Fig. 4.39: Sinus gas composition of the samples taken from *Grampus griseus* with different decomposition codes illustrating the contribution of each gas to the total amount in µmol percentage

More samples were recovered from the heart and veins. All the samples obtained from fresh *Grampus griseus* were composed of nitrogen, CO_2 and oxygen. On the other hand samples from a more autolytic animal were composed of hydrogen, CO_2 and nitrogen. In one fresh animal it was found a smaller content of nitrogen (54%) and higher levels of CO_2 percentage (46%) compared to the rest of the samples where the mean values of nitrogen and CO_2 were of 76 and 15% with standard deviations of 7 and 9 respectively.

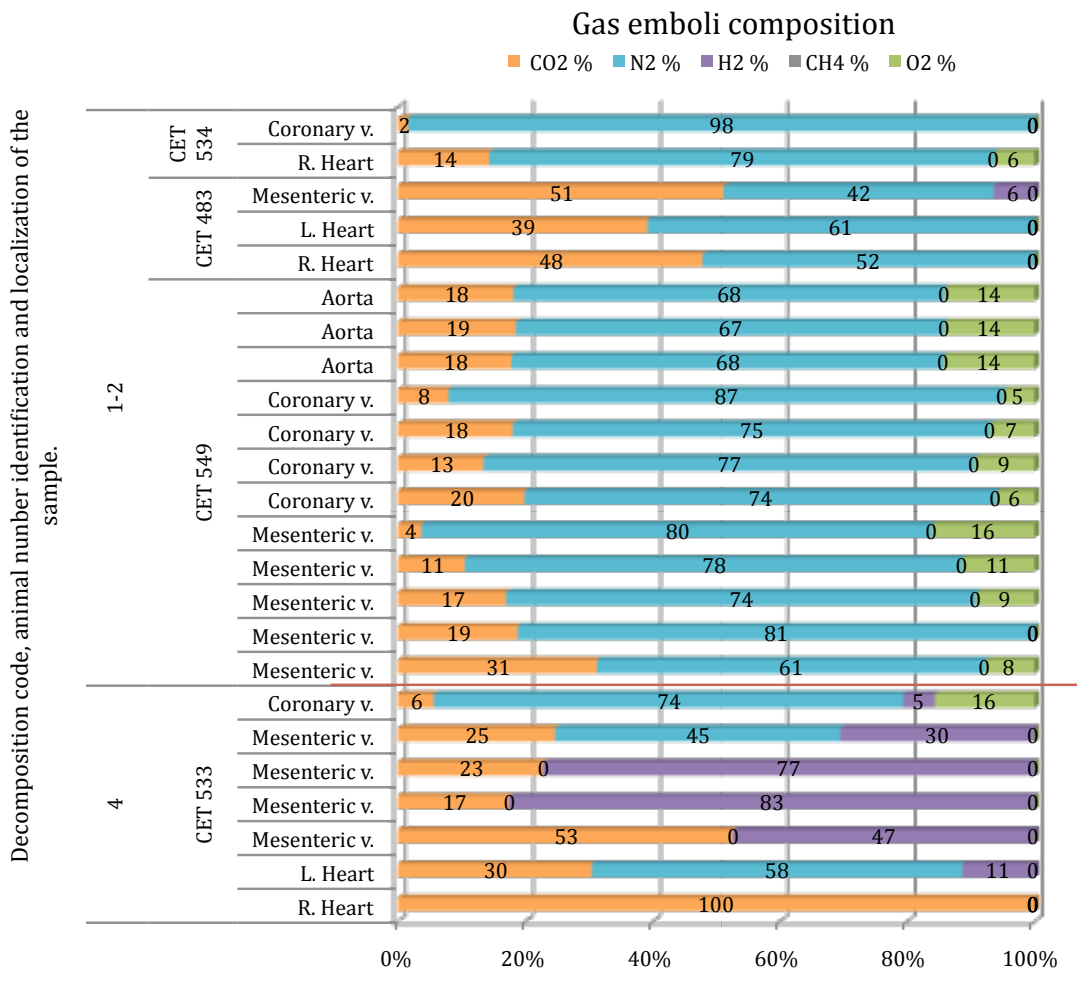

Fig. 4.40: Gas embolism composition sampled form different localizations and with different decomposition codes, illustrating the contribution of each gas to the total amount in percentage µmol. The solid red line is separating decomposition code 4 from the more fresh samples, since samples from decomposition code 4 had a clear different gas composition.

SEPARADOR ZIFIOS

4.3.2.5 *Ziphiidae*

4.3.2.5.1 Free gas in tissues and/or veins

Presence and abundance of free gas in tissues and veins was evaluated with the grading system described under material and methods section in this chapter as well as in appendix 9.2. Since PM time was unknown for most of the cases, animals were arranged first by decomposition code, and secondly in mounting order of the summation of free gas in the different tissues, in order to detect more clearly tendencies or disparities within the dataset. Some stranding circumstances that might be of relevance are described together with the cetacean number (for identification purposes) and gas bubble scores.

Table 4.9: Cetacean number, specie, stranding circumstances and gas bubble score for *Ziphiidae* included in the study

Cetacean number	Specie	Decomposition code	Active stranding	Mass stranding	Frozen	Bubbles	Subcutaneous v.	Mesenteric v.	Lumbo-caudal Venous plexus	Coronary v.	Subcapsular emphysema	Summation	Diagnosis
CET 379	*Mesoplodon bidens*	2	?	no	no	yes	0	2	1	1	1	5	Trauma Septicaemia
CET 471	*Ziphius cavirostris*	2	?	no	no	yes	2	0	1	1	2	6	Chronic renal failure
CET 510	*Mesoplodon europaeus*	3	?	no	no	yes	1	1	2	1	1	6	Trauma Possible viral disease
I181/09	*Mesoplodon bidens*	3	yes	yes	no	yes	0	2	1	2	1	6	pending
I182/09	*Mesoplodon bidens*	3	no	yes	no	yes	0	1	2	2	1	6	pending
I183/09	*Mesoplodon bidens*	3	?	yes	no	yes	1	2	2	1	1	7	pending
I184/09	*Mesoplodon bidens*	4	?	yes	no	yes	0	1	2	2	2	7	pending
CET 547	*Mesoplodon europaeus*	4	?	no	no	yes	1	2	2	2	2	9	not determined
I185/09	*Mesoplodon bidens*	5	no	yes	no	yes	2	2	2	2	2	10	pending

All the beaked whales presented bubbles and all of them had summation of bubble score equal or higher than five regardless decomposition codes. All of them had bubbles in the coronary veins and in the lumbo-caudal venous plexus except for one case (CET 471) they all had bubbles in the mesenteric veins as well. Emphysema was present in the freshest carcasses too.

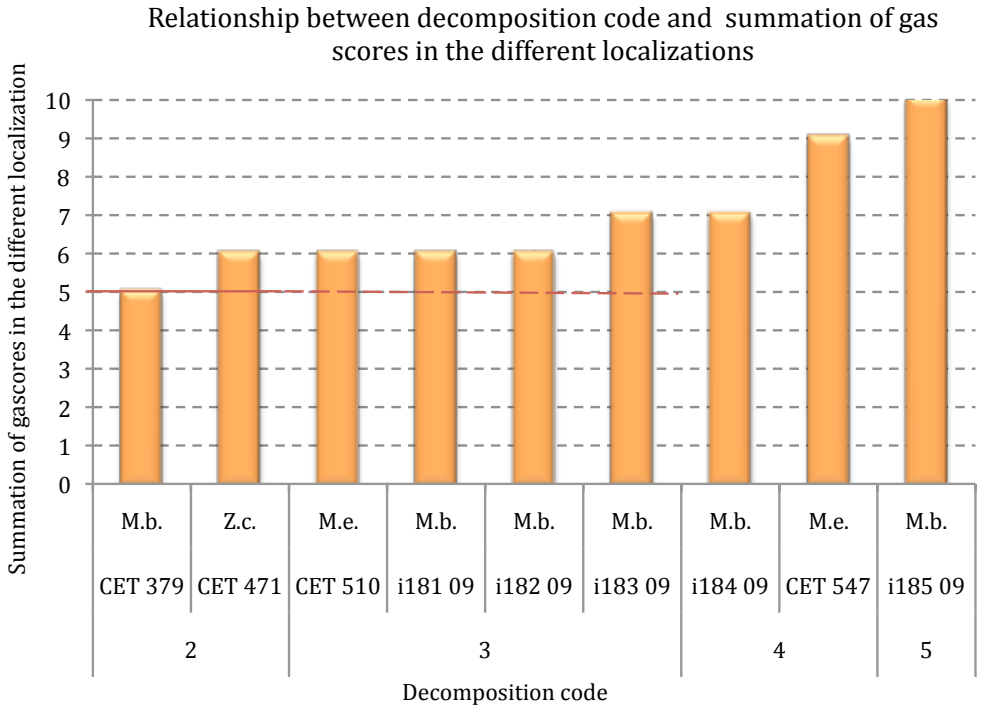

Fig. 4.41: Cumulative gas appearance in tissues and veins of each beaked whale included in the study within its corresponding decomposition code.

4.3.2.5.2 Gas composition

130 gas samples were obtained. Detailed gas composition of each analyzed sample expressed as percentage of average mole fraction is given in appendix 7.2.2. Samples were arranged following the same order as in the graphs of free gas abundance in tissues and veins: first by decomposition code and then by gas abundance in tissues.

For the first time we found intestinal gas composition quite homogenous between animals and between decomposition codes. Intestinal gas was composed of CO_2 and hydrogen. Nitrogen if presented, it was in very low amounts except for one sample (i181/09) where it reached a concentration of 45%. The highest levels of CO_2 were always found in samples from *Mesoplodon europaeus* intestine. Methane was not present at all, and oxygen was only present in one sample.

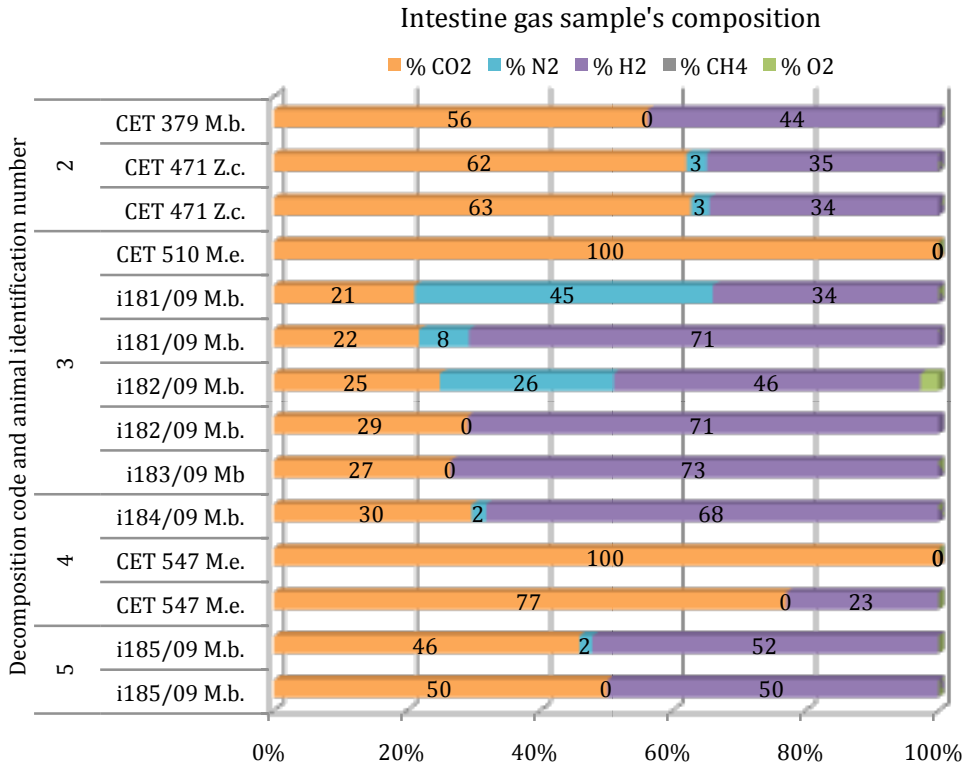

Fig. 4.42: Intestine gas composition from *beaked whales* within different decomposition codes illustrating the contribution of each gas to the total amount in µmol percentage

Few samples from emphysema were obtained but with similar gas composition. Similarly to the intestinal gas, subcapsular emphysema was composed of CO_2 and hydrogen. These two samples were taken from the liver that presented marked putrefactive emphysema besides their decomposition code.

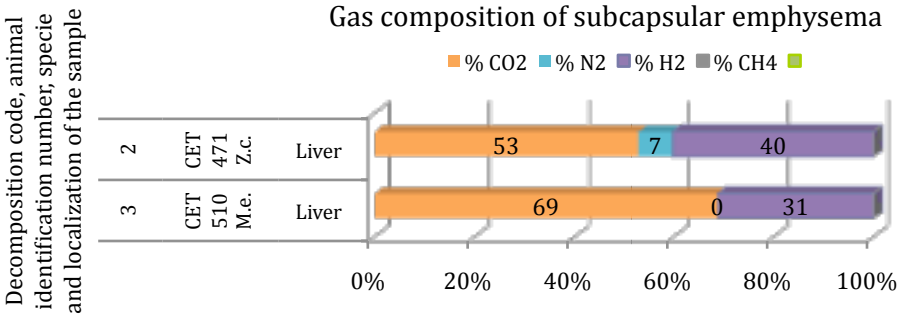

Fig. 4.43: Subcapsular emphysema composition of the samples taken from different localizations from Ziphidae with different decomposition codes illustrating the contribution of each gas to the total amount in µmol percentage.

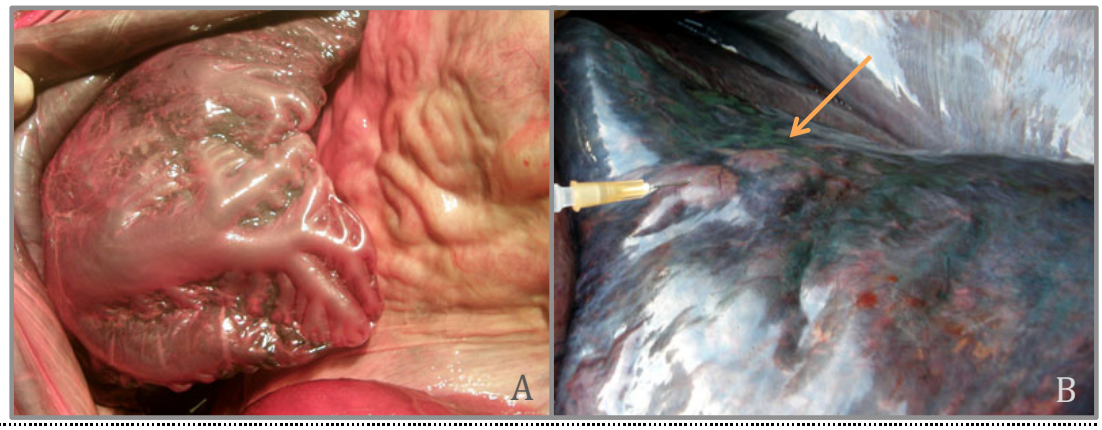

Fig. 4.44: Putrefactive aspect of liver subcapsular emphysema from CET 471 (A) and CET 510 (3).

On the other hand, gas composition of the sinuses was found as well to be very stable but with a completely different composition. The major compound was nitrogen that was present in very high concentrations (70-90%) regardless decomposition code. In one animal (CET 510), nitrogen levels were smaller but still high (around 60%). Only one sample presented oxygen and in other sample with decomposition code 5 hydrogen was found.

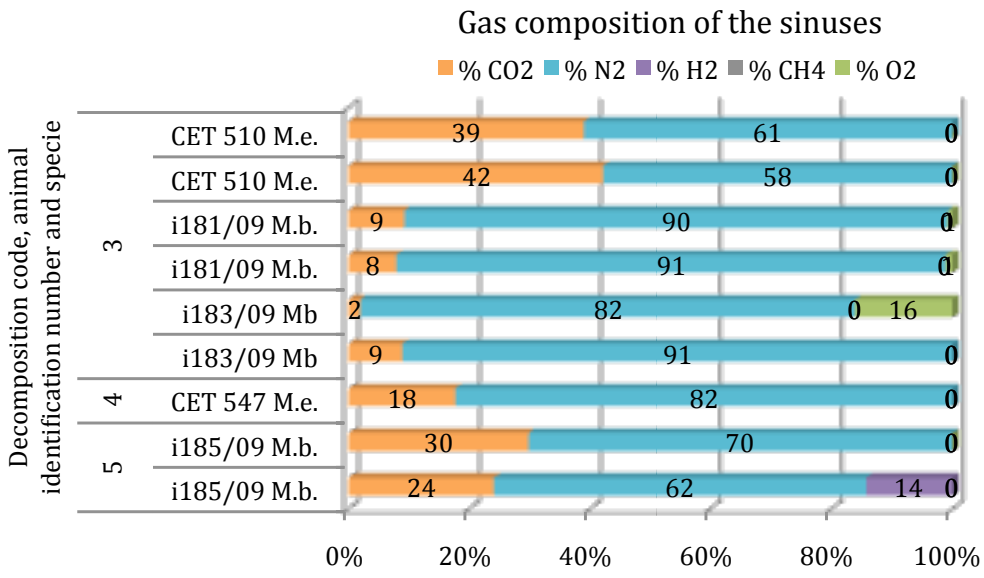

Fig. 4.45: Sinus gas composition of the samples taken from *Ziphiidae* with different decomposition codes illustrating the contribution of each gas to the total amount in µmol percentage

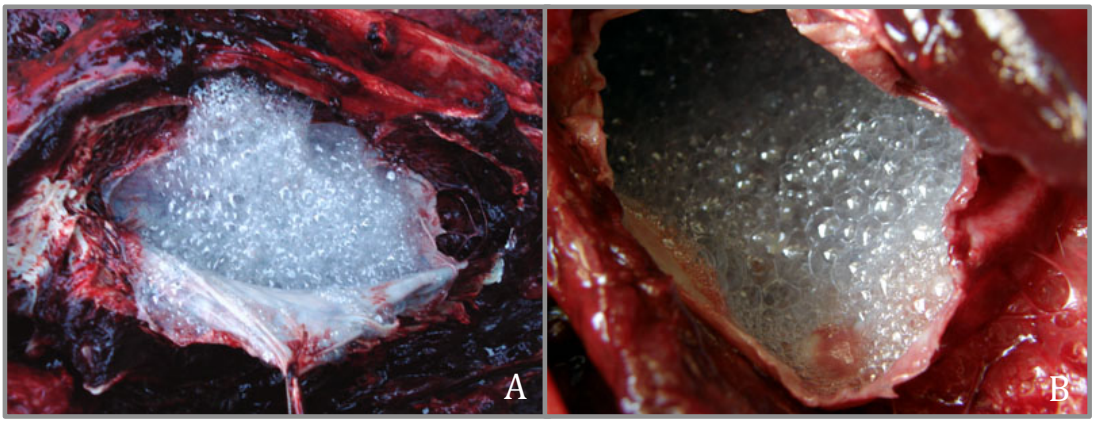

Fig. 4.46: Illustrations of pterygoid sinus with filled with gas foam.

Regarding composition of gas found in the circulatory system of *Ziphiidae*, a large variation was found. There are samples within the same animal with high nitrogen content (higher than 70%) and low or any oxygen while other samples had hydrogen.

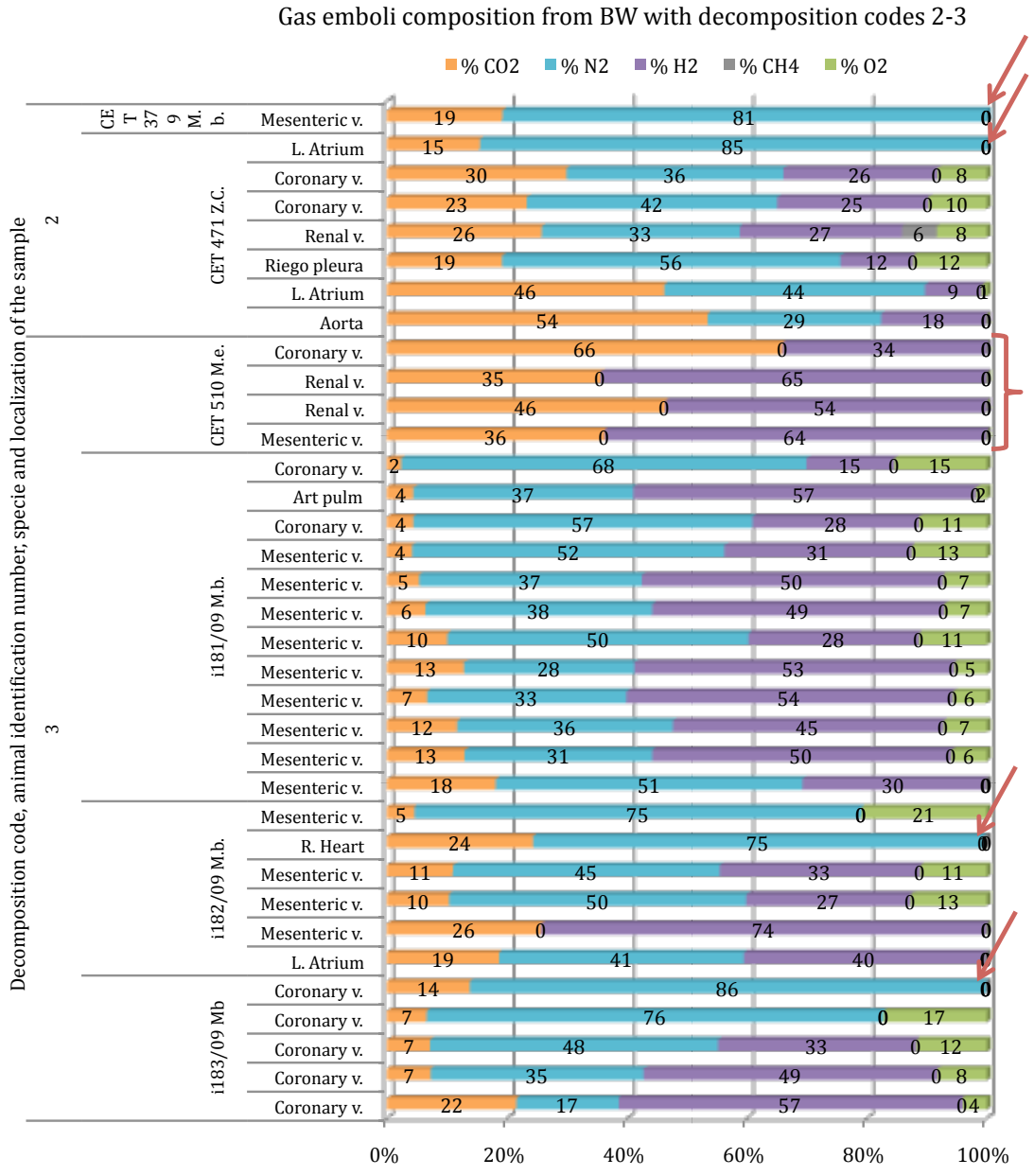

Fig. 4.47: Sinus gas composition of the samples taken from *Ziphiidae* with different decomposition codes illustrating the contribution of each gas to the total amount in µmol percentage. Red arrows are indicating gas samples with high nitrogen content (>70%) and without oxygen ruling out air pollution. The bracket is showing a very different gas composition from the rest of the samples from decomposition codes 2 and 3. This gas composition resembles to that found with decomposition code 5, also in brackets. The red circles in enclosing a data set composition that does not match with the other samples from decomposition code 4.

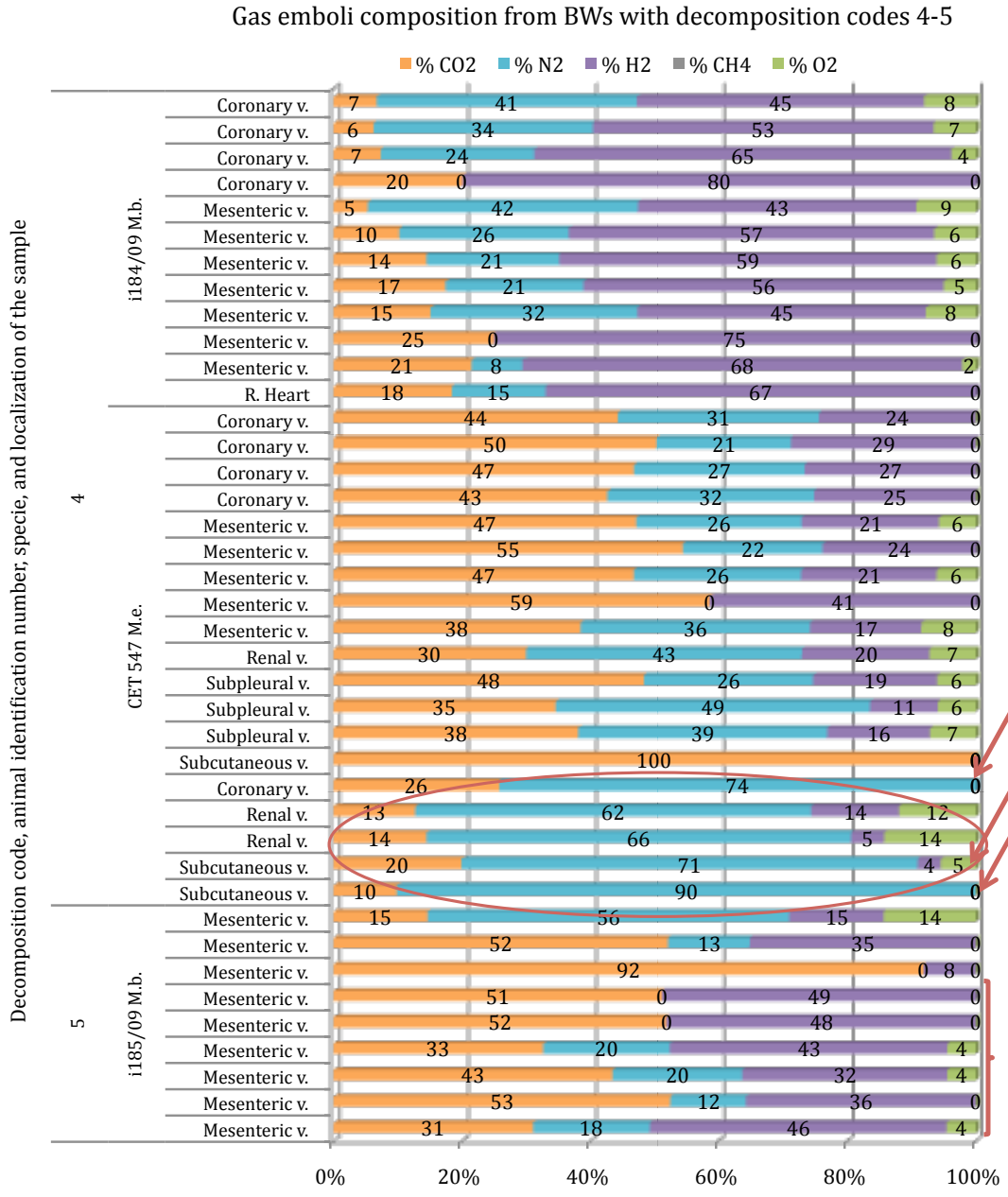

(Follow up) Fig. 4.47: Sinus gas composition of the samples taken from *Ziphiidae* with different decomposition codes illustrating the contribution of each gas to the total amount in µmol percentage. Red arrows are indicating gas samples with high nitrogen content (>70%) and without oxygen ruling out air pollution. The bracket is showing a very different gas composition from the rest of the samples from decomposition codes 2 and 3. This gas composition resembles to that found with decomposition code 5, also in brackets. The red circles in enclosing a data set composition that does not match with the other samples from decomposition code 4.

4.4 DISCUSSION

Marine mammals were not considered to suffer from decompression sickness since gas supersaturation was not expected to occur because the gas available for supersaturation is limited to that of the lungs, which are compressed during the dive forcing the residual air to the upper airways where non-gas exchange should take place. In addition, partial pressure of nitrogen in the blood would decrease as nitrogen is distributed among tissues (Piantadosi and Thalmann, 2004).

However, recently, VGE was described in an atypical BWs mass stranding related to military maneuvers that occurred in the Canary Islands in 2002. BWs (8 out of 8) presented gas bubble lesions consistent with acute decompression like sickness (Fernandez et al., 2005; Jepson et al., 2003). In addition chronic gas-bubble lesions were also reported in single strandings of Risso's dolphin (3 out of 24), common dolphins (3 out of 342), harbour porpoises (1 out of 1035) and in Blainville's beaked whale (1 out of 1) stranded in the United Kingdom (Jepson et al., 2003; Jepson et al., 2005). Osteonecrosis (a chronic bone pathology also related to repetitive decompression mechanisms in humans) has been described to occur in sperm whales (Moore and Early, 2004). Moore et al. (2009) described grossly a high incidence of intravascular bubbles in bycaught seals and dolphins trapped at depth (15 out of 23) compared to stranded marine mammals (1 out of 41).

Our results show that 56 out 93 stranded animals presented macroscopically bubbles during the necropsy. This represents 60% of the animals that were studied in the present thesis, and it clearly indicates that the presence of gas bubble within the cardiovascular system in stranded cetaceans is a common gross finding during necropsy.

These animals belonged to 13 different marine mammal's species from 18 that were studied in the thesis. This clearly demonstrates that the presence of gas bubbles in stranded marine mammals is not a specie-specific phenomenon. However, the presence of gas bubbles in the studied stranded cetaceans also showed some relevant

relationships that involve factors that merit to be analyzed either individually or in groups of animals.

We have considered the following main common factors: decomposition animal code, stranding type, either active (found alive) or passive (found dead), and diving profile (deep or non-deep divers).

In forensic human pathology the presence of intravascular gas in carcasses linked to decomposition under different environmental conditions is well known and widely reported (Knight, 1996). This observation has also been demonstrated in our experimental rabbit model in which dead rabbits were necropsied under well-controlled environmental conditions and scheduled PM time intervals (chapter III). In that experiment it was detected the appearance and accumulation of gas within veins and/or tissues from none in fresh animals to a high amount in highly decomposed carcasses directly linked to PM time and decomposition codes (R^2 = 0.8982 and P < 0.001).

Most of the stranded cetaceans are found dead on the beach or floating near the coast exposed to different environmental conditions. Defining a precise PM time when necropsy is done is certainly very difficult, therefore, instead of establishing a PM time, a body decomposition code is adjudged to each stranded cetacean following a cetacean international necropsy standard protocol (Kuiken and García-Hartmann, 1991), which also takes referenced PM criteria described in human and animal pathology (Knight, 1996). This protocol and criteria were also used in the rabbits experimental models carried out in this thesis (chapter III), in addition to PM times. A strong correlation between PM time and decomposition codes used was confirmed (r=0.9591; P<0.001), allowing us a comparative discussion using decomposition codes.

From the total of marine mammals included in the study, the incidence of intravascular gas bubbles was of 13/39 (33.3%) in fresh or very fresh animals (decomposition codes 1 and 2), 16/23 (69.6%) in those with incipient autolysis

(decomposition code 3), and 27/27 (100%) in the carcasses in an advanced or very advanced putrefaction state (decomposition codes 4 and 5). The last data demonstrates that intravascular gas bubbles due to putrefaction is a constant finding in these stranded cetaceans, as it occurs in humans and in domestic animals, directly related to PM time and to the corresponding decomposition codes which were influenced by different environmental conditions (specially temperature) (King et al., 1989; Knight, 1996).

Putrefaction is a continual process of gradual decay and disorganization of organic tissues and structures after death that results in the production of liquids, simple molecules and gases (intravascular gas and/or putrefactive emphysema)(Lerner and Lerner, 2006; Vass et al., 2002). This gas producing process may overlap or mask the presence of "in vivo" gas producing phenomena, related to diving physiology and physiopathology (Knight, 1996). That effect would be high or very high in decomposition codes 4 and 5, but lower in decomposition code 3, when putrefaction is still incipient as we saw in the putrefaction experimental model (see chapter II).

As there is a unanimous consensus on that, we have ruled out code 4 and 5 cetaceans, in order to approach one of our key objectives, that is, do gas bubbles found in stranded cetaceans at necropsy with decomposition code 1 and 2 are "*in vivo*" formed? In addition, code 3 animals, were included sometimes, when gas amount and its composition (discussed later on) indicated a most likely "in vivo" gas-producing phenomenon.

It is very unusual to find gas bubbles within the cardiovascular system in fresh necropsied domestic animals or humans (King et al., 1989; Knight, 1996). In humans, its presence should include as first differential diagnosis, iatrogenic air embolism and gas embolism linked to diving fatalities (Knight, 1996; Muth and Shank, 2000).

Attending to these well-known pathologies in humans, our experimental rabbit model for putrefaction had provided strong evidences of no intravascular bubbles in

rabbits necropsied in decomposition code 1 and 2. These evidences together with the fact that marine mammals are constantly diving, suggests that the most feasible explanation for the presence of small quantities of intravascular bubbles in code 1 and 2 stranded cetaceans would be related to bubble formation / growth involved in diving physiology (Tikuisis and Gerth, 2003) instead of putrefaction processes.

Another common factor, was the stranding type, active stranded cetaceans presented a higher prevalence of bubbles (7/14) what means 50% of the animals, in contrast to 3 out of 15 (20%) passive stranded cetaceans that showed also gas bubbles. Thus active stranding seems to be related with a higher incidence in bubble presence, but it should be considered that some of the passive stranding might be animals that beached alive but were found dead. Due to the importance of clarification of the role of stranding on bubble formation and growth in cetaceans, this is a significant point that would merit to be investigated further.

The third factor is based on the fact that different species have different diving behavior. It was found a clear relationship between deep diving species and incidence of bubbles in animals with decomposition codes 1 and 2. 60% of the deep divers presented intravascular bubbles compared to 25% of non-deep divers. This difference was of 100% *versus* 50% with decomposition code 3. This marked difference let us segregate the data in two groups: deep-divers and non-deep divers. This subdivision is important to avoid comparing very different diving profile (levels of exposure), in addition to the well known inter and intra-individual bubble formation variability described at any level of exposure (Eckenhoff et al., 1990), fact that was also demonstrated in our experimental decompression rabbit model (chapter III).

The higher incidence of intravascular bubbles related to the diving behavior of the species suggest that these bubbles are linked to the diving physiology and that deep divers might have higher risk to suffer from decompression.

Related to this, the extreme diving profile of BWs, not previously observed in other marine mammals, such as very deep foraging dives (up to 2000 msw and as long as 90 min), relatively slow controlled ascents followed by a series of bounce dives of 100-400 msw (Hooker and Baird, 1999; Tyack et al., 2006) were considered to induce nitrogen supersaturation (Hooker et al., 2009) that would drive growth of bubbles in a manner similar to decompression sickness in humans (Cox et al., 2006).

The amount of intravascular bubbles in the venous system (bubble grade) measured by means of ultrasound has been shown to be statistically correlated with DCS in humans (Sawatzky, 1991). Moreover, we have previously demonstrated (in chapter III) a clear relationship between high bubble grades (evaluated *in vivo* with the ultrasound) and high gas summation scores measured in tissues and veins during the necropsies of the rabbits from the compression/decompression model. In forensic human pathology as well as we have seen in our decompression experimental rabbit model, the amount of intravascular visible gas bubbles plays a key point to approach a condition of decompression like sickness (Knight, 1996).

To determine what is a high summation of gas score in cetaceans and what is not, a cut-off guideline was established taken as a reference the results of the experimental rabbit models and taking into consideration the results obtained in stranded cetaceans. This cut-off guideline was defined in half of the total gas score summation.

In experimental rabbit model, this cut-off line clearly distinguished between venous gas embolism and putrefaction gases up to decomposition code 3. On the other hand, we should be more cautious in stranded cetaceans since a higher gas production seems to be produced, thus this cut-off line can also be clearly established for decomposition codes 1 and 2, but not for decomposition code 3, being necessary an individual analysis in order to get a conclusion.

Following this method, we found high summation of gas scores in 3 out of 14 (21, 4%) in deep divers versus 0 out of 25 (0%) in non-deep divers within decomposition

code 1 and 2. With decomposition code 3, we found them in 6 out of 9 (66, 6%) and 2 out of 14 (14, 3%) animals respectively. These results indicate that an "in vivo" gas bubble formation is most likely to have occurred in all these animals, being more prevalent in deep divers, which therefore would be at a higher risk to suffer from decompression.

Summarizing our results using the score system, we can conclude that the presence of bubbles detected macroscopically during the necropsy in stranded cetaceans is not something unusual but the quantity of them is more important than the merely presence versus absence of bubbles.

Intravascular gas bubbles were first described in BWs (extreme deep divers) stranded in spatiotemporal concordance with military maneuvers (Fernandez et al., 2005; Jepson et al., 2003). Authors suggested a decompression-like disease as a plausible mechanism for explaining that new pathological entity in cetaceans. This hypothesis raised an important public controversy and a scientific replay in *Nature 2004* (Piantadosi and Thalmann, 2004), which clearly disagreed with that interpretation, requiring investigations on analysis of the composition of the gas in the bubbles in order to approach a diagnosis of DCS.

In order to answer this question, one of the objectives of the present thesis, was to develop and innovate a field methodology, not previous done in marine mammals, that enables *in situ* gas sampling from stranded cetaceans, storage, and transport to the laboratory and its analysis, attempting to avoid air pollution, as main problem, during all the steps of the methodology (chapter II).

In addition, three experiments were set up using rabbits under well-controlled circumstances in order to establish referenced guidelines on intravascular gases produced firstly by putrefaction, second, by air embolism and third, compression and decompression in an experimental hyperbaric chamber (chapter III).

With these referenced data, and following the methodology described in chapter II, 496 gas samples were obtained from 92 animals belonging to 18 different mammal species (1 pinniped specie and 17 cetacean species) and were analyzed.

Nitrogen, oxygen, CO_2, hydrogen, CH_4 and SH_2 represented the most common detected gases found in our thesis, as it has been reported in cadavers from different species, including humans and laboratory animals (Bajanowski et al., 1998; Keil et al., 1980; Pierucci and Gherson, 1968; Pierucci and Gherson, 1969), and confirmed in our experimental rabbit model (chapter II).

As it has been addressed in the literature (Keil et al., 1980; Pierucci and Gherson, 1968), sample contamination by atmospheric air is a serious problem, on which we have put high attention. Although, preventive measures were taken (chapter I), some samples were contaminated by air, which were analytically defined as those with nitrogen and oxygen levels in similar proportion to atmospheric air composition (79% Nitrogen and 21% oxygen). All these samples were ruled out for further analysis or interpretations.

A non-unusual gas analytical finding was related to significant differences of composition among samples taken in the same animal. So, one or two samples showed a very different gas composition from the rest. These samples contained low concentrations of CO_2 or other gases, and nitrogen and oxygen were present in proportions similar to atmospheric air composition. In these cases, we have considered as a first option, a likely contamination of air during sampling, and therefore, those data were also ruled out for further analysis and interpretations.

Once excluded these polluted samples, the rest of the gas samples obtained from stranded cetaceans with an advanced or very advanced autolysis (code 4 and 5) showed a similar gas composition to those obtained from rabbits with the same decomposition codes experimentally induced. The composition consisted of a mixture of a high concentration of CO_2, presence of hydrogen, low concentration of nitrogen

(mostly lower than 40%) and very small quantities of oxygen, when present. CH_4 and SH_2 were randomly present and in trace levels. These last two gases reached higher values only in the intestine of few cetaceans.

These data point out that detection of hydrogen and/or high levels of CO_2 are "signal" gases indicative of putrefaction, while nitrogen decreases progressively until disappearing (not detected chromatographically) in carcasses with the highest decomposition code (code 5). Similar results have been described in humans and laboratory animals (Bajanowski et al., 1998; Keil et al., 1980; Pierucci and Gherson, 1968; Pierucci and Gherson, 1969). In this sense, we can state that hydrogen in stranded cetaceans is also a key putrefaction marker with few unexplained exceptions.

These exceptions were 4 cetacean carcasses (code 1 and 2) which showed a significant proportion of intravascular hydrogen. These gas results should be taken into account when a whole individual diagnostic analysis (including pathology, microbiology, toxicology, etc.) would be done. Speculatively, we have considered acute gastrointestinal diseases as primary source of hydrogen or due to overlapping with other pathogenic processes.

As it was concluded in chapter II, gas composition from air embolism and decompression is certainly similar and therefore difficult to make differences.

Gas composition found in most of the samples recovered from cardiovascular system from fresh stranded cetacean carcasses (decomposition codes 1 and 2) showed high concentrations of nitrogen (>70%) and values of CO_2 around 20%. Similar results were obtained from both, air embolism and compression/decompression experimental model in contrast to the gas analytical results obtained in our putrefaction rabbit model (chapter II). These values confirm what has been reported for gas analysis in cases of air embolism and/or decompression sickness in humans and laboratory animals (Armstrong, 1939; Bajanowski et al., 1998; Bert, 1878; Ishiyama, 1983; Pierucci and Gherson, 1968; Smith-Sivertsen, 1976).

Considering gas analytical results of the thesis as reference guideline and coming back to the conclusion that gas bubbles is not an unusual necropsy finding in different stranded species, we are going to do a diagnostic approach apply considering presence, amount and gas composition in order to try to reach a final diagnosis of animal death. On this regard and using our gas analysis results, the following cases will be discussed.

Among of our cases, the best example of an iatrogenic air embolism was demonstrated in a sea lion which died after an acute massive severe pneumomediastinum and subcutaneous emphysema (Fig. 4.16) due to rupture of the visceral pleura during an inappropriate digestive intubation. Necropsy was done four hours after death (code 1). Gas composition of samples taken from emphysematous tissues showed high nitrogen levels (>70%), CO_2 concentrations of around 15-20%, and low oxygen content, approximately 5% (Fig. 4.15).

In stranded cetaceans the demonstration of a similar case of air embolism, is not as simple. From our cases, we have considered a mass stranding of sperm whales occurred in Italy. They stranded alive (Fig. 4.25) and died within a period of time of 48 hours. They suffered of a prolonged lateral recumbence before dying. Pathological studies were carried out in three animals that presented different decomposition codes (from 2 to 3) at necropsy.

Pneumothorax and pneumomediastinum (Fig.4.26) were seen in these whales. Gas embolism (gas bubble score 1 or 2) was detected in the coronary veins. They were composed mainly of 70% of N_2, 15% of CO_2 and 15% of O_2 in the freshest animal, in contrast to gas composition around 30% of N_2, 30% of CO_2, 6% of O_2 and 33% of H_2 in the most decomposed animal (Fig. 4.29). Intestinal gases were mainly composed of CO_2 combined either with CH_4 or hydrogen (Fig.4.27). Nitrogen was absent or in low quantities (<20%) except for one sample where it reached high values (around 70%). Gas composition of the gas bubbles found in the coronary veins did not match with intestinal gases composition.

Bubbles were not widely distributed, nor either massively, throughout the rest of the body. According to our results from chapter II distribution and gas abundance (measured by the summation of gas score) might help to distinguish between decompression and air embolism. Gases from decompression are more widely distributed and in higher score since immediately after death when significant differences were found (chapter III).

Taking this into consideration, gas analysis of these animals allowed us to approach two different possibilities. First, an air embolism due to a severe respiratory distress (overbreathing with overexpansion of the passively congested lungs, rupture of alveolar walls as well as the pleura connective tissue), and secondly, bubbles can gas-off from supersaturated tissues since sperm whales may have a high saturation of nitrogen in tissues as deep-divers. Therefore, we can speculate with the concurrence of two "*in vivo*" and "*perimortem*" gas producing processes in the stranded sperm whales during beaching.

In this mass stranding as well as in stranded sperm whales in Canary Islands, it was also demonstrated a direct association between sperm whale decomposition and gas analysis. Nitrogen decreased with decomposition code (R^2=0.96) and at the same time hydrogen and CO_2 values increased (Fig. 4.30). Hydrogen started to appear with decomposition code 3. All of this plenty confirms the conclusions of this thesis respecting putrefaction and gas analysis (chapter III).

Regarding presence, amount and gas analysis in relationship to described decompression (chapter III) the most consistent cases we found were two *Grampus grisseus* (Fig. 4.37). They both were fresh carcasses (code2) with a large amount of bubbles within the cardiovascular system macroscopically found during necropsy.

One Grampus (CET 483) showed complete non-digested neon flying squid *Ommastrephes bartramii* in the stomach as well as fighting evidences in the esophagus and head skin.

Gas recovered from the right and left heart contained nitrogen in concentrations of 50-60% and CO_2 in 50-40% (Fig.4. 40). Even though this gas composition does not match exactly to what has been mainly reported (Bert 1878; Ishiyama 1983; Smith-Sivertsen 1976), is not that far from these values. Actually (1939) reported values of 60-65% of nitrogen and around 30% of CO_2, and us, have several samples from the compression/decompression model similar to what was found in the *Grampus* and that differed from all the rest of the samples. However, these were not just a few samples and a deep discussion about the role of CO_2 in DCS can be found in chapter III.

We proposed severe changes in the diving profile caused by the interaction with the squid as the most plausible mechanism to explain the abundant bubble formation within the cardiovascular system as well as other gas related lesions consistent with DCS in humans and experimental animals including our rabbit model (chapter III) (Bert, 1878; Francis and Simon, 2003; Harris et al., 1945a; Harris et al., 1945b; Smith-Sivertsen, 1976).

A second grampus (CET 549) (Fig. 4.36) with a poor body condition also showed a complete non digested squid in the stomach. At necropsy, main gross findings were systemic gas embolism, pneumomediastinum, pneumothorax and active pleural healing lesions. This animal presented the highest bubble score summation (Fig. 4.21) and gas composition falls in the range of what is widely described for air embolism and/or decompression (Armstrong, 1939; Bajanowski et al., 1998; Bert, 1878; Elsner, 1999; Ishiyama, 1983; Pierucci and Gherson, 1968) with nitrogen values of 60-80%, CO_2 values of 15-30% and oxygen levels of 5-15%, what is consistent with a likely overlapping of both pathogenic processes, decompression and air embolism.

During the last 20 years, stranded beaked whales have received an special attention due to their involvement in several atypical mass strandings linked to military maneuvers and antisubmarine sonar activities (Cox et al., 2006). Since gas bubble lesions were the main pathological finding to make a consistent diagnosis of DC like Sickness (Fernandez et al., 2005; Jepson et al., 2003) in BWs, these species are to be expected to contribute to clarify many of the questions of this sensitive and controversial environmental issue.

Our results demonstrate that decomposition is still the principal inconvenience to achieve good results in stranded beaked whales. From our cases, only two BWs were fresh (code 2), while all the rest showed decomposition code 3 or higher at necropsy. Most of the samples presented hydrogen confirming that this gas is an important putrefaction marker also in BWs.

However, BWs showed larger amounts of gas than expected attending to decomposition codes when compared to other stranded cetaceans or to our rabbit experimental decompression model. In addition, there were some samples (indicated with a red arrow in figures 4. 47) that contained a high level of nitrogen (60-90%), CO_2 concentrations of 10-30%, and no oxygen (ruling out atmospheric air pollution), leading us to suggest "in vivo" silent bubbles or *perimortem* gas-off bubble formation.

BWs with decomposition code 4 showed either high CO_2 content, or high hydrogen content, with some nitrogen (10-40%) until they reached decomposition code 5, when it CO_2 and hydrogen were found almost exclusively and in similar proportions. This gas composition is the same as that for intestinal gases regardless decomposition code. This was an unusual finding since a large variation in the intestinal gas composition of other species was commonly found, with difficulties to observe any trend. Unlikely other cetaceans the intestinal gas had almost no nitrogen (except for one sample with 45% of nitrogen).

Contrarily, gas from pterygoideal sinuses showed always-high concentrations of nitrogen reaching sometimes 90% of total gas composition (Fig 4.45 and 4.46). Similar values were obtained in some fresh non-deep divers. This was an additional finding that needs further investigation, as those anatomical areas are directly communicated with the tympanic areas of the ears, where gas bubbles were also grossly observed in beaked whales.

Piantadosi and Thalmann requested the gas analysis as necessary information to make a proper diagnosis of DCS in cetaceans when intravascular gas bubbles are found during necropsy. The present thesis answers Piantidosi`s request, presenting a good field method to gas sampling and storing, as well as laboratory analysis, and may conclude that gas analysis of bubbles can help pathologists to define more precisely body decomposition as well as to make a better approach in defining decompression related processes and/or air embolism in stranded cetaceans.

Gas analysis is not a conclusive diagnosis for DC like Sickness in stranded cetaceans, but may contribute complementarily with other data obtained by imaging analytical techniques, a systematic necropsy, histopathology, microbiology, toxicology and other possible future analyses to reach a definitive diagnosis of decompression disease

4.5 REFERENCES

2004. Policy on sound and marine mammals. In: Commission TMM, editor. Beaked whale technical workshop. Baltimore, Maryland.

Aguilar de Soto N. 2006. Acoustic and diving behaviour of the short finned pilot whale (Globicephala macrorhynchus) and Blainville's beaked whale (Mesoplodon densirostris) in the Canary Islands. Implications of the effects of man-made noise and boat collisions. La Laguna, Tenerife, Spain: La Laguna University.

Arbelo M. 2007. Patología y causas de la muerte de los cetáceos varados en las Islas Canarias (1999-2005) [Doctoral thesis]. Las Palmas de Gran Canaria: University of Las Palmas de Gran Canaria.

Armstrong HG. 1939. Analyisi of gas emboli. Engineering Section Memorandum Report. Wright Field, Ohio.

Astruc G, Beaubrun P. 2005. Do Mediterranean cetaceans diets overlap for the same resources? European Research on Cetaceans 19:81.

Bajanowski T, Kohler H, DuChesne A, Koops E, Brinkmann B. 1998. Proof of air embolism after exhumation. International Journal of Legal Medicine 112(1):2-7.

Bert P. 1878. La Pression Barometrique: Recherches de Physiologie Expérimentale. Hitchcock MA, Hitchcock FA, translator. Paris: Masson.

Cox TM, Ragen TJ, Read AJ, Vos E, Baird RW, Balcomb K, Barlow J, Caldwell JM, Cranford T, Crum LA, D'Amico A, D'Spain G, Fernandez A, Finneran JJ, Gentry R, Gerth WA, Gulland FMD, Hildebrand J, Houser D, Hullar T, Jepson PD, Ketten D, MacLeod CD, Miller P, Moore S, Mountain DC, Palka D, Ponganis PJ, Rommel S, Rowles T, Tyack PL, Wartzok D, Gisiner R, Mead J, Benner L. 2006. Understanding the impacts of anthropogenic sound on beaked whales. Journal of Cetacean Research and Management 7(3):117-187.

Croll DA, Acevedo-Gutierrez A, Tershy BR, Urban-Ramirez J. 2001. The diving behavior of blue and fin whales: is dive duration shorter than expected based on oxygen stores? Comparative Biochemistry and Physiology a-Molecular & Integrative Physiology 129(4):797-809.

Eckenhoff RG, Olstad CS, Carrod G. 1990. HUMAN DOSE-RESPONSE RELATIONSHIP FOR DECOMPRESSION AND ENDOGENOUS BUBBLE FORMATION. Journal of Applied Physiology 69(3):914-918.

Elsner R. 1999. Living in water: solutions to physiological problems. In: Reynolds JE, III, Rommel S, editors. Biology of Marine Mammals. Washington, DC.: Smithsonian Institution Press. p 73-116.

Fernandez A, Edwards JF, Rodriguez F, de los Monteros AE, Herraez P, Castro P, Jaber JR, Martin V, Arbelo M. 2005. "Gas and fat embolic syndrome" involving a mass stranding of beaked whales (Family Ziphiidae) exposed to anthropogenic sonar signals. Veterinary Pathology 42(4):446-457.

Francis TJR, Simon JM. 2003. Pathology of Decompression Sickness. In: Brubakk AO, Neuman TS, editors. Bennett and Elliott's Physiology and Medicing of Diving: Saunders. p 530-556.

Gannier A. 1998. Variation saisonnière de l'affinité bathymétrique des cétacés dans le bassin Luguro-provençal (Méditerranée occidentale). Vie Milieu 48:25-34.

Geraci JR, Lounsbury VJ. 2005. Marine Mammals Ashore: a Fiel Guide for Strandings. Second ed. Baltimore, MD: National Aquarium in Baltimore.

Harris M, Berg WE, Whitaker DM, Twitty VC. 1945a. THE RELATION OF EXERCISE TO BUBBLE FORMATION IN ANIMALS DECOMPRESSED TO SEA LEVEL FROM HIGH BAROMETRIC PRESSURES. Journal of General Physiology 28(3):241-251.

Harris M, Berg WE, Whitaker DM, Twitty VC, Blinks LR. 1945b. Carbon dioxide as a facilitating agent in the initiation and growth of bubbles in animals decompressed to simulated altitudes. Journal of General Physiology 28(3):225-240.

Hooker S, Baird RW. 1999. Deep-diving behaviour of the northern bottlenose whale, Hyperoodon ampullatus (Cetacea: Ziphiidae). Proceedings of the Royal Society of London B 266:671-676.

Hooker SK, Baird RW, Fahlman A. 2009. Could beaked whales get the bends? Effect of diving behaviour and physiology on modelled gas exchange for three species: Ziphius cavirostris, Mesoplodon densirostris and Hyperoodon ampullatus. Respiratory Physiology & Neurobiology 167(3):235-246.

Ishiyama A. 1983. Analysis of gas composition of intra vascular bubbles produced by decompression. Bulletin of Tokyo Medical and Dental University 30(2):25-36.

Jepson PD, Arbelo M, Deaville R, Patterson IAP, Castro P, Baker JR, Degollada E, Ross HM, Herraez P, Pocknell AM, Rodriguez F, Howie FE, Espinosa A, Reid RJ, Jaber JR, Martin V, Cunningham AA, Fernandez A. 2003. Gas-bubble lesions in stranded cetaceans - Was sonar responsible for a spate of whale deaths after an Atlantic military exercise? Nature 425(6958):575-576.

Jepson PD, Deaville R, Patterson IAP, Pocknell AM, Ross HM, Baker JR, Howie FE, Reid RJ, Colloff A, Cunningham AA. 2005. Acute and chronic gas bubble lesions in

cetaceans stranded in the United Kingdom. Veterinary Pathology 42(3):291-305.

Kaiser H. 1947. Die berechnung der nachweisempfindlichkeit. Spectrochimica Acta 3(1):40-67.

Keil W, Bretsxhneider K, Patzelt D, Behning I, Lignitz E, Matz J. 1980. Luftembolie oder Fäulnisgas? Zur Dianostik der cardialen Luftembolie an der Leiche. Beiträge zur Gerichtlichen Medizin 38:395-408.

King JM, Dodd DC, Newson ME, Roth L. 1989. The Necropsy Book. New York State College of Veterinary Medicine CU, editor. Ithaca, E.E.U.U.: Charles Louis Davis, D.V.M. Foundation.

Knight B. 1996. Forensic Pathology. Arnold, editor. London.

Kooyman GL. 2009. Diving Physiology. In: Perrin WF, Würsig B, Thewissen JGM, editors. Encyclopedia of Marine Mammals. 2nd edition ed. San Diego, CA: Academic Press. p 327-332.

Kuiken T, García-Hartmann M. Dissection techniques and tissues sampling. In: Newsletter, editor; 1991; Leiden, Netherlands.

Lerner L, Lerner BW. 2006. Decomposition. World of Forensic Science: eNotes.com.

Martin V, Servidio A, Tejedor M, Arbelo M, Brederlau B, Neves S, Perez-Gil M, Urquiola E, Perez-Gil E, Fernandez A. Cetaceans and conservation in the Canary Islands; 2009; Quebec, Canada.

Moore MJ, Bogomolni AL, Dennison SE, Early G, Garner MM, Hayward BA, Lentell BJ, Rotstein DS. 2009. Gas Bubbles in Seals, Dolphins, and Porpoises Entangled and Drowned at Depth in Gillnets. Veterinary Pathology 46(3):536-547.

Moore MJ, Early GA. 2004. Cumulative sperm whale bone damage and the bends. Science 306(5705):2215-2215.

Muth CM, Shank ES. 2000. Primary care: Gas embolism. N Engl J Med 342(7):476-482.

Piantadosi CA, Thalmann ED. 2004. Pathology: whales, sonar and decompression sickness. Nature 428(6984):1 p following 716; discussion 712 p following 716.

Pierucci G, Gherson G. 1968. Experimental study on gas embolism with special reference to the differentiation between embolic gas and putrefaction gas. Zacchia 4(3):347-373.

Pierucci G, Gherson G. 1969. Further contribution to the chemical diagnosis of gas embolism. The demonstration of hydrogen as an expression of "putrefactive component". Zacchia 5(4):595-603.

Sawatzky KD. 1991. The relationship between intravascular Doopler-detected gas bubbles and decompression sickness after bounce diving in humans [MSc thesis]. Toronto, Canada: York University.

Smith-Sivertsen J. The origin of intravascular bubbles produced by decompression of rats killed prior to hypebaric exposure. In: Lambertsen CJ, editor; 1976; Washington, DC. Bethesda MD. p 303-309.

Stewart BS. 2009. Diving behavior. In: Perrin WF, Würsig B, Thewissen JGM, editors. Encyclopedia of Marine Mammals. 2nd edition ed. San Diego, CA: Academic Press. p 321-327.

Tikuisis P, Gerth WA. 2003. Decompression theory. In: Brubakk AO, Neuman TS, editors. Physiology and Medicine of Diving. Saunders ed: Saunders. p 419-454.

Tyack PL, Johnson M, Soto NA, Sturlese A, Madsen PT. 2006. Extreme diving of beaked whales. Journal of Experimental Biology 209(21):4238-4253.

Unit of Cetaceans Research ULPGC. 2006. Necropsies of cetaceans stranded in Canary Islands in 2006 report. Canary Islands Government.

Unit of Cetaceans Research ULPGC. 2007. Necropsies of cetaceans stranded in Canary Islands in 2007 report. Canary Islands Government.

Unit of Cetaceans Research ULPGC. 2008. Necropsies of cetaceans stranded in Canary Islands in 2008 report. Canary Islands Government.

Unit of Cetaceans Research ULPGC. 2009. Necropsies of cetaceans stranded in Canary Islands in 2009 report. Canary Islands Government.

Unit of Cetaceans Research ULPGC. 2010. Necropsies of cetaceans stranded in Canary Islands in 2010 report. Canary Islands Government.

Vass AA, Barshick SA, Sega G, Caton J, Skeen JT, Love JC, Synstelien JA. 2002. Decomposition chemistry of human remains: A new methodology for determining the postmortem interval. Journal of Forensic Sciences 47(3):542-553.

Watwood SL, Miller PO, Johnson M, Madsen J, Tyack PL. 2006. Deep-diving foraging behaviour of sperm whales (Physerter macrocephalus). Journal of Animal Ecology 75:814-825.

West KL, Walker WA, Baird RW, White W, Levine G, Brown E, Schofield D. 2009. Diet of pygmy sperm whales (Kogia breviceps) in the Hawaiian Archipelago. Marine Mammal Science 25(4):931-943.

5 CONCLUSIONS

Chapter II: Development of a Methodology for gas embolism studies.

1. We have developed, implemented and standardized through laboratory validations, a handy feasible methodology with non-easy breakable materials, that enables gas sampling during *in situ* necropsies, as well as their storage and transport in vacuum tubes with non-statistical significant changes in gas composition, for their final analysis in the laboratory.

Chapter III: Experimental models of gas embolism.

2. Based on our rabbit experimental models a semi-quantitative method has been established to evaluate the presence and abundance of intravascular and tissular gas in carcasses during necropsy with forensic aims.

3. During necropsy of the rabbits (with decomposition codes 1 and 2) of the putrefaction experimental model, no atmospheric air was found to enter into vessels as a result of dissection. Considering all decomposition codes, a statistic significant lineal relationship was found between putrefaction and presence and quantity of gas.

4. Massive presence of gas within the cardiovascular system of rabbits with decomposition codes 1 and 2 in our experimental models should be interpreted as a systemic "*in vivo*" gas embolism. Rabbits dying after decompression showed a higher significant quantity and wider distribution of gas within the vascular system involving subcutaneous, femoral, cava, mesenteric, coronary veins as well as heart cavities, compared to rabbits which died due to experimental air embolism.

5. Putrefaction gases in rabbits were composed of presence of hydrogen and/or high levels of CO_2, low concentration of nitrogen (mostly lower than 40%) and very small quantities of oxygen when present. CH_4 and SH_2 were randomly present in trace levels.

6. Gas composition from samples obtained in codes 1 and 2 rabbits from air embolism and decompression experiments were very similar being composed of 70%-80% nitrogen and 20%-30% CO_2, and therefore quite difficult to make a difference.

Chapter IV: Gas embolism in stranded cetaceans.

7. The presence of bubbles detected within the cardiovascular system and tissues during the necropsy of stranded cetaceans is a common finding related to "*in vivo"* and/or PM process.

8. There is a direct relationship between decomposition codes in stranded cetaceans and increasing amount of bubbles. Postmortem processes were analytically related to the presence of hydrogen and/or high levels of CO_2 as demonstrated in the rabbit experimental models. To try to avoid these putrefactive masking gases, necropsy and gas sampling must be performed as soon as possible, before 24 hours PM as recommendation but preferably within 12 hours PM.

9. A small amount of intravascular bubbles is not an uncommon gross finding in fresh or very fresh stranded cetaceans showing a gas composition of 70% nitrogen and 30% CO_2. This observation is highly consistent with physiological "*in vivo silent bubbles*", more frequently observed in stranded deep divers. This may also be an evidence of predisposition of these species to suffer from decompression, attending to our results.

10. At necropsy, quantity of bubbles in decomposition codes 1 and 2 stranded cetaceans is more important than the merely presence versus absence of bubbles. High amount and widely distributed intravascular gas bubbles in these animals with gas composition higher than 70% nitrogen and around 20% CO_2 would be related to "*antemortem*" bubble formation / growth involved in physiopathological processes.

11. Gas analysis as a single diagnostic test is not a conclusive diagnosis for Decompression like Sickness in stranded cetaceans, but may contribute complementarily with other data obtained by imaging analytical techniques, a systematic necropsy, histopathology, microbiology, toxicology and other possible future analyses to reach a definitive diagnosis of decompression disease.

6 SUMMARY

A new pathological entity named "Gas Bubble Disease" or “Decompression like Sickness" was described in stranded beaked whales linked to military sonar by our research group. Attempts have been made to analyze the gas produced during decompression, using a wide variety of methods in humans and experimental animal pathology but not, so far, in cetaceans. However, appropriate and accurate measurement of respiratory gases while avoiding atmospheric air is difficult, and the peculiar circumstances of cetacean strandings and *in situ* necropsies make this goal even more difficult.

In this direction, this thesis addresses generically “what” (gas analysis) and “how” (gas sampling and storing) addressing the following specific objectives:

To develop and standardize an accurate and handy feasible methodoly that enables gas analysis and sampling for field necropsy of stranded cetaceans. To obtain experimentally in rabbits referenced guideline data (presence, amount and analysis) of intravascular gas bubbles generated either “*in vivo*” (compression / decompression or iatrogenic venous gas embolism) and “*postmortem*” (putrefaction model). To use this gas analysis for diagnosis of gas embolic related pathologies in stranded cetaceans.

In the present thesis, we have developed, implemented and standardized through laboratory validations, a handy feasible methodology than enables gas sampling during *in situ* necropsies, as well as their storage and transport in vaccum tubes with non-statistical significant changes in gas composition for their final analysis in the laboratory.

Based on our rabbit experimental models a semi-quantitative method has been established to evaluate the presence and abundance of intravascular and tissular gas in carcasses during necropsy with forensic aim.

During necropsy of the rabbits (with decomposition codes 1 and 2) of the putrefaction experimental model, no atmospheric air was found to enter into vessels as a result of dissection. In codes 3, 4 and 5 a statistic significant lineal relationship was found between putrefaction and presence and quantity of gas.

Massive presence of gas within the cardiovascular system of rabbits with decomposition codes 1 and 2 in our experimental models should be interpreted as a systemic "in vivo" gas embolism. Rabbits dying during or after compression and decompression showed a higher quantity and wider distribution of gas within the vascular system involving subcutaneous, femoral, cava, mesenteric, coronary veins as well as heart cavities compared to rabbits which died due to experimental air embolism.

Putrefaction gases in rabbits were composed of presence of hydrogen and / or high levels of CO2, low concentration of nitrogen (mostly lower than 40%) and very small quantities of oxygen when present. CH4 and SH2 were randomly present in trace levels.

Gas composition from samples obtained in codes 1 and 2 rabbits from air embolism and decompression experiments were very similar being composed of 70%-80% Nitrogen and 20%-30% CO2, and therefore quite difficult to make a difference.

The presence of bubbles detected within the cardiovascular system and tissues during the necropsy of stranded cetaceans is a common finding related to "*in vivo* and / or *postmortem*" process.

There is a direct relationship between decomposition codes and increasing amount of bubbles. *Postmortem* processes were analytically related to the presence of hydrogen and/or high levels of CO_2 as demonstrated in the rabbit experimental models. To try to avoid these putrefactive masking gases, necropsy and gas sampling must be performed as

soon as possible, before 24 hours *PM* as recommendation but preferably within 12 hours *PM*.

A small amount of intravascular bubbles is not an uncommon gross finding in fresh or very fresh stranded cetaceans showing a gas composition of 70% Nitrogen and 30% C02. This observation is highly consistent with physiological *"in vivo* silent bubbles", more frequently observed in stranded deep divers. This may also be an evidence of predisposition of these species to suffer from decompression, attending to our results.

At necropsy, quantity of bubbles in decomposition codes 1 and 2 stranded cetaceans is more important than the merely presence versus absence of bubbles. High amount and widely distributed intravascular gas bubbles in these animals with gas composition of around 70% Nitrogen and 30% CO2 would be related to "*antemortem"* bubble formation / growth involved in physiopathological processes.

Gas analysis is not a conclusive diagnosis for DC like Sickness in stranded cetaceans, but may contribute complementarily with other data obtained by imaging analytical techniques, a systematic necropsy, histopathology, microbiology, toxicology and other possible future analyses to reach a definitive diagnosis of decompression disease.

7 RESUMEN EXTENDIDO

7.1 INTRODUCCIÓN

La preocupación sobre los posibles efectos o impactos del sonido de origen antropogénico en el medio marino ha ido en aumento en los últimos años, provocando resoluciones por parte de distintos organismos, siendo probablemente la del Parlamento europeo (2004) una de las más significativas.

Esta resolución (no vinculante) anima, a sus estados miembros, a adoptar una moratoria para el uso de los sónares activos de alta frecuencia hasta que se realice una evaluación global del impacto ambiental acumulativo sobre los mamíferos marinos, peces u otros organismo marinos (European-Parliament, 2004).

A consecuencia de ello, España se comprometió, en el congreso de los diputados (2004a), a instaurar una moratoria en régimen de restricción en las aguas territoriales españolas y en el nivel de recomendación en las aguas internacionales. La moratoria adoptada por España consiste en la prohibición absoluta de maniobras militares en la zona oriental de las Islas Canarias, prohibición de sónares de cualquier frecuencia, y no más cerca de 50 millas de las aguas de jurisdicción.

Una de las causas que conllevó a la adopción de esta moratoria fueron los varamientos masivos atípicos (varamientos que implican a más de 2 animales excluyendo madre y cría, en ocasiones de diversas especies y que llegan a una misma costa dispersados en un período corto de tiempo) de zifios relacionados con maniobras militares, donde el elemento común es el uso de sónar antisubmarino. Los zifios (familia *Ziphiidae*) son las especies de cetáceos que más varan bajo estas circunstancias.

Los varamientos masivos de zifios no se han referenciado con anterioridad al año 1963 (época a partir de la cual se empezó a desarrollar la tecnología del sónar antisubmarino). Desde entonces, se han sucedido varios varamientos masivos de zifios en distintas localizaciones geográficas como Bonnarie 1974, Canarias 1985, 1988, 1989, 2002, Grecia 1996 y Bahamas 2000. Teniendo todas ellas en común la relación espacial y temporal con maniobras militares (Cox et al., 2006).

En los casos anteriores a Bahamas no se realizó ningún tipo de estudio patológico, con el objetivo de estudiar la causa de la muerte y/o varamiento, en los cetáceos varados. En el caso de Bahamas, se realizó un estudio parcial y se concluyó como diagnóstico un trauma acústico, siendo la única hipótesis que se barajaba hasta el varamiento de Canarias de 2002.

Los resultados sobres los estudios patológicos completos, llevados a cabo sobre el varamiento masivo atípico de zifios que tuvo lugar en Fuerteventura en el año 2002, dieron lugar a una hipótesis alternativa, pero no exclusiva que explicaría la relación entre las actividades militares con uso de sónar y los varamientos de zifios. Se demostró la presencia de lesiones compatibles con burbujas, sugiriéndose un mecanismo similar al de la enfermedad descompresiva como posible causa de las mismas (Fernandez et al., 2005; Jepson et al., 2003).

La nueva entidad patológica denominada “Gas Bubble disease” (enfermedad de las burbujas) o “Decompression like Sickness” (enfermedad similar a la descompresiva), fue ampliamente discutida en un Workshop específico con la participación de reconocidos expertos en las distintas materias relacionadas (Policy on sound and marine mammals, 2004b). Una de las conclusiones de este Workshop fue que la enfermedad de las burbujas es un mecanismo patológico posible, que explicaría la mortandad de cetáceos asociada a ejercicios militares con uso de sónar y, por tanto, era necesario iniciar líneas de investigación al respecto.

Se propusieron varios mecanismos que pudieran inducir directa o indirectamente la enfermedad de las burbujas (Cox et al., 2006), la mayoría de ellos relacionados con una alteración causada por una señal acústica que pudiera:

A. Provocar una respuesta en el animal, rompiendo su perfil de buceo favoreciendo la acumulación de nitrógeno en tejidos, y aumentando por ello, el riesgo de sufrir una enfermedad descompresiva.

B. Activar micronúcleos gaseosos pre-existentes que crecerían por difusión pasiva.

C. Favorecer el crecimiento de micronúcleos gaseosos pre-existentes por difusión rectificada.

Entre estas posibles causas se destacó, en particular, la hipótesis de que la señal acústica provocara un cambio comportamental del animal, que podría dar lugar a la formación de burbujas de gas, causando daños en múltiples órganos o interfiriendo con su normal fisiología (Cox et al., 2006).

Los últimos hallazgos sobre los perfiles de buceo en algunas especies de zifios demuestran que estos animales realizan inmersiones mucho más extremas que otras especies. Éstas se caracterizan por su gran profundidad de inmersión (hasta 2000 m y durante 90 min), una velocidad lenta de ascenso, seguida por unas inmersiones de menos profundidad (100-400m) llamadas inmersiones de amortiguación (Bounce dives) (Hooker and Baird, 1999; Tyack et al., 2006).

Se considera que unas alteraciones en estos perfiles de buceo tan extremos podría conllevar una excesiva acumulación de nitrógeno en tejidos, favoreciendo el crecimiento de las burbujas de manera muy similar a la enfermedad descompresiva (Cox et al., 2006).

Sin embargo, la descripción de esta enfermedad similar a la descompresiva en cetáceos, ha sido hasta la fecha objeto de una intensa y controvertida discusión científica, sugiriéndose la realización del análisis del gas para justificar estas lesiones desde un punto de vista diagnóstico (Piantadosi and Thalmann, 2004).

Las aguas de las Islas Canarias constituyen una de las regiones con mayor riqueza y diversidad del Atlántico nororiental, habiéndose citado 28 especies diferentes de cetáceos, de los cuales 21 son especies de odontocetes y 7 de misticetos. De estas 28 especies, al menos 26 han varado en las costas de las Islas Canarias (Martin et al., 2009).

Esta aguas son un área de extremado valor natural debido a su situación estratégica en la ruta de muchas especies migratorias y a sus particularidades oceanográficas (temperaturas, grandes profundidades cerca de la costa al carecer de plataforma continental, abundantes cefalópodos, zona de calmas en el sur-sureste insular, etc.). Todo ello ha dado lugar al establecimiento de poblaciones residentes de cetáceos como el delfín mular (*Tursiops truncatus*), calderón tropical (*Globicephala macrorhynchus*), calderón gris (*Grampus griseus*), cachalotes (*Physeter macrocephalus*), zifio de Cuvier (*Ziphius cavirostris*) y el zifio de Blainville (*Mesoplodon densirostris*).

Esta alta riqueza en especies, incluyendo cetáceos de buceo profundo y superficial, hace de las Islas Canarias un laboratorio natural inmejorable para el estudio del embolismo gaseoso en cetáceos con distintos perfiles de buceo.

Para abordar la problemática del análisis del gas en cetáceos se requiere abordar los siguientes objetivos:

1. Desarrollar una metodología estandarizada, precisa y práctica, que permita el análisis y muestro del gas de cetáceos varados.

2. Obtener unos valores de referencia (en cuanto a presencia, abundancia y composición) de gas intravascular generado por procesos "*in vivo*" (como la descompresión o el embolismo aéreo iatrogénico) y *postmortmen* (putrefacción).

3. Utilizar el análisis del gas para diagnosticar patologías embólicas gaseosas en cetáceos varados.

7.2 CAPÍTULO II: DESARROLLO DE METODOLOGÍA PARA EL ESTUDIO DEL EMBOLISMO GASEOSO

La cromatografía gaseosa es una técnica válida para distinguir entre los gases de putrefacción y los gases por aeroembolismo (Pierucci and Gherson, 1968; Pierucci and Gherson, 1969), por ello ha sido utilizada con este fin en medicina forense humana (Bajanowski et al., 1998).

Asimismo, se han realizado varios intentos mediante diversos métodos para analizar los gases producidos por descompresión (Armstrong, 1939; Bert, 1878; Harris et al., 1945; Ishiyama, 1983; Lillo et al., 1992; Smith-Sivertsen, 1976). Sin embargo, esto nunca se había realizado antes en cetáceos.

El mayor obstáculo que suponen los varamientos al análisis gaseoso es precisamente el contexto en el que se engloban los mismos. En numerosas ocasiones, los cetáceos varan en costas de difícil acceso, por lo que la necropsia se realiza "*in situ*". De aquí se deriva uno de los mayores problemas, o se desarrolla una metodología que permita el análisis *in situ* e instantáneo de las muestras, o hay que almacenarlas y transportarlas.

El análisis de la composición química de estas muestras de gases se debe realizar mediante el empleo de la Cromatografía de Gases (CG). Si bien existen cromatógrafos portátiles que permitirían el análisis de las muestras "in situ", esta opción resulta inviable si pensamos que, por la naturaleza de estos gases, éstos deben ser analizados mediante detección por ionización a la llama (FID). En efecto, la respuesta de hidrocarburos de bajo peso molecular o moléculas orgánicas simples, es muchísimo más intensa en este tipo de detectores que en el detector convencional que incorpora el cromatógrafo de gases portátil.

El tipo de detector convencional, no destructivo y universal, que tienen estos equipos, como detector único, es uno que se basa en la disminución de la temperatura de un filamento caliente de tungsteno. Ese enfriamiento se transforma en una señal eléctrica gracias al concurso de un termopar. Dicho detector se denomina detector de conductividad térmica (TCD). La situación óptima para el cromatógrafo a emplear en el procesado de las muestras directamente en la zona de varamiento, sería la que corresponde con un equipo que presente, la combinación en serie de dos detectores, un TCD no destructivo y, posteriormente, un FID destructivo.

El primero de los detectores es eficaz a la hora de recoger las señales correspondientes a los gases permanentes que no dan respuesta en el FID; y, el segundo, sería eficaz para la detección de aquellos hidrocarburos de bajo peso molecular que se pueden producir en función del tiempo de descomposición. El principal problema de este equipo es que necesita como combustible para alimentar la llama del FID, hidrógeno. Este gas no puede transportarse a las zonas de varamiento por motivos de seguridad.

En consecuencia, se debe disponer de una metodología que permita un traslado riguroso de las muestras desde la zona de varamiento hasta el laboratorio donde efectuar el análisis. La metodología que se propone en este trabajo de Tesis Doctoral es original y fundamentalmente es sencilla. La estrategia estriba en utilizar dispositivos de recogida de muestras que no supongan grandes complicaciones logísticas para su traslado, téngase en cuenta que, en algunas ocasiones, la localización de los varamientos, resulta inaccesible desde el punto de vista orográfico.

Fig 7.1: Intentando localizar el animal varado en un acantilado en la costa norte de Tenerife (A). Traslado del material por la costa rocosa hasta el lugar del varamiento para realizar la necropsia in situ (B).

Por tanto, la metodología debe cumplir con dos aspectos fundamentales: sencillez y rigor. Para establecerla es necesario conocer la ubicación y la morfología de las muestras gaseosas en el cetáceo varado.

Se pueden distinguir tres tipos de muestras susceptibles de ser analizadas: unas en las oquedades corporales (tubo digestivo, senos pterigoideos…); burbujas en el sistema venoso que por su tamaño permitan su extracción mediante una jeringa adecuada, (generalmente esto es posible sólo en los vasos de mayor calibre, ya que los de menos calibre se colapsan rápidamente); y, gases del interior del corazón para cuya extracción es necesario tener un sistema que nos separe el gas (no disuelto en forma de burbujas) de la sangre.

Se necesita, pues, de un sistema de extracción de las muestras gaseosas diverso, y además es necesario utilizar un sistema para el transporte de las mismas desde el lugar donde se han tomado hasta el laboratorio para el posterior análisis. Este sistema de almacenaje temporal debe garantizar la estanqueidad suficiente como para que la muestra no sufra ningún tipo de pérdida.

De todos los sistemas, con mayor o menor estanqueidad, que se investigaron, el que se eligió por su sencillez y menor coste, fue el de los tubos vacutainer. Básicamente son tubos de vidrio no rompible, a los que se les realiza un vacío en su interior gracias al cual se extrae la sangre en medicina clínica.

Los vacutainer son los recipientes que se usaron para el traslado con independencia de la metodología que se utilice en la toma de muestras.

Fig 7.1: Varios vacutainers utilizados comúnmente en medicina clínica, con distintos aditivos identificados con su correspondiente color en el tapón

Esta decisión tuvo que refrendarse con una serie de experimentos encaminados a ver el grado de fiabilidad de estos tubos en cuanto a la pérdida de material muestral (por difusión) a lo largo del tiempo y en función de la temperatura. Además, se probaron diferentes tipos de vacutainers, con o sin aditivos. Los estudios realizados para estos tubos con inyección de un volumen conocido (1 mL) de aire atmosférico, demuestran que las pérdidas por difusión no llegan al 1% por día en volumen. Este resultado se obtuvo mediante el cálculo de un modelo de regresión con una $R^2 = 0,944$ ($P < 0,001$).

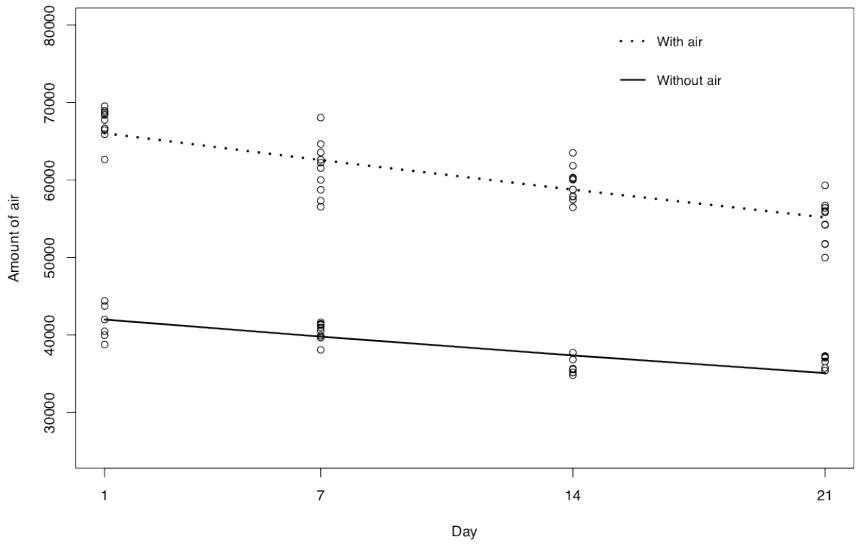

Fig 7.2: Contenido de aire (eje de ordenadas) de los vacutainer a los días 1, 7 , 14 y 21 (eje de abscisas) para los dos tipos de vacutainer 5 mL sin aditivos (línea contínua) y 3,5 mL con aditivos (línea discontinua).

En cuanto a la temperatura de conservación se demuestra que someter los tubos vacutainer a las temperaturas de los congeladores hace que se produzca un aumento en la señal del aire, debido a la diferencia de los coeficientes de dilatación del sello de caucho y del material del tubo. Esas diferencias provocan la incorporación de aire desde el exterior al vacutainer, perdiéndose el vacío y equilibrándose las presiones interna y externa.

Se hizo un estudio sobre la reutilización de los vacutainer para ello se sometió un mismo vacutainer a sucesivos pinchazos encontrándose un incremento en las señales por incorporación de aire, con independencia de la temperatura de conservación del tubo, pero viéndose más afectado los tubos conservados a temperatura de congelación.

Finalmente, los estudios de difusión realizados sobre diferentes gases demuestran un comportamiento similar en todos ellos en función del tiempo.

Por último, no se encontraron diferencias significativas en el contenido de las muestras recogidas en los tubos cuando se trasladaron en avión. (P= 0,137 para el oxígeno y P= 0,056 para el nitrógeno).

En resumen, se puede validar los vacutainer como procedimiento de conservación temporal de las muestras hasta la llegada al laboratorio, dentro del intervalo de confianza considerado (95%), si se cumple con los siguientes requisitos:

Disponer de varios vaccutainer para muestras y blancos.

Someter todos los vacutainer a idénticas condiciones durante el traslado.

No demorar el análisis más tiempo del necesario, recuérdese que hay una pérdida de menos de un 1% de material en volumen por día.

Conservar en condiciones de temperatura ambiente o en refrigeración moderada.

Tal y como se mencionó al principio de este resumen, las muestras pueden ser tomadas de tres formas, mediante aplicación directa del vacutainer, con jeringa o mediante un sistema que nos separe el gas de la sangre. Para este último, se necesita de un dispositivo de recogida basado en el desplazamiento del gas a través de un medio continuo (agua) , por aplicación de un gradiente de presión.

Uno de los sistemas que se utiliza para la recogida de burbujas en vasos es mediante jeringas especiales provistas de sistema de bloqueo que se usan con mucha frecuencia en la inyección de muestras gaseosas, a través de los sistemas Split-splitless de los cromatógrafos de gases. Este tipo de jeringas garantizan estanqueidad, gracias al sistema de bloqueo, pero incorporan un elevado grado de sofisticación en cuanto al cuidado que se debe tener con ellas, y su elevado costo. Además, en el proceso de extracción de las muestras gaseosas es factible incorporar en la jeringa algo de fluido sanguíneo que obligaría a una limpieza del émbolo de la jeringa antes de continuar, y que pudiera dar lugar al deterioro de la jeringa (específica para muestras gaseosas), o bien a la contaminación cruzada. La metodología que se desarrolla en este trabajo, propone en su lugar el uso de jeringas de insulina de un solo uso validado previamente mediante la realización de diferentes ensayos.

Fig 7.3: Jeringa desechable de insulina.

El primero de los ensayos de validación consistió en inyectar diferentes volúmenes de aire en el interior de los tubos vacutainer mediante esta jeringa y analizar posteriormente su contenido mediante cromatografía. Se obtuvo una ajuste por regresión de R^2= 0,99594. Esto demostró que este sistema de toma de muestras es muy sensible y exacto en relación con el volumen medido en ella.

Además no se observaron diferencias significativas ni para el oxígeno (P = 0,336) ni para el nitrógeno (P = 0,337) del aire de fondo (background) de la jeringa. Esto significa que la jeringa de insulina no incrementa el contenido de aire del background de esta metodología.

Para las muestras de gases contenidas en las cavidades de los animales varados se utiliza un dispositivo denominado Aspirómetro que nos permite separar el gas (no disuelto en forma de burbujas) de la sangre.

El aspirómetro fue desarrollado por Dyrenfurth (Dyrenfurth, 1928), pero nosotros lo hemos modificado para que se adapte de una manera más eficiente a las condiciones de campo en la que se encuentran los animales varados, y recogida de la muestra. Las principales modificaciones fueron: Minimización del tamaño y eliminación de los ángulos muertos para evitar las pérdidas del volumen de gas recogido.

La idea que subyace en el aspirómetro es presentar una barrera física que permita separar la sangre que inevitablemente va a contaminar las muestras de gases que se tomen.

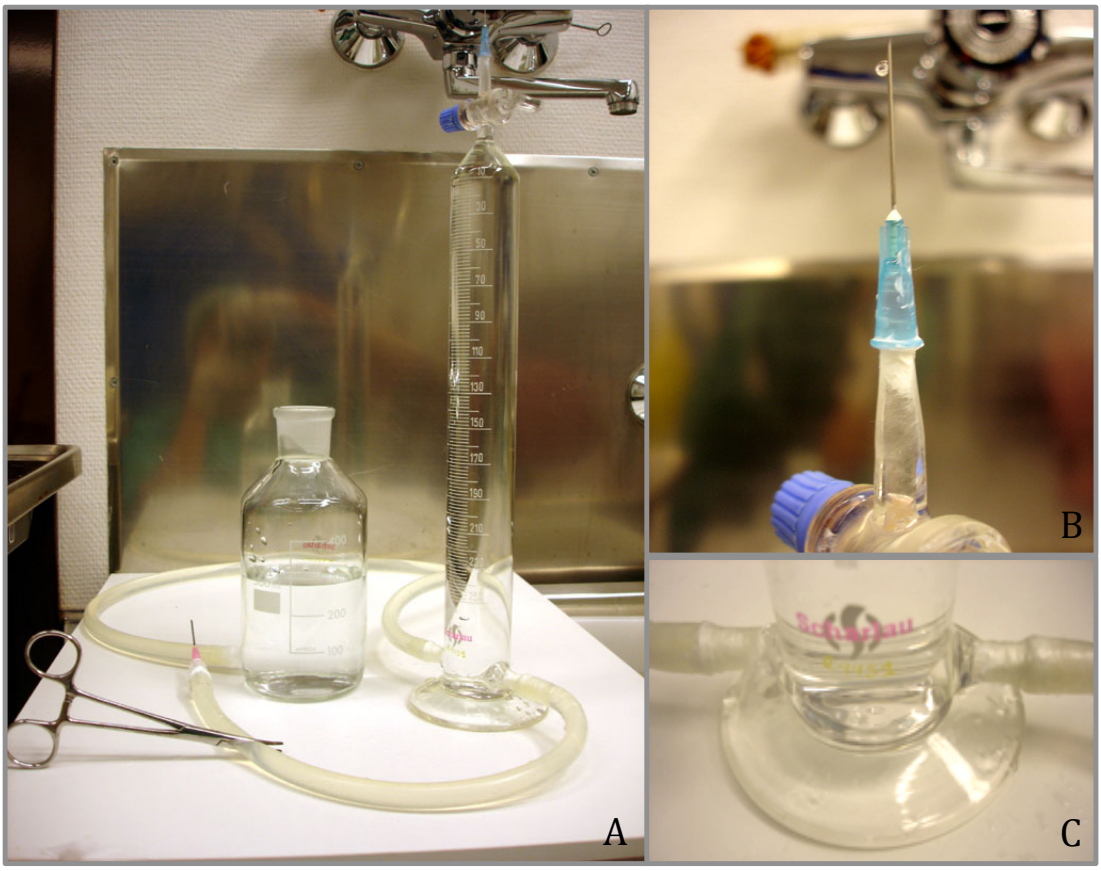

Fig 7.4: Aspirómetro (A9, detalle del sellado con silicona en la bureta de gases invertida junto con la aguja (B), y de los tubos con el espirómetro (C).

La validación de este dispositivo se realizó comparando la recogida de un volumen conocido de muestra simulada de aire o de gas estándar, a través de este sistema, con la inyección directa a los tubos vacutainer. Analizando los gases recogidos en la parte superior del aspirómetro y efectuando la correspondiente estadística a las señales obtenidas en el cromatógrafo se encontró que el líquido que se utiliza en el aspirómetro juega un papel importante desde el punto de vista de la composición del gas recolectado en la parte superior, comparando esta composición con la correspondiente a la que se recoge directamente desde los tubos vacutainer. Aemás, estas experiencias se realizaron también usando una disolución de NaCl al 20% a pH 4, en vez de agua, tal y como habían descrito algunos autores (Pierucci and Gherson, 1968). Se observó un incremento en la señal de oxígeno y nitrógeno, y una disminución

en la señal de dióxido de carbono. Este incremento se puede observar claramente en la Tabla siguiente donde se compara el pinchazo de 1 mL de H_2 o de CO_2 a través del aspirómetro con el pinchazo directo del mismo volumen al tubo vacutainer.

Además la tabla recoge las señales correspondientes al empleo de agua destilada de una disolución salina de NaCl al 20% en peso y ajustada a pH 4. También, se aprecia el aumento provocado en la señal del oxígeno y nitrógeno del gas recogido en la parte superior aspirómetro con respecto a la señal que le corresponde a 1 mL del gas inyectado al tubo vacutainer, respectivamente, subíndices "asp" y "ctrl". Por el contrario, la señal correspondiente al CO_2 y procedente del gas recogido en el aspirómetro experimenta una disminución con respecto a la inyección en el tubo vacutainer.

Tabla 7.1: mL y unidades de area (u.á.) de H2 y CO_2 junto con su contenido residual de O2 y N2 recuperados desde el aspirómetro cuando se fuerza 1 mL de H2 o de CO2 puro a pasar por el líquido barrera con el que está relleno el aspirómetro comparado con la inyección directa de 1 mL de estos mismos gases en los vacutainers.

H_2 agua destilada	ml recogidos	H_2 (u.á.)	O_2 (H_2) (u.á.)	N_2 (H_2) (u.á.)
med_{asp}	1,1 (2.5E-08)	293,10	4338,80	14982,70
med_{ctrl}	1	245,50	3042,40	11193,90
med_{asp} - med_{ctrl}	+ 0.1	47,60	1296,40	3788,80
med_{ctrl} / med_{asp}	0.91	0,84	0,70	0,75
CO_2 agua destilada	ml recogidos	CO_2 (u.á.)	O_2 (CO_2) (u.á.)	N_2 (CO_2) (u.á.)
medasp	0,64	2688,20	3924,20	14163,70
medctrl (SE)	1	6505,95	2881,40	10347,05
medasp - medctrl	-0,36	-3817,75	1042,80	3816,65
medctrl / medasp	1,56	2,42	0,73	0,73
CO_2 solución salina	ml recogidos	CO_2 (u.á.)	O_2 (CO_2) (u.á.)	N_2 (CO_2) (u.á.)
medasp	1	5868,7	3308,45	11646,6
medctrl (SE)	1	6505,95	2881,40	10347,05
medasp - medctrl	0,00	-637,25	427,05	1299,55
medctrl / medasp	1,00	1,11	0,87	0,89

Aplicando a estas observaciones un análisis estadístico es posible establecer una serie de factores de corrección al aspirómetro debido a la interacción del gas recolectado cuando se hace pasar por agua destilada. Estos factores de corrección no son muy diferentes de la unidad para el caso del H_2, O_2 y N_2. Además, el empleo de la disolución salina de NaCl al 20% en peso y a pH 4, acerca los factores de conversión a la unidad. Otra de las consideraciones que hay que realizar es que el incremento que aparece en las señales de O_2 y N_2 cuando se inyecta H_2 o CO_2 es muy similar, lo que está relacionado con un fenómeno de arrastre del gas inyectado sobre el que está previamente disuelto en el agua destilada. En otras palabras, el incremento en la señal es prácticamente independiente de la naturaleza química del gas y la aportación es prácticamente igual para todos.

No obstante, la señal del CO_2 experimenta una interesante disminución debido fundamentalmente a que este gas interacciona fuertemente con el agua solubilizándose de forma apreciable. El factor de corrección a aplicar sería de 2,42 de acuerdo con el análisis estadístico utilizado. Es decir, para corregir la señal del CO_2 medido a partir de una muestra en el aspirómetro, la señal la debemos multiplicar por dicho factor.

Con objeto de averiguar a qué se debe ese valor desde el punto de vista estadístico, se intentó aplicar un modelo basado en un balance de materia al CO_2 a su paso por el aspirómetro, suponiendo en este modelo que se tiene agua destilada como líquido de relleno, y suponiendo que el CO_2 cumple en las condiciones ambientales de recogida la Ley de Henry.

$$\frac{C_{O_2}^{aq}}{C_{O_2}^{g}} = K_{H,c}^{O_2} \cdot RT$$

$$\frac{C_{O_2}^{aq}}{C_{O_2}^{g}} = 0.0013\left(\frac{mol}{atm \cdot L}\right) \cdot 0.082\left(\frac{atm \cdot L}{K \cdot mol}\right) \cdot 298.15(K) = 0.0318 \qquad (7.1)$$

Aplicando estas ecuaciones al CO2, se aprecia un factor de corrección, $1 + K_{H,c}^{i} RT$, a la temperatura de 298,15 K de 1,82. Este factor es capaz de explicar el 75% del que se obtiene a partir de la estadística. La explicación de esta desavenencia debe encontrarse

en que además de la solubilización por la Ley de Henry, este gas experimenta una serie de equilibrios químicos tipo ácido-base con el agua:

$$CO_2(g) + H_2O \rightleftharpoons H_2CO_3(aq)$$
$$H_2CO_3(aq) + H_2O \rightleftharpoons HCO_3^-(aq) + H_3O^+(aq) \quad (7.2)$$

Estos equilibrios hacen que el valor de la corrección a aplicar aumente.

Cuando se utiliza la disolución acuosa de NaCl al 20% en peso y a pH 4 se minimiza drásticamente este factor, siendo prácticamente idéntica la recogida en el aspirómetro comparada con la del tubo vacutainer. No obstante, el empleo de este líquido, más viscoso que el agua destilada, plantea inconvenientes de recogida de gases "in situ" sobre todo cuando se incorpora restos de sangre junto con el gas recogido, produciéndose obstrucciones que dificultan la llegada del gas a la parte superior del aspirómetro.

Las señales se han medido en unidades de cuenta de área usando para ello un cromatógrafo de gases con dos detectores en serie: uno de ellos no destructivo de, TCD; y el otro destructivo, FID. El cromatógrafo utilizado estaba provisto de un sistema de dos columnas (tándem) formado por una columna capilar con una fase estacionaria de tamiz molecular (MolSieve 5A), muy útil para la separación de gases permanentes, y sobre todo para la resolución óptima de los gases del aire (O_2 y N_2). La otra columna capilar presenta una fase estacionaria polar denominada Porabond Q óptima para la separación de CO2 y de hidrocarburos de pequeño peso molecular.

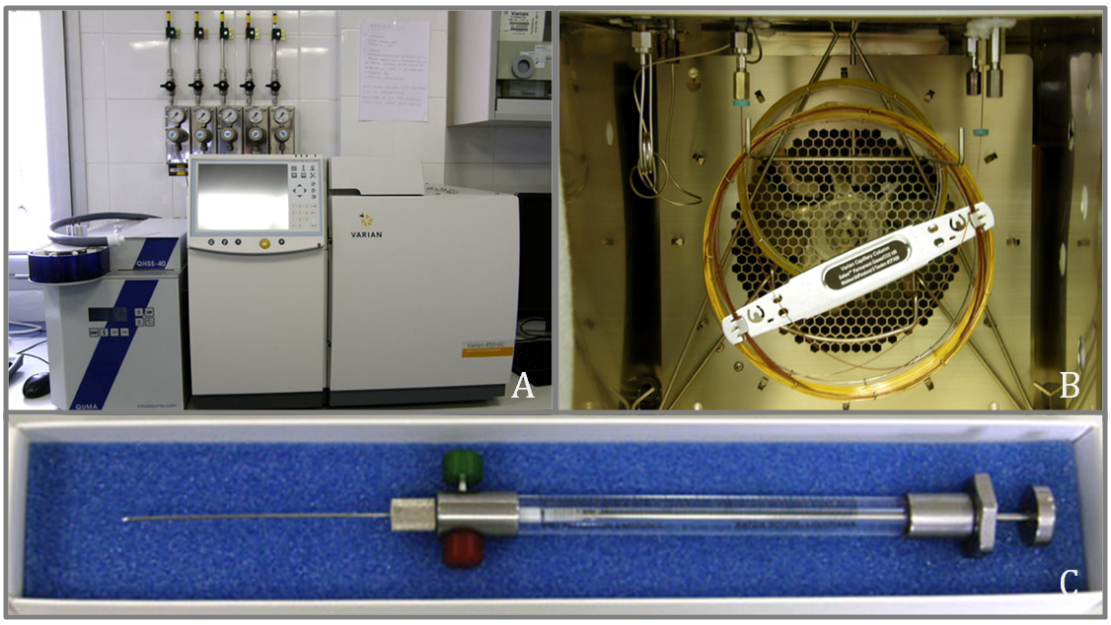

Fig 7.5: Cromatógrafo de gases (A), Columna tandem (B), jeringa de inyección manual para gases (C).

Se ha usado como herramienta de calibración, para evaluar las fracciones molares, la curva de calibrado. Y los límites de detección se estimaron usando la propuesta de Kaiser (1947).

En resumen, proponemos las siguientes metódicas:

- Gas de cavidades. Empleo directo de Vacutainer de 5 mL provisto con su adaptador plástico y una aguja de doble terminación. El gas recolectado se transfiere de forma directa a los tubos de vacutainer. Para evitar al aire atmosférico procedente de la cavidad, se introduce primero la aguja en la cavidad (purgándose) y luego se acopla el vacutainer. El vacutainer con la muestra recolectada debe retirarse antes de extraer la aguja de la cavidad con el mismo fin. Se necesitan varios tubos vacíos a modo de blancos.

- Gas procedente de burbujas subcutáneas. Empleo directo de la jeringa de insulina, y transferencia de las burbujas recolectadas a los tubos vacutainer.

Empleo de una jeringa nueva para cada burbuja y de un vacutainer único para cada burbuja. Se necesitan varios tubos vacíos a modo de blancos.

- Gas procedente de la cavidad cardiaca. Aquí se hace necesario el empleo del aspirómetro para separar la sangre del gas recolectado. Utilizaremos agua destilado como líquido barrera. Para evitar la intrusión de aire procedente de la cavidad pericárdica, ésta se rellenará así mismo con agua destilada. Una vez que el gas se ha recogido en la parte superior del aspirómetro (bureta invertida) se procede a inyectar ahí el vacutainer, abriéndose simultáneamente la llave de la bureta.

- Las muestras se transportan al laboratorio en los vacutainer y se almacenan a temperatura ambiente, intentando que el período de almacenaje no supere el día.

- El mínimo de blancos debe ser de 3 para realizar posteriormente la corrección que corresponda.

- El análisis de las muestras se realiza en un cromatógrafo de gases con dos detectores en serie: Uno universal, no destructivo, TCD; y otro de ionización a la llama para analizar la posible presencia de hidrocarburos de pequeño peso molecular. El cromatógrafo tiene que usar un sistema doble de columnas en tándem de forma que se puedan separar simultáneamente los gases permanentes en una de ellas; y los hidrocarburos y el CO2 en la otra. Las muestras se inyectan desde el vacutainer mediante microjeringas específicas para muestras gaseosas, con sistema de bloqueo.

- El límite de detección se obtiene a partir de la media de las señales de los blancos aplicando el criterio de Kaiser.

7.3 CAPÍTULO III: MODELOS EXPERIMENTALES EN EMBOLISMO GASEOSO

El embolismo gaseoso es la presencia de gas en el sistema circulatorio. Cuando está en el sistema venoso se llama embolismo gaseoso venoso, y puede deberse a distintas causas, como accidentes quirúrgicos (Muth and Shank, 2000), trauma, intervenciones criminales, barotraumas (Knight, 1996) o por separación de la fase gaseosa de los tejidos por descompresión (Hamilton and Thalmann, 2003). Con respecto a este último caso, hay que destacar que la cantidad de embolismo gaseoso venoso, evaluado por técnicas de ultrasonido, está estadísticamente correlacionado con la enfermedad descompresiva (Sawatzky, 1991).

Cuando el origen del gas es aire atmosférico, como sucede en casos de trauma o intervenciones criminales, lo denominaremos "aeroembolismo". Este tipo de embolismo gaseoso ha sido de especial interés en la medicina forense dado su alto carácter iatrogénico (Knight, 1996). Quizás por ello podemos encontrar desde estudios en animales de laboratorio, intentando distinguir los gases de la putrefacción del aeroembolismo, mediante análisis de su composición química, hasta su aplicación directa en medicina forense (Bajanowski et al., 1998; Keil et al., 1980; Pierucci and Gherson, 1968; Pierucci and Gherson, 1969).

Por el contrario, si bien se sugirió el análisis de gas como método diagnóstico para la enfermedad descompresiva, esta técnica no se utiliza normalmente en medicina forense. Es más, son muy pocas las publicaciones con datos (obtenidos mediante distintos métodos) de análisis de gases producidos durante la descompresión (Armstrong, 1939; Bert, 1878; Harris et al., 1945; Ishiyama, 1983; Lillo et al., 1992; Smith-Sivertsen, 1976). A esto se le suma la amplia diversidad de la metodología empleada, tipo de modelo animal, tipo de tratamiento (hiperbárico, hipobárico, tiempo de exposición, tiempo de descompresión, etc.) y momento de recogida de los gases (vivo/muerto y horas post-mortem).

Dadas las pocas referencias en humana y/o animales de experimentación, su variabilidad y la ausencia total de datos similares en cetáceos, nos propusimos evaluar en modelos experimentales, aplicando la metodología desarrollada en el capítulo II, 3 tratamientos: putrefacción experimental, inducción del aeroembolismo e inducción de la enfermedad descompresiva.

Un total de 41 conejos blancos neozelandeses, de género masculino y el mismo peso y edad, subdividos en 3 grupos, fueron sometidos a los distintos tratamientos. Todos los tratamientos recibidos fueron bajo anestesia profunda y los distintos protocolos fueron aprobados por los pertinentes comités éticos.

Los tratamientos consistieron es:

1. Putrefacción experimental. Los animales fueron primeramente anestesiados y posteriormente eutanasiados. Se les realizó una necropsia reglada a distintos intervalos de tiempo *post-mortem* (PM), desde inmediatamente después de la muerte hasta las 67 horas PM, donde se recogieron muestras de gas.

2. Aeroembolismo. Se les inyectó 2,2 mL/min de aire hasta causarles la muerte, y se realizaron necropsias regladas a los mismos intervalos de tiempo que en el modelo de putrefacción experimental.

3. Hiperbárico. Los animales fuero sometidos a 8 atmósferas absolutas de presión (el equivalente a 70 metros bajo el agua aproximadamente) durante 45 minutos y fueron descomprimidos rápidamente (0,33m/s). Este tratamiento agresivo, tenía por objetivo inducir una enfermedad descompresiva explosiva. Una vez fuera de la cámara hiperbárica, se midió el grado de burbujas *in vivo* mediante la técnica del ultrasonido. Las burbujas se observaron como puntos brillantes dentro de la arteria pulmonar. La escala utilizada fue la publicada por Eftedal y Brubakk (1997).

Los animales que no fallecieron por el tratamiento fueron sacrificados transcurrida una hora desde la descompresión. Finalmente, se realizaron necropsias regladas a los mismos tiempos utilizados en los experimentos anteriores. Este último modelo experimental fue realizado en la Universidad Noruega de Ciencia y Tecnología (NTNU), Trondheim, con la colaboración y asesoramiento del grupo de medicina hiperbárica de la misma.

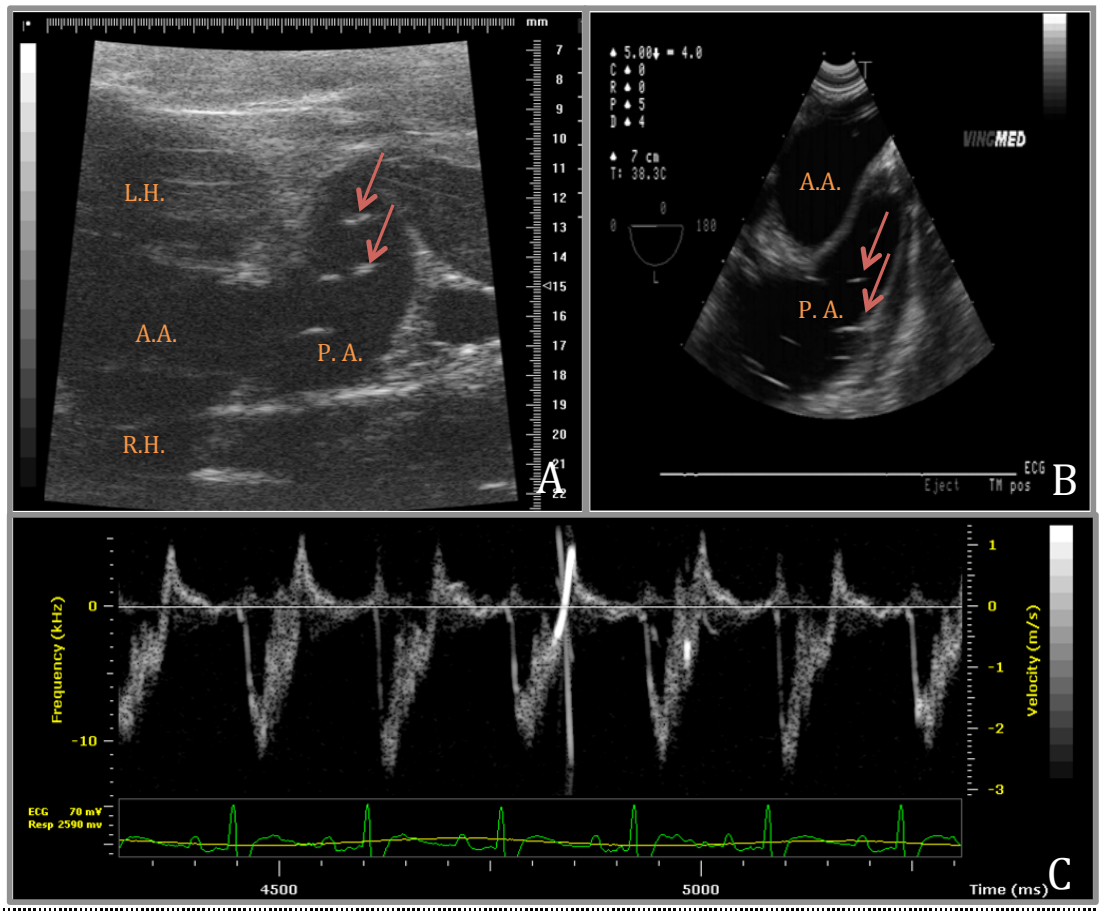

Fig. 7.6: Imágenes de ultrasonido obtenidas en corazón de ratas (utilizadas a modo de ejemplo) con una escala de embolismo gaseoso venoso de 3 (A) y de 4 (B). Las flechas rojas están señalando burbujas. Las estructuras anatómicas que se están observando en estas imágenes son corazón izquierdo (Left Heart = L.H.), corazón derecho (Right Heart = R.H.), Arco aórtico (A.A.) y arteria pulmonar (Pumonary Artery = P.A.). Imágen de Dopler (C) donde se distingue una marca blanca más opaca (es el ruido causado por la reflexión en la superficie de la burbuja del Dopler) sobre un fondo gris (ruido causado por el flujo sanguíneo). Estas imágenes han sido utilizadas con permiso de la NTNU.

Tabla 7.2: Escala para la cuantificación del embolismo venoso gaseoso mediante la técnica de ultrasonido de acuerdo con Eftedal y Brubakk (1997)

Escala	Definición
0	Sin burbujas
1	Alguna burbuja ocasional
2	Una burbuja por cada 4 ciclos cardiacos
3	Una burbuja por cada ciclo cardiaco
4	Burbujeo continuo
5	Bubujeo masivo (no se puede contar)

Todos los animales de los distintos modelos experimentales fueron sometidos al mismo procedimiento PM (condiciones de conservación PM, tiempos PM y protocolo de necropsia).

Además de los tiempos PM, se le adjudicó a cado conejo un código de descomposición (1-5) basado en el protocolo de necropsias de cetáceos de la Sociedad Europea de Cetáceos (Kuiken and García-Hartmann, 1991) donde el código 1 corresponde a un animal muy fresco (recién muerto); código 2, cuando está fresco; 3, cuando tiene signos de autolisis; 4, autolisis avanzada y 5, autolisis muy avanzada.

El propósito de asignarles a los conejos códigos de descomposición es el de facilitar las comparaciones con los cetáceos varados cuyas horas PM se desconocen en la mayoría de los casos. Por lo tanto, se analizó asimismo la utilidad de estos códigos obteniéndose una fuerte asociación lineal con el tiempo PM, siendo el coeficiente de correlación de Pearson de 0,9591 (P<0,001). De modo que ambas variables tienen el mismo valor predictivo para el nivel de gas según el tratamiento.

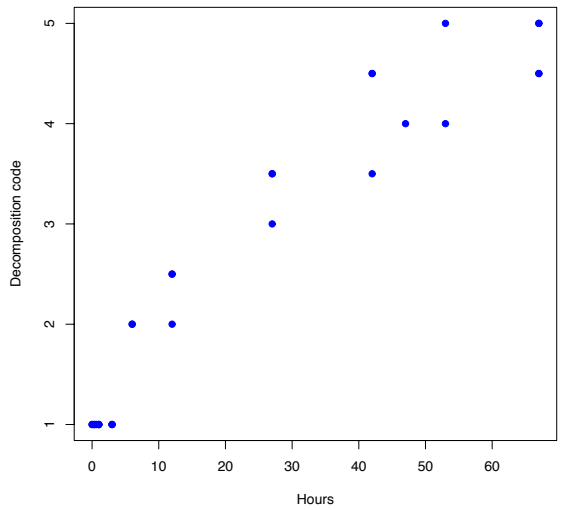

Fig. 7.7: Correlación lineal entre el tiempo PM (horas) en el eje de abscisas y los códigos de descomposición el eje de ordenadas.

El protocolo de necropsias utilizado tanto en los modelos experimentales como en los cetáceos varados, está basado en el protocolo de necropsias de cetáceos estandarizado por Kuiken y García-Hartmann (1991), la guía de varamientos de mamíferos marinos de Geraci y Lounsbury (2005) y el libro de necropsias de animales domésticos de King y colaboradores (1989), con algunas innovaciones debido a la incorporación de la metodología desarrollada para el análisis de los gases y discutida en el capítulo II.

Las modificaciones incluídas en el protocolo de necropsia consisten básicamente en una disección cuidadosa, evitando cortar grandes vasos, hasta que se observe y muestree el gas de todo el sistema circulatorio (incluído el corazón). Una vez que hayan sido muestreados los gases, se puede proseguir con el protocolo normal de necropsia.

Una innovación añadida aportada en esta tesis es un sistema semi-cuantitativo para valorar la presencia y/o abundancia del gas encontrado macroscópicamente durante la necropsia en los distintos vasos y tejidos. Se evaluó mediante este método la presencia de gas en venas subcutáneas, mesentéricas, femorales, vena cava, aurícula derecha y venas coronarias. La gradación propuesta fue la siguiente:

Tabla 7.3: Gradación para la evaluación de la presencia de gas intravenoso hallado macroscópicamente durante la realización de la necropsia.

Grado	Definición
0	Sin burbujas/Vasos congestivos
I	Alguna burbuja ocasional
II	Muy pocas burbujas y pequeñas/Algunas disontinuidades de flujo sanguíneo en las venas.
III	Abundantes discontinuidades en las venas pero no están rellenas de gas.
IV	Presencia moderada de burbujas
V	Presencia abundante de burbujas
VI	Secciones completas de las venas rellenas de gas.

De manera similar, se evaluó el enfisema subcapsular o en la serosa (según órgano) y el enfisema en tejido graso (fundamentalmente grasa abdominal pero también subcutánea y coronaria).

Tabla 7.4: Gradación para la evaluación de la presencia de gas intravenoso hallado macroscópicamente durante la realización de la necropsia.

Grado	Definición
0	Ausencia de gas
1	Presencia escasa de gas (afectando solo a un órgano)
2	Presencia moderada de gas (afectando a más de un órgano)
3	Presencia abundante de gas (afectando muchos órganos)

Sumando las gradaciones de burbujas en sangre (gradación del 0-VI en 6 loalizaciones distintas) más la presencia de gas sucapsular o en serosa (0-3) y enfisema en tejido graso (0-3) obtenemos una escala total de 0-43 puntos.

Esta semi-cuantificación nos ha permitido explorar la aparición/producción de los gases y su tendencia a lo largo del tiempo, o de lo que es lo mismo, los códigos de descomposición. Se obtuvo el siguiente modelo con un R^2 ajustado de 0,8982:

$$E\left[Gas\right] = \alpha + \tau_2 T_2 + \tau_3 T_3 + \beta_1 T_1 HOURS + \beta_2 T_2 \log\left(1 + HOURS\right) + \beta_3 T_3 \log\left(1 + HOURS\right)$$

Tabla 7.5: Definición, estimación (y desviación estándar) así como su P-valor asociado de los parámetros que definen el modelo de la evolución de cantidad de los gases en venas y tejidos según tratamiento y tiempo PM.

Parámetros	Estimación (SE)	P-valor
α	-0.797 (2.090)	0.7061 (NS)
τ_2 (efecto tto 2 respecto tto 1 en hora 0)	11.986 (2.913)	< .001
τ_3 (efecto tto 3 respecto tto 1 en hora 0)	33.112 (2.739)	< .001
β_1 (tasa crecimiento tto1)	0.409 (0.051)	< .001
β_2 (creciento gases según log-horas tto 2)	6.228 (0.793)	< .001
β_3 (creciento gases según log-horas tto 3)	1.051 (0.808)	0.2047 (NS)

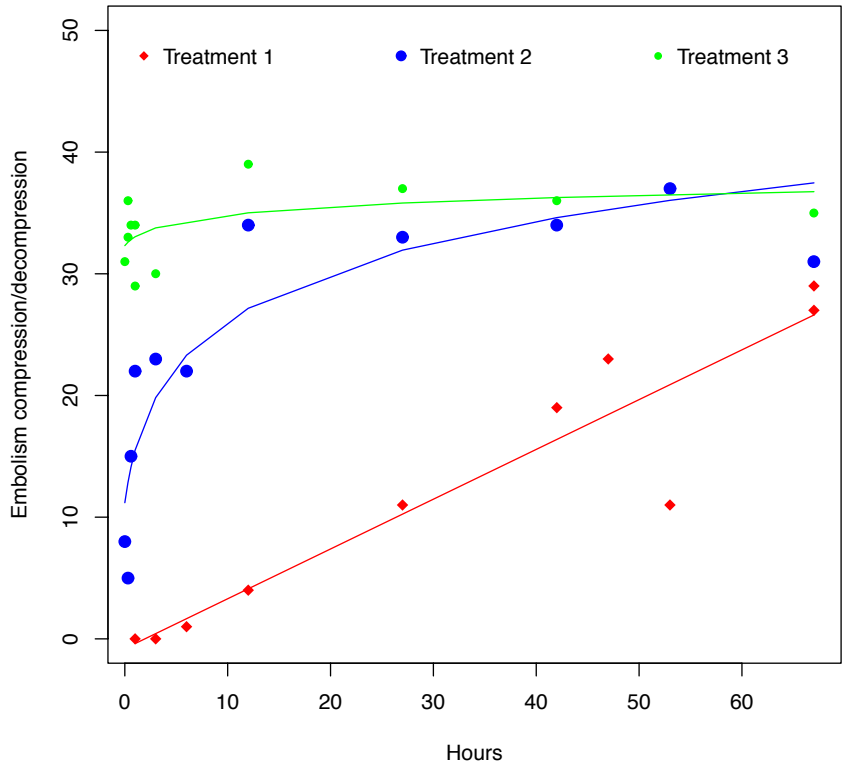

Fig. 7.7: Evolución del nivel de gases medidos con nuestra gración (eje de ordenadas) a lo largo del tiempo postmorten en horas (eje de abscisas) y según tratamiento recibido: 1 putrefacción (en rojo), 2 aeroembolismo (en azul) y 3 tratamiento hiperbárico (en verde).

De los resultados se desprende, en primer lugar, que los valores iniciales de gas son distintos para los 3 tratamientos, habiéndose encontrado diferencias estadísticamente significativas entre los mismos. El patrón de crecimiento para los gases por putrefacción (tratamiento 1) es lineal, con una tasa de crecimiento esperada por día de 0,409 ± 0,051 unidades de grado. Para el tratamiento 2 (aeroembolismo), hay un crecimiento logarítmico significativo, mientras que para el tratamiento 3 (hiperbárico), el crecimiento no es significativo, dado que los valores iniciales de gas son similares a los valores finales en el tiempo comprendido dentro del estudio.

Las diferencias son muy evidentes macroscópicamente entre los animales con código de descomposición 1 y 2, como se puede observar en las siguientes figuras. El embolismo venoso gaseoso debido a una descompresión es más severo y extendido que en el aeroembolismo. Esto fue obsersavdo especialmente en venas subcutáneas. En ambos casos se puede producir la acumulación de gas en bazo, pero sólo mediante la descompresión se observa el tejido graso enfisematoso en todos los tiempos postmortem.

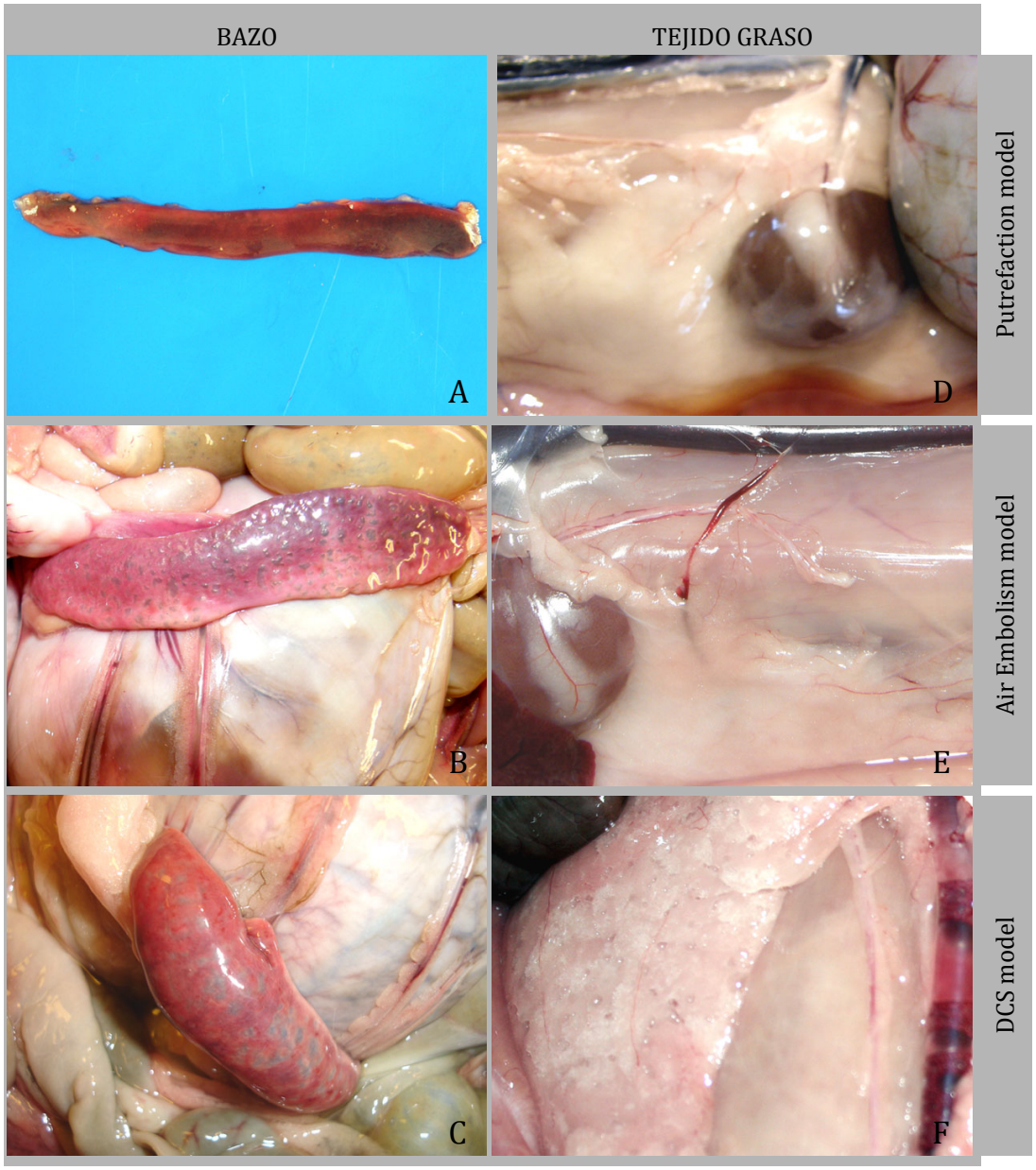

Fig 7.8: Distinta apariencia del bazo con código 1 y 2 en animales de putrefacción(A), sometidos a aeroembolismo (B) y a una exposición hiperbárica (C). Distinta apariencia del tejido adiposo con código 1 y 2 en animales de putrefacción(D), sometidos a aeroembolismo (E) y a una exposición hiperbárica (F).

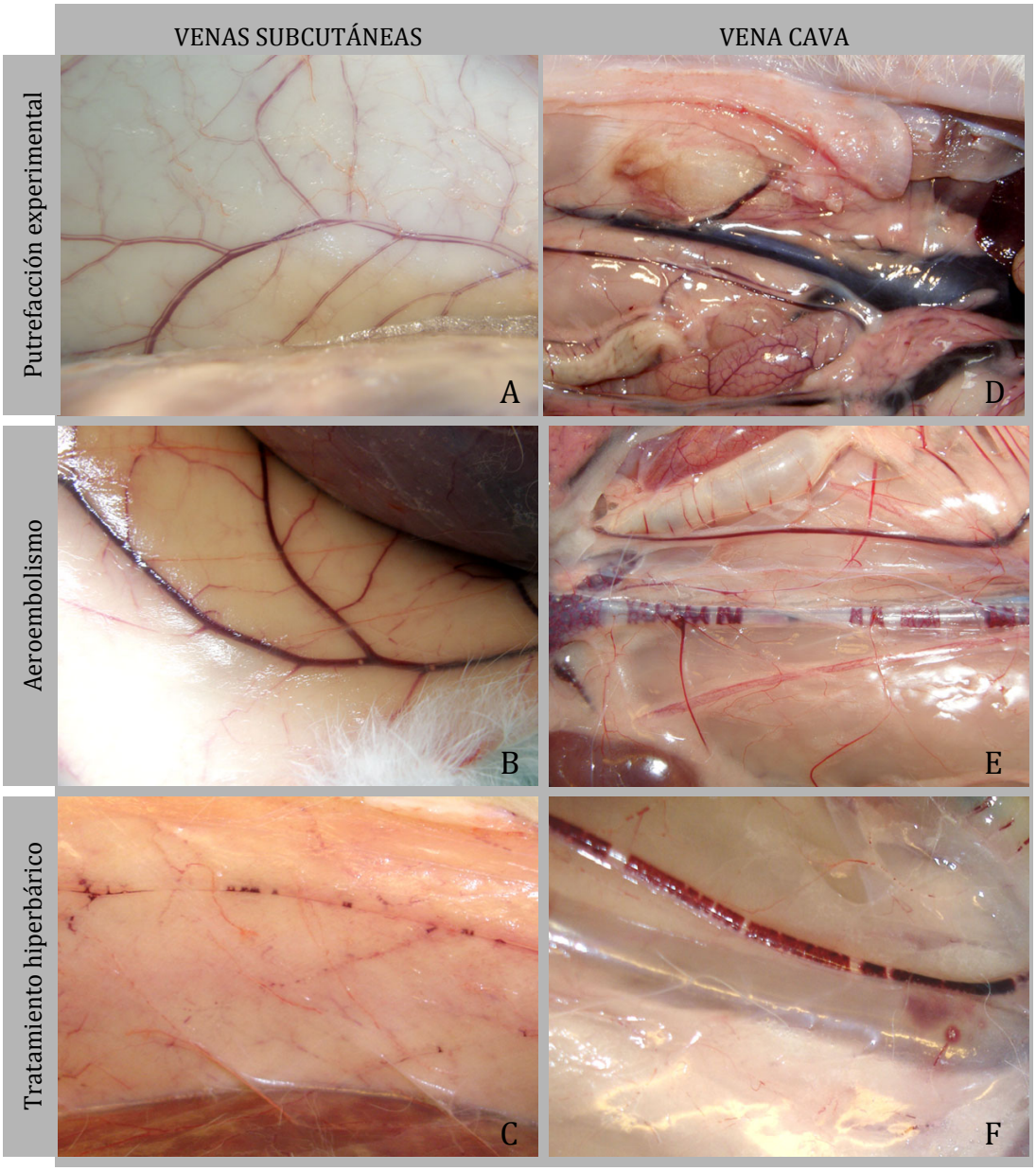

Fig 7.8: Distinta presencia y abundancia de gas en los mismos tejidos, con los mismos códigos de descomposición (código 1 y 2) según tratatmiento recibido. Venas subcutáneas del modelo de putrefacción (A), aeroembolismo (B) y tratamiento hiperbárico (C). Vena cava en el modelo de putrefacción (D), aeroembolismo (E) y tratamiento hiperbárico (F).

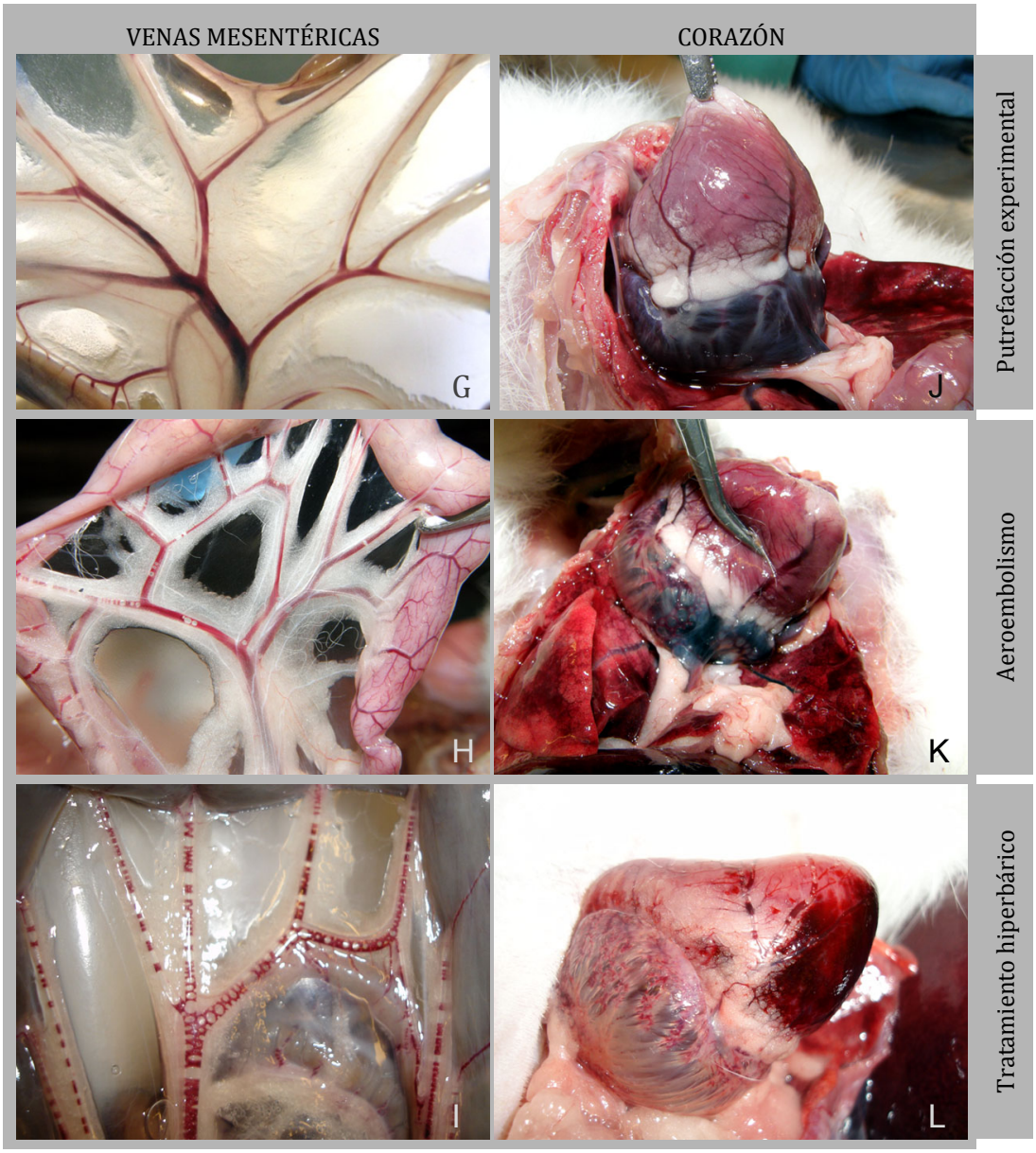

Fig 7.8: Distinta presencia y abundancia de gas en los mismos tejidos, con los mismos códigos de descomposición (código 1 y 2) según tratatmiento recibido. Venas mesentércias en el modelo de putrefacción (G), aeroembolismo (H) y tratamiento hiperbárico (I). Corazón en el modelo de putrefacción (J), aeroembolismo (K) y tratamiento hiperbárico (L).

Respecto a la composición química de los gases, analizados cromatográficamente, observamos que los gases recogidos en el modelo de putrefacción experimental están compuestos por una mezcla de N_2, H_2, CO_2 y O_2.

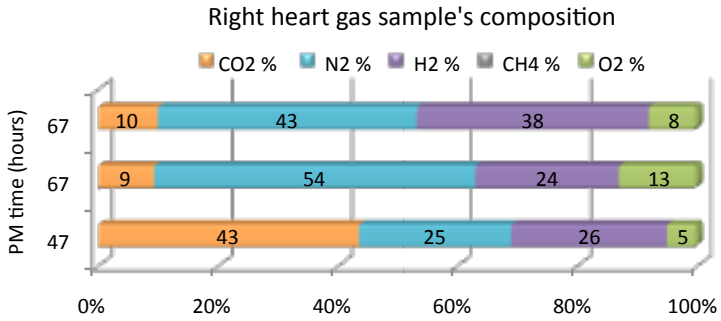

Fig. 7.9: Composición de cada muestra de gas (en % de µmol) recogidas del corazón derecho de animales distintos con su tiempo PM indicado en horas.

Nos encontramos composiciones similares a partir de las 42 horas PM (código de descomposición 4) en los distintos modelos.

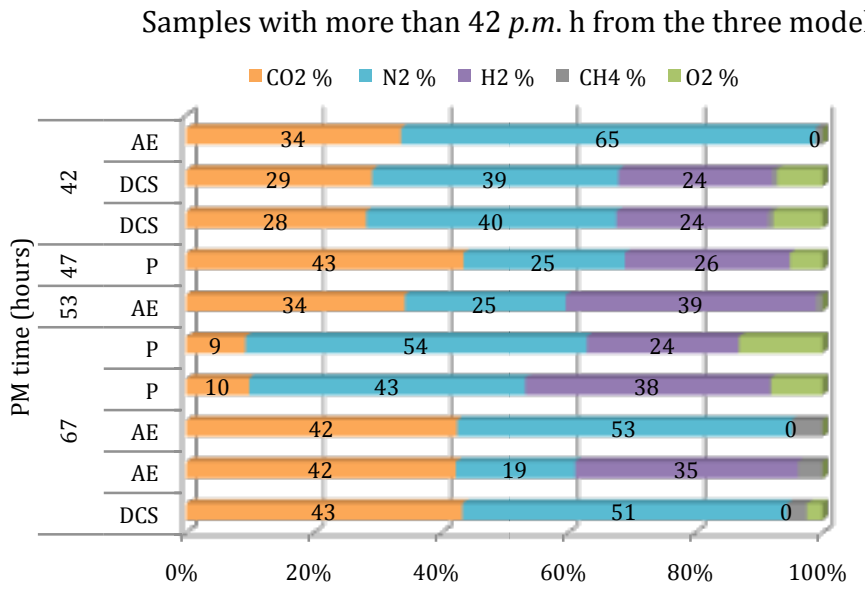

Fig. 7.10: Composición del gas en % µmol de muestras de gas recogidas del sistema circulatorio en animales expuestos a los distintos tratamientos: putrefacción (P), aeroembolismo (AE), hiperbárico (DCS) estudiados a partir de 27 horas PM.

Por el contrario, la composición gaseosa de los modelos de aeroembolismo e hiperbárico recogidas anteriormente al código de descomposición 4, poseen una composición química completamente distinta a los gases de putrefacción descritos anteriormente. Esta composición consiste en altas concentraciones de N_2 (superiores al 70%) y CO_2 (en torno al 30%).

Encontramos sutiles diferencias entre el modelo del aeroembolismo y el descompresivo o hiperbárico. En este último encontramos mayores cantidades de CO_2 que en el caso del aeroembolismo, cuyas muestras gaseosas recogidas experimentalmente, rara vez contenían valores de CO_2 superiores al 25% (indicado con una línea discontinua roja en la siguiente figura).

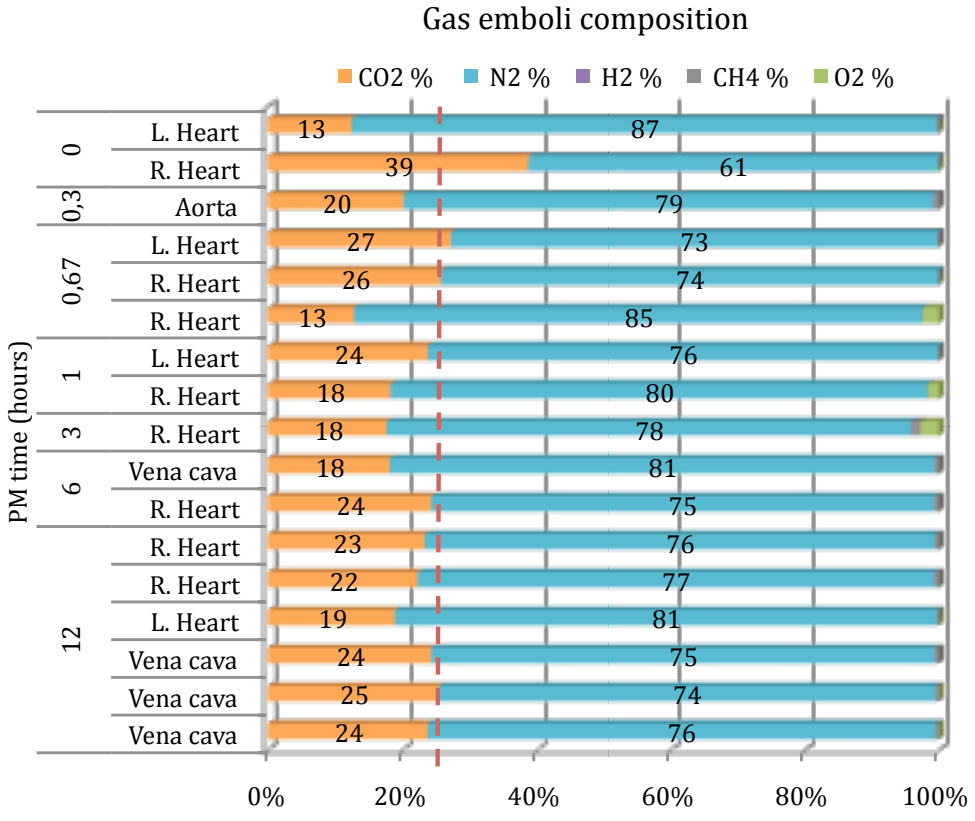

Fig. 7.11: Composición del gas en % µmol de muestras de gas recogidas del sistema circulatorio en animales a los que se les indujo un embolismo gaseoso, estudiados dentro de las primeras 12 horas PM.

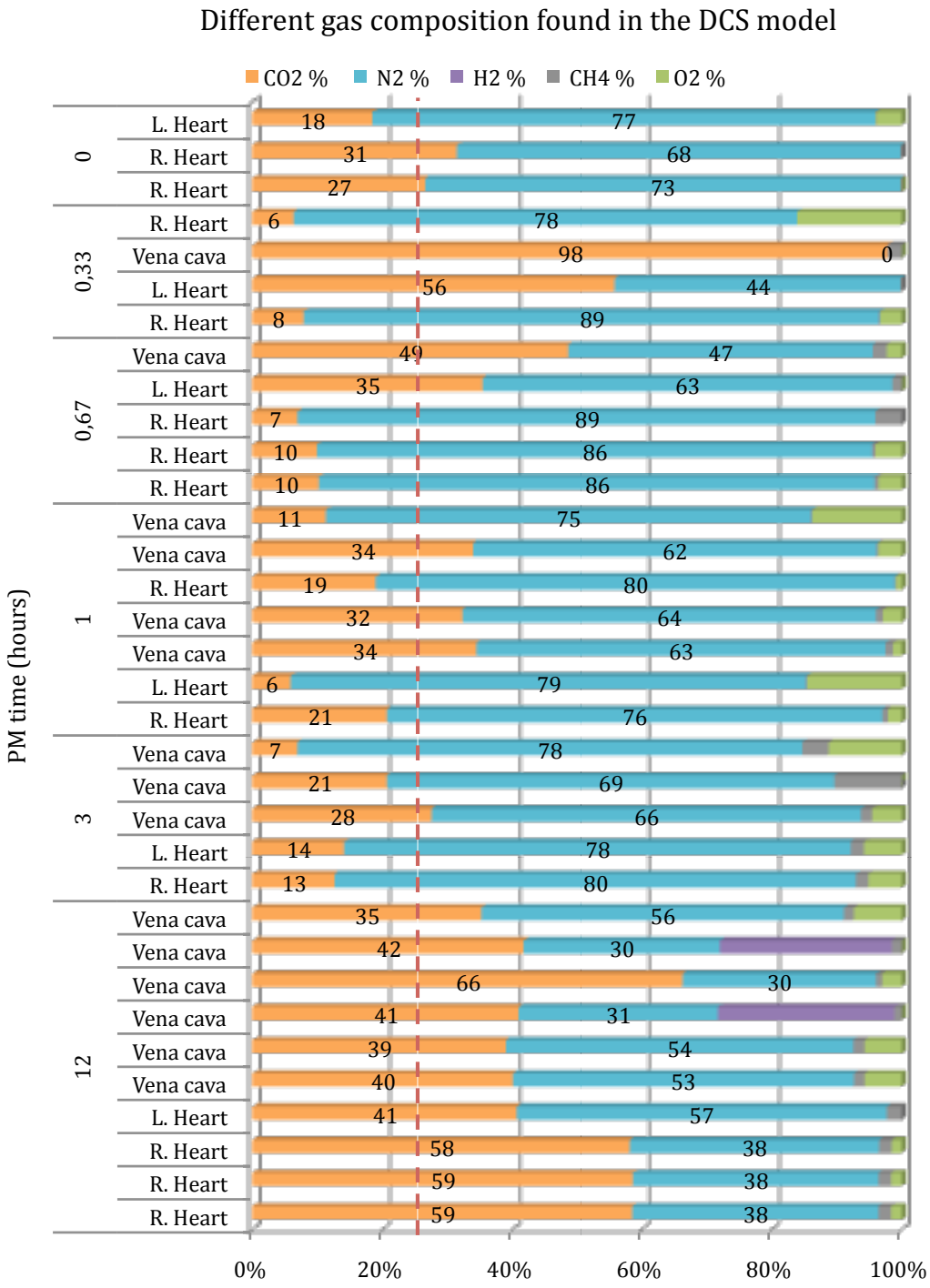

Fig. 7.12: Composición del gas en % µmol de muestras de gas recogidas del sistema circulatorio en animales a los que se les sometió a un tratamiento hiperbárico, estudiados dentro de las primeras 12 horas PM.

La ausencia total de H_2 en las muestras frescas (aquellas recogidas dentro de las 12 horas PM) indica que el H_2 es un marcador de gases de putrefacción.

Poniendo estos datos en conjunto, observamos altas concentraciones iniciales de N_2 que decrecen a favor del CO_2 en los modelos de aeroembolismo e hiperbárico. A partir de las 42 horas PM identificamos claramente gases producidos por la putrefacción que se superponen a los producidos *in vivo* por los distintos modelos experimentales. Se establece, por tanto, un equilibrio dinámico contínuo que observamos en las siguientes figuras.

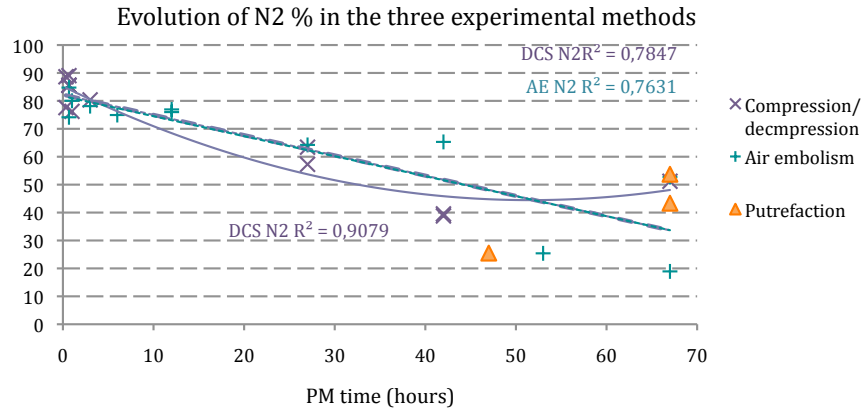

Fig. 7.13: Evolución del contenido de N_2 % µmol (eje de ordenadas) en las muestras de gas recogidas del sistema circulatorio a distintas horas PM (eje de ordenadas) y según tratamiento: putrefacción experimental en naranja, aeroembolismo en azul e hiperbárico en lila.

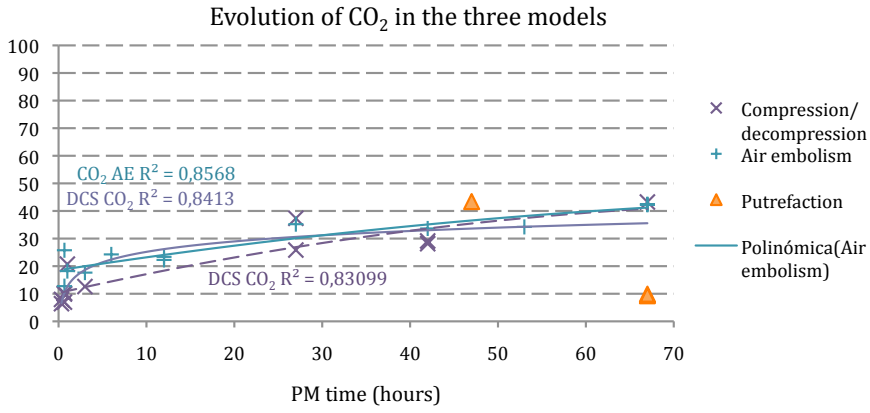

Fig. 7.14: Evolución del contenido de CO_2 % µmol (eje de ordenadas) en las muestras de gas recogidas del sistema circulatorio a distintas horas PM (eje de ordenadas) y según tratamiento: putrefacción experimental en naranja, aeroembolismo en azul e hiperbárico en lila.

7.4 CAPÍTULO IV: EMBOLISMO GASEOSO EN CETÁCEOS VARADOS

Para el estudio del embolismo gaseoso en cetáceos varados se utilizaron animales varados en las Islas Canarias entre 2006 y 2010, zifios de un varamiento masivo que tuvo lugar en Azores en el año 2009, cachalotes de otro varamiento masivo que ocurrió en Italia también en el año 2009, y finalmente 2 pinnipedos procedentes de parques acuáticos que fueron remitidos a nuestra institución. En este estudio se incluyeron un total de 93 mamíferos marinos, pertenecientes a 18 especies distintas, de los cuales se obtuvieron 496 muestras de gases que fueron analizadas cromatográficamente.

A cada cetáceo se le adjudicó un código de descomposición (1-5) basado en el protocolo de necropsias de cetáceos de la Sociedad Europea de Cetáceos (Kuiken and García-Hartmann, 1991) donde el código 1 corresponde a un animal muy fresco (recién muerto); código 2, cuando está fresco; 3, cuando tiene signos de autolisis; 4, autolisis avanzada y 5, autolisis muy avanzada. Este mismo código se utilizó también en los modelos experimentales en conejos (capítulo III).

El protocolo de necropsias fue el mismo que utilizamos para conejos: está basado en el protocolo de necropsias de cetáceos estandarizado por Kuiken y García-Hartmann (1991), la guía de varamientos de mamíferos marinos de Geraci y Lounsbury (2005) y el libro de necropsias de animales domésticos de King y colaboradores (1989), con algunas innovaciones debido a la incorporación de la metodología desarrollada para el análisis de los gases y discutida en el capítulo II.

Del mismo modo, también se evaluaron semi-cuantitativamente la presencia y abundancia de gases en venas y tejidos. Sin embargo, esta gradación en cetáceos se realizó retrospectivamente mediante el uso de soporte gráfico, por lo que hubo que simplificar la escala a utilizar. Las localizaciones que se estudiaron en este caso fueron

venas subcutáneas, mesentéricas, plexo venoso lumbo-caudal y venas epicárdicas. Las gradación propuesta es la siguiente:

Tabla 7.6: Gradación para la evaluación retrospectiva de la presencia de gas intravenoso hallado macroscópicamente durante la realización de la necropsia en cetáceos varados.

Grado	Definición
0	Ausencia de burbujas/ Vasos congestivas
I	Presencia de pocas burbujas.
II	Muchas burbujas.

Tabla 7.7: Gradación para la evaluación retrospectiva de la presencia de gas en tejidos (enfisema) macroscópicamente durante la realización de la necropsia en cetáceos varados.

Grado	Definición
0	Ausencia de enfisema
1	Presencia escasa de enfisema (afectando a 1 ó 2 órganos)
2	Presencia moderada-abundante de enfisema (distribución generalizada)

Nuestros resultados mostraron la presencia de burbujas en 56 de los 93 animales estudiados, lo que representa un 60%, demostrando que la presencia de burbujas en cetáceos varados no es algo inusual.

Asimismo, se observó que la incidencia de burbujas aumentaba con los códigos de descomposición, habiéndose encontrado 13/39 (33.3%) en animales frescos o muy frescos (códigos de descomposición 1 y 2), 16/23 (69.6%) en animales con autolisis incipiente (código de descomposición 3), y 27/27 (100%) en los cadáveres con autolisis avanzada o muy avanzada (códigos 4 y 5).

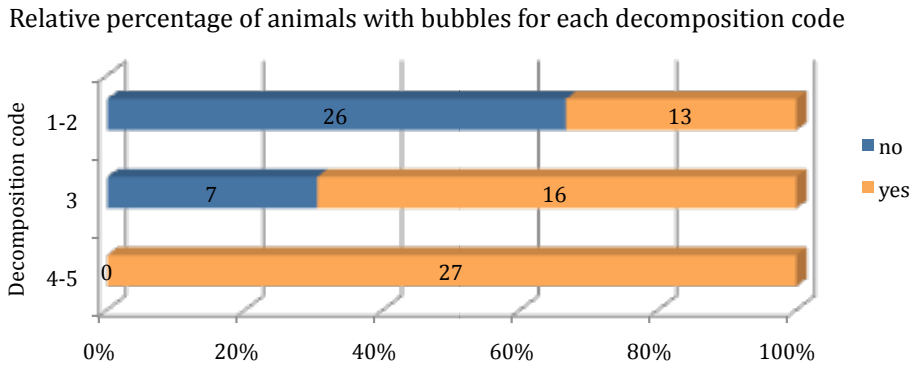

Fig. 7.15: Número y porcentaje relativo (eje de abscisas) de animales que presentan burbujas (en naranja) con respecto a los que no los presentan (en azul) para distintos códigos de descomposición (eje de ordenadas).

Con el objetivo de identificar posibles procesos productores de gas *in vivo*, se excluyeron para este estudio los animales con evidencias de putrefacción (códigos 3, 4 y 5), analizándose exclusivamente los animales con códigos de descomposición 1 y 2.

Uno de los factores que mostró una mayor relación con la incidencia de burbujas fue el perfil de buceo de los animales estudiados. Segregamos los cetáceos en buceadores profundos (aquellos que bajan más de 500 m para alimentarse de modo rutinario) y los de buceo superficial (que aunque ocasionalmente pudieran bajar a estas profundidades, no lo hacen de modo rutinario para alimentarse).

Según nuestros resultados, el 57% de los buceadores profundos mostraron burbujas comparados con el 20% de los cetáceos de buceo superficial con códigos 1 y 2 de descomposición. Se observó una mayor diferencia para el código de descomposición 3, habiéndose encontrado burbujas en el 100% de los buceadores profundos *vs.* 50% de los buceadores superficiales.

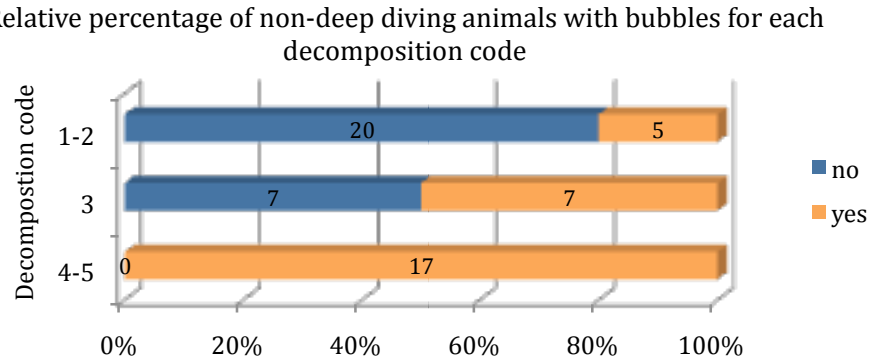

Fig. 7.16: Número y porcentaje relativo (eje de abscisas) de animales de buceo superficial que presentan burbujas (en naranja) con respecto a los que no los presentan (en azul) para distintos códigos de descomposición (eje de ordenadas).

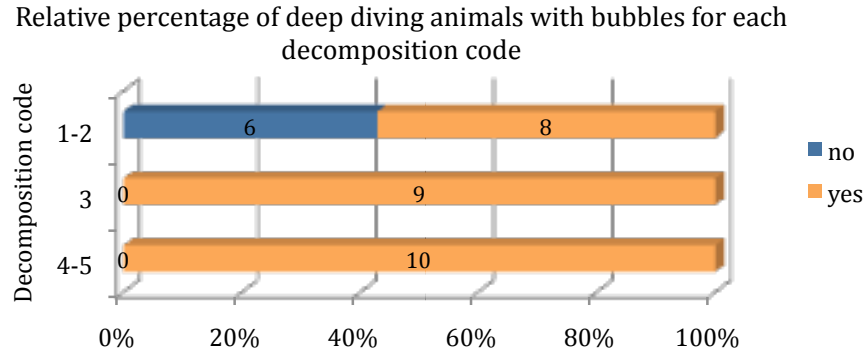

Fig. 7.17: Número y porcentaje relativo (eje de abscisas) de animales de buceo profundo que presentan burbujas (en naranja) con respecto a los que no los presentan (en azul) para distintos códigos de descomposición (eje de ordenadas).

La distinta incidencia de burbujas intravasculares observada en cetáceos de buceo profundo *vs.* cetáceos de buceo superficial, junto con la ausencia total de burbujas en conejos con código 1 y 2 de descomposición (pertenecientes al modelo de putrefacción experimental, capítulo III), nos hace pensar que la presencia de estas burbujas en cetáceos está relacionada con la fisiología del buceo. Por tanto, los animales de buceo profundo tendrían más probabilidades de sufrir una enfermedad similar a la descompresiva.

En medicina humana, hoy en día, se sabe que se producen burbujas en casi todas las descompresiones (Eckenhoff et al., 1990) y que pueden estar presentes en el sistema venoso sin ninguna manifestación clínica (Nishi et al., 2003). A estas burbujas se les conoce como burbujas silenciosas o "silent bubbles".

También se ha descrito que la descompresión puede favorecer la formación de burbujas aún después de la muerte (Brown et al., 1978). Esto es una dificultad añadida para los patólogos, ya que está generalmente reconocido que la presencia de, al menos, algunas de estas burbujas pudieran ser artefactuales por "*off-gasing*" después de la muerte. Por ello, la diferencia entre una posible enfermedad descompresiva y las burbujas silenciosas y/o el "*off-gasing"* es una diferencia cuantitativa más que cualitativa (Knight, 1996).

Se ha demostrado que la incidencia de enfermedad descompresiva está relacionada estadísticamente con la cantidad de burbujas intravasculares evaluadas mediante la técnica de ultrasonido (Sawatzky, 1991). En nuestro estudio experimental, en conejos sometidos a tratamiento descompresivo, se ha demostrado una relación directa entre altas gradaciones de burbujas medidas con ultrasonido y burbujas intravasculares encontradas durante la necropsia (semi-cuantificadas con el sistema de gradación desarrollado en la presente tesis).

De modo adicional, pudimos diferenciar estadísticamente los distintos procesos productores de gas (in vivo y *PM*) en los modelos experimentales mediante el método desarrollado para evaluar la presencia y/o abundancia de gas durante las necropsias, siendo el proceso descompresivo el que mostraba una mayor abundancia de gas.

Por tanto, procedimos a analizar la cantidad de burbujas en los cetáceos varados mediante nuestro método. Decidimos establecer una línea orientativa que nos permitiera distinguir aquellos animales que tuvieran cantidades de gas muy superiores al resto. La situación de la misma (gradación 5) se estableció en base a las gradaciones obtenidas en los modelos experimentales (capítulo III) y a los resultados de los propios cetáceos.

Nuestros resultados revelaron que ningún cetáceo de buceo superficial (0 de 25) presentó una gradación superior a 5 con códigos 1 y 2, y tan sólo el 14, 3% (2 de 14) con código 3 se encontraron por encima de este límite, comparado con el 13,3% (2 de 15) y el 66, 6% (6 de 9) en buceadores profundos.

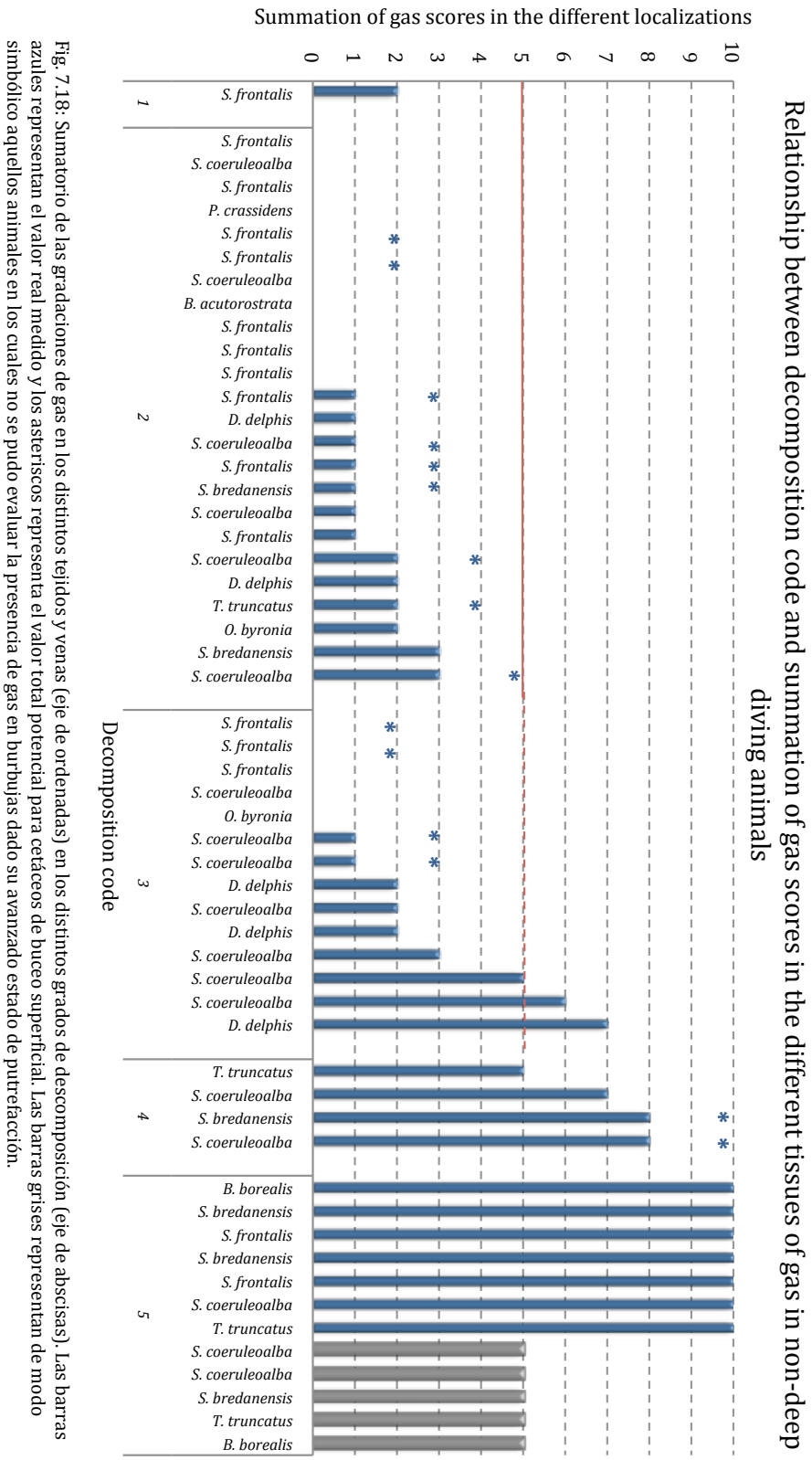

Fig. 7.18: Sumatorio de las gradaciones de gas en los distintos tejidos y venas (eje de ordenadas) en los distintos grados de descomposición (eje de abscisas). Las barras azules representan el valor real medido y los asteriscos representa el valor total potencial para cetáceos de buceo superficial. Las barras grises representan de modo simbólico aquellos animales en los cuales no se pudo evaluar la presencia de gas en burbujas dado su avanzado estado de putrefacción.

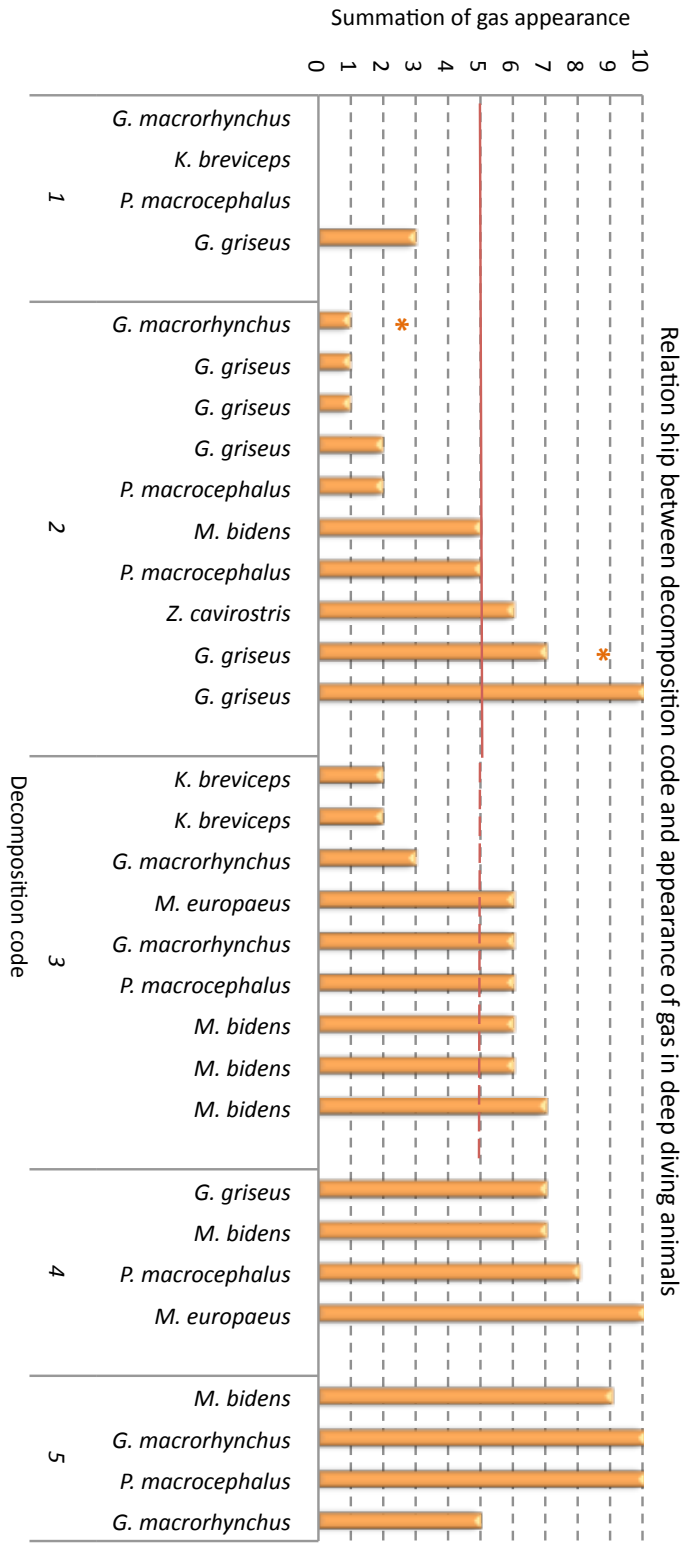

Fig. 7.19: Sumatorio de las gradaciones de gas en los distintos tejidos y venas (eje de ordenadas) en los distintos grados de descomposición (eje de abscisas). Las barras naranjas representan el valor real medido y los asteriscos representa el valor total potencial. para cetáceos de buceo profundo. Las barras grises representan de modo simbólico aquellos animales en los cuales no se pudo evaluar la presencia de gas en burbujas dado su avanzado estado de putrefacción.

Según el método desarrollado en nuestra tesis, los animales que presentaron una mayor abundancia de burbujas intravasculares durante la necropsia, fueron 2 animales de buceo profundo (*Grampus griseus)*.

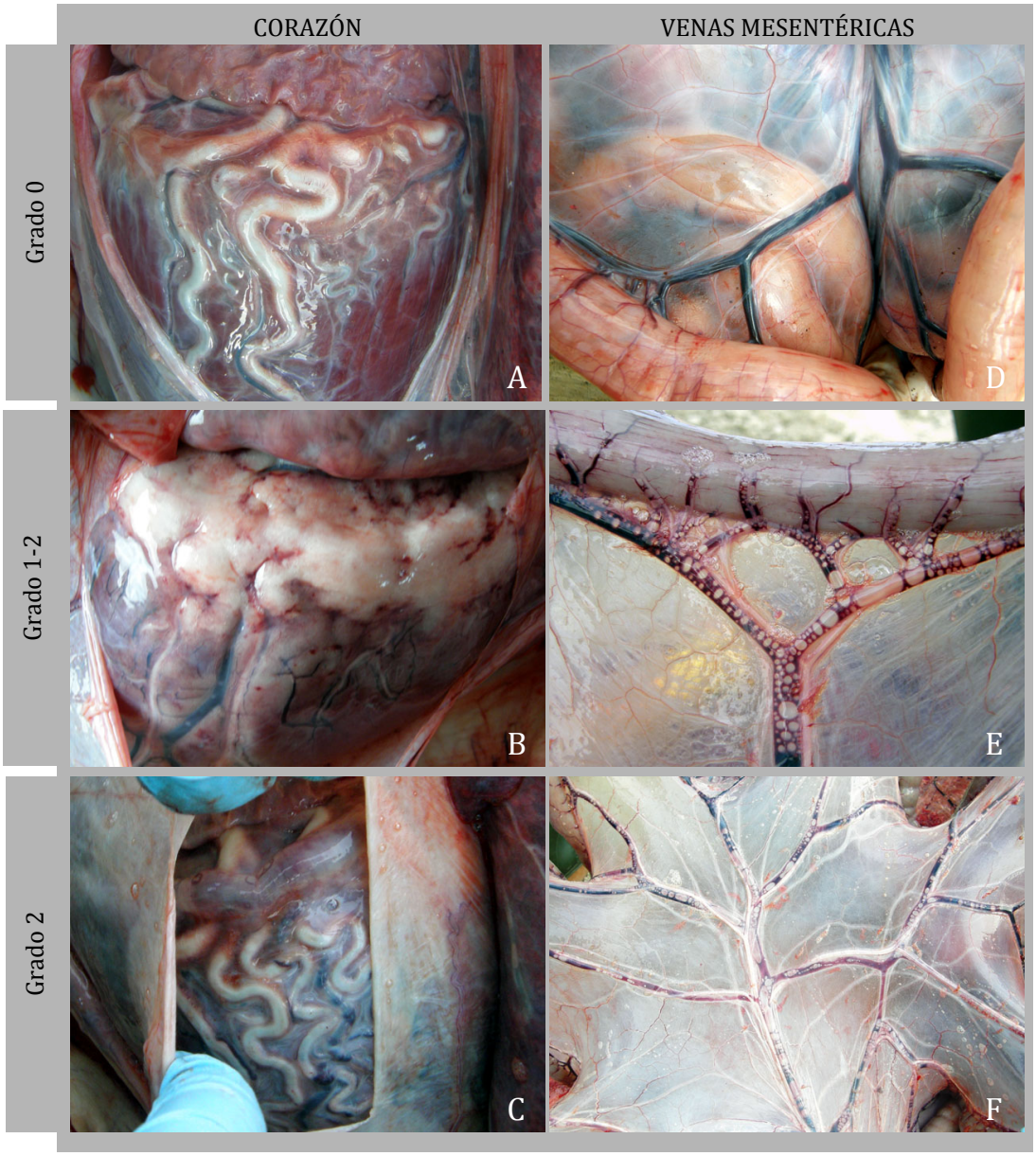

Fig. 7.20: Imágenes de corazón (A-C), venas mesentéricas (D-F) con distintos grados de burbujas en *Grampus* frescos (códigos de descomposición 1-2).

En cuanto a la composición química de las muestras de gas recogidas de cetáceos varados se observaron varias similitudes con respecto a los modelos experimentales.

Las muestras de gas de los animales con un mayor código de putrefacción estaban compuestas fundamentalmente por hidrógeno y altas concentraciones de CO_2. Los niveles de nitrógeno fueron pequeños llegando incluso a no estar presente. El SH_2 y el CH_4 fueron detectados ocasionalmente y en valores traza, demostrando que no son gases putrefactivos importantes en cetáceos, como tampoco lo fueron en los conejos de los modelos experimentales.

Salvo en algunas excepeciones, las muestras obtenidas de animales frescos estaban compuestas por altos niveles de N_2 (aproximadamente un 70%) y concentraciones de CO_2 de alrededor del 30%, de manera similar a la composición de gases encontrada en los conejos de aeroembolismo y descompresión. Estos resultados refuerzan la idea de que las burbujas que observamos en animales con código 1-2 de descomposición podrían corresponderse con "*silent bubbles*".

El análisis químico del contenido gaseoso de los émbolos encontrados en cetáceos varados puede colaborar a establecer, con mayor precisión, el estado de putrefacción de los animales encontrados muertos, bien en la playa o flotando en el mar, de los que se desconoce el momento exacto de la muerte.

Igualmente este tipo de análisis puede contribuir como un diagnóstico etiológico de naturaleza química, descartando fenómenos putrefactivos o colaborando en el diagnóstico de la enfermedad, reforzando la posibilidad de que esos émbolos gaseosos se hayan producido *in vivo* y estén relacionados bien con mecanismos descompresivos, o por la entrada de gas intravascular procedente de lesiones pulmonares o de perforaciones transcutáneas por traumas inciso perforantes.

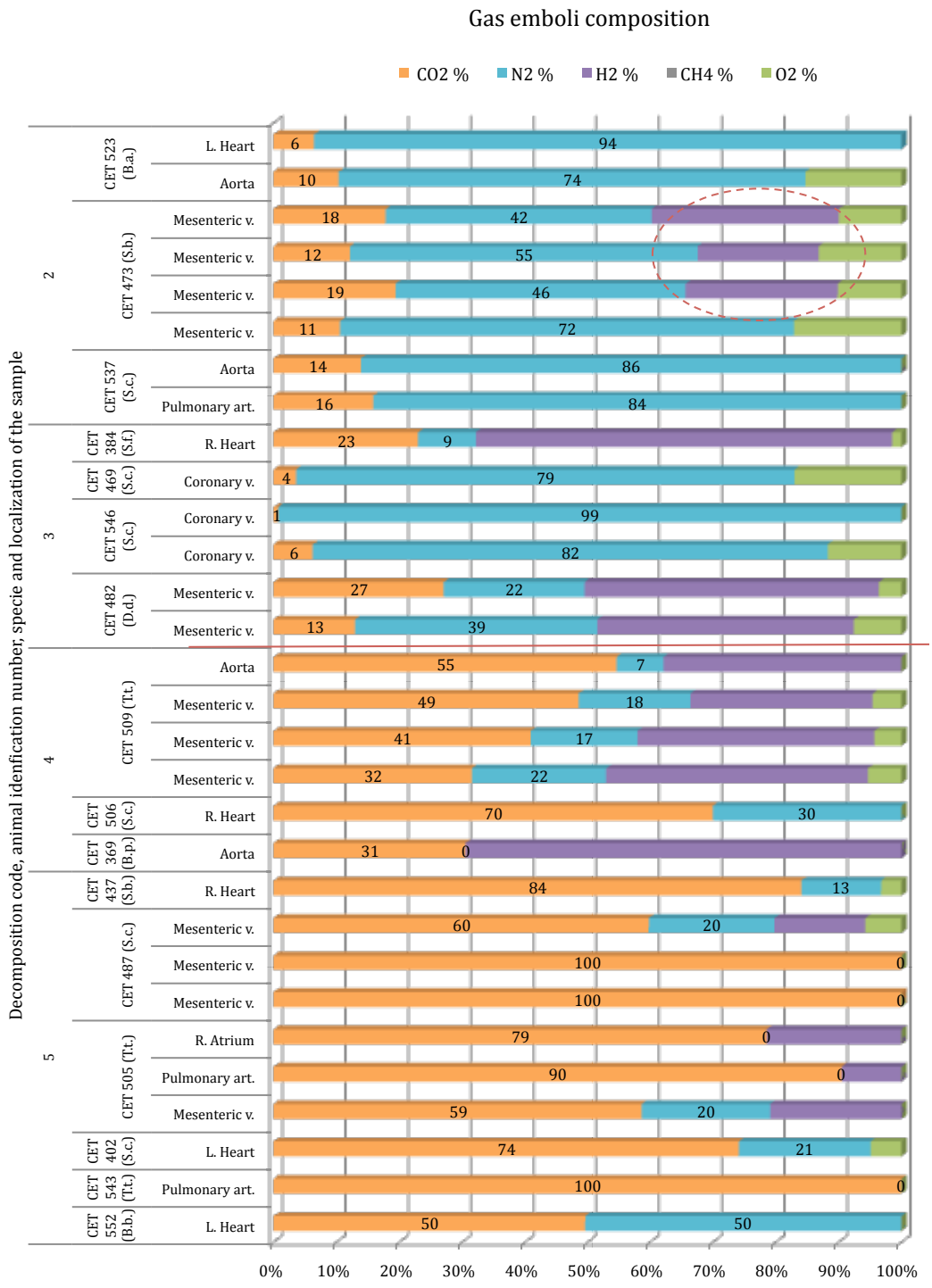

Fig. 7.21: Composición del gas en % µmol (eje de abscisas) de muestras de gas recogidas del sistema circulatorio en cetáceos de buceo superficial con distintos códigos de descomposición (eje de ordenadas).

7.5 CONCLUSIONES

Capítulo II: Desarrollo de metodología para el estudio del emboliso gaseoso.

Hemos desarrollado, innovado y estandarizado mediante validaciones en el laboratorio, una metodología precisa y práctica que permite el muestreo, incluso en necropsias que se realicen *in situ*, así como el almacenamiento y transporte de las muestras en tubos vacuatiners sin que se den diferencias significativas en su composición para finalmente analizar las mismas en el laboratorio.

Capítulo III: Modelos experimentales en embolismo gaseoso .

De acuerdo a nuestros modelos experimentales con conejos hemos desarrollado una metodología semicuantitativa que permite evaluar la presencia y abundancia de gas intravascular y tisular en cadáveres durante la realización de la necropsia con fines forenses.

Durante la necropsia de los conejos (con código de descomposición 1 y 2) del modelo de putrefacción experimental, no se observó que entrara aire en las venas como resultado de la disección. Se encontró una relación lineal, estadísticamente significativa, entre los códigos de putrefacción y el incremento en la presencia y abundancia del gas.

La presencia abundante de gas en el sistema cardiovascular de conejos con códigos de descomposición 1 y 2 de nuestros modelos experimentales debieran interpretarse como indicador de embolismo gaseoso venoso "*in vivo*". Los conejos que murieron por la descompresión mostraron mayor cantidad y distribución de gas en el sistema vascular, afectando venas subcutáneas, femorales, vena cava, mesentéricas, coronarias

y en cavidades cardiacas comparado con los conejos que murieron por inyección intravenosa de aire.

La composición de gases de putrefacción en conejos está constituida por una mezcla de gases caracterizados por la presencia de H_2, altos niveles de CO_2, concentraciones bajas de nitrógeno (en la mayoría de los casos inferior al 40%) y muy pequeñas cantidades de oxigeno, cuando las hay. El CH_4 y el SH_2 aparecieron muy ocasionalmente y en valores traza.

La composición química de las muestras de gas obtenidas de conejos con código de putrefacción 1 y 2, en los modelos de aeroembolismo y descompresión resultaron muy similares, con un 70-80% de N_2 y un 20-30% de CO_2, no siendo posible diferenciarlos analíticamente.

La presencia de burbujas detectadas en el sistema cardiovascular y tejidos durante la necropsia de cetáceos varados es un hallazgo común relacionado con procesos "*in vivo*" y/o PM.

Capítulo IV: Embolismo gaseoso en cetáceos varados.

Existe una relación directa entre los códigos de descomposición en cetáceos y el incremento de presencia y abundancia de burbujas. Los procesos PM fueron analíticamente relacionados con la presencia de H_2 y/o altas concentraciones de CO_2, como fue corroborado en los modelos experimentales en conejos. Para evitar el enmascaramientos procesos "*in vivo"* por los de putrefacción, se debe realizar la necropsia y toma de las muestras lo antes posible, siendo recomendable realizarla antes de las 24 horas PM y preferiblemente 12 horas PM.

La presencia de unas pocas burbujas intravasculares es un hallazgo común en animales frescos con una composición de 70% N_2 y 30% CO_2. Esta observación es altamente consistente con la presencia fisiológica de burbujas silenciosas "*in vivo*", que

fueron además encontradas con mayor frecuencia en buceadores profundos. Esto sugiere que estas especies de cetáceos pudieran estar más predispuestas a sufrir una descompresión, de acuerdo a nuestros resultados.

La cantidad de burbujas durante la necropsia de cetáceos con código de descomposición 1 y 2 es más importante que la mera presencia *vs.* ausencia de las mismas. Grandes volúmenes de gas y ampliamente distribuidos intravascularmente de modo difuso y con una composición de entre 70% de N_2 y 30% de CO_2 estarían relacionados con la formación/crecimiento de las burbujas antemortem mediante procesos fisiopatológicos.

Los análisis de gas por sí mismos, no son conclusivos de diagnóstico para una enfermedad similar a la descompresiva en cetáceos varados, pero pueden contribuir complementariamente junto con otros datos de técnicas de imagen, la realización de necropsias regladas, histopatología, microbiología, toxicología y otros futuros análisis, para alcanzar un diagnóstico de enfermedad descompresiva.

7.6 BIBLIOGRAFÍA

2004a. Diario de sesiones del congreso de los diputados. In: Diputados Cdl, editor.

2004b. Policy on sound and marine mammals. In: Commission TMM, editor. Beaked whale technical workshop. Baltimore, Maryland.

Armstrong HG. 1939. Analyisi of gas emboli. Engineering Section Memorandum Report. Wright Field, Ohio.

Bajanowski T, Kohler H, DuChesne A, Koops E, Brinkmann B. 1998. Proof of air embolism after exhumation. International Journal of Legal Medicine 112(1):2-7.

Bert P. 1878. La Pression Barometrique: Recherches de Physiologie Expérimentale. Hitchcock MA, Hitchcock FA, translator. Paris: Masson.

Brown CD, Kime W, Sherrer EL. 1978. POSTMORTEM INTRA-VASCULAR BUBBLING - DECOMPRESSION ARTIFACT. Journal of Forensic Sciences 23(3):511-518.

Cox TM, Ragen TJ, Read AJ, Vos E, Baird RW, Balcomb K, Barlow J, Caldwell JM, Cranford T, Crum LA, D'Amico A, D'Spain G, Fernandez A, Finneran JJ, Gentry R, Gerth WA, Gulland FMD, Hildebrand J, Houser D, Hullar T, Jepson PD, Ketten D, MacLeod CD, Miller P, Moore S, Mountain DC, Palka D, Ponganis PJ, Rommel S, Rowles T, Tyack PL, Wartzok D, Gisiner R, Mead J, Benner L. 2006. Understanding the impacts of anthropogenic sound on beaked whales. Journal of Cetacean Research and Management 7(3):117-187.

Dyrenfurth F. 1928. Über den qualitativen und quantitativen nachweis von sauerstoff in lungenund darmgasen von leichen und seine anwendung bei der gerischtsärztlichen feststellung der atmung neugeborener. Dtsch Z ges gerichtl Med 12:23-29.

Eckenhoff RG, Olstad CS, Carrod G. 1990. HUMAN DOSE-RESPONSE RELATIONSHIP FOR DECOMPRESSION AND ENDOGENOUS BUBBLE FORMATION. Journal of Applied Physiology 69(3):914-918.

Eftedal O, Brubakk AO. 1997. Agreement between trained and untrained observers in grading intravascular bubble signals in ultrasonic images. Undersea & Hyperbaric Medicine 24(4):293-299.

European-Parliament. 2004. European Parliament resolution on the environment effects of high-intensity naval sonars.

Fernandez A, Edwards JF, Rodriguez F, de los Monteros AE, Herraez P, Castro P, Jaber JR, Martin V, Arbelo M. 2005. "Gas and fat embolic syndrome" involving a mass stranding of beaked whales (Family Ziphiidae) exposed to anthropogenic sonar signals. Veterinary Pathology 42(4):446-457.

Geraci JR, Lounsbury VJ. 2005. Marine Mammals Ashore: a Fiel Guide for Strandings. Second ed. Baltimore, MD: National Aquarium in Baltimore.

Hamilton RW, Thalmann ED. 2003. Decompression practice. In: Brubakk AO, Neuman TS, editors. Bennett and Elliott's Physiology and Medicing of Diving: Saunders. p 455-500.

Harris M, Berg WE, Whitaker DM, Twitty VC, Blinks LR. 1945. Carbon dioxide as a facilitating agent in the initiation and growth of bubbles in animals decompressed to simulated altitudes. Journal of General Physiology 28(3):225-240.

Hooker S, Baird RW. 1999. Deep-diving behaviour of the northern bottlenose whale, Hyperoodon ampullatus (Cetacea: Ziphiidae). Proceedings of the Royal Society of London B 266:671-676.

Ishiyama A. 1983. Analysis of gas composition of intra vascular bubbles produced by decompression. Bulletin of Tokyo Medical and Dental University 30(2):25-36.

Jepson PD, Arbelo M, Deaville R, Patterson IAP, Castro P, Baker JR, Degollada E, Ross HM, Herraez P, Pocknell AM, Rodriguez F, Howie FE, Espinosa A, Reid RJ, Jaber JR, Martin V, Cunningham AA, Fernandez A. 2003. Gas-bubble lesions in stranded cetaceans - Was sonar responsible for a spate of whale deaths after an Atlantic military exercise? Nature 425(6958):575-576.

Kaiser H. 1947. Die berechnung der nachweisempfindlichkeit. Spectrochimica Acta 3(1):40-67.

Keil W, Bretsxhneider K, Patzelt D, Behning I, Lignitz E, Matz J. 1980. Luftembolie oder Fäulnisgas? Zur Dianostik der cardialen Luftembolie an der Leiche. Beiträge zur Gerichtlichen Medizin 38:395-408.

King JM, Dodd DC, Newson ME, Roth L. 1989. The Necropsy Book. New York State College of Veterinary Medicine CU, editor. Ithaca, E.E.U.U.: Charles Louis Davis, D.V.M. Foundation.

Knight B. 1996. Forensic Pathology. Arnold, editor. London.

Kuiken T, García-Hartmann M. Dissection techniques and tissues sampling. In: Newsletter, editor; 1991; Leiden, Netherlands.

Lillo RS, Maccallum ME, Caldwell JM. 1992. Intravascular bubble composition in guinea-pigs a possible explanation for differences in decompression risk among different gases. Undersea Biomedical Research 19(5):375-386.

Martin V, Servidio A, Tejedor M, Arbelo M, Brederlau B, Neves S, Perez-Gil M, Urquiola E, Perez-Gil E, Fernandez A. Cetaceans and conservation in the Canary Islands; 2009; Quebec, Canada.

Muth CM, Shank ES. 2000. Primary care: Gas embolism. N Engl J Med 342(7):476-482.

Nishi RY, Brubakk AO, Eftedal O. 2003. Bubble detection. In: Brubakk AO, Neuman TS, editors. Bennett and Elliott's Physiology and Medicine of Diving. 5th Edition ed: Saunders. p 501-529.

Piantadosi CA, Thalmann ED. 2004. Pathology: whales, sonar and decompression sickness. Nature 428(6984):1 p following 716; discussion 712 p following 716.

Pierucci G, Gherson G. 1968. Experimental study on gas embolism with special reference to the differentiation between embolic gas and putrefaction gas. Zacchia 4(3):347-373.

Pierucci G, Gherson G. 1969. Further contribution to the chemical diagnosis of gas embolism. The demonstration of hydrogen as an expression of "putrefactive component". Zacchia 5(4):595-603.

Sawatzky KD. 1991. The relationship between intravascular Doopler-detected gas bubbles and decompression sickness after bounce diving in humans [MSc thesis]. Toronto, Canada: York University.

Smith-Sivertsen J. The origin of intravascular bubbles produced by decompression of rats killed prior to hypebaric exposure. In: Lambertsen CJ, editor; 1976; Washington, DC. Bethesda MD. p 303-309.

Tyack PL, Johnson M, Soto NA, Sturlese A, Madsen PT. 2006. Extreme diving of beaked whales. Journal of Experimental Biology 209(21):4238-4253.

8 GLOSSARY

8.1 ABBREVIATIONS

a	Type
A	Cross-sectional area of the fluid
A.A.	Aortic Arch
AE	Air embolism
ATA	Absolute Atmospheres
b	Day
B.a.; B. acutorostrata	Balaenoptera acutorostrata, minke whale
B.b.; B. borealis	Balaenoptera borealis, sei whale
B.p.; B. physalus	Balaenoptera physalus, fin whale
BW	Beaked Whales
CT	Computed Tomography
d	Distance between two areas
D	Net Diffusion Rate
D.d.; D. delphis	Delphinus delphis, common dolphin
DCS	Decompression Sickness
FID	Flame-Ionization Detector
Fig.	Figure
GC	Gas chromatograph
G.g.; G. griseus	*Grampus griseu*s, Risso's dolphin
G.m.; G. macrorhynchus	*Globicephala macrorhynchus*, short-finned pilot whale
K.b.; K. breviceps	*Kogia breviceps*, pygmy sperm whale
K.s.; K. sima	*Kogia sima*, dwarf sperm whale
L.H, L. Heart	Left Heart

M	Molsieve 5 A column
M.b.; M. bidens	*Mesoplodon bidens*, Sowerby's beaked whale
M.e.; M. europaeus	*Mesoplodon europaeus*, Gervais' beaked whale
MRI	Magnetic Resonance Imaging
msw	Meters of Sea Water
MW	Molecular Weight
NZWR	New Zeeland White Rabbits
O.b.; O. byronia	*Otaria byronia*, south American sea lion
P	Pressure
P	Putrefaction
P.A.	Pulmonary Artery
P.c.; P. crassidens	*Pseudorca crassidens*, false killer whale
P.m.; P.macrocephalus	Physeter macrocephalus, sperm whale
PM	Post-mortem
Q	PoraBOND Q column
R	Interface Radius of Curvature
R.H., R. Heart	Right Heart
RBC	Red Blood Cells
S	Solubility Coefficient
S.b.; S. bredanensis	*Steno bredanensis*, rough-toothed dolphin
S.c.; S. coeruloealba	Stenella coeruleoalba, striped dolphin
S.f.; S. frontalis	*Stenella frontalis*, atlantic spotted dolphin
SWs	Sperm Whales
T.t.; T.truncatus	*Tursiops truncatus*, bottle-nose dolphin
TCD	Thermal-Conductivity Detector
VC	Vena Cava
VGE	Venous Gas Emboli
VOCs	Volatile Organic Compounds

y	molar fraction
Z.c.; Z.cavirostris	*Ziphius cavirostris*, Cuvier's beaked whale
σ	Gas–Liquid Interface Surface Tension

8.2 DEFINITIONS

Active strandings	Cetaceans that had been observed to strand alive.
Adhesive forces	It is the attraction between molecules of different nature and it differs for different pair of substances.
Air embolism	It is the entry of atmospheric or alveolar air into the vascular system and is mainly a iatrogenic problem.
Aortic bulb	It is the dilation of the aorta.
Arterial Gas Emboli	It is the presence of bubbles on the aterial side of the circulatory system.
Atypical mass stranding	An stranding of more than two animals, which sometimes includes several species that came ashore during a relatively short period of time, but in different places of the coasts.
Autolysis	It is the spontaneous self-destruction of tissues by the body enzymes present in the cells, without any bacterial interference.
Cohesive force	It is the attraction between molecules of the same nature.
Decomposition	It is the continual process of gradual decay and disorganization of organic tissues and structures after death.
Decompression illness	Diseases caused by intravascular or extravascular bubbles that are formed as a result of reduction in environmental pressure (decompression).
Decompression sickness	It is the disease caused by bubble formation due to gas phase separation in the body.
Deep diver cetaceans	Those species supposed to dive usually deeper than 500m for foraging (*Kogia, Physeter, Ziphius, Mesoplodon, Globicephala and Grampus*).

Flame-ionization detector	It is a selective hydrocarbon destructive detector.
Gas Emboli	It is the presence of gas bubbles on the circulatory system.
Gas nuclei	In vivo bubble precursors.
Homogenous nucleation	It is the formation of spontaneous gas bubbles from supersaturated liquid phases.
Net diffusion	It is the net movement of molecules from the concentrated area to the most diluted one.
Partial pressure	It is the pressure of each gas in a system.
Passive stranding	When the animal beached already death.
Permanent gases	Gases that cannot be liquefied at ambient temperatures.
Pre-existing gas nuclei	They are persistent bodies of undissolved gas.
Pressure	It is the impact of the random movements of the molecules against the walls of the system.
Pulmonary barotraumas	When gas in the alveoli expands (in diving is normally caused by a reduction in ambient pressure) and ruptures the alveolar capillaries.
Putrefaction	It is the breakdown by microorganisms such as bacteria, fungi and protozoa (from the intestine and the environment) and follows autolysis.
Resolution limit	The minimum distance or angular separation between two point objects, which allows them to be resolved according to the Rayleigh criterion.
Respiratory or pulmonary membrane	It is the overall membrane surfaces where gaseous exchange takes place.
Retia mirabilia	They are plexus of anastomosing arteries and veins wich occur along the vertebrae and base of the skull.

Supersaturation	It is the excess of partial pressure compared to barometric pressure on a given fluid.
Surface tension	Is the force per unit length of the cohesive energy present at an interface of a liquid that prevent vaporization.
Surfactants	They are amphilic molecules with a polar hydrophilic and a lipophilic group.
Surgical anesthesia	When the animal has lost blink reflexes, pupils become fixed and respiration is regular because of the adequate anesthesia dose.
Thermal-conductivity detector	It is a universal detector for permanent gases.
Total pressure (P_t)	It is the sum of different molecules hitting the surface. It is the sum of the partial pressures of the different gases of a mixture.
Typical mass stranding	Refers to two or more cetaceans, other than a female and her calf, coming ashore at the same time and location.
Vacutainers	They are glass tubes sealed with a partial vacuum inside using rubber stoppers.
Venous Gas Emboli	It is the presence of bubbles on the venous side of the circulatory system.
Volatile organic compounds	They are intermediate products of decomposition

9 GRADING SYSTEMS USED

9.1 BUBBLE GRADE

In rabbits compressed and decompressed, the pulmonary artery was monitored just after surfacing every 15 minutes with ultrasound. Bubbles were detected as bright spots, the number of gas bubbles was evaluated using a grading scale from 0 to 5 (Eftedal and Brubakk 1997).

Table 9.1: Bubble grade scale from (Eftedal and Brubakk 1997)

Bubble grade	Definition
0	No bubbles
1	Occasional bubble
2	One bubbles every fourth heart cycle
3	One bubble every heart cycle.
4	Continuous bubbling.
5	Massive bubbling.

9.2 *POST MORTEM* STUDIES

9.2.1 DECOMPOSITION CODE

The decomposition code of the body was determined following the parameters and classifications established in the protocol of necropsies of cetaceans referenced by the European Cetacean Society (Kuiken and García-Hartmann 1991)

Table 9.2: Decomposition code based on kuiken and García-Hartmann (1991).

Decomposition code	Definition
1	Very fresh
2	Fresh
3	Incipient autolysis/moderate decomposition
4	Advanced decomposition
5	Very advanced decomposition

9.2.2 PRESENCE OF BUBBLES IN VEINS

9.2.2.1 Rabbits

To evaluate macroscopically bubbles abundancy found in different vessels during dissection of rabbits, we stablished a grading system from 0 to IV.

Table 9.3: Bubble score used to evaluate macroscopically bubbles found during dissection of rabbits.

Bubble score	Definition
0	No bubbles/Congestive veins
I	Occasional bubble
II	Few bubbles/Small discontinuities on blood flow
III	Abundant and larger discontinuities on blood flow, but nof filled with gas
IV	Moderate presence of gas bubbles within an specific vein
V	Abundant presence of bubbles
VI	Complete sections of the veins are filled with gas

9.2.2.2 Marine mammals

Evaluation of free gas in tissues and veins was done in most of the cases retrospectively, using photos and data written in the necropsy report, thus a more simple system than that of the rabbits was used. A question mark was noted when some information was missing.

Table 9.4: Bubble score used to evaluate macroscopically bubbles found during necropsy of cetaceans.

Bubble score	Definition
0	No bubbles/Congestive veins
I	Few bubbles
II	Abundant presence of bubbles

9.2.3 FREE GAS IN TISSUES

9.2.3.1 Rabbits

When evaluating gas within fat tissues or subcapsular gas presence, a simpler grading from 0 to 3 was used.

Table 9.5: Gas score used to evaluate subacapuslar emphysema found druing dissection of rabbits.

Bubble score	Definition
0	Absence of gas
1	Scarce presence of gas (affecting only a target organ)
2	Moderate presence of gas (affecting more than one organ)
3	Abundant presence of gas (affecting many different organs).

9.2.3.2 Marine mammals

Evaluation of free gas in tissues and veins was done in most of the cases retrospectively, using photos and data written in the necropsy report, thus a more simple system than that of the rabbits was used. A question mark was noted when some information was missing.

Table 9.6: Gas score used to evaluate subacapuslar emphysema found druing necropsies of cetaceans.

Bubble score	Definition
0	Absence of subcapsular gas
1	Scarce presence of gas (affecting only one or two organs)
2	Moderate-abundant presence of gas (widely distributed)

9.2.4 GAS ACCUMULATION IN THE SPLEEN

In the rabbits, the spleen was sometimes observed to be filled with free gas. Therefore it is been recorded as 0 with no gas and 1 with gas.

10 APPENDIX FOR GAS ANALYSIS RESULTS

10.1 GAS COMPOSITION RESULTS OF THE EXPERIMENTAL MODELS (CHAPTER III)

10.1.1 GAS ANALYSIS RESULTS OF THE PUTREFACTION MODEL

41 gas samples were obtained. A summary of average mole fraction expressed as a percentage of gas composition of samples of each animal can be observed bellow:

Table 10.1: Gas sample composition of each animal expressed in percentages. In the last column it is represented the contribution of each gas to the total composition.

1hP	Remarks	% H_2	% O_2	% N_2	% CH_4	% CO_2	
Intestine 1		36.48	0.00	45.10	0.25	18.17	
Intestine 2		38.09	0.00	44.80	0.33	16.78	
AVERAGE	Intestine	37,28	0,00	44,95	0,29	17,47	N_2>H_2>CO_2

3hP	Remarks	% H_2	% O_2	% N_2	% CH_4	% CO_2	
Intestine 1		0,00	0,00	11,15	28,76	60,09	CO_2>>CH_4>N_2
Intestine 2		0,00	0,00	56,19	1,01	42,80	N_2> CO_2
Intestine 3		0,00	0,00	45,93	2,26	51,81	CO_2≈ N_2

6hP	Remarks	% H_2	% O_2	% N_2	% CH_4	% CO_2	
Intestine 1		0,00	0,00	35,93	5,33	58,74	CO_2> N_2
Intestine 2		0,00	0,00	57,25	0,20	42,55	N_2> CO_2
Intestine 3		0,00	0,87	19,11	3,57	76,45	CO_2>> N_2

12hP	Remarks	% H_2	% O_2	% N_2	% CH_4	% CO_2	
Intestine 1		4,25	0,00	61,55	1,85	32,35	N_2> CO_2>H_2
Intestine 2		0,00	0,00	27,98	4,11	67,91	CO_2>> N_2
Intestine 3		0,00	0,00	0,00	0,00	0,00	Empty

(Follow up) Table 10.1: Gas sample composition of each animal expressed in percentages. In the last column it is represented the contribution of each gas to the total composition.

27hP	Remarks	% H_2	% O_2	% N_2	% CH_4	% CO_2	
Intestine 1		9,04	0,00	50,80	9,58	30,58	N_2> CO_2>H_2
Intestine 2		0,00	0,00	18,97	28,07	52,95	CO_2> N_2> CH_4
Intestine 3		5,68	0,00	36,04	15,57	42,72	CO_2≈ N_2> CH_4> H_2
Emphysema	Pericardic sac	0,00	19,36	78,07	0,07	2,51	Air pollution?

42hP	Remarks	% H_2	% O_2	% N_2	% CH_4	% CO_2	
Intestine 1		0,00	0,00	8,60	23,97	67,43	CO_2>>CH_4>N_2
Intestine 2		8,27	0,00	21,19	13,74	56,80	CO_2> N_2> CH_4>H_2
Intestine 3		0,00	8,43	30,28	16,96	44,33	CO_2> N_2> CH_4>O_2
R. Heart	0.6 mL	0,00	19,89	80,03	0,08	0,00	Air pollution?

47hP	Remarks	% H_2	% O_2	% N_2	% CH_4	% CO_2	
Intestine 1		0,00	0,00	7,60	25,39	67,02	CO_2>>CH_4>N_2
R. Heart	1.8mL	25,94	5,05	25,48	0,12	43,41	CO_2> N_2> CH_4>H_2

53hP	Remarks	% H_2	% O_2	% N_2	% CH_4	% CO_2	
Intestine 1		0,00	0,00	11,59	7,28	81,13	CO_2>> N_2> CH_4
Intestine 2		0,00	0,86	21,82	10,76	66,55	CO_2>> N_2> CH_4
Intestine 3		0,00	0,00	13,26	8,55	78,19	CO_2>> N_2> CH_4

67hAP	Remarks	% H_2	% O_2	% N_2	% CH_4	% CO_2	
Intestine 1		2,89	0,00	16,60	13,16	67,35	CO_2>>N_2> CH_4>H_2
Intestine 2		2,28	0,00	11,94	11,28	74,50	CO_2>>N_2> CH_4>H_2
Emphysema		29,00	11,63	41,81	0,75	16,81	N_2>H_2>CO_2>O_2
Emphysema		26,52	9,91	38,53	0,19	24,84	N_2>H_2≈CO_2>O_2
Emphysema		27,54	9,01	34,80	0,57	28,09	N_2>H_2≈CO_2> O_2
R. Heart		23,78	13,03	53,71	0,21	9,27	N_2 >H_2>O_2>CO_2
Vena cava		18,01	4,79	58,32	0,28	18,60	N_2 >H_2≈CO_2> O_2
Vena cava		39,01	0,00	21,79	0,72	38,48	H_2≈CO_2>N_2
Vena cava		34,87	0,00	32,66	0,71	31,76	H_2≈CO_2≈N_2

(Follow up) Table 10.1: Gas sample composition of each animal expressed in percentages. In the last column it is represented the contribution of each gas to the total composition.

67hBP	Remarks	% H_2	% O_2	% N_2	% CH_4	% CO_2	
Intestine 1		32,62	0,00	22,95	0,51	43,91	CO_2>H_2>N_2
R. Heart		38,44	8,03	43,35	0,31	9,87	N_2> H_2>CO_2>O_2
L. Heart		31,99	4,85	43,44	0,22	19,51	N_2>H_2>CO_2>O_2
Emphysema		26,21	8,71	31,05	2,91	31,13	N_2> CO_2≈H_2 >O_2
Vena cava		28,81	0,00	39,75	0,41	31,02	N_2> CO_2≈H_2
Vena cava		19,67	0,00	14,67	13,36	52,30	CO_2> H_2> N_2
Vena cava		36,24	0,00	21,80	0,51	41,45	CO_2> H_2> N_2

10.1.2 GAS ANALYSIS RESULTS OF THE INDUCED AIR EMBOLISM MODEL

56 gas samples were obtained. A summary of average mole fraction expressed as a percentage of gas composition of samples of each animal can be observed bellow:

Table 10.2: Gas sample composition of each animal expressed in percentages. In the last column it is represented the contribution of each gas to the total composition.

0hAE	Remarks	% H_2	% O_2	% N_2	% CH_4	% CO_2	
R. Heart	0,8 mL	0,00	0,00	61,24	0,06	38,70	N_2> CO_2
L. Heart	0,5 mL	0,00	0,00	87,12	0,38	12,50	N_2>> CO_2

20minAE	Remarks	% H_2	% O_2	% N_2	% CH_4	% CO_2	
Intestine 1		0,00	0,00	65,72	18,29	15,99	N_2>> CO_2
Intestine 2		0,00	0,00	0,00	0,67	99,33	CO_2
Aorta	0,7 mL	0,00	0,00	78,97	0,86	20,18	N_2>> CO_2

40minAE	Remarks	% H_2	% O_2	% N_2	% CH_4	% CO_2	
Intestine 1		0	0	17	0,459	82,54	CO_2>>N_2
R. Heart	4,5 mL	0	2,38	84,8	0,097	12,76	N_2>> CO_2
R. Heart	3,5 mL	0	0	74,1	0,105	25,76	N_2>> CO_2
L. Heart	1 mL	0	0	72,5	0,243	27,22	N_2>> CO_2

1hAE	Remarks	% H_2	% O_2	% N_2	% CH_4	% CO_2	
Intestine 1		4,55	0,00	68,15	0,43	26,87	N_2>CO_2 >H_2
Intestine 2		0,00	0,00	7,66	1,71	90,62	CO_2>>N_2
R. Heart	4 mL	0,00	1,63	80,04	0,12	18,22	N_2>> CO_2
L. Heart	0,2 mL	0,00	0,00	76,11	0,14	23,74	N_2>> CO_2

3hAE	Remarks	% H_2	% O_2	% N_2	% CH_4	% CO_2	
Intestine 1	SH_2	0,00	0,00	24,10	0,16	75,74	CO_2 >>N_2
Intestine 2		0,00	0,00	0,00	0,00	100,00	CO_2
R. Heart	2,6 mL	0,00	2,73	78,13	1,48	17,66	N_2>> CO_2
L. Heart	0,5 mL	0,00	19,73	80,09	0,18	0,00	Air polluted

(Follow up) Table 10.2: Gas sample composition of each animal expressed in percentages. In the last column it is represented the contribution of each gas to the total composition.

6hAE	Remarks	% H_2	% O_2	% N_2	% CH_4	% CO_2	
Intestine 1	SH_2	0,00	0,00	25,05	0,12	74,82	CO_2>> N_2
Intestine 2		0,00	0,00	0,00	0,00	0,00	Empty
Intestine 3	SH_2	0,00	0,00	24,02	0,12	75,86	CO_2>> N_2
R. Heart	2,2 mL	0,00	0,00	74,93	0,80	24,26	N_2>> CO_2
Vena cava	0,8 mL	0,00	0,00	81,23	0,70	18,07	N_2>> CO_2

12hDCSA	Remarks	% H_2	% O_2	% N_2	% CH_4	% CO_2	
Intestine 2		0,00	1,23	72,09	4,48	22,20	N_2>> CO_2>CH_4
Intestine 3		43,59	0,00	15,15	1,06	40,20	H_2≈CO_2> N_2
R. Heart	1,3 mL	0,00	0,00	75,98	0,65	23,37	N_2>> CO_2
R. Heart	4,7 mL	0,00	0,00	76,94	0,80	22,26	N_2>> CO_2
L. Heart	0,2 mL	0,00	0,00	80,79	0,37	18,84	N_2>> CO_2
Cava v.	1 mL	0,00	0,00	75,09	0,62	24,29	N_2>> CO_2
Cava v.	1 mL	0,00	0,00	74,09	0,57	25,34	N_2>> CO_2
Cava v.	1 mL	0,00	0,00	75,68	0,59	23,73	N_2>> CO_2

27hAE	Remarks	% H_2	% O_2	% N_2	% CH_4	% CO_2	
R. Heart	0,1 mL	0,00	0,00	64,23	0,56	35,21	N_2> CO_2
L. Heart	0,6 mL	0,00	0,00	59,48	2,41	38,11	N_2> CO_2

42hAE	Remarks	% H_2	% O_2	% N_2	% CH_4	% CO_2	
R. Heart	0,8 mL	0,00	0,00	65,31	1,03	33,66	N_2> CO_2
Cava v.	0,6 mL	0,00	0,00	64,91	4,74	30,35	N_2> CO_2
Cava v.	1 mL	10,80	0,00	57,05	5,00	27,15	N_2> CO_2> H_2>CH_4
Cava v.	0,9 mL	5,33	0,00	49,03	4,85	40,79	N_2> CO_2> H_2≈CH_4

(Follow up) Table 10.2: Gas sample composition of each animal expressed in percentages. In the last column it is represented the contribution of each gas to the total composition.

53hAE	Remarks	% H_2	% O_2	% N_2	% CH_4	% CO_2	
Intestine 1		37,76	0,00	13,50	5,25	43,49	CO_2≈ H_2>N_2> CH_4
Intestine 2		37,51	1,61	15,27	4,91	40,69	CO_2≈ H_2>N_2> CH_4
Intestine 3		40,94	0,00	12,91	5,25	40,90	CO_2≈ H_2>N_2> CH_4
Intestine 4		14,57	0,00	11,34	13,73	60,36	CO_2> H_2≈N_2≈ CH_4
R. Heart	Accident	0,00	19,56	77,67	0,02	2,75	Air polluted
R. Heart	0,6 mL	39,37	0,00	25,40	1,01	34,22	H_2≈CO_2 >N_2
R. Heart	Accident	0,00	19,55	78,18	0,02	2,26	Air polluted
L. Heart	1,1 mL	10,79	11,65	59,96	0,20	17,40	N_2> CO_2>O_2≈ H_2
Cava v.	1 mL SH_2	21,13	0,00	18,38	0,57	59,93	CO_2> H_2≈N_2
Cava v.	1 mL	53,97	0,00	44,73	1,30	0,00	H_2≈ N_2
Cava v.	0,6 mL	34,52	0,00	43,89	0,93	20,66	N_2>H_2>CO_2
Emphysema abdominal cavity	0,2 mL	26,03	0,00	0,00	2,62	71,34	CO_2>H_2

67hAE	Remarks	% H_2	% O_2	% N_2	% CH_4	% CO_2	
Intestine 1		0,00	0,00	10,28	26,54	63,18	CO_2> CH4> N_2
Intestine 2		2,44	0,00	15,79	28,05	53,72	CO_2> CH4> N_2
Intestine 3		3,85	0,00	19,88	30,76	45,50	CO_2> CH4> N_2
R. Heart	2,5 mL	35,00	0,00	18,93	3,85	42,23	CO_2> H2> N_2
R. Heart	0,7 mL	0,00	0,00	52,71	4,82	42,48	N_2> CO_2
L. Heart		0,00	0,00	43,58	2,17	54,25	CO_2>N_2
Cava v.	1 mL	0,00	0,00	0,00	0,00	0,00	Empty

10.1.3 GAS ANALYSIS RESULS OF THE COMPRESSION / DECOMPRESSION MODEL

71 gas samples were obtained in total. A summary of average mole fraction expressed as a percentage of gas composition of samples of each animal can be observed bellow. Animals not represented here had no gas samples were recovered successfully.

Table 10.3: Gas sample composition of each animal expressed in percentages. In the last column it is represented the contribution of each gas to the total composition.

0hDCSB	Remarks	% H_2	% O_2	% N_2	% CH_4	% CO_2	
R. Heart	3 mL	0,00	0,00	73,27	0,14	26,58	N_2>> CO_2
R. Heart	1 mL	0,00	0,00	68,39	0,14	31,46	N_2>> CO_2
L. Heart	0,6 mL	0,00	3,89	77,47	0,18	18,45	N_2>> CO_2>O_2

20minDCSA	Remarks	% H_2	% O_2	% N_2	% CH_4	% CO_2	
Intestine 1		0,00	0,93	26,20	64,98	7,89	CH_4> N_2> CO_2
R. Heart	3 mL	0,00	3,29	88,64	0,14	7,94	N_2>> CO_2>O_2
L. Heart	0,25 mL	0,00	0,00	43,94	0,17	55,89	CO_2≈ N_2
Vena cava	0,25 mL	0,00	0,00	0,00	2,17	97,83	CO_2

20minDCSB	Remarks	% H_2	% O_2	% N_2	% CH_4	% CO_2	
Intestine 1		0,00	0,00	0,00	0,00	0,00	Empty
R. Heart	1 mL	0,00	16,00	77,59	0,00	6,41	N_2>> O_2> CO_2

40minDCSB	Remarks	% H_2	% O_2	% N_2	% CH_4	% CO_2	
R. Heart	3 mL	0,00	3,54	85,62	0,60	10,24	N_2>> CO_2
R. Heart	2,5 mL	0,00	4,03	85,53	0,52	9,91	N_2>> CO_2
R. Heart	1 mL	0,00	0,00	89,04	4,00	6,96	N_2>> CO_2
L. Heart	1 mL	0,00	0,00	63,18	1,41	35,42	N_2> CO_2
Vena cava	0,38 mL	0,00	2,31	47,06	2,09	48,55	CO_2≈ N_2>O_2

1hDCSA	Remarks	% H_2	% O_2	% N_2	% CH_4	% CO_2	
Intestine		0,00	0,00	8,43	0,10	91,47	CO_2> N_2
R. Heart	4 mL	0,00	2,14	76,25	0,87	20,74	N_2>> CO_2>O_2
L. Heart	1,2 mL	0,00	14,52	79,47	0,14	5,87	N_2>> O_2> CO_2
Vena cava	3 mL	0,00	1,30	63,04	1,16	34,50	N_2> CO_2>O_2
Vena cava	2,5 mL	0,00	2,85	63,75	1,06	32,34	N_2> CO_2>O_2

(Follow up) Table 10.3: Gas sample composition of each animal expressed in percentages. In the last column it is represented the contribution of each gas to the total composition.

1hDCSB	Remarks	% H_2	% O_2	% N_2	% CH_4	% CO_2	
Intestine		0,00	0,00	12,82	0,08	87,10	CO_2> N_2
R. Heart	2,9	0,00	0,88	79,94	0,17	19,00	N_2>> CO_2>O_2
L. Heart	microbubbles	0,00	0,00	0,00	0,00	0,00	Empty
Vena cava	1	0,00	3,57	62,22	0,24	33,96	N_2> CO_2>O_2
Vena cava	0,24	0,00	13,75	74,82	0,16	11,27	N_2>> CO_2≈O_2

3hDCSB	Remarks	% H_2	% O_2	% N_2	% CH_4	% CO_2	
Intestine		0,00	0,00	0,00	0,00	0,00	Empty
R. Heart	3,5 mL asp.	0,00	5,07	80,36	1,95	12,62	N_2>> CO_2>O_2
L. Heart	1 mL asp.	0,00	5,79	78,03	2,05	14,13	N_2>> CO_2>O_2
Vena cava	1,2 mL asp.	0,00	4,52	66,16	1,71	27,61	N_2>> CO_2>O_2
Vena cava	0,28	0,00	0,00	69,00	10,31	20,69	N_2>> CO_2> CH_4
Vena cava	0,22	0,00	11,19	77,83	4,08	6,90	N_2>> O_2> CO_2

6hDCS	Remarks	% H_2	% O_2	% N_2	% CH_4	% CO_2	
R. Heart (A)	0.1 mL	0,00	11,73	55,63	21,67	10,97	N_2> CH_4>O_2≈CO_2
Intestine (B)		0,00	0,00	38,94	14,57	46,49	CO_2>N_2> CH_4
R. Heart (B)	0.35 mL	0,00	17,27	73,84	0,00	8,89	N_2>> O_2> CO_2

12hDCSA	Remarks	% H_2	% O_2	% N_2	% CH_4	% CO_2	
Intestine 1		0,00	2,02	20,35	13,47	64,16	CO_2>>N_2> CH_4>O_2
R. Heart	5 mL	0,00	1,57	37,94	1,95	58,54	CO_2> N_2>O_2
R. Heart	3,5 mL	0,00	1,59	37,82	1,94	58,65	CO_2> N_2>O_2
R. Heart	3,3 mL	0,00	1,54	38,30	1,96	58,20	CO_2> N_2>O_2
L. Heart	0,6 mL	0,00	0,00	57,08	2,28	40,64	N_2> CO_2
Vena cava	1 mL	0,00	5,65	52,58	1,71	40,06	N_2> CO_2>O_2
Vena cava	1 mL	0,00	5,72	53,52	1,72	39,04	N_2> CO_2>O_2
Vena cava	1,1 mL	0,00	7,29	55,92	1,55	35,24	N_2> CO_2>O_2
Vena cava	0,4 mL	0,00	30,45	67,43	0,09	2,03	N_2> O2> CO_2
Vena cava	1 mL	0,00	3,01	29,71	0,95	66,33	CO_2> N_2>O_2
Vena cava	1 mL	26,44	0,00	30,26	1,54	41,76	CO_2> N_2>H_2
Vena cava	1 mL	27,17	0,00	30,77	1,09	40,98	CO_2> N_2>H_2

(Follow up) Table 10.3: Gas sample composition of each animal expressed in percentages. In the last column it is represented the contribution of each gas to the total composition.

12hDCSB	Remarks	% H_2	% O_2	% N_2	% CH_4	% CO_2	
Intestine 1		0,00	0,00	24,08	8,82	67,09	CO_2> N_2>CH_4
R. Heart	0,25 mL	0,00	11,57	74,97	0,39	13,08	N_2>> CO_2≈ O_2

27hDCSA	Remarks	% H_2	% O_2	% N_2	% CH_4	% CO_2	
Intestine 1		0,00	0,00	0,00	4,14	95,86	CO_2>> CH_4
R. Heart	0,25 mL	0,00	16,82	76,46	0,19	6,54	N_2>> O2 ≈ CO_2

27hDCSB	Remarks	% H_2	% O_2	% N_2	% CH_4	% CO_2	
Intestine		0,00	0,00	21,86	12,67	65,46	CO_2> N_2>CH_4
R. Heart	2,5	0,00	2,29	57,28	3,08	37,35	N_2> CO_2>O_2
R. Heart	0,5	0,00	8,95	63,41	1,79	25,84	N_2>> CO_2>O_2
Vena cava	0,1 mL	0,00	16,41	71,37	0,79	11,43	N_2>> O_2>CO_2
Vena cava	0,5 mL	0,00	9,28	63,10	2,20	25,42	N_2>> CO_2> O_2
Vena cava	0,35 mL	0,00	11,14	65,30	1,37	22,19	N_2>> CO_2> O_2
Vena cava	0,7 mL	0,00	9,46	61,12	1,81	27,61	N_2>> CO_2> O_2

42hDCSA	Remarks	% H_2	% O_2	% N_2	% CH_4	% CO_2	
Intestine		0,00	0,00	27,44	9,59	62,97	CO_2> N_2>CH_4
R. Heart	2,8 mL	23,77	7,68	39,53	0,89	28,14	N_2> CO_2>O_2
R. Heart	2,7 mL	24,13	7,07	38,79	0,88	29,13	N_2>CO_2>O_2
L. Heart	0,6 mL	22,55	0,00	36,39	0,89	40,18	CO_2>N_2> O_2
Vena cava	0,6 mL asp.	23,01	0,00	39,59	0,96	36,45	N_2>> CO_2> O_2

42hDCSB	Remarks	% H_2	% O_2	% N_2	% CH_4	% CO_2	
Intestine		0,00	1,24	17,21	14,03	67,52	N_2>> CO_2
R. Heart	0,25	0,00	13,90	73,20	0,41	12,50	N_2>> CO_2≈ O_2
L. Heart	microbubbles	0,00	15,75	75,03	0,00	9,22	N_2>> O2≈ CO2

(Follow up) Table 10.3: Gas sample composition of each animal expressed in percentages. In the last column it is represented the contribution of each gas to the total composition.

67hDCSB	Remarks	% H_2	% O_2	% N_2	% CH_4	% CO_2	
Intestine		0,00	0,00	32,44	10,11	57,45	CO_2> N_2>CH_4
R. Heart	2	0,00	2,43	51,21	3,11	43,25	N_2> CO_2>O_2
L. Heart	0,4	0,00	0,00	66,75	4,32	28,92	N_2> CO_2
Vena cava	1	0,00	0,00	45,94	2,31	51,74	N_2≈CO_2
Vena cava	1	0,00	0,00	51,31	2,34	46,35	N_2≈CO_2
Vena cava	1	0,00	0,00	43,23	2,29	54,48	N_2≈CO_2
Vena cava	0,74	0,00	7,94	84,16	0,30	7,59	N_2> CO_2≈O_2

10.2 GAS COMPOSITION RESULTS OF STRANDED CETACEANS (CHAPTER IV)

Gas composition is summarized as percentage of the mole fraction.

In many cases blood was recovered from the heart. When using the aspirometer, it could be seen how only blood was being suctioned, thus there are no gas samples of the heart in these cases. If the sample was taken directly with vacuum tubes and little blood entered the tube, the headspace was analyzed, but considered as the headspace of the blood and not as free gas found inside the heart (although some gas might have entered into the tube together with the blood). If there was too much blood inside the tube, it was not analyzed for protecting the gas-tight syringes and the column of the gas cromatograph. On the other hand, if the heart was not sampled because of special circumstances, this is clearly stated below the corresponding table.

On the last box of the table, gas composition is summarized in degrees of gases contribution to the total amount. If a gas was found in concentrations higher than twice the following major compound, this was represented with a double symbol: “>>”. When an atmospheric air composition was found this was indicated besides the gas compounds. Since atmospheric concentrations of CO2 are too small to be detected by gas chromatography, it was used as an indicative of gases stem inside the carcass. But if it was found in very low concentrations and there was a very similar atmospheric air composition, air pollution was suggested as a plausible phenomenon. Additionally, very small gas samples are indicated below the corresponding table. These samples have only one gas compound in concentrations slightly higher than the established detection limit, typically CO_2 or H_2. Since the background of the vacuum tubes contains mainly O_2 and N_2, their detection limit is always higher than CO_2 and H_2. Thus, when these conditions were met, the sample was identified as very little and not considered representative of its original composition.

SH_2 was not quantified, but identified qualitatively. When found, it is noted in the remarks.

Volume of bubbles sampled with the insulin syringe is reported in mL in the remarks box. If a sample was taken with the aspirometer, this is note with “asp” together with the volume of gas recovered.

10.2.1 GAS ANALYSIS RESULTS FOR THE NON-DEEP DIVING SPECIES

222 gas samples were obtained. A summary of average mole fraction expressed as a percentage of gas composition of samples of each animal can be observed bellow. Samples were arranged following the same order as in the graphs of free gas abundance in tissues and veins: first by decomposition code and then by gas abundance in tissues.

10.2.1.1 With decomposition code 1

Table 10.4: Gas sample composition of each animal with decomposition code 1 expressed in percentages. In the last column it is represented the contribution of each gas to the total composition.

CET 362 *S. frontalis*	Remarks	% H_2	% O_2	% N_2	% CH_4	% CO_2	
Aorta	Blood	0	20	80	0	0	Air

* The heart was not sampled. Only scarce and small bubbles were observed in the lumbo-caudal venous plexus.

10.2.1.2 With decomposition code 2

Table 10.5: Gas sample composition of each animal with decomposition code 2 expressed in percentages. In the last column it is represented the contribution of each gas to the total composition.

CET 371 *S. frontalis*	Remarks	% H_2	% O_2	% N_2	% CH_4	% CO_2	
Intestine		45	0	0	0	55	CO_2>H_2
R. Heart	Blood	34	0	0	0	66	CO_2>H_2
L. Heart	Blood	22	0	13	0	65	CO_2>H_2> N_2
Porta v.	Blood	43	0	0	0	57	CO_2>H_2
Torax		0	0	0	0	0	Empty

*Only blood was recovered from the heart. No bubbles were observed.

CET 380 *S.coeruleoalba*	Remarks	% H_2	% O_2	% N_2	% CH_4	% CO_2	
Intestine		0	20	79	0	0	Air
R. Heart	Blood	99	0	0	0	1	H_2>> CO_2
L. Heart		0	29	71	0	0	Air

*No gas was recovered from the heart. No bubbles were observed.

CET 393 *S. frontalis*	Remarks	% H_2	% O_2	% N_2	% CH_4	% CO_2	
Intestine		2	0	62	0	37	N_2> CO_2> H_2
R. Heart		0	0	0	0	0	Empty

*No gas was recovered from the heart. No bubbles were observed.

CET 413 *P. crassidens*	Remarks	% H_2	% O_2	% N_2	% CH_4	% CO_2	
Intestine		2	0	73	0	25	N_2>> CO_2> H_2
R. Heart	Blood	0	0	40	0	60	CO_2 >N_2
L. Heart		0	21	79	0	0	Air

*No gas was recovered from the heart. Probably there was air pollution during sampling in the left heart and intestine. No bubbles were observed.

CET 418 *S. frontalis*	Remarks	% H_2	% O_2	% N_2	% CH_4	% CO_2	
Intestine		2	19	79	0	1	Air polluted?
R. Heart	Blood	1	0	80	0	20	N_2>> CO_2> H_2

*Only blood was recovered from the heart. No bubbles were observed.

(Follow up) Table 10.5: Gas sample composition of each animal with decomposition code 2 expressed in percentages. In the last column it is represented the contribution of each gas to the total composition.

CET 421 *S. frontalis*	Remarks	% H_2	% O_2	% N_2	% CH_4	% CO_2	
Intestine		0	0	0	0	0	Empty
R. Heart	Blood	0	6	61	0	33	N_2> CO_2>O_2
L. Heart		0	0	0	0	0	Empty

*No gas was recovered from the heart. No bubbles were observed.

CET 474 *S.coeruleoalba*	Remarks	% H_2	% O_2	% N_2	% CH_4	% CO_2	
Intestine		0	12	67	0	21	N_2>> CO_2≈ O_2
L. Heart		0	0	0	0	0	Empty

*No gas was recovered from the heart. No bubbles were observed.

CET 523 *B.acutorostrata*	Remarks	% H_2	% O_2	% N_2	% CH_4	% CO_2	
Intestine 1		0	0	34	0	66	CO_2> N_2
Intestine 2		16	0	19	0	65	CO_2> N_2 ≈ H_2
R. Heart	Blood	0	0	34	0	66	CO_2> N_2
L. Heart		0	0	94	0	6	N_2>> CO_2
Aorta		0	15	74	0	10	N_2>> CO_2≈ O_2

*No bubbles were observed.

CET 530 *S. frontalis*	Remarks	% H_2	% O_2	% N_2	% CH_4	% CO_2	
Intestine 1		30	0	3	0	67	CO_2> H_2> N_2
Intestine 2		34	0	13	0	53	CO_2> H_2> N_2
L. Heart		0	21	79	0	0	Air
Aorta	Blood	0	0	51	0	49	N_2≈ CO_2
Emphysema	Aorta	0	20	80	0	0	Air

*No gas was recovered from the heart. No bubbles were observed.

CET 531 *S. frontalis*	Remarks	% H_2	% O_2	% N_2	% CH_4	% CO_2	
Intestine 2		0	0	73	0	27	N_2>> CO_2
Intestine 3		29	6	39	0	26	N_2>H2≈CO_2>O_2
R. Heart		0	0	0	0	0	Empty
L. Heart		0	22	77	0	0	Air

*No gas was recovered from the heart. No bubbles were observed.

(Follow up) Table 10.5: Gas sample composition of each animal with decomposition code 2 expressed in percentages. In the last column it is represented the contribution of each gas to the total composition.

CET 548 *S. frontalis*	Remarks	% H_2	% O_2	% N_2	% CH_4	% CO_2	
Intestine 2		0	0	52	0	48	$N_2 \approx CO2$
Intestine 3		0	0	35	0	64	$CO_2 > N_2$
R. Sinus		0	0	0	0	0	Empty
R. Heart		0	0	0	0	0	Empty

*No gas was recovered from the heart. No bubbles were observed.

CET 363 *S. frontalis*	Remarks	% H_2	% O_2	% N_2	% CH_4	% CO_2	
Intestine		0	0	0	0	0	Empty
R. Heart		0	0	0	0	0	Empty
L. Heart		0	0	0	0	0	Empty

*No gas was recovered from the heart. No bubbles were observed.

CET 373 *D. delphis*	Remarks	% H_2	% O_2	% N_2	% CH_4	% CO_2	
Intestine		0	21	79	0	0	Air
L. Heart		0	0	0	0	0	Empty
R. Heart	Blood	0	19	81	0	0	Air

*No gas was recovered from the heart. No bubbles were observed.

CET 376 *S.coeruleoalba*	Remarks	% H_2	% O_2	% N_2	% CH_4	% CO_2	
Intestine		68	0	0	0	32	$CO_2 > H_2$
R. Heart	Blood	69	0	0	0	31	$CO_2 > H_2$
L. Heart		100	0	0	0	0	H_2

*Very little gas was recovered from the left heart. No bubbles were observed.

CET 395 *S. frontalis*	Remarks	% H_2	% O_2	% N_2	% CH_4	% CO_2	
Intestine		0	0	0	0	0	Empty
R. Heart	Blood	0	21	79	0	0	Air
L. Heart		0	0	0	0	0	Empty

*No gas was recovered from the heart. No bubbles were observed.

(Follow up) Table 10.5: Gas sample composition of each animal with decomposition code 2 expressed in percentages. In the last column it is represented the contribution of each gas to the total composition.

CET 419 *S.bredanensis*	Remarks	% H_2	% O_2	% N_2	% CH_4	% CO_2	
Intestine		0	19	81	0	0	Air
R. Heart	Blood	0	18	80	0	2	Air polluted?
L. Heart	Blood	0	0	81	0	19	N_2>> CO_2

*Only blood was recovered from the heart. No bubbles were observed.

CET 476 *S.coeruleoalba*	Remarks	% H_2	% O_2	% N_2	% CH_4	% CO_2	
R. Heart		0	19	81	0	0	Air
L. Heart		0	0	0	0	0	Empty

*No gas was recovered from the heart (gas analyzed in the right heart is the head space from the blood). No bubbles were observed.

CET 515 *S. frontalis*	Remarks	% H_2	% O_2	% N_2	% CH_4	% CO_2	
Intestine 1		0	0	0	0	0	Empty
Intestine 2		0	0	0	0	0	Empty
R. Heart		0	0	0	0	0	Empty
L. Heart		0	0	0	0	0	Empty

*No gas was recovered from the heart. Scarce and small bubbles were only observed in the mesenteric veins.

CET 400 *S.coeruleoalba*	Remarks	% H_2	% O_2	% N_2	% CH_4	% CO_2	
Intestine		39	0	0	0	61	CO_2> H2
R. Heart	Blood	0	0	0	0	100	CO_2
L. Heart		0	0	0	0	0	Empty

*Very little gas was recovered from the right heart. No bubbles were observed.

CET 517 *D. delphis*	Remarks	% H_2	% O_2	% N_2	% CH_4	% CO_2	
Intestine 1		0	0	29	0	71	CO_2>>N_2
Intestine 2		0	0	42	0	58	CO_2>N_2
Intestine 3	SH_2!!!	46	0	7	0	47	CO_2≈ H_2>N_2
Emphysema Kidney		14	2	44	0	40	N_2≈ CO_2>H_2>O_2
Torax	SH_2!!!	33	0	22	0	45	CO_2> H_2> N_2

*Only blood was recovered from the heart. No bubbles were observed.

(Follow up) Table 10.5: Gas sample composition of each animal with decomposition code 2 expressed in percentages. In the last column it is represented the contribution of each gas to the total composition.

CET 526 *T. truncatus*	Remarks	% H_2	% O_2	% N_2	% CH_4	% CO_2	
Intestine 1	SH_2!!!	36	0	0	0	64	CO_2>H_2
Intestine 2		26	0	9	0	64	CO_2>>H_2>N_2
L. Heart	Blood	0	0	0	0	100	CO_2
Mesenteric v.	0.3 mL	0	0	0	0	0	Empty

*Only blood was recovered from the heart. Scarce and small bubbles were only observed in the mesenteric veins.

I 344/07 *O. byronia*	Remarks	% H_2	% O_2	% N_2	% CH_4	% CO_2	
Torax		0	6	81	0	13	N_2>>CO_2>O_2
Emphysema subcutaneous		0	1	78	0	21	N_2>>CO_2>O_2
Distension of the oesophagus		0	4	74	0	21	N_2>>CO_2>O_2

*The heart was not sampled. Severe pneumomediastinum and subcutaneous emphysema was observed.

CET 473 S.bredanensis	Remarks	% H_2	% O_2	% N_2	% CH_4	% CO_2	
Intestine		0	0	0	0	100	CO_2
Mesenteric v.	0.4 mL	30	10	42	0	18	N_2>H_2>CO_2>O_2
Mesenteric v.	0.25 mL	19	13	55	0	12	N_2> H_2>O2≈CO2
Mesenteric v.	0.55 mL	24	10	46	0	19	N_2>H_2>CO_2>O_2
Mesenteric v.	0.15 mL	0	17	72	0	11	N_2>O_2>CO_2
torax		0	0	0	0	0	Empty
Sinus		0	0	82	0	18	N_2>>CO_2

*Only blood was recovered from the heart. Scarce and small bubbles were only observed in the mesenteric veins.

CET 537 *S.coeruleoalba*	Remarks	% H_2	% O_2	% N_2	% CH_4	% CO_2	
Intestine 2		0	0	0	0	0	Empty
L. Heart		0	0	0	0	0	Empty
Aorta		0	0	86	0	14	N_2>>CO_2
Pulmonary art.		0	0	84	0	16	N_2>>CO_2
R. Sinus		0	20	80	0	1	Air polluted?

*No gas was recovered from the heart but it was from aorta and pulmonary artery. Scarce and small bubbles were observed diffusely.

10.2.1.3 With decomposition code 3

Table 10.6: Gas sample composition of each animal with decomposition code 3 expressed in percentages. In the last column it is represented the contribution of each gas to the total composition.

CET 368 *S. frontalis*	Remarks	% H_2	% O_2	% N_2	% CH_4	% CO_2	
Intestine		0	0	53	0	47	$N_2 \approx CO_2$

*The heart was not sampled. No bubbles were observed.

CET 384 *S. frontalis*	Remarks	% H_2	% O_2	% N_2	% CH_4	% CO_2	
Intestine		58	3	12	0	27	$H_2 > CO_2 > N_2 > O_2$
R. Heart		66	2	9	0	23	$H_2 > CO_2 > N_2 \approx O_2$
L. Heart	Blood	0	0	34	0	66	$CO_2 > N_2$

*Gas was recovered from the heart successfully. No bubbles were observed.

CET 522 *S. frontalis*	Remarks	% H_2	% O_2	% N_2	% CH_4	% CO_2	
Intestine 1		0	0	0	0	0	Empty
Intestine 2		0	1	84	0	15	$N_2 > CO_2 > O_2$
Intestine 3		2	1	83	0	14	$N_2 > CO_2 > H_2$
Pulmonary art.	Asp! Accident with sampling!	0	17	82	0	1	Air polluted?
R. Sinus		0	0	80	0	20	$N_2 > CO_2$
L. Sinus		0	3	87	0	10	$N_2 > CO_2 > O_2$

*Only blood was recovered from the heart. No bubbles were observed.

CET 527 *S.coeruleoalba*	Remarks	% H_2	% O_2	% N_2	% CH_4	% CO_2	
Intestine 2		15	0	69	0	16	$N_2 > CO_2 \approx H_2$
Intestine 3		0	0	0	0	0	Empty
L. Heart		0	0	0	0	0	Empty
Aorta	Blood	0	14	80	0	6	$N_2 > O_2 > CO_2$

*Only blood was recovered from the heart, but gas was successfully sampled from the aorta. No bubbles were observed.

(Follow up) Table 10.6: Gas sample composition of each animal with decomposition code 3 expressed in percentages. In the last column it is represented the contribution of each gas to the total composition.

I 134/07 *O. byronia*	Remarks	% H_2	% O_2	% N_2	% CH_4	% CO_2	
Intestine		0	11	82	0	8	N_2>>O_2>CO_2
R. Heart	Blood	**0**	0	0	0	100	CO_2
L. Heart	Blood	60	0	17	0	24	H_2>CO_2>N_2

*Very little gas was recovered from the right heart. No bubbles were observed.

CET 375 *S.coeruleoalba*	Remarks	% H_2	% O_2	% N_2	% CH_4	% CO_2	
Intestine		100	0	0	0	0	CO_2
R. Heart	Blood	0	0	58	0	42	N_2>CO_2
L. Heart	Blood	76	0	23	0	1	H_2>>N_2>CO_2

*Only blood was recovered from the heart. No bubbles were observed.

CET 409 *S.coeruleoalba*	Remarks	% H_2	% O_2	% N_2	% CH_4	% CO_2	
Intestine		0	0	0	0	0	Empty
R. Heart	Blood	0	0	68	0	32	N_2>CO_2

*Only blood was recovered from the heart. No bubbles were observed.

CET 364 *D. delphis*	Remarks	% H_2	% O_2	% N_2	% CH_4	% CO_2	
Intestine		0	0	0	0	0	Empty
R. Heart		0	0	0	0	0	Empty
L. Heart		0	0	0	0	0	Empty
Aorta	Blood	0	0	77	0	23	N_2>>CO_2
Torax		0	19	81	0	0	Air

*No gas was recovered from the heart. Scarce and small bubbles were only observed in the lumbo-caudal venous plexus.

CET 374 *S.coeruleoalba*	Remarks	% H_2	% O_2	% N_2	% CH_4	% CO_2	
Intestine		53	0	18	0	29	H_2>CO_2>N_2
R. Heart		99	0	0	0	1	H_2>CO_2
L. Heart		100	0	0	0	0	H_2

*Very little gas was recovered from the heart. Scarce and small bubbles were observed in the coronary veins as well as in the lumbo-caudal venous plexus.

(Follow up) Table 10.6: Gas sample composition of each animal with decomposition code 3 expressed in percentages. In the last column it is represented the contribution of each gas to the total composition.

CET 382 *D. delphis*	Remarks	% H_2	% O_2	% N_2	% CH_4	% CO_2	
Intestine		46	0	13	0	40	$H_2 \approx CO_2 > N_2$
R. Heart	Blood	22	0	39	0	39	$N_2 \approx CO_2 > H_2$
L. Heart		0	0	0	0	0	Empty

*No gas was recovered from the heart. Scarce and small bubbles were only observed in the coronary veins.

CET 370 *S.coeruleoalba*	Remarks	% H_2	% O_2	% N_2	% CH_4	% CO_2	
Intestine		100	0	0	0	0	H_2
R. Heart	Blood	0	0	34	0	66	$CO_2 > N_2$
L. Heart	Blood	0	0	62	0	38	$N_2 > CO_2$
Aorta	Blood	0	14	82	0	4	$N_2 > O_2 > CO_2$

*Only blood was recovered from the heart. Scarce and small bubbles were only observed subcutaneously and in the lumbo-caudal venous plexus.

CET 469 *S.coeruleoalba*	Remarks	% H_2	% O_2	% N_2	% CH_4	% CO_2	
R. Heart		0	0	0	0	100	CO_2
Intestine		0	0	0	0	0	Empty
Coronary v.	0.2 mL	0	17	79	0	4	$N_2 > O_2 > CO_2$

*Very little gas was recovered from the heart. Scarce and small bubbles were observed diffusely.

CET 546 *S.coeruleoalba*	Remarks	% H_2	% O_2	% N_2	% CH_4	% CO_2	
Intestine 2		46	0	0	0	54	$CO_2 > H_2$
Intestine 3		44	0	6	0	50	$CO_2 > H_2 > N_2$
Coronary v.	0.8 mL	0	0	99	0	1	$N_2 >> CO_2$
Coronary v.	0.2 mL	0	12	82	0	6	$N_2 >> O_2 \approx CO_2$
Coronary v.	0.1 mL	0	16	82	0	2	Air polluted
Emphysema Kidney		6	15	66	0	13	$N_2 >> O_2 \approx CO_2 > H_2$

*Only blood was recovered from the heart. Small to large bubbles were observed diffusely.

(Follow up) Table 10.6: Gas sample composition of each animal with decomposition code 3 expressed in percentages. In the last column it is represented the contribution of each gas to the total composition.

CET 482 *D. delphis*	Remarks	% H_2	% O_2	% N_2	% CH_4	% CO_2	
Intestine		67	0	7	0	26	H_2>>CO_2>N_2
R. Heart	Blood	0	0	21	0	79	CO_2>>N_2
L. Heart		0	21	79	0	0	Air
Mesenteric v.	1 mL	47	4	22	0	27	H_2>CO_2≈N_2>O_2
Mesenteric v.	0.11 mL	41	8	39	0	13	H_2> N_2>CO_2>O_2
Mesenteric v.	0,5 mL	0	18	79	0	3	Air polluted

*Gas was recovered successfully from the right heart. Small to large bubbles were observed diffusely.

10.2.1.4 With decomposition code 4

Table 10.7: Gas sample composition of each animal with decomposition code 4 expressed in percentages. In the last column it is represented the contribution of each gas to the total composition.

CET 509 *T. truncatus*	Remarks	% H_2	% O_2	% N_2	% CH_4	% CO_2	
R. Heart		0	0	0	0	0	Empty
L. Heart		0	0	0	0	0	Empty
Pulmonary art.		0	0	0	0	0	Empty
Aorta		38	0	7	0	55	CO_2>H_2> N_2
Mesenteric v.	1 mL	29	5	18	0	49	CO_2>H_2>N_2>O_2
Mesenteric v.	1 mL	38	4	17	0	41	CO_2≈H_2>N_2>O_2
Mesenteric v.	0.65 mL	42	5	22	0	32	H_2 >CO_2>N_2>O_2
Emphysema Liver		42	0	0	0	58	CO_2>H_2

*No gas was recovered from the heart, but it was from aorta. Scarce and small bubbles were observed diffusely.

CET 506 *S. coeruleoalba*	Remarks	% H_2	% O_2	% N_2	% CH_4	% CO_2	
Intestine 3		0	0	0	0	0	Empty
R. Heart	SH_2!!! Asp.	0	0	30	0	70	N_2>CO_2
Intestine 2		0	0	62	0	38	N_2>CO_2
R. Sinus		0	18	79	0	3	Air polluted?
L. Sinus		0	19	77	0	4	Air polluted?

*Gas was successfully recovered from the right heart. Scarce and small bubbles were observed diffusely.

CET 430 *S. bredanensis*	Remarks	% H_2	% O_2	% N_2	% CH_4	% CO_2	
Intestine		18	4	16	0	62	CO_2>H_2>N_2>O_2
R. Heart		0	19	81	0	0	Air
Torax		20	4	15	0	61	CO_2>H_2>N_2>O_2

*No gas was recovered from the heart. Large bubbles were observed diffusely.

(Follow up) Table 10.7: Gas sample composition of each animal with decomposition code 4 expressed in percentages. In the last column it is represented the contribution of each gas to the total composition.

CET 460 *S.coeruleoalba*	Remarks	% H_2	% O_2	% N_2	% CH_4	% CO_2	
Intestine		10	0	22	4	64	N_2>CO_2
R. Heart		0	0	0	0	0	Empty
L. Heart		0	0	0	0	100	CO_2
Emphysema Lung		32	0	26	0	42	N_2>O_2>CO_2

*Very little gas was recovered from the left heart. Large bubbles were observed diffusely.

CET 369 *B. physalus*	Remarks	% H_2	% O_2	% N_2	% CH_4	% CO_2	
Intestine		25	0	0	0	75	CO_2>H_2
L. Heart		0	0	0	0	0	Empty
Aorta		69	0	0	0	31	H_2>CO_2

*No gas was recovered from the heart, but it was from the aorta. It could happen that the needle was not large enough to go through the heart wall. No data gas recorded regarding gas bubble presence.

CET 381 *D. delphis*	Remarks	% H_2	% O_2	% N_2	% CH_4	% CO_2	
Intestine		64	0	0	0	36	H_2>CO_2
R. Heart	blood	0	0	70	0	30	N_2>CO_2
L. Heart	blood	77	0	0	0	23	H_2>CO_2

*Only blood was recovered from the heart. No data gas recorded regarding gas bubble presence.

CET 425 *D. delphis*	Remarks	% H_2	% O_2	% N_2	% CH_4	% CO_2	
Intestine		0	0	0	0	0	Empty
R. Heart		0	0	0	0	0	Empty
L. Heart		0	0	0	0	0	Empty

*No gas was recovered from the heart. No data gas recorded regarding gas bubble presence.

10.2.1.5 With decomposition code 5

Table 10.8: Gas sample composition of each animal with decomposition code 5 expressed in percentages. In the last column it is represented the contribution of each gas to the total composition.

CET 372 *B. borealis*	Remarks	% H_2	% O_2	% N_2	% CH_4	% CO_2	
Intestine		0	0	0	0	100	CO_2
R. Heart		0	0	0	0	0	Empty
L. Heart		0	0	0	0	0	Empty

*No gas was recovered from the heart. It could happen that the needle was not large enough to go through the heart wall. Large bubbles were observed diffusely.

CET 434 *S. bredanensis*	Remarks	% H_2	% O_2	% N_2	% CH_4	% CO_2	
Intestine		0	4	16	0	80	CO_2>>N_2>O_2
R. Heart		0	17	73	0	10	Air polluted?
L. Heart		0	14	86	0	0	Air

*Gas recovered from the heart was probably mixed during sampling with atmospheric air. Large bubbles were observed diffusely.

CET 435 *S. frontalis*	Remarks	% H_2	% O_2	% N_2	% CH_4	% CO_2	
Intestine		0	0	0	0	0	Empty
R. Heart		0	0	0	0	0	Empty
L. Heart		0	0	0	0	0	Empty

*No gas was successfully recovered from the heart. Large bubbles were observed diffusely.

CET 437 *S. bredanensis*	Remarks	% H_2	% O_2	% N_2	% CH_4	% CO_2	
R. Heart		0	3	13	0	84	CO_2>>N_2>O_2
L. Heart		0	0	0	0	100	CO_2
Intestine		18	15	64	0	3	N_2>H_2≈O_2>CO_2

*Gas was successfully recovered from the heart. Large bubbles were observed diffusely.

(Follow up) Table 10.8: Gas sample composition of each animal with decomposition code 5 expressed in percentages. In the last column it is represented the contribution of each gas to the total composition.

CET 462 *S. frontalis*	Remarks	% H_2	% O_2	% N_2	% CH_4	% CO_2	
Intestine 1		0	0	0	0	0	Empty
Intestine 2		0	0	0	0	100	CO_2
Intestine 3		0	20	80	0	0	Air
L. Heart	Bad sampling	0	15	85	0	1	Air polluted?
Torax		0	0	89	0	11	N_2>>CO_2

*No gas was recovered from the heart. Large bubbles were observed diffusely.

CET 487 *S.coeruleoalba*	Remarks	% H_2	% O_2	% N_2	% CH_4	% CO_2	
Intestine		2	0	0	0	98	CO_2>>H_2
R. Heart		0	0	0	0	0	Empty
L. Heart		0	0	0	0	0	Empty
Mesenteric v.	1 mL	14	6	20	0	60	CO_2>N_2≈H_2>O_2
Mesenteric v.	1 mL	0	0	0	0	100	CO_2
Mesenteric v.	0.11 mL	0	0	0	0	100	CO_2
Mesenteric v.	0.05 mL	0	21	76	0	3	Air polluted
Pericardic sac		14	0	0	0	86	CO_2>>H_2

*No gas was recovered from the heart. Large bubbles were observed diffusely.

CET 505 *T. truncatus*	Remarks	% H_2	% O_2	% N_2	% CH_4	% CO_2	
Intestine		14	0	0	0	86	CO_2>>H_2
R. Heart		0	0	0	0	0	Empty
R. Atrium		21	0	0	0	79	CO_2>>H_2
Pulmonary art.		10	0	0	0	90	CO_2>>H_2
Coronary v.	1 mL	0	0	0	0	0	Empty
Mesenteric v.	1 mL	21	0	20	0	59	CO_2≈ H_2
Mesenteric v.	0.7 mL	0	0	0	0	0	Empty
Mesenteric v.	0.7 mL	0	19	78	0	3	Air polluted?
Mesenteric v.	0.7 mL	0	17	82	0	1	Air polluted?

*Gas was successfully recovered from the right atrium. Large bubbles were observed diffusely.

CET 367 *S.coeruleoalba*	Remarks	% H_2	% O_2	% N_2	% CH_4	% CO_2	
Torax		27	0	24	0	49	CO_2>H_2≈N_2

*****The heart was not sampled. The advanced decay hampered the observation of the veins.

(Follow up) Table 10.8: Gas sample composition of each animal with decomposition code 5 expressed in percentages. In the last column it is represented the contribution of each gas to the total composition.

CET 402 *S.coeruleoalba*	Remarks	% H_2	% O_2	% N_2	% CH_4	% CO_2	
Intestine		18	0	0	0	82	CO_2>>H_2
R. Heart		0	0	0	0	0	Empty
L. Heart		0	5	21	0	74	CO_2>N_2>O_2

*Gas was successfully recovered from the left heart. The advanced decay hampered the observation of the veins.

CET 438 *S. bredanensis*	Remarks	% H_2	% O_2	% N_2	% CH_4	% CO_2	
R. Heart		0	0	0	0	100	CO_2
L. Heart		0	34	66	0	0	Air

*Very little gas was recovered from the right heart. The advanced decay hampered the observation of the veins.

CET 543 *T. truncatus*	Remarks	% H_2	% O_2	% N_2	% CH_4	% CO_2	
R. Heart		0	0	0	0	0	Empty
L. Heart		0	0	0	0	0	Empty
Pulmonary art.		0	0	0	0	100	CO_2
R. Sinus		0	0	30	0	70	CO_2>>N_2
L. Sinus		0	21	71	0	8	Air polluted?

*Gas was not recovered from the heart but it was from the pulmonary artery. The advanced decay hampered the observation of the veins.

CET 552 *T. borealis*	Remarks	% H_2	% O_2	% N_2	% CH_4	% CO_2	
Intestine 1		4	0	0	0	96	CO_2>>H_2
Intestine 2		5	0	0	0	95	CO_2>>H_2
Intestine 3		0	0	0	10	90	CO_2>>CH_4
R. Heart		0	19	81	0	0	Air
L. Heart		0	0	50	0	50	CO_2≈N_2

*Gas was successfully recovered from the left heart. The advanced decay hampered the observation of the veins.

(Follow up) Table 10.8: Gas sample composition of each animal with decomposition code 5 expressed in percentages. In the last column it is represented the contribution of each gas to the total composition.

CET 521 *D. delphis*	Remarks	% H_2	% O_2	% N_2	% CH_4	% CO_2	
L. Heart		0	0	0	0	0	Empty
R. Heart		0	0	0	0	0	Empty
Pericardic sac		18	0	2	0	79	CO_2>>H_2>N_2

*Gas was not recovered from the left heart. No data gas recorded regarding gas bubble presence.

10.2.2 GAS ANALYSIS RESULTS OF THE DEEP DIVING SPECIES

274 gas samples were obtained from deep diving species A summary of average mole fraction expressed as a percentage of gas composition of samples of each animal can be observed bellow. The data was first segregated by genera or family as follows: *Kogiidae*, *Physeteridae, Globicephala*, *Grampus* and Ziphidae (includes the genera *Ziphius* and *Mesoplodon*,). Samples were arranged following the same criteria as in the graphs of free gas abundance in tissues and veins: first by decomposition code and then by gas abundance in tissues.

10.2.2.1 Gas analysis results of samples taken from *Kogiidae*

10.2.2.1.1 With decomposition code 1

Table 10.9: Gas sample composition of each *Kogia* included in the study with decomposition code 1 expressed in percentages. In the last column it is represented the contribution of each gas to the total composition.

CET 404	Remarks	% H_2	% O_2	% N_2	% CH_4	% CO_2	
Intestine		0	0	0	0	0	Empty
R. Heart		0	0	0	0	0	Empty
L. Heart		0	0	0	0	0	Empty

* No gas was recovered from the heart. No bubbles were observed.

10.2.2.1.2 With decomposition code 3

Table 10.10: Gas sample composition of each *Kogia* included in the study with decomposition code 3 expressed in percentages. In the last column it is represented the contribution of each gas to the total composition.

CET 397	Remarks	% H_2	% O_2	% N_2	% CH_4	% CO_2	
Intestine		22	0	17	0	61	$CO_2>N_2\approx O_2$
R. Heart		0	0	87	0	13	$N_2>>CO_2$
L. Heart		0	21	79	0	0	Air

*Gas was successfully recovered from the right heart. Small and scarce bubbles were only observed in the lumbo-caudal venous plexus.

CET 459	Remarks	% H_2	% O_2	% N_2	% CH_4	% CO_2	
Intestine		0	0	9	32	59	$CO_2>CH_4>N_2$
R. Heart		0	20	80	0	0	Air
L. Heart		0	21	79	0	0	Air

*No gas was recovered from the heart. . Small and scarce bubbles were only observed in the mesenteric veins and in the lumbo-caudal venous plexus,

10.2.2.1.3 With decomposition code 4

Table 10.11: Gas sample composition of each *Kogia* included in the study with decomposition code 4 expressed in percentages. In the last column it is represented the contribution of each gas to the total composition.

CET 542	Remarks	% H_2	% O_2	% N_2	% CH_4	% CO_2	
R. Heart		0	20	80	0	0	Air
R. Atrium		7	16	72	0	4	$N_2>O_2>H_2\approx CO_2$
L. Heart		0	21	79	0	0	Air
Pulmonary art.		12	0	69	0	19	$N_2>CO_2\approx H_2$

*Gas was successfully recovered from the right heart. Small and scarce bubbles were only observed in the lumbo-caudal venous plexus.

10.2.2.1 Gas analysis results of samples taken from *Physeteridae*

10.2.2.1.1 With decomposition code 1

Table 10.12: Gas sample composition of each *Physeter* included in the study with decomposition code 1 expressed in percentages. In the last column it is represented the contribution of each gas to the total composition.

CET 463	Remarks	% H_2	% O_2	% N_2	% CH_4	% CO_2	
Intestine		0	16	80	0	4	Air polluted?
R. Heart		0	0	0	0	0	Empty
L. Heart		0	0	76	0	24	N_2>>CO_2

* Gas was successfully recovered from the left heart. No bubbles were observed.

10.2.2.1.2 With decomposition code 2

Table 10.13: Gas sample composition of each *Physeter* included in the study with decomposition code 2 expressed in percentages. In the last column it is represented the contribution of each gas to the total composition.

I298/09	Remarks	% H_2	% O_2	% N_2	% CH_4	% CO_2	
Intestine		71	0	0	0	29	H_2>>CO_2
Torax		0	21	76	0	3	N_2>>O_2>CO_2
Coronary v.	0.15 mL	0	18	77	0	4	N_2>>CO_2
Coronary v.	0.15 mL	0	18	75	0	7	N_2>>O_2>CO_2
Coronary v.	1 mL	0	13	66	0	21	N_2>>CO_2>O_2
Coronary v.	1 mL	0	14	68	0	18	N_2>>CO_2≈O_2
Coronary v.	1 mL	0	14	66	0	20	N_2>>CO_2>O_2
Coronary v.	1 mL	0	15	69	0	16	N_2>>CO_2≈O_2
Coronary v.	1 mL	0	13	66	0	20	N_2>>CO_2>O_2

* The heart was not sampled. Few bubbles were only observed in the coronary veins.

(Follow up) Table 10.13: Gas sample composition of each *Physeter* included in the study with decomposition code 2 expressed in percentages. In the last column it is represented the contribution of each gas to the total composition.

I299/09	Remarks	% H_2	% O_2	% N_2	% CH_4	% CO_2	
Intestine		0	0	6	6	89	CO_2>>N_2≈CH_4
Subcutaneous v.	0.9 mL	0	0	0	0	0	Empty
Peritoneo		0	19	76	0	5	N_2>>O_2>CO_2
Coronary v.	1 mL	0	13	63	0	24	N_2>>CO_2>O_2
Coronary v.	1 mL	0	13	65	0	22	N_2>>CO_2>O_2
Coronary v.	1 mL	0	14	64	0	22	N_2>>CO_2>O_2
Coronary v.	1 mL	0	14	66	0	20	N_2>>CO_2>O_2
Coronary v.	0.5 mL	0	0	49	0	51	CO_2≈N_2

* The heart was not sampled. Large amount of bubbles were only observed in the coronary veins and few in the subcutaneous veins.

10.2.2.1.3 With decomposition code 3

Table 10.14: Gas sample composition of each *Physeter* included in the study with decomposition code 3 expressed in percentages. In the last column it is represented the contribution of each gas to the total composition.

I300/09	Remarks	% H_2	% O_2	% N_2	% CH_4	% CO_2	
Stomach		0	3	68	0	30	N_2>>CO_2>O_2
Intestine		0	0	19	26	55	CO_2>CH4>N_2
Emphysema Intestine		58	3	15	0	24	H_2>CO_2>N_2>O_2
Emphysema Intestine		58	2	10	0	29	H_2>CO_2>N_2>O_2
Coronary v.	1 mL	34	6	29	0	31	H_2≈CO_2≈N_2>O_2
Coronary v.	1 mL	36	5	25	0	34	H_2≈CO_2>N_2>O_2
Coronary v.	1 mL	30	8	36	0	26	N_2≈H_2>CO_2>O_2
Coronary v.	1 mL	31	7	33	0	29	N_2≈H_2≈CO_2>O_2
Coronary v.	1 mL	30	8	36	0	27	N_2≈H_2≈CO_2>O_2
Coronary v.	1 mL	37	5	24	0	34	H_2≈CO_2>N_2>O_2

* The heart was not sampled. Large amount of bubbles were only observed in the coronary and mesenteric veins.

10.2.2.1.4 With decomposition code 4

Table 10.15: Gas sample composition of each *Physeter* included in the study with decomposition code 4 expressed in percentages. In the last column it is represented the contribution of each gas to the total composition.

CET 520	Remarks	% H_2	% O_2	% N_2	% CH_4	% CO_2	
Intestine	SH_2!!!	47	0	0	0	53	$CO_2 \approx H_2$
Coronary v.	1 mL	39	0	19	0	42	$CO_2 \approx H_2 > N_2$
Coronary v.	1 mL	38	3	22	0	38	$CO_2 \approx H_2 > N_2 > O_2$
Coronary v.	1 mL	39	3	20	0	38	$H_2 \approx CO_2 > N_2 > O_2$
Coronary v.	1 mL	0	21	79	0	0	Air
Coronary v.	1 mL	45	0	12	0	43	$H_2 \approx CO_2 > N_2$
Mesenteric v.	1 mL	34	3	17	0	46	$CO_2 > H_2 > N_2 > O_2$

* The heart was not sampled. Large bubbles were observed diffusely.

10.2.2.1.5 With decomposition code 5

Table 10.16: Gas sample composition of each *Physeter* included in the study with decomposition code 5 expressed in percentages. In the last column it is represented the contribution of each gas to the total composition.

CET 544	Remarks	% H_2	% O_2	% N_2	% CH_4	% CO_2	
Intestine 1		0	0	0	0	0	Empty
Intestine 2	SH_2!!!	5	0	0	1	94	$CO_2 >> H_2 > CH_4$
Intestine 3	SH_2!!!	0	0	0	21	79	$CO_2 >> CH_4$

* The heart was not sampled. Large bubbles were observed diffusely.

10.2.2.1 Gas analysis results of samples taken from *Globicephala*

10.2.2.1.1 With decomposition code 1

Table 10.17: Gas sample composition of each *Globicephala macrorhynchus* included in the study with decomposition code 1 expressed in percentages. In the last column it is represented the contribution of each gas to the total composition.

CET 360	Remarks	% H_2	% O_2	% N_2	% CH_4	% CO_2	
Intestine		0	6	80	0	14	N_2>>CO_2
R. Heart	Blood	0	17	81	0	1	Air polluted?
Aorta		0	16	74	0	10	N_2>>O_2>CO_2

*No gas was recovered from the heart, but it was from the Aorta. No bubbles were observed.

10.2.2.1.2 With decomposition code 2

Table 10.18: Gas sample composition of each *Globicephala macrorhynchus* included in the study with decomposition code 2 expressed in percentages. In the last column it is represented the contribution of each gas to the total composition.

CET 339	Remarks	% H_2	% O_2	% N_2	% CH_4	% CO_2
¿?						

*Several samples were taken but no blanks were kept. Calculations could not be properly done.

10.2.2.1.3 With decomposition code 3

Table 10.19: Gas sample composition of each *Globicephala macrorhynchus* included in the study with decomposition code 3 expressed in percentages. In the last column it is represented the contribution of each gas to the total composition.

CET 390	Remarks	% H_2	% O_2	% N_2	% CH_4	% CO_2	
R. Heart		1	18	76	0	5	Air polluted?
L. Heart		25	0	10	0	64	CO_2>>H_2>N_2

*Gas was successfully recovered from the left heart. Scarce and small bubbles were observed in the coronary veins as well as in the lumbo-caudal venous plexus.

(Follow up) Table 10.19: Gas sample composition of each *Globicephala macrorhynchus* included in the study with decomposition code 3 expressed in percentages. In the last column it is represented the contribution of each gas to the total composition.

CET 512	Remarks	% H_2	% O_2	% N_2	% CH_4	% CO_2	
Intestine 1		37	0	0	0	63	CO_2>H_2
Intestine 2		0	0	0	0	0	Empty
L. Sinus		0	19	79	0	2	N_2>O_2>CO_2
Coronary v.	1 mL	0	0	0	0	100	CO_2
Coronary v.	1 mL	0	17	81	0	2	Air polluted
Mesenteric v.	1 mL	27	0	41	0	33	N_2>CO_2≈H_2
Mesenteric v.	1 mL	20	10	48	0	23	N_2>CO_2≈H_2>O_2
Mesenteric v.	1 mL	46	0	0	0	54	CO_2>H_2
Mesenteric v.	1 mL	55	0	0	0	45	CO_2>H_2
Peritoneo	1 mL	4	9	70	0	17	N_2>CO_2>H_2≈O_2
Peritoneo	0,8 mL	0	0	0	0	0	Empty
Plexo rep	1 mL	6	0	68	0	27	N_2>CO_2>H_2
Plexo rep	1 mL	7	0	66	0	27	N_2>CO_2>H_2
Vena Porta	1 mL	19	0	43	0	38	N_2≈CO_2>H_2
Rectal v.	1 mL	42	0	0	0	58	CO_2>H_2

*No gas was recovered from the heart, but it was from the Vena Porta. Bubbles were observed diffusely especially in the mesenteric and coronary veins.

10.2.2.1.4 With decomposition code 4

Table 10.20: Gas sample composition of each *Globicephala macrorhynchus* included in the study with decomposition code 4 expressed in percentages. In the last column it is represented the contribution of each gas to the total composition.

CET 464	Remarks	% H_2	% O_2	% N_2	% CH_4	% CO_2	
Intestine		24	0	4	0	72	CO_2>H_2>N_2
R. Heart		38	0	7	1	55	CO_2>H_2>N_2
L. Heart		34	0	12	0	55	CO_2>H_2>N_2

*Gas was successfully recovered from the heart. Bubbles were observed in the mesenteric veins and in the lumbo-caudal venous plexus but the rest of the veins were not properly studied.

(Follow up) Table 10.20: Gas sample composition of each *Globicephala macrorhynchus* included in the study with decomposition code 4 expressed in percentages. In the last column it is represented the contribution of each gas to the total composition.

CET 504	Remarks	% H_2	% O_2	% N_2	% CH_4	% CO_2	
Intestine		34	0	0	0	66	CO_2>H_2
R. Heart		21	0	18	0	61	CO_2>H_2≈N_2
L. Heart	Blood	18	0	0	0	82	CO_2>>H_2
Aorta		0	0	0	0	0	Empty
Mesenteric v.	1 mL	24	0	29	0	47	CO_2> N_2≈H_2
R. Sinus		0	19	80	0	2	N_2>O_2>CO_2

*Gas was successfully recovered from the right heart. Bubbles were observed in the mesenteric veins but the rest of the veins were not properly studied.

10.2.2.1.5 With decomposition code 5

Table 10.21: Gas sample composition of each *Globicephala macrorhynchus* included in the study with decomposition code 5 expressed in percentages. In the last column it is represented the contribution of each gas to the total composition.

CET 399	Remarks	% H_2	% O_2	% N_2	% CH_4	% CO_2	
Intestine		0	0	0	0	0	Empty
R. Heart		43	0	0	0	57	CO_2>H_2
Aorta		0	0	0	0	0	Empty

*Gas was successfully recovered from the right heart. Large amount of bubbles were diffusely observed.

CET 361	Remarks	% H_2	% O_2	% N_2	% CH_4	% CO_2	
R. Heart		0	19	81	0	0	Air
L. Heart		25	0	10	0	64	CO_2>>H_2>N_2

*Gas was successfully recovered from the left heart. The veins could not be clearly distinguished from the rest of the tissues.

10.2.2.1 Gas analysis results of samples taken from *Grampus grisseus*

10.2.2.1.1 With decomposition code 1

Table 10.22: Gas sample composition of each *Grampus* included in the study with decomposition code 1 expressed in percentages. In the last column it is represented the contribution of each gas to the total composition.

CET 534	Remarks	% H_2	% O_2	% N_2	% CH_4	% CO_2	
Intestine 1		0	0	0	0	100	CO_2
Intestine 2		7	0	73	0	20	N_2>> CO_2> H_2
Intestine 3		0	0	0	0	0	Empty
R. Sinus		0	0	64	0	36	N_2>> CO_2
Sinus izq		0	0	0	0	0	Empty
R. Heart	Asp.	0	6	79	0	14	N_2>> CO_2> O_2
Coronary v.	0.15 mL	0	0	98	0	2	N_2>> CO_2

* No gas was recovered from the left heart. No bubbles were observed, except for some few in the coronary veins.

10.2.2.1.2 With decomposition code 2

Table 10.23: Gas sample composition of each *Grampus* included in the study with decomposition code 2 expressed in percentages. In the last column it is represented the contribution of each gas to the total composition.

CET 431	Remarks	% H_2	% O_2	% N_2	% CH_4	% CO_2	
Intestine		0	4	86	0	10	N_2>> CO_2> O_2
R. Heart	Blood	0	0	0	0	100	Blood polluted
L. Heart	Blood	0	?	?	?	?	Blood polluted
Torax		0	4	83	0	13	N_2>> CO_2> O_2

*Only blood was recovered from the heart. No bubbles were observed. Possible pneumotorax.

(Follow up) Table 10.23: Gas sample composition of each *Grampus* included in the study with decomposition code 2 expressed in percentages. In the last column it is represented the contribution of each gas to the total composition.

CET 472	Remarks	% H_2	% O_2	% N_2	% CH_4	% CO_2	
Intestine		0	1	86	0	14	N_2>> CO_2> O_2
Emphysema	Kidney	0	17	82	0	2	Air pollution?
L. Heart		0	21	79	0	0	Air pollution

*Only blood was recovered from the heart. Probably there was air pollution during sampling in the left heart. No bubbles were observed.

CET 456	Remarks	% H_2	% O_2	% N_2	% CH_4	% CO_2	
Emphysema	Urine bladder	0	0	89	0	11	N_2>> CO_2
Emphysema	Stomach	0	3	83	0	14	N_2>> CO_2> O_2
Emphysema	Kidney	0	0	94	1	5	N_2>> CO_2
Emphysema	Liver	0	0	78	0	22	N_2>> CO_2
Lymphatic v.	0.32 mL	0	12	87	0	1	N_2>> CO_2> O_2

*Only blood was recovered from the heart. No bubbles were observed, but large emphysema was observed in different gases. In addition, gas was observed within the lymphatic vessels.

CET 483	Remarks	% H_2	% O_2	% N_2	% CH_4	% CO_2	
Intestine		7	0	43	0	51	CO_2> N2> H_2
R. Heart		0	0	52	0	48	N_2≈ CO_2> O_2
L. Heart		0	0	61	0	39	N_2> CO_2> O_2
Mesenteric v.		6	0	42	0	51	CO_2> N2> H_2

*Gas was recovered from both hearts. In addition, large amount of bubbles were found in the veins.

(Follow up) Table 10.23: Gas sample composition of each *Grampus* included in the study with decomposition code 2 expressed in percentages. In the last column it is represented the contribution of each gas to the total composition.

CET 456	Remarks	% H_2	% O_2	% N_2	% CH_4	% CO_2	
Intestine 2		0	0	0	0	0	Empty
Intestine 3		0	0	0	0	0	Empty
Thorax		0	0	84	0	16	N_2>> CO_2
Subcutaneous v.	0.10 mL	0	21	78	0	1	Air pollution?
Mesenteric v.	1 mL	0	8	61	0	31	N_2>> CO_2> O_2
Mesenteric v.	0.2 mL	0	0	81	0	19	N_2>> CO_2
Mesenteric v.	0.4 mL	0	9	74	0	17	N_2>> CO_2> O_2
Mesenteric v.	0.2 mL	0	11	78	0	11	N_2>> $CO_2 \approx O_2$
Mesenteric v.	0.5 mL (Asp)	0	16	80	0	4	N_2>> O_2> CO_2
Coronary v.	1 mL	0	6	74	0	20	N_2>> CO_2> O_2
Coronary v.	0.2 mL	0	9	77	0	13	N_2>> CO_2> O_2
Coronary v.	? mL	0	7	75	0	18	N_2>> CO_2> O_2
Coronary v.	3.2 mL (Asp)	0	5	87	0	8	N_2>> $CO_2 \approx O_2$
Aorta	Asp.	0	14	68	0	18	N_2>> $CO_2 \approx O_2$
Aorta	Asp.	0	14	67	0	19	N_2>> $CO_2 \approx O_2$
Aorta	Asp.	0	14	68	0	18	N_2>> $CO_2 \approx O_2$

*No gas was recovered from the heart, but large quantities of gas were recovered from the aorta (more than 100 mL). In addition, large amount of bubbles were found in all the screened veins.

10.2.2.1.3 With decomposition code 4

Table 10.24: Gas sample composition of each *Grampus* included in the study with decomposition code 4 expressed in percentages. In the last column it is represented the contribution of each gas to the total composition.

CET 533	Remarks	% H_2	% O_2	% N_2	% CH_4	% CO_2	
Intestine		41	0	0	0	59	CO_2> H_2
R. Heart	SH_2!!!	0	0	0	0	100	CO_2, SH_2
L. Heart		11	0	58	0	30	N_2> CO_2> H_2
Thorax		0	20	79	0	1	Air pollution?
Sinus		0	0	0	0	0	Empty
Mesenteric v.	1 mL	47	0	0	0	53	CO_2≈ H_2
Mesenteric v.	0,6 mL	83	0	0	0	17	H_2 >CO_2
Mesenteric v.	0,5 mL	77	0	0	0	23	H_2 >CO_2
Mesenteric v.	1 mL	30	0	45	0	25	N_2> H_2 > CO_2
Coronary v.	0,92 mL	5	16	74	0	6	Air polluted? / Mixture with putrefaction gases

Gas was successfully recovered from the heart. Bubbles were observed diffusely, especially in the mesenteric veins.

10.2.2.1 Gas analysis results of samples taken from *Ziphidae*

10.2.2.1.1 With decomposition code 2

Table 10.25: Gas sample composition of each *Ziphidae* included in the study with decomposition code 2 expressed in percentages. In the last column it is represented the contribution of each gas to the total composition.

CET 379 *M. bidens*	Remarks	% H_2	% O_2	% N_2	% CH_4	% CO_2	
Intestine		44	0	0	0	56	$CO_2>H_2$
R. Heart	Blood	0	17	77	0	6	$N_2>O_2>CO_2$
Torax		0	19	81	0	0	Air
Mesenteric v.		0	0	81	0	19	$N_2>>CO_2$
Peritoneum v.		0	0	0	0	100	CO_2
Renal v.		0	0	0	0	100	CO_2

*No gas was recovered from the heart. Very little gas was recovered from the bubbles of the peritoneum and renal veins. Scarce and small bubbles were observed diffusely.

CET 471 Z. cavirostris	Remarks	% H_2	% O_2	% N_2	% CH_4	% CO_2	
Intestine		34	0	3	0	63	$CO_2>H_2>N_2$
Stomach		35	0	3	0	62	$CO_2>H_2>N_2$
Torax		7	0	51	0	42	$N_2>CO_2>H_2$
Aorta		18	0	29	0	54	$CO_2>N_2>H_2$
L. Atrium		9	1	44	0	46	$CO_2\approx N_2>H_2$
L. Heart		0	19	76	0	5	Air polluted
Emphysema Liver		40	0	7	0	53	$CO_2>H_2>N_2$
Pleura v.		12	12	56	0	19	$N_2>CO_2\approx H_2\approx O_2$
Renal v.		27	8	33	6	26	$N_2\approx H_2\approx CO_2>O_2\approx CH_4$
Coronary v.	0.7 mL	25	10	42	0	23	$N_2>CO_2\approx H_2>O_2$
Coronary v.	1 mL	26	8	36	0	30	$N_2\approx CO_2\approx H_2>O_2$
Subcutaneous v.	0.1 mL	0	19	81	0	0	Air
Subcutaneous v.	0.8 mL	0	18	80	0	2	Air polluted
Subcutaneous v.	1 mL	0	19	79	0	2	Air polluted
Artifact	0.2 mL	8	17	68	0	7	Air polluted
Subcutaneous v.	0.2 mL	0	17	78	0	5	Air polluted

*Gas was successfully recovered from the left atrium and aorta. Scarce and small bubbles were observed diffusely. Very little gas was recovered from the bubbles of the peritoneum and renal veins.

10.2.2.1.2 With decomposition code 3

Table 10.26: Gas sample composition of each *Ziphidae* included in the study with decomposition code 3 expressed in percentages. In the last column it is represented the contribution of each gas to the total composition.

CET 510 *M. europaeus*	Remarks	% H_2	% O_2	% N_2	% CH_4	% CO_2	
Intestine		0	0	0	0	100	CO_2
R. Heart		0	0	0	0	0	Empty
L. Heart		0	21	79	0	0	Air
Pulmonary art.		0	0	0	0	0	Empty
L. Sinus		0	0	58	0	42	N_2>CO_2
R. Sinus		0	0	61	0	39	N_2>CO_2
Capsular	Liver	31	0	0	0	69	CO_2>H_2
Subescapular v.		0	0	0	0	100	CO_2
Mesenteric v.	0.15 mL	0	0	0	0	100	CO_2
Mesenteric v.	0.1 mL	0	0	0	0	100	CO_2
Mesenteric v.	0.1 mL	64	0	0	0	36	H_2>CO_2
Renal v.	0.45 mL	54	0	0	0	46	H_2>CO_2
Renal v.	0.2 mL	65	0	0	0	35	H_2>CO_2
Renal v.	0.1 mL	0	0	0	0	0	Empty
Coronary v.	0.2 mL	0	20	80	0	0	Air
Coronary v.	0.15 mL	34	0	0	0	66	CO_2>H_2

*No gas was recovered from the heart. Scarce and small bubbles were observed diffusely. Very little gas was recovered from the mesenteric and sub-scapular veins.

(Follow up) Table 10.26: Gas sample composition of each *Ziphiidae* included in the study with decomposition code 3 expressed in percentages. In the last column it is represented the contribution of each gas to the total composition.

i181/09 *M. bidens*	Remarks	% H_2	% O_2	% N_2	% CH_4	% CO_2	
Intestine	SH_2!!!	71	0	8	0	22	$H_2>CO_2>N_2$
Stomach		34	0	45	0	21	$N_2>H_2>CO_2$
L. Heart		0	22	77	1	0	Air
Art pulm	1 mL	57	2	37	0	4	$H_2>N_2>CO_2\approx O_2$
Mesenteric v.	1 mL	30	0	51	0	18	$N_2>H_2>CO_2$
Mesenteric v.	1 mL	50	6	31	0	13	$H_2>N_2>CO_2>O_2$
Mesenteric v.	1 mL	45	7	36	0	12	$H_2>N_2>CO_2>O_2$
Mesenteric v.	1 mL	54	6	33	0	7	$H_2>N_2>CO_2\approx O_2$
Mesenteric v.	1 mL	53	5	28	0	13	$H_2>N_2>CO_2>O_2$
Mesenteric v.	1 mL	28	11	50	0	10	$N_2>H_2>O_2\approx CO_2$
Mesenteric v.	0.98 mL	49	7	38	0	6	$H_2>N_2>O_2\approx CO_2$
Mesenteric v.	0.3 mL	50	7	37	0	5	$H_2>N_2>O_2\approx CO_2$
Mesenteric v.	0.2 mL	31	13	52	0	4	$N_2>H_2>O_2>CO_2$
Coronary v.	0.2 mL	28	11	57	0	4	$N_2>H_2>O_2>CO_2$
Coronary v.	0.6 mL	15	15	68	0	2	$N_2>H_2\approx O_2>CO_2$
R. Sinus		0	1	91	0	8	$N_2>>CO_2>O_2$
L. Sinus		0	1	90	0	9	$N_2>>CO_2>O_2$

*No gas was recovered from the heart due to problems with the aspirometer. Small and large bubbles were observed diffusely.

i182/09 *M. bidens*	Remarks	% H_2	% O_2	% N_2	% CH_4	% CO_2	
R. Heart	SH_2!!!	0	0	75	1	24	$N_2>>CO_2$
R. Atrium		0	17	83	0	0	Air
L. Atrium	SH_2!!!	40	0	41	0	19	$N_2\approx H_2>CO_2$
Intestine	SH_2!!!	71	0	0	0	29	$H_2>>CO_2$
Stomach	SH_2!!!	46	3	26	0	25	$H_2>N_2\approx CO_2>O_2$
Mesenteric v.	1 mL	74	0	0	0	26	$H_2>>CO_2$
Mesenteric v.	0.55 mL	27	13	50	0	10	$N_2>H_2>O_2\approx CO_2$
Mesenteric v.	0.3 mL	0	20	80	0	0	Air
Mesenteric v.	0.23 mL	0	20	80	0	0	Air
Mesenteric v.	0.15 mL	33	11	45	0	11	$N_2>H_2>O_2\approx CO_2$
Mesenteric v.	0.2 mL	0	21	75	0	5	Air polluted

*Gas was successfully recovered from the heart. Small and large bubbles were observed diffusely.

(Follow up) Table 10.26: Gas sample composition of each *Ziphiidae* included in the study with decomposition code 3 expressed in percentages. In the last column it is represented the contribution of each gas to the total composition.

i183/09 *M. bidens*	Remarks	% H_2	% O_2	% N_2	% CH_4	% CO_2	
Intestine		73	0	0	0	27	$H_2>>CO_2$
L. Heart		0	0	0	0	0	Empty
Aorta		0	0	0	0	0	Empty
Coronary v.	1 mL	57	4	17	0	22	$H_2>CO_2>N_2>O_2$
Coronary v.	0.35 mL	49	8	35	0	7	$H_2>N_2>O_2\approx CO_2$
Coronary v.	0.25 mL	33	12	48	0	7	$N_2>H_2>O_2\approx CO_2$
Coronary v.	0.9 mL	0	17	76	0	7	$N_2>O_2>CO_2$
Coronary v.	0.6 mL	0	0	86	0	14	$N_2>CO_2$
Coronary v.	0.11 mL	0	19	78	0	3	Air polluted
R. Sinus		0	0	91	0	9	$N_2>>CO_2$
L. Sinus		0	16	82	0	2	Air

*No gas was recovered from the heart due to problems with the aspirometer. Small and large bubbles were observed diffusely.

10.2.2.1.3 With decomposition code 4

Table 10.27: Gas sample composition of each *Ziphiidae* included in the study with decomposition code 4 expressed in percentages. In the last column it is represented the contribution of each gas to the total composition.

i184/09 *M. bidens*	Remarks	% H_2	% O_2	% N_2	% CH_4	% CO_2	
Intestine		0	0	0	0	0	Empty
Stomach		68	0	2	0	30	$H_2>CO_2>N_2$
R. Heart		67	0	15	0	18	$H_2>CO_2\approx N_2$
Mesenteric v.	1 mL	68	2	8	0	21	$H_2> CO_2>N_2\approx O_2$
Mesenteric v.	1 mL	75	0	0	0	25	$H_2>>CO_2$
Mesenteric v.	1 mL	45	8	32	0	15	$H_2>N_2>CO_2>O_2$
Mesenteric v.	1 mL	56	5	21	0	17	$H_2>N_2\approx CO_2>O_2$
Mesenteric v.	0.35 mL	59	6	21	0	14	$H_2>N_2>CO_2\approx O_2$
Mesenteric v.	0.28 mL	57	6	26	0	10	$H_2>N_2>CO_2>O_2$
Mesenteric v.	0.24 mL	43	9	42	0	5	$H_2\approx N_2>O_2\approx CO_2$
Coronary v.	0.6 mL	80	0	0	0	20	$H_2>>CO_2$
Coronary v.	0.35 mL	65	4	24	0	7	$H_2>N_2>CO_2\approx O_2$
Coronary v.	0.35 mL	53	7	34	0	6	$H_2>N_2>CO_2\approx O_2$
Coronary v.	0.11 mL	45	8	41	0	7	$H_2\approx N_2>CO_2\approx O_2$

*Gas was successfully recovered from the right heart. Small and large bubbles were observed diffusely.

(Follow up) Table 8.17: Gas sample composition of each *Ziphiidae* included in the study with decomposition code 4 expressed in percentages. In the last column it is represented the contribution of each gas to the total composition.

CET 547 *M. bidens*	Remarks	% H_2	% O_2	% N_2	% CH_4	% CO_2	
Intestine. 1	SH_2!!!	23	0	0	0	77	$CO>>_2H_2$
Intestine. 2		0	0	0	0	100	CO_2
Intestine. 3		0	0	0	0	0	Empty
L. Heart	0.1 mL	0	19	73	1	7	Air polluted
Sinus		0	0	82	0	18	$N_2>>CO_2$
Subcutaneous v.	0.2 mL	0	0	90	0	10	$N_2>>CO_2$
Subcutaneous v.	1 mL	4	5	71	0	20	$N_2>>CO_2>H_2\approx O_2$
Subcutaneous v.	0.1 mL	0	0	0	0	100	CO_2
Renal v.	0.9 mL	20	7	43	0	30	$N_2>CO_2>H_2>O_2$
Renal v.	0.75 mL	5	14	66	0	14	$N_2>CO_2\approx O_2>H_2$
Renal v.	0.8 mL	14	12	62	0	13	$N_2>H_2\approx CO_2\approx O_2$
Sub pleural v.	1 mL	16	7	39	0	38	$N_2\approx CO_2>H_2>O_2$
Sub pleural v.	1 mL	11	6	49	0	35	$N_2>CO_2>H_2>O_2$
Sub pleural v.	1 mL	19	6	26	0	48	$CO_2>N_2>H_2>O_2$
Mesenteric v.	1 mL	17	8	36	0	38	$CO_2\approx N_2>H_2>O_2$
Mesenteric v.	1 mL	41	0	0	0	59	$CO_2> H_2$
Mesenteric v.	1 mL	21	6	26	0	47	$CO_2>N_2\approx H_2>O_2$
Mesenteric v.	1 mL	24	0	22	0	55	$CO_2>H_2\approx N_2>O_2$
Mesenteric v.	1 mL	21	6	26	0	47	$CO_2>N_2\approx H_2>O_2$
Coronary v.	1 mL	0	0	74	0	26	$N_2>>CO_2$
Coronary v.	1 mL	25	0	32	0	43	$CO_2>N_2>H_2$
Coronary v.	1 mL	27	0	27	0	47	$CO_2>N_2\approx H_2$
Coronary v.	1 mL	29	0	21	0	50	$CO_2> H_2>N_2$
Coronary v.	1 mL	24	0	31	0	44	$CO_2>N_2>H_2$

*No gas was recovered from the heart. Large bubbles were observed diffusely.

10.2.2.1.4 With decomposition code 5

Table 8.17: Gas sample composition of each *Ziphiidae* included in the study with decomposition code 5 expressed in percentages. In the last column it is represented the contribution of each gas to the total composition.

i185/09 *M. bidens*	Remarks	% H_2	% O_2	% N_2	% CH_4	% CO_2	
Intestine		50	0	0	0	50	$H_2 \approx CO_2$
Stomach		52	0	2	0	46	$H_2 \approx CO_2 > N_2$
R. Sinus		14	0	62	0	24	$N_2 > CO_2 > H_2$
L. Sinus		0	0	70	0	30	$N_2 > CO_2$
Mesenteric v.	1 mL	46	4	18	0	31	$H_2 > CO_2 > N_2 > O_2$
Mesenteric v.	1 mL	36	0	12	0	53	$CO_2 > H_2 > N_2$
Mesenteric v.	1 mL	32	4	20	0	43	$CO_2 > H_2 > N_2 > O_2$
Mesenteric v.	1 mL	43	4	20	0	33	$H_2 > CO_2 > N_2 > O_2$
Mesenteric v.	1 mL	48	0	0	0	52	$CO_2 > H_2$
Mesenteric v.	1 mL	49	0	0	0	51	$CO_2 > H_2$
Mesenteric v.	1 mL	8	0	0	0	92	$CO_2 >> H_2$
Mesenteric v.	1 mL	35	0	13	0	52	$CO_2 > H_2 > N_2$
Mesenteric v.	0.58 mL	15	14	56	0	15	$N_2 > CO_2 \approx H_2 \approx O_2$

*No gas was recovered from the heart due to problems with the aspirometer. Large bubbles were observed diffusely.

11 AGRADECIMIENTOS/ACKNOWLEDGMENTS

Nunca se me ha dado bien escribir, y menos expresar mis sentimientos. No sé cómo reflejar mi agradecimiento a todas las personas que de distintos modos me han ayudado, apoyado, guiado, sufrido y disfrutado conmigo a lo largo de esta etapa de mi vida tan importante para mí. Pero si algo sé, es que soy muy afortunada.

I have never been good at writing, and even least at expressing my feelings. I don't know how to reflect my gratitude to all the people that in different manners have helped me, supported me, guided me, suffered and enjoyed with me along this stage in my life so important to me. But if I know something, is that I am very fortunate.

Soy afortunada por haber podido disfrutar de mucho más que un director de tesis, a la vez que tutor, con una mente privilegiada, sino de una persona cuya calidad humana supera con creces su extraordinaria mente. Una persona que ha confiado en mí más que yo misma, que ha apostado por mí, que se ha arriesgado conmigo, que siempre ha antepuesto mi bienestar y futuro a sus intereses personales, que ha sido en ocasiones casi como un padre, y que espero que haya disfrutado tanto de esta experiencia conjunta como yo lo he hecho. Por todo ello, le estaré siempre agradecida. Gracias Toño.

Soy afortunada por haber tenido además como codirector a otra persona de una gran calidad humana, una persona tan inteligente como optimista. Una persona que más allá de sus valiosos conocimientos fundamentales para el desarrollo de esta tesis, es experta en solucionar problemas, en subrayar los aspectos positivos sobre los negativos, las virtudes sobre los defectos. Una persona que en muchas ocasiones me ha desatascado, me ha sacado adelante, me ha enseñado a ver las cosas desde otras perspectivas. Gracias Óscar.

Soy afortunada por haber podido contar con la ayuda y guía de otra persona con una gran mente matemática, metódica, meticulosa y perfeccionista, pero sobretodo de una persona con una paciencia infinita siempre preocupada de que lo haya entendido y que ambos quedáramos satisfechos. Gracias Pedro.

Soy afortunada por haber tenido unos compañeros estupendos, cooperativos, dinámicos, con una gran mentalidad de equipo, y que crean un inmejorable ambiente de trabajo; unos con sus chistes, otros con sus comidas, otros con su alegría, etc.. En definitiva, personalidades dispares que conforman un equipo peculiar en un ambiente envidiable. Quiero agradecer a todo el personal que forma parte del IUSA y del departamento de histología y anatomía patológica y en especial a todos aquellos que en algún momento han pasado por el mundo de los cetáceos.

Soy afortunada por la ayuda y guía desinteresada prestada desde el primer día de mi llegada (cuando estaba más perdida que una perdiz) por alguien que estaba muy ocupado. A pesar de ello, se preocupó y se interesó por mí, y lo ha seguido haciendo durante todos estos años. Por ello, quiero darte especialmente las gracias Manolo.

Soy afortunada porque una grandísima compañera se convirtió con el paso del tiempo, en una amiga de verdad, de las que duran para todo la vida. Gracias Eva por haber sido mi compañera y amiga y haber compartido conmigo a nivel profesional y personal las distintas emociones de estos años de tesis. Estoy segura de que seguiremos compartiendo más momentos importantes para ambas en un futuro no muy lejano. Muchísimas gracias Eva.

Soy afortunada por contar con una compañera que a pesar “de ser madera”, mantiene el sentido de humor aún en los momentos de alto estrés y además se mantiene maquillada y estupenda hasta dentro de un cachalote! Gracias Simona por tu alegría.

I am very fortunate for having the honor to learn and discuss with Alf O. Brubakk whose broad knowledge about diving physiology and medicine have been key for the completion of this thesis. But this collaboration would have never been possible without the intervention of Andreas Møllerløkken whose enthusiasm (until the very last day of the completion of this thesis) and willing of collaboration made me possible to join a wonderful professional team and to learn from them. All the components of the Baromedical Research Group at the Norwegian University of Science and Technology gave me a warm welcome and put all their efforts in helping and teaching me about decompression sickness, thus all of them deserve at least my acknowledgments. I would like to thanks specially to Marianne Bjordal who has always being there for me, for teaching me much more things than decompression sickness like netting or cooking wafles ☺, but specially for making me feel at home. Thanks to Alf, Andreas, Marianne and to all the baromedical Group.

I would like to thanks Woods Hole Oceanographic Institute for providing a interdisciplinary discussion forum where to put things together and inviting us to participate actively in the discussion and to collaborate in the behavioral response Studies.

Thanks to Paul Jepson, for a continuous collaboration, for being a great colleague and for supporting and teaching me how to defend the decompression hypothesis in cetaceans in non-favorable environment.

I would like to thanks and congratulate as well to Mónica Almeida e Silva, Rui Petro, the volunteers and the authorities from Azores for allowing us to collaborate in the beaked whale mass stranding, for a magnificent stranding response and for taking so much care of us while we were there.

My acknowledgments and congratulations to Sandro Mazzariol, Giovani Di guardo and all the scientific researchers and volunteers, for a profitable collaboration and an

amazing efficient and coordinated stranding response to the mass stranding of sperm whales in the Adriatic coast of Southern Italy.

Soy muy afortunada por tener una familia a la que quiero y me quiere con locura. Una familia que igual sin entender mucho lo que hago o por qué lo hago, me apoya incondicionalmente, aún sabiendo que en la mayoría de los casos supone estar lejos de ellos. Gracias por entender que necesito crecer como persona de una manera distinta, gracias por entender mis ausencias, gracias por quererme simplemente como soy. Gracias yayos, tíos, primos, pero muy especialmente:

A mis padres. No soy afortunada por teneros como padres, soy mucho más que eso, soy una privilegiada. Habéis hecho de mis sueños los vuestros, de mis inquietudes las vuestras, de mis éxitos y fracasos los vuestros. Habéis dado todo lo que estaba en vuestra mano y más, para que yo pudiera ser feliz. Y si soy feliz, es por teneros como padres. Gracias mamá, gracias papá.

A mis hermanos. Somos 3 hermanos y 3 mundos distintos, y a pesar de que no nos ponemos de acuerdo ni para vivir en la misma ciudad y tenemos que quedar en los aeropuertos, siempre están ahí. Gracias por apoyarme en las distancias, gracias por entender mis ausencias. Gracias Tania y Yago.

Soy afortunada por tener unas amigas que son desde hace mucho tiempo en verdad parte de mi familia. Amigas de Pamplona inseparables desde los 3 años, que me han seguido por mis ires y venires de la vida, ya me fuera al polo norte (Tromso, Noruega) o a las cálidas islas canarias. Ellas estaban ahí, y sé que seguirán, vaya donde vaya, y que yo las seguiré a ellas. Porque sois únicas, por formar parte de mi familia, gracias Adriana, Amaya, Arantza, Iraia, Marieta, Miriam y Patricia.

Soy muy afortunada por tener a una amiga que me cocinaba cenas caltentitas para cuando llegaba de varamiento, y la pobre escuchaba con mucha entereza las

"guarradas" que le contaba en el desayuno. Jenny gracias por escuchar e interesarte por mis historias y por la participación activa en el diseño de este documento.

Finalmente quisiera agradecer a todas las instituciones gubernamentales y no gubernamentales que han financiado o participado de distintos modos en el desarrollo de esta tesis o en el estudio en general para la conservación de los cetáceos.

Esta tesis ha sido financiada con una beca FPU del Ministerio de Educación, con fondos del Instituto Universitario de Sanidad Animal y Seguridad Alimentaria así como con dos proyecto del plan nacional de I+D: "Valoración del estado sanitario de cetáceos de la familia *Ziphiidae* (zifios) en el archipiélago canario" (AGL2005-07947) 2005-2008 Y "Patología embólica (geseosa/grasa) en Cetáceos" (CGL 2009/12663) (Subprograma BOS) 2010-2012.

Quisiera agradecer en especial a la SECAC y a Canarias Conservación primero y lo más importante, por su interés e ilusión en la conservación y protección de las especies en nuestras islas y en segundo lugar por su participación activa y colaboración con nuestro grupo y por tanto, con esta tesis. Muchas gracias porque cada uno me habéis ayudado a mí en particular de una forma diferente, pero sobre todo gracias por el gran aporte que hacéis a la sociedad.

Y a todos aquellos que habéis creído en mí y hecho que esto fuera posible (Edu, Nico, Pilar,Yoli, y muchos más!)

Gracias a todos y todas.

Thank you to all of you.